

Aus dem Institut für Management ländlicher Räume
der Agrar- und Umweltwissenschaftlichen Fakultät

**GIS-based interpolation methods for soil CO₂ respiration data in
a temperate deciduous forest**

Dissertation
zur Erlangung des akademischen Grades
doctor agriculturae (Dr. agr.)
an der Agrar- und Umweltwissenschaftlichen Fakultät
der Universität Rostock

vorgelegt von
Dipl. Umweltwiss. Albrecht Jordan
aus Göttingen

Rostock, 01. Februar 2010

urn:nbn:de:gbv:28-diss2010-0120-2

Gutachter:

Prof. Dr. Stephan Glatzel:

Professur für Landschaftsökologie und Standortkunde, Institut für Management ländlicher Räume, Agrar- und Umweltwissenschaftliche Fakultät, Universität Rostock

Prof. Dr.-Ing. Ralf Bill:

Professur für Geodäsie und Geoinformatik, Institut für Management ländlicher Räume, Agrar- und Umweltwissenschaftliche Fakultät, Universität Rostock

PD Dr. Gerd Gleixner:

Abteilung für Biogeochemische Prozesse, Max-Planck-Institut für Biogeochemie, Jena

PD Dr. Hermann Jungkunst:

Abteilung Landschaftsökologie, Geographisches Institut, Fakultät für Geowissenschaften und Geographie, Universität Göttingen

Tag der Verteidigung: 15. Juni 2010 in Rostock

Table of contents

1.	Introduction	6
1.1	Motivation	6
1.2	Current state of research.....	7
1.3	Main objectives and hypothesis of this study.....	9
1.4	The “Hainich” project	10
2.	Materials and methods	12
2.1	Site description	12
2.1.1	Geography	12
2.1.2	Geology and general soil characteristics.....	13
2.1.3	Climate and hydrology	14
2.1.4	Vegetation	15
2.1.5	Land use history	17
2.2	Sampling design	20
2.2.1	The nested series	20
2.2.2	The random series	20
2.3	Sampling procedures	21
3.	Small scale spatial heterogeneity of soil respiration	24
3.1	Methods	24
3.1.1	Statistical analysis and calculations	24
3.2	Results	30
3.2.1	Seasonal variation of soil respiration	30
3.3	Spatial distribution	35
3.3.1	Hydrological gradient & spatial trends	35
3.3.2	Outlier analysis.....	38
3.3.3	Number of measurement locations required	40
3.3.4	Kriging preparation	41
3.3.5	Semivariograms.....	41
3.3.6	Maps of soil respiration.....	46
3.3.7	Maps of soil respiration incorporating soil moisture and temperature.....	46
4.	Fine root biomass of trees as a predictor of root respiration.....	49
4.1	Materials and methods	50
4.1.1	Surveying and mapping of trees.....	50
4.1.2	Calculating point specific potential relative fine root biomass	50

4.1.3	Calculating area-wide potential relative fine root biomass	53
4.1.4	Model validation	54
4.1.5	Statistical analysis & Regression kriging.....	55
4.2	Results	58
4.2.1	Validation results.....	58
4.2.2	Stand structure parameters	58
4.2.3	Calculated point specific potential fine root biomass	59
4.2.4	Correlations between potential fine root biomass and soil respiration at different seasons.....	60
4.2.5	Maps of seasonal ash root respiration	62
5.	Discussion	65
5.1	Small scale spatial heterogeneity of soil respiration	65
5.1.1	The influence of soil temperature.....	65
5.1.2	The influence of soil moisture.....	65
5.1.3	Spatial heterogeneity of soil respiration.....	66
5.1.4	Optimizing the parameters for interpolation	68
5.1.5	Interpolated maps	69
5.1.6	The standardisation approach.....	70
5.2	Fine root biomass of trees as a predictor of soil respiration.....	71
5.2.1	Limitations	71
5.2.2	Spatial patterns	71
5.2.3	Seasonal patterns	72
5.2.4	Microbial and physical controls	72
5.2.5	Synthesis.....	73
6.	Conclusion.....	75
7.	Summary	76
8.	Zusammenfassung.....	78
9.	References	80
10.	List of abbreviations.....	91
11.	List of tables	93
12.	List of figures	94
13.	Appendix	97
13.1	Soil respiration data.....	97
13.2	Soil moisture data.....	111

13.3	Soil temperature data.....	121
13.4	Semivariograms of soil respiration measurements.....	131
13.5	Java application – Source code	144
13.6	Potential relative fine root distribution patterns of different tree species	150
14.	Declaration	154
15.	Acknowledgements	155
16.	THESIS	157

1. Introduction

1.1 Motivation

Soil CO₂ efflux is one of the largest carbon flux components. Globally it accounts for 20-40% (50-75 Gt C/yr) of the total annual input of carbon dioxide into the atmosphere (Houghton, Woodwell 1989; Raich, Schlesinger 1992; Schimel 1995; Lankreijer et al. 2003). Even small shifts between carbon release and photosynthetic uptake can have a significant influence on the atmospheric carbon budget (Pregitzer, Euskirchen 2004).

Therefore, a better scientific understanding of the key factors driving soil respiration is of great interest, due to its potential for changing climate and thus temperature and precipitation (Jenkinson et al. 1991; Raich, Schlesinger 1992; Schimel 1995; Goulden et al. 1996; Davidson et al. 1998, S. 218).

4.1 billion hectares of land on earth are covered with boreal, temperate and tropical forests containing up to 80% of the terrestrial aboveground carbon and 40% of total soil C (Dixon et al. 1994; Pregitzer, Euskirchen 2004). Ecosystem productivity as well as soil respiration is thereby related to climatic gradients. The lowest mean rates of soil respiration occur in the coldest (tundra) and driest (deserts) biomes, whereas the highest rates can be found in ecosystems with high temperatures and high moisture availability (tropical moist forest) (Raich, Schlesinger 1992). However, mean soil efflux rates do not only vary between the major biome types, they also show high variability within the same biome and even within the same measurement site (Raich, Schlesinger 1992; Rayment, Jarvis 2000; Soe, Buchmann 2005; Herbst et al. 2009). Thus, there are large uncertainties in the annual averages of site specific soil efflux rates (a site is understood here as a particular ecosystem e.g., a forest or a wetland).

Small-scale heterogeneities in soil efflux rates are, *inter alia*, caused by the high variability of soil structure (Bouma, Bryla 2000), soil moisture (Davidson et al. 1998), bacterial & fungal communities (Gomoryova 2004), root density (Hanson et al. 2000; Soe, Buchmann 2005), soil organic matter content (Fang et al. 1998), wind speed at the soil surface and pressure patterns (Lankreijer et al. 2003; Martin, Bolstad 2005).

In recent years, the term "spatial heterogeneity" occurred mainly within studies comparing soil respiration values between different measurement sites. Most of these sites are selected just because of their different sample characteristics, for example their different soil or vegetation type, stand structure or stand age (Law et al. 2001; Salimon et al. 2004; Vogel et al. 2005). Studies describing within site "spatial heterogeneity", that means micro scale spatial

heterogeneity within old growth temperate deciduous forests with otherwise relatively homogeneous site conditions, are rare.

Many studies in the past few years partitioned soil respiration into autotrophic and heterotrophic components (Kuzyakov, Larionova 2006; Subke et al. 2006) and advances have been made in understanding the dynamics of a wide range of soil C pools and their effects on soil respiration (Baggs 2006; Kalbitz et al. 2000; Ryan, Law 2005). However, it still remains unclear on which scales factors influencing soil respiration vary, while influencing total soil respiration rate.

The following brief summary of a selection of important controls of within-site heterogeneity illustrates the need for investigations aiming at deciphering this neglected issue, which generally is reported as a mere by-product of soil respiration studies.

1.2 Current state of research

Forest age

The quantity of carbon cycling and storage in forests clearly depends on forest age. Intermediate-aged forests have a higher net primary productivity (NPP) and net ecosystem productivity (NEP) than older forests (<120 years) on the biome level (Ryan et al. 1997; Pregitzer, Euskirchen 2004) It is still uncertain to what extent old growth forest are less productive compared to younger stands (Carey et al. 2001). Thus, uneven-aged forests might show a high spatial heterogeneity of soil efflux rates.

Soil texture

Sandy soils have a low water holding capacity, which stimulates root growth and thereby higher root respiration rates, reflected in higher total efflux rates at the soil surface (Sotta et al. 2006). On the other hand clayey soils inhibit the percolation of water as well as the diffusion of soil CO₂ efflux (Adachi et al. 2006; Sotta et al. 2006). Waterlogging impedes O₂ diffusion and limits microbial and root activity (Soe, Buchmann 2005). Schwendenmann et al. (2003) assume that an increase in soil water content not only impedes the diffusion of CO₂ from the soil to the atmosphere, but also reduces the CO₂ production.

The contribution of CO₂ storage to the efflux is very small because the amount of CO₂ accumulated in the whole profile is only 7 to 10 times higher than the efflux per hour (Schwendenmann et al. 2003). It accounts only for about 0.1 -2% of soil respiration, which leads to the assumption that the observed decrease of soil respiration during high moisture contents is mainly caused by a decrease in CO₂ production due to a limitation of oxygen.

Topographic position

Sotta et. al. (2006) investigated the role of topographic position on soil respiration. Comparing annual mean values led to the assumption that there is no effect, but analyzing the seasonal variation of each topographic position demonstrated significant differences between them. These may be caused by variations in soil water content or by different amounts of litter and soil organic matter. Sotta et al. (2006) detected a systematic difference in soil water content along a topographical gradient, which might be caused by water redistribution throughout the year.

Micro topography

Rayment & Jarvis (2000) related spatial heterogeneity to variations in micro-topography in a boreal peat bog. Soil respiration in hummocks varied more strongly than in hollows, where fluctuations in soil moisture led to a strong variability of soil respiration. (Rayment, Jarvis 2000). Saiz et al. (2006) observed significantly higher respiration rates to be associated with a higher thickness of the organic layer. The importance of layer thickness, water content and the microbial and soil soluble carbon pools for spatial variation was also supported in a study at a high elevation subalpine forest (Scott-Denton et al. 2003): Spatial variation of soil respiration was determined by the thickness of the organic layer, which depended on the distance to the nearest trees.

Soil properties

A negative correlation between the spatial variability of CN ratio and soil respiration was described within the same forest in Ontario, explaining 51% of the respiration heterogeneity. This might be due to fungal activities because fungi are in need of high nitrogen substrate content and play an important role in decomposition (Khomik et al. 2006).

Stand structure

Soil respiration emanates from the heterotrophic microbial decay of organic matter, and as autotrophic respiration from the rhizosphere and associated mycorrhiza (Hanson et al. 2000). Root respiration significantly contributes to net carbon dioxide (CO_2) flux from soils (Raich, Schlesinger 1992; Epron et al. 1999), but its reliable quantification is difficult (Baggs 2006). The usual measured total soil respiration rates at the soil surface do not allow drawing conclusions on its specific components (Kelting et al. 1998). Therefore in recent years various techniques were developed to separate different fractions of soil respiration with both direct (i.e. girdling, trenching) and indirect methodologies (i.e. stable and radioactive C isotopes) (Rodeghiero, Cescatti 2006; Hanson et al. 2000; Kuzyakov, Larionova 2006). The reliability of the results is bound by assumptions and simplifications on which the applied

methodologies are based on (Rodeghiero, Cescatti 2006). Separation methods like trenching which is commonly used in forest ecosystems involve strong impacts on the root-soil system by increasing soil water content and rising rhizodeposition (Kelting et al. 1998; Epron et al. 1999; Hanson et al. 2000; Baggs 2006; Rodeghiero, Cescatti 2006). The decomposition of severed fine roots can persist for several months (Moyano et al. 2008). Isotope labelling techniques reduce soil-plant disturbances but the accuracy of these methods is relatively low (Baggs 2006; Kuzyakov, Larionova 2006). Depending on the method used for separation, rhizospheric respiration is related to microbial soil respiration (measurements on intact or excised roots) or to autotrophic root respiration (trenching) (Kelting et al. 1998; Widen, Majdi 2001; Hanson et al. 2000). Thereby the methods themselves can be a remarkable source of difference between the presented values of respiration components of different studies (Kuzyakov, Larionova 2006).

Having in mind these restrictions, the contribution of root respiration to total soil CO₂ efflux ranges from 10% to 90% in various studies within forest ecosystems (Hanson et al. 2000; Subke et al. 2006). Moyano (2008), working in the Hainich National Park at the same study site as this study, observed average rhizosphere respiration rates of 44±2 percent of the total, using a micro-mesh partitioning method with meshes of different pore sizes to separate root and rhizomicrobial respiration (Moyano 2008). To further increase the reliability of the interpolation of soil respiration data within forested study sites, there is a need for parameters with a long term temporal stability and simple determinability. Having in mind the high percentage rates of root respiration, it is obvious that the absence as well as the presence of roots has a huge influence on total soil respiration rates in forest ecosystems.

1.3 Main objectives and hypothesis of this study

This brief summary illustrates that various factors must be taken into account when reliable estimates of site scale flux rates are to be extrapolated from point measurements. It is very likely that these factors do not take effect on the same scales within a given site. Thus, an approach spanning various spatial scales seems to be adequate.

Therefore, in the first part of the present study a three-fold strategy was adopted. First nested groups of sampling measurement locations were set up. Second, data from stratified random measurement locations were recorded. Third, additional information gathered at the sampling points was used via kriging to improve the reliability of the site scale estimates of soil efflux rates. With this approach a better understanding of the spatial variability of soil respiration in

old growth temperate deciduous forests has been strived for. Specifically the following hypotheses were tested:

1. The environmental controls for soil respiration vary on different spatial scales within old growth temperate deciduous forest sites. Therefore, a multiple scale sampling approach improves the reliability of site scale soil efflux rate estimates extrapolated from point measurements.
2. The consideration of seasonal parameters like soil temperature and soil moisture further improves the interpolation results.

The objectives of the second part of the study are to improve the regionalisation of root respiration within an old growth beech forest. In the first analysis, the hypothesis that calculated potential fine root biomass at randomly located soil respiration measurement locations is correlated with measured total soil CO₂ efflux rates is tested. It is expected that the significance of the correlation is higher in summer than in winter, due to higher relative contributions of root respiration to total soil efflux (Epron et al. 2001; Widen, Majdi 2001; Moyano et al. 2008) compared to winter respiration rates (Kuzyakov, Larionova 2006). Preparing this analysis, stand structure parameters like location, breast height diameter (at 1.3m dbh) and type of each tree were recorded and potential fine-root biomass rates were calculated at each soil respiration measurement location using an adapted modeling approach of Ammer and Wagner (2005). In a second analysis, it is examined whether the expected correlation results can be used to improve the regionalisation of total soil respiration measurements. Therefore a regression kriging procedure (Odeh et al. 1995) using calculated potential fine root biomass rates of the entire study area and total soil respiration data is performed. It is studied how tree type and seasonal dynamics of root growth and mortality influence the quality of the regression kriging results.

1.4 The “Hainich” project

This study, focusing on the spatial and temporal variability of soil respiration in the Hainich National Park, is embedded in a larger scientific context. The scientific uncertainties described above and the determination of unexpectedly high carbon (C) storage rates in the context of the European-CARBOEUROFLUX project in the Hainich National Park (Thuringia), inspired scientific curiosity. These rates contradict the idea of the carbon dioxide neutrality of old forests and raise question about their countability as carbon sinks in terms of the Kyoto-protocol. In the context of European projects it cannot be clarified however, how

these high storage rates are and where in the system the C remains. In this context, the DFG - (Deutsche Forschungsgemeinschaft) funded project “Carbon storage in an unused beech forest in the Hainich national park - Differentiation of the soil carbon source and sink considering land use history” hypothesized that due to historical C-export, e.g. due to litter export, soils in the Hainich were depleted and the C store is again filled up now. This hypothesis was revised by three scientific partners, investigating:

- the extent of the C-export due to land use, type and extent of biomass use in its temporal and local variation. Data were reconstructed from archives. (University of Freiburg, Institute of Forest- and Environmental Policy, workgroup for forest history, Germany)
- how much C-input is stored and exported by water. To achieve this, ^{13}C and ^{14}C isotope ratios in soil gases as well as dissolved and particular soil C were determined. (Max-Planck-Institute for Biogeochemistry, Jena, Germany)
- and which portions of the C input are respired as soil respiration (this study). (University of Rostock, Faculty of Agricultural and Environmental Sciences, Institute for Management of Rural Areas, Landscape Ecology and Land Evaluation, Germany)

2. Materials and methods

2.1 Site description

2.1.1 Geography

The study site is located in the southern part of the “Hainich-Dün” growing-region in western Thuringia, Germany, between the cities of Mühlhausen (to the north), Bad Langensalza (to the east) and Eisenach (to the south-west). The investigation area was part of the forest growing region called “Weberstedter Holz”, measures about 5ha in size at an elevation of 440m a.s.l. ($51^{\circ}04'46''\text{N}$, $10^{\circ}27'08''\text{E}$) and its borders marks the catchment area (fetch) of an Eddy-covariance facility within the core zone of the “Hainich National Park” (Fig. 2.1).

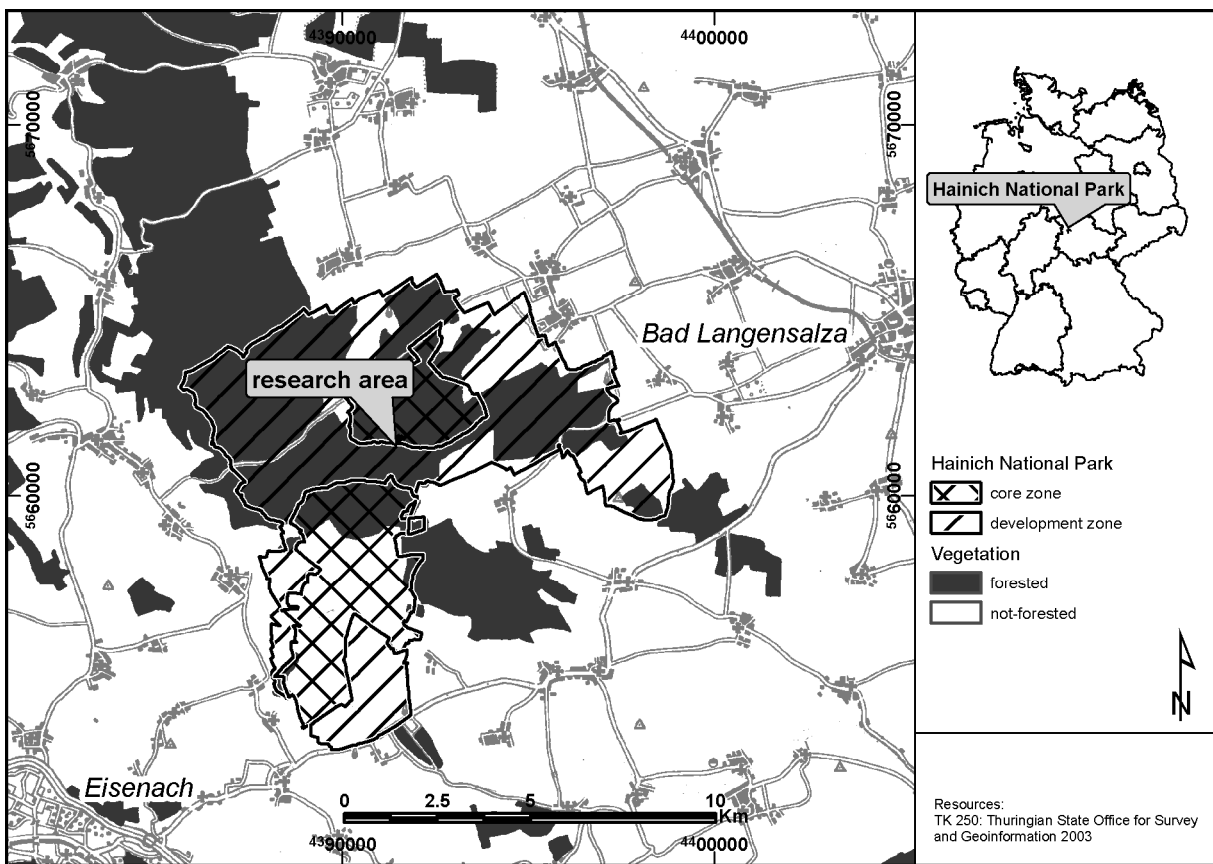


Fig. 2.1 Location of study site in the Hainich National Park

Both, the “Hainich” and the “Dün” are forested mountain ranges, separated by the Unstrut valley, forming together the northwestern corner of the “Thuringian basin”. Due to their same subatlantic climate and natural growing conditions, they are united into the same growing district, which is part of the superior region “Mitteldeutsches Trias-Berg- und Hügelland”(Schramm 1997). The size of the Hainich region amounts to about 15000ha and the narrow mountain range extends from southeast to northwest about 22km long and 4 to

8km wide(Stephan 2000; Ahrns, Hofmann 1998; Klaus, Reisinger 1995). The altitude of the upper plateau reaches more than 400m about sea level and the highest point is called “Alter Berg” with about 494m in height. Therewith, the Hainich plateau is about 100 to 200m higher than the adjacent “Thuringian basin”. It gently slopes towards the basin in northeastern direction and the terrain is characterised by a lot of v-shaped valleys at intervals of 0.8 to 1.2 km. The south-western border of the Hainich plateau suddenly plunges down to the valley of the river “Werra” and the hillside is formed by strong fluvial erosion processes of the river “Werra” and its tributary streams (Klaus, Reisinger 1995).

2.1.2 Geology and general soil characteristics

The Hainich mountain range consists of a limestone bed rock on a basement of mottled sandstone formed during the Trias, 200-250m years ago. The limestone package slopes in northeastern direction and can be divided into lower, middle and upper limestone. The upper limestone forms a wide band from north to south at the border of the Thuringian basin. To the west it is followed by a narrow band of middle limestone and a wider band of lower limestone. These bands are interrupted several times by other types of limestone. The southern border of the Hainich is dominated by the Eichenberg-Gotha-Saalfelder fault zone, which is about 120km long and characterized by upthrows and shiftings (Fig. 2.2).

The study site is dominated by upper limestone which consists of alternating layers of limestone and marl (Klaus, Reisinger 1995; Mönninghoff 1998; Seidel 2003).

In many areas, the limestone is covered by a Pleistocene loess layer. Its thickness (10-50cm) depends on the physiography of the underlying limestone bedrock. Thicker layer can be typically found in the bottom of the valleys. The loess is responsible for the high fertility of the Hainich, but its uneven distribution is also responsible for the high spatial heterogeneity of the soil formation processes. Other parts of the Hainich with little or non loess are covered with terra fusca or if the clay content is very low with rendzina.

The study site is characterised by terra fusca (international notation: chromic cambisol FAO et al. 1998), like many plateaus, shallow domes and pits in the Hainich (Grossmann 2007) with a depth of 50 – 60 cm and by a large clay content (45 – 65 %). The overriding humus form is mull. Especially beneath the ash, no litter remains are found during the summer months. In contrast to the beech stands a thin litter horizon is present, which leads to F-mull humus horizon.

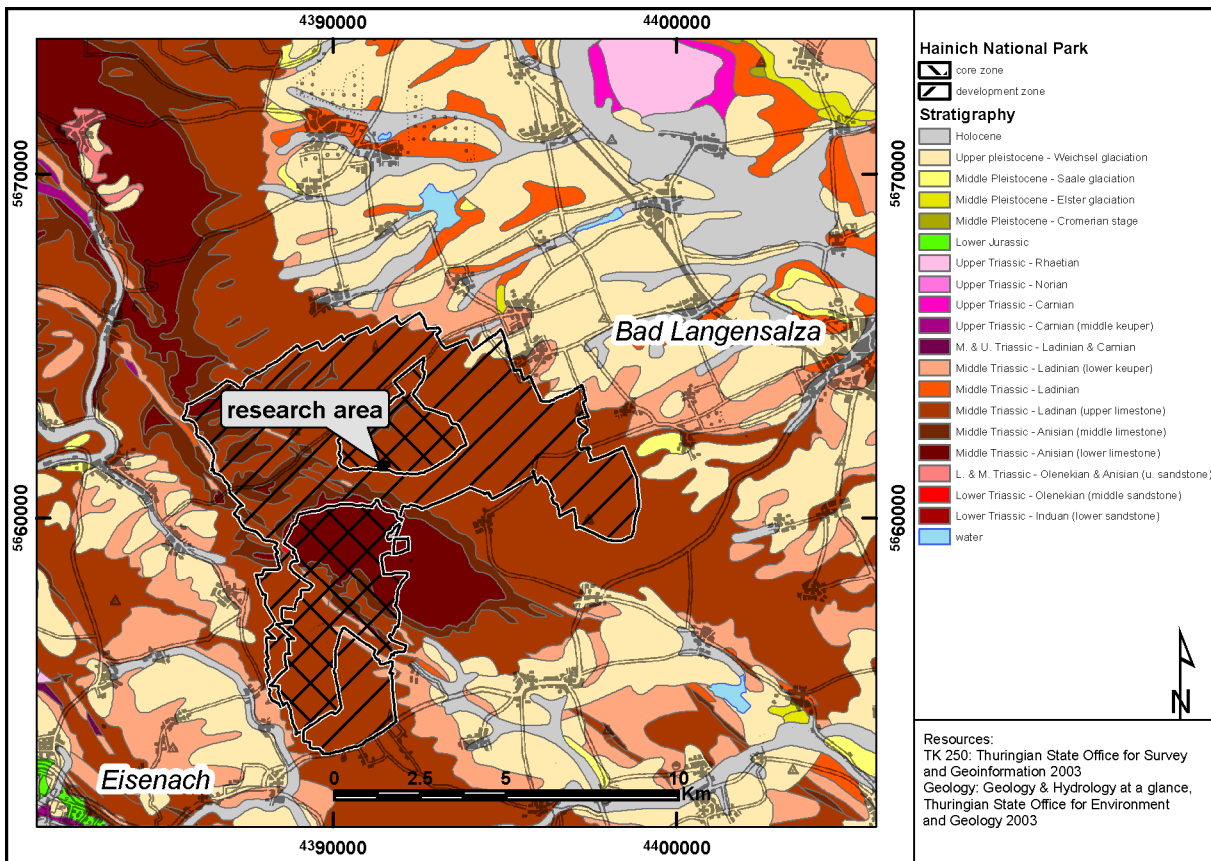


Fig. 2.2 Geology at the Hainich-Dün growing region

2.1.3 Climate and hydrology

The western scarp of the Hainich escarpment retains much of the upcoming rainfall from the predominantly western direction. As a consequence the Hainich can be divided into three climatic zones. The average rainfall at the western border of the Hainich at the river Werra is less than 650mm per year, the climate can be described as subatlantic. Only the upper parts of the Hainich are characterized as suboceanic-submontane with long-term annual means: 6-7 °C air temperature and about 750 mm precipitation. The precipitation has its maximum in summer (July and August) and half of it occurs during the growing season. The temperature amplitude ranges between 16°C in July and -1°C in January. More than 160 days of the year are without frost. On more than 40 days per year fog occurs in the mountain range, whereas the plain side around Bad Langensalza has less than 30 days with fog (Klaus, Reisinger 1995; Ahrns, Hofmann 1998). In addition it is noticeable that the cloud amount is about 7.0 to 7.2, which is very high. The climate classification system of Thuringia classifies the study site as "Klimastufe Vff" (very humid lower mountain range) (Schramm 1997).

Much more moderate climatic conditions (continental climate) can be found in the lee side of the Hainich plateau at the eastern border towards the thuringian basin which lower precipitation of 550-650mm and average annual temperatures of 7-8°C.

The Hainich belongs to two different river catchments, the Unstrut-Saale-Elbe river basin in the northeast and the Werra-Weser river shed to the southwest (Klaus, Stephan 1998). Much of the limestone bedrock of the Hainich especially the western escarpment consists of karsts. As a consequence of the karsts' porosity, many of the small streams exist only periodically during snow melting in springtime or after heavy rainfall. A huge amount of water percolates through the karsts until it reaches the underlying mottled sandstone (Seidel 2003). This mottled sandstone consists of clay and marl, so it works as impermeable stratum. The groundwater flows as interflow until it leaves the soil at several karsts springs at the slopes of the plateau in northern direction. A number of springs are well known between Mühlhausen and Bad Langensalza (Klaus, Reisinger 1995). The outflow of the area averages at 200 to 240 mm, which means 6 to 8 l/s km², but the seasonal variation is very high (Bauer, Weinitzschke 1974; Seidel 2003). Due to the high porosity, the Hainich plateau is an area with a high water deficiency, even though they produce a high amount of fresh groundwater (Seidel 2003). The frequency and duration of periodically occurring summer droughts is much higher at hillsides with southern exposure, but even at the northern exposed study side summer droughts occur occasionally.

2.1.4 Vegetation

The leading vegetation community, occupying predominantly the mountain range of the Hainich is called Fagion sylvaticae and the sub-formations Galio odorati Fagenion (woodruff) and Hordelymo-Fagetum / Elymo-Fagetum (wood barley). The most frequent tree species is European Beech (*Fagus sylvatica* L.), complemented by ash (*Fraxinus excelsior* L.), elm (*Ulmus glabra* Huds.) and maple (*Acer pseudoplatanus* L. and *Acer platanoides* L.). The climatic gradient from west to east plays a crucial role for the formation of the tree species. Regional differences in local climate and soil conditions are also responsible for the variations in plant community structures (Bauer, Weinitzschke 1974; Hofmann 1965, Hofmann 1974; Klaus, Reisinger 1995). At the escarpments with shallow soil depths also occurs the photophilic Carici-Fagenion (orchidaceous), whereas at some sites near Mühlhausen and Craula historic forest management encouraged the position of *Quercus petraea* L. (oak). Nevertheless, the main plant community of the Hainich is Elymo-Fagetum (wood barley). Due to the dense canopy, the young-growth forest and several shrubs like *Daphne mezereum*, *Lonicera xylosteum*, and *Crataegus* spec. grow sparsely. In contrast to the shrubs, the herb layer is well developed: *Hordelymus europaeus* (wood barley), *Asarum europaeum* (European

Wild Ginger), Melica uniflora (Wood Melick), Galeobdolon luteum (Yellow Archangel), Mercurialis perennis (Dog's Mercury) and others are dominating it (Klaus, Reisinger 1995).

At the study site, a wide age class range up to the age of 250 years was established, as a consequence of the absence of forest management (Fig. 2.3 & 2.4).

Following my own plant survey at the experimental site (described in chapter 4.1.1), the dominant tree species is beech (*Fagus sylvatica L.*), covering 87 % of the trees, followed by 7 % of ash (*Fraxinus excelsior L.*) and 2 % of maple (*Acer pseudoplatanus L.* and *Acer platanoides L.*) with minor abundance of European hornbeam (*Carpinus betulus L.*) and elm (*Ulmus glabra Huds.*). The age-class composition is much diversified, the tree density is about 489 trees per hectare and the maximum breast height diameter is about 92cm.

The herb layer consists of Ramsons (*Allium ursinum L.*), Dog's Mercury (*Mercurialis perennis L.*) and European thimbleweed (*Anemone nemorosa L.*) and is fully developed between April and October. The growing season starts with the bud break of the trees between the end of April and the beginning of May, leading to a leaved period until October. A special feature of the study site region called "Weberstedter Holz" is its richness of deadwood of about 30m³/ha, which is half the average of other European primeval forests (Klaus, Reisinger 1995).

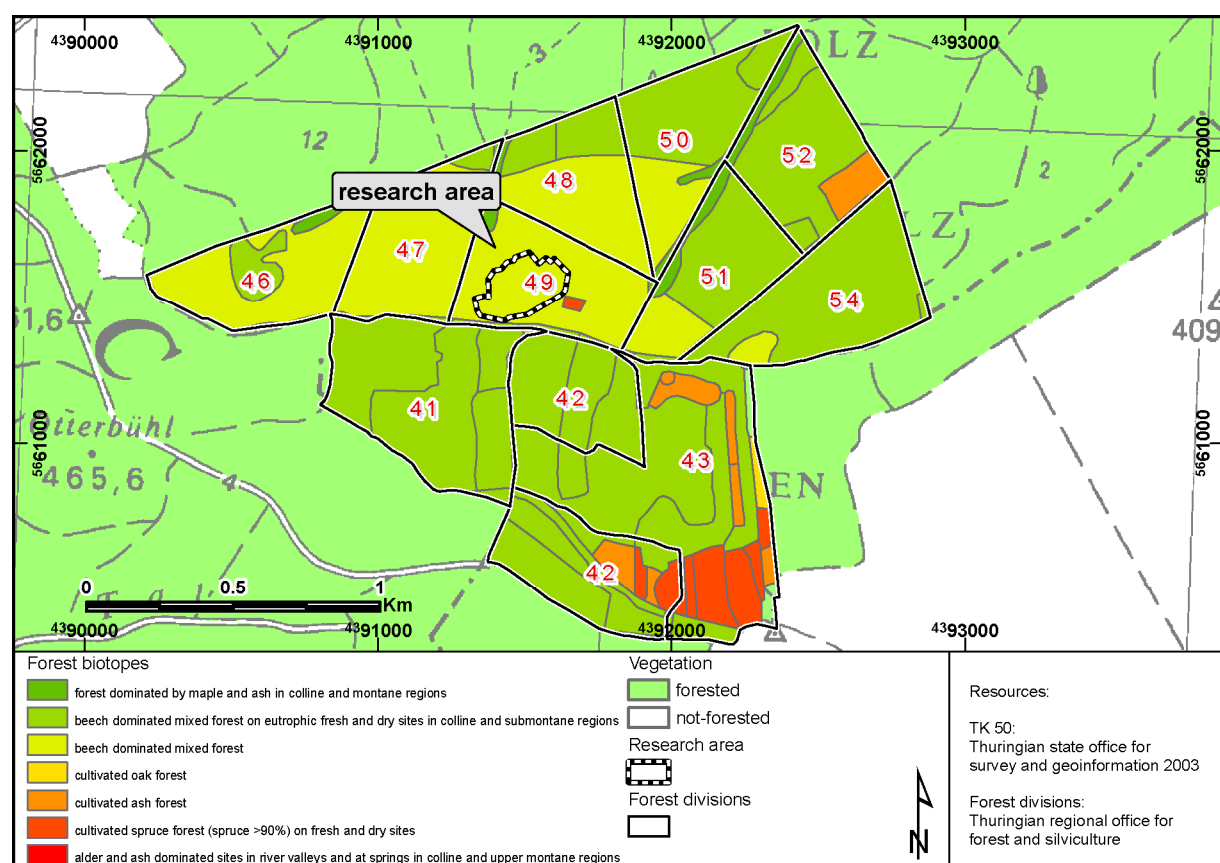


Fig. 2.3 Distribution of vegetation communities around the study site

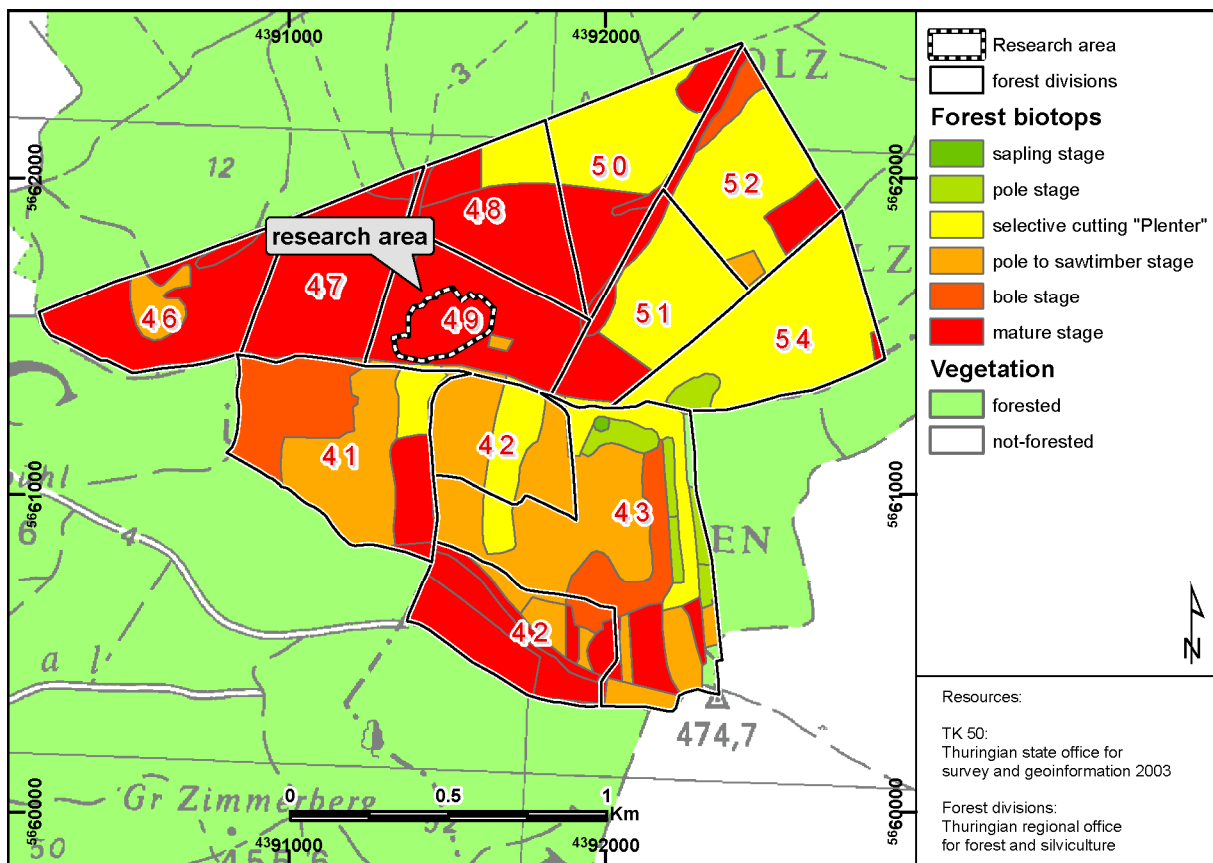


Fig. 2.4 Age class distribution around the study site

2.1.5 Land use history

The knowledge of former and present forest and land use history of the Hainich and the study site is essential for understanding and interpreting the measurement of soil respiration data, especially in the context of the given hypotheses described above. A detailed investigation of the forest history at the study site is being carried out by project partners from the University of Freiburg, searching for documents stored in historical archives, so the following paragraph gives only a brief overview.

Since 750 to 500 B.C. humans left marks in the Hainich region. Until the mediaeval times, the Hainich history is badly documented. Since that time different parts of the Hainich including small villages belonged to frequently changing owners. Rivalries between various noble landowners inhibited the continuity of a consistent use of the forest resources. The frequent changes of forest ownership also mean changes in silvicultural practices. Before the 12th century the forest use was characterise by irregular selective cutting and extensive grazing. Between the 12th and the 15th century five types of use where dominant: (1) selective cutting in hardly accessible or far away sites, (2) regular and organized harvest of fire wood, close to settlements, (3) grazing by goats, sheep, cows, pigs and horses, (4) combination of harvesting and forest pasture, (5) conversion of forest to cropland. Between the 16th till the 18th century,

the coppice system was widely used with rotation length of 13 years, often combined with forest pasture. The local people still collected all pieces of wood and leaf litter. From the 16th century the different forest using practices in more detail can be localized. Unfortunately, the study site is located in the southern Hainich in the “Weberstedter Holz”, where forest management details are rare. The site belonged to the elector of Saxony and presumably it was intensively managed as a coppice with standards and forest grazing. Usually local people from the adjacent villages obtained the right to use small parcels of forest as a closed community (“Laubgenossenschaft”). Houseowners living in Weberstedt also obtained the right to harvest pasture and to collect deadwood. Since 1803 respectively 1814/15, the complete Hainich was assigned to Prussia.

At the end of the 19th century adjacent forest sites were selectively cut high forests, the transmission phase of the study site to a selectively cut high forest started not before 1920. This was a result of socioeconomic structural changes, that means the direct use of timber increased, compared to other ways of forest utilisation (Klaus, Reisinger 1995). From 1926 till the beginning of World War II the study site was selectively cut about 2.1 m³ timber per year (Mund 2004). In the following years, the planned timber harvest increased up to 6.5 m³. After the war, the forest administration in Mühlhausen was established and private property of forested land was forbidden. Planning's to substitute the selection cutting system by grouped shelterwood cuttings were never realised. Since 1965, the study site at the “Weberstedter Holz” was used by the National People’s Army (NVA) as part of a large military training area (5700ha) of the GDR. This was not the first military site of the region. The adjacent Kindel at the southern border of the Hainich was used by military since 1935, first by the “Wehrmacht”, later on by the “Soviet-Army”. At the study site it is assumed that about 2m³ per year were still selectively cut, during the military period. As a result the forest, which was used more or less intensively for centuries, recovered to a natural broadleaved forest with a high amount of dead wood and an increased diversity of different species (Klaus, Reisinger 1995). In the 1980, only very valuable maple trees were cut selectively. After the fall of the iron curtain in 1990 the administration of the entire Hainich was taken over by the “Bundesforstverwaltung”. It remains unclear if any cuttings were performed at the study site at that time. In 1992 the last cutting of about 20 m³ of valuable timber was carried out (Mund 2004). Since 1997 the study site is part of the new established “Hainich National Park”, at the southern end of the Hainich mountain range, which protects the largest unmanaged beech forest in Central Germany covering a total area of 7512 ha (Stephan 2000) This area is divided into two type of protecting zones. In the first zone, in which the study site is part of, the forest is highly

protected, totally unused and can develop on its own. For the second protecting zone, a catalogue of objectives and measurements were determined, although natural development is also the main goal. In 2006 90% of the total area is completely out of forest or agricultural use. Only small parts of coniferous forest stands, which are not domestic in the Hainich region, are still under management (Thüringer Ministerium für Landwirtschaft, Naturschutz und Umwelt 2007).

2.2 Sampling design

Various factors have to be taken into account to get reliable estimates of site scale flux rates from point measurements. Two different sampling approaches were implemented to account for these factors which do not take effect on the same scales within a given site.

2.2.1 The nested series

On the one hand, a double nested, stratified random approach (nested series) to determine the maximum range of autocorrelation as a prerequisite for interpolation was implemented (Fig. 2.5). The first design was established at the 14th of April 2005. 79 measurement locations were arranged in this series. A grid on a map of the site was superimposed that divides it into 43 rectangular cells with an edge length of 34 m. In each of the grid cells one measurement location was placed in a random location to reduce the maximum distance between the points and to avoid large gaps between them. Thus, 43 measurement locations were distributed in a stratified random layout across the whole study site using an extension for ArcGIS 9.2 (ESRI, Redlands, USA) called “Hawth’s Analysis Tool” (<http://www.spatialecology.com>). To obtain spatially nested measurement locations 2 cells were chosen randomly from the grid and 36 measurement locations were placed in 4 groups within them resulting in two small and two larger measurement location groupings nested within each other (see Fig. 2.5 for details). This double nested approach allowed computing soil respiration data with three different spatial resolutions. At last 20 measurement locations were distributed along a hydrologic gradient, divided into 5 groups, each group consisting of four measurement locations. One group is located 200m north outside the catchments area of the eddy covariance tower at the bottom of the valley.

2.2.2 The random series

The second design was installed at the 25th of August 2005 at 81 randomly selected points, in almost the same catchment area of the eddy covariance facility. These sampling points were given beforehand by the Max-Planck-Institute for Biogeochemistry (Jena). They had extracted soil cores with an auger in 2000 and 2004, to determine soil physical and chemical parameters. This design has been retained unchanged till the end of measurements at 13th of June 2007. All twenty measurement locations along the hydrologic gradient, introduced during the build-up of the first design, were additionally probed during the measurement events of the second design (Fig. 2.5).

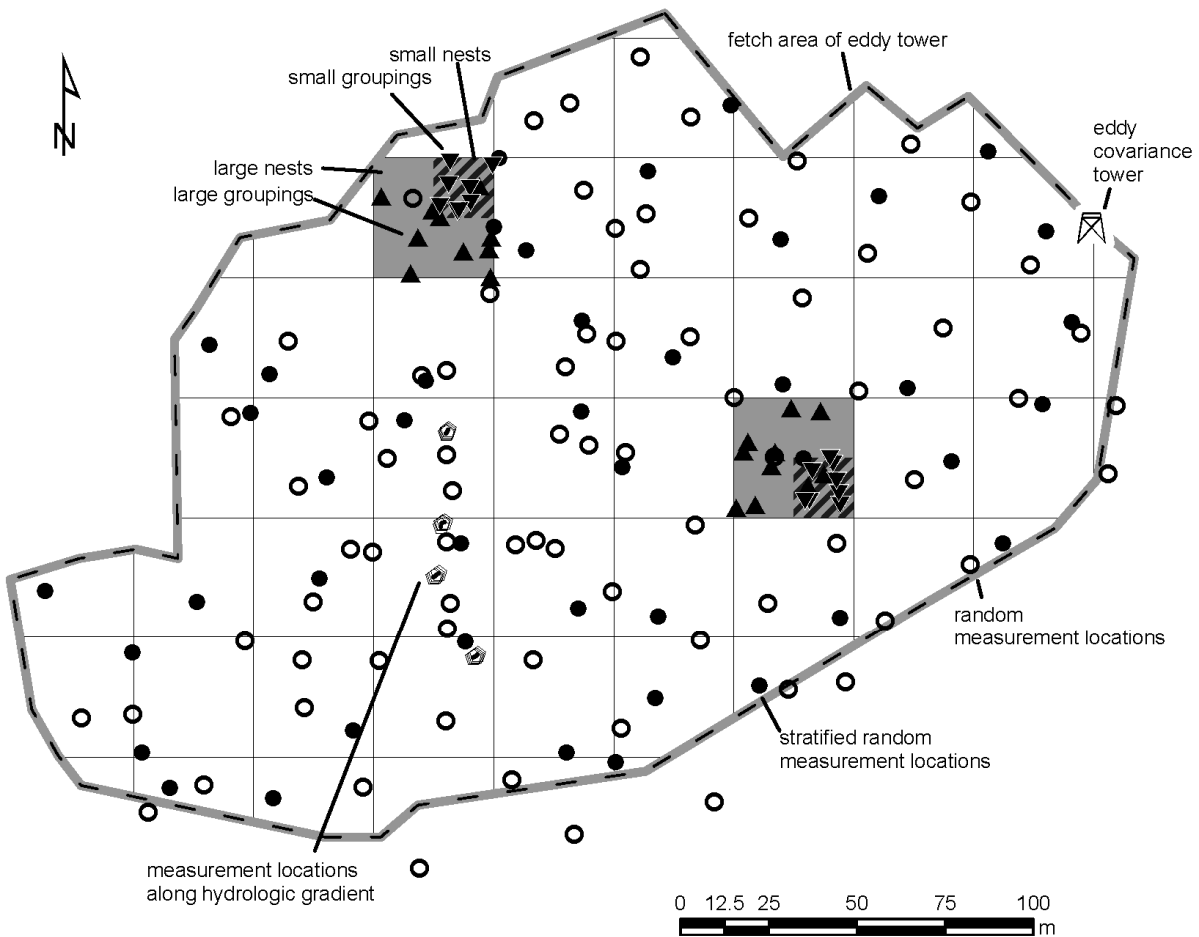


Fig. 2.5 Distribution of sampling locations in two series. Sampling locations of the random series (81 open circles) are distributed completely random across the site. Sampling locations of the nested series (43 dark circles and 36 triangles and 34m grid squares) are arranged in a stratified random way in 2 nested groupings: Two of the cells were chosen randomly from the grid. In both, 9 measurement locations are distributed randomly (large groupings). Both cells are further divided into quarters and in one quarter 9 measurement locations are placed at random (small groupings).

2.3 Sampling procedures

Both series were sampled biweekly. For the nested series sampling was carried out from April 2005 to April 2006. The random series was sampled from August 2005 to June 2007. During the time when both series were sampled (August 2005 to April 2006) the biweekly sampling was carried out alternately.

Beside the determination of soil respiration, measurements were made of soil temperature and soil moisture simultaneously. At the beginning of both measurement series, soil samples were also taken singularly for determining the soil bulk density.

Soil respiration

All sampling points of both measurement series were ordered and numbered in a consistent sequence depending on their distance to ensure the uniformity of the measurement events.

Soil respiration was recorded with a portable infrared gas analyser (IRGA, EGM-4) connected to a closed soil respiration chamber (SRC-1), both devices by PP Systems, Hitchin, UK. The soil respiration rate was calculated as the rate of change in CO₂ concentration within the chamber headspace. The EGM-4 allows for an automatic calculation of emission rates provided that the volume of the chamber and the surface area of the soil are set. The CO₂ concentration was monitored each 4.8 s over an interval of 124 s. Only the final results were saved and recorded. In preparation of both measurement series, a set of comparative measurements was performed using a second soil respiration measurement device (LiCor 6400-09, LiCor, Inc., Lincoln, Nebraska, USA), to ensure the quality of the recorded data. Due to the high reproducibility and the stability of both measurement results, the EGM-4 measurements were seen as reliable and sufficient.

The soil CO₂-efflux is calculated as:

$$R = \frac{\Delta c}{\Delta t} * \frac{p}{1000} * \frac{273}{273 + T_c} * \frac{44.01}{22.41} * \frac{V}{a}$$

R	CO ₂ -efflux [g*m ⁻² *h ⁻¹]
Δc	Variation of CO ₂ concentration [ppm]
Δt	Time
V	Volume
A	Area [cm ²]
p	Pressure [mbar]
T _c	inner temperature of the system

Soil temperature

In addition to the recording of respiration rates soil temperature was measured next to each measurement location at a depth of 0–10cm below the litter layer by digital precision thermometers (Greisinger, Regenstauf, Germany for the nested series; Testo, Lenzkirch, Germany for the random series). Due to the year round measurement campaigns, a few data gaps occurred at ground frost events. These were closed with data from the 20 continuously measuring soil sensors of the Max-Planck-Institute for Biogeochemistry, Jena. These sensors collect data at depths of -2, -5, -15, -30 and -50 cm. To assure comparability, the average temperature of the sensors in the depths of -2 and -5 cm was calculated. These values showed a very close and significant correlation with the average value of the own measurements at non-ground frost days.

Bulk density

The bulk density next to each measurement location was determined singularly at the beginning of each measurement campaign. Therefore undisturbed soil cores (100cm^3) were taken, oven dried at 105°C for at least 48h and weighted. The measured weights were multiplied with the constant factor of 0.01 to get the correct bulk density in [$\text{g}\cdot\text{cm}^{-3}$] (Schlichting et al. 1995).

Soil moisture

From April 14, 2005 until April 12, 2006 soil moisture was determined gravimetrically. During each measurement event, gravimetric soil water content was determined next to each measurement location. Hereto, soil samples were taken twice at each measurement location with a small auger up to a depth of -15 cm . These wet samples were weighted, oven-dried for 24 h at 105°C to stable weight and weighted again. The soil moisture was calculated as the percentage difference between wet and dry weight. From April 2006 until the end of the measurements soil moisture was determined with frequency domain reflectrometry (fdr) at 0– 6 cm soil depth below the litter layer with the ThetaProbe Soil Moisture Sensor – ML-2x and the Soil Moisture Meter – HH2 (AT-Delta-T Devices Ltd., Cambridge, UK). In contrast to soil temperature, data gaps during ground frost periods could not be closed using data from the eddy covariance tower, because of the large spatial variability of soil moisture measurements at single measurement dates.

3. Small scale spatial heterogeneity of soil respiration

In this section spatial heterogeneity of soil respiration was investigated using soil moisture and soil temperature values.

3.1 Methods

3.1.1 Statistical analysis and calculations

Tests for normal distribution with the Kolmogoroff-Smirnoff testing algorithm showed that non-parametric testing procedures were necessary, so I proceeded with Spearman rank correlations. All statistical calculations were carried out with STATISTICA 7.0 (Statsoft, Oklahoma, USA).

To estimate the dependency of seasonal variation of soil respiration from soil temperature, the temperature functions were fitted by regression to the simple exponential equation:

$$R = ke^{aT} \quad (1)$$

with R = soil respiration [$\text{g CO}_2 \text{ m}^{-2} \text{ a}^{-1}$], T = soil temperature (0-10cm) [$^\circ\text{C}$], k and a are constants(Davidson et al. 1998; Knohl et al. 2008). Q_{10} represents the temperature response of soil respiration and is calculated with the formula:

$$Q_{10} = e^{a10} \quad (2)$$

Saiz et al. (2006) and Stoyan et al. (2000) found that soil moisture is more important for the determination of spatial effects in temperate deciduous forests than soil temperature. Therefore, soil moisture is considered in the model (Eq. 3).

$$R = ke^{aT} e^{b\theta}, \quad \text{or} \quad \ln(R) = \ln(k) + a(t) + b(\theta) \quad (3)$$

with θ = soil moisture measured at 0-6cm [vol%] and a, b are fitted constant. The exponential equation taken from Knohl et al. (2008), was log-transformed to a linear model in order to conduct linear regression for the estimation of the parameters (Fig. 3.1). Soil respiration rates were standardized using soil moisture and soil temperature. Eq. 4 presents the modified version of Eq. 3, where $R_{\delta_T \delta_\theta}$ represents the modeled soil respiration for each measurement location, T and θ are the standardized soil temperature and soil moisture. δ_T and δ_θ are the differences between standardized and measured temperature and moisture values and k, a and b are constants again.

$$\begin{aligned}
R_{\delta_T \delta_\theta} &= k e^{a(T+\delta T)} e^{b(\theta+\delta\theta)} \\
&= k e^{aT} e^{a\delta_T} e^{b\theta} e^{b\delta_\theta} \\
&= R e^{a\delta_T} e^{b\delta_\theta}
\end{aligned} \tag{4}$$

$$R_{\text{standard}} = \frac{R_{\delta_T \delta_\theta}}{e^{a\delta_T} e^{b\delta_\theta}} \tag{5}$$

Eq. 4 can be transformed to separate R , so R is replaced by R_{standard} (Eq. 5). The modeled $R_{\delta_T \delta_\theta}$ term in Eq. 5 can be substituted by the measured soil respiration values.

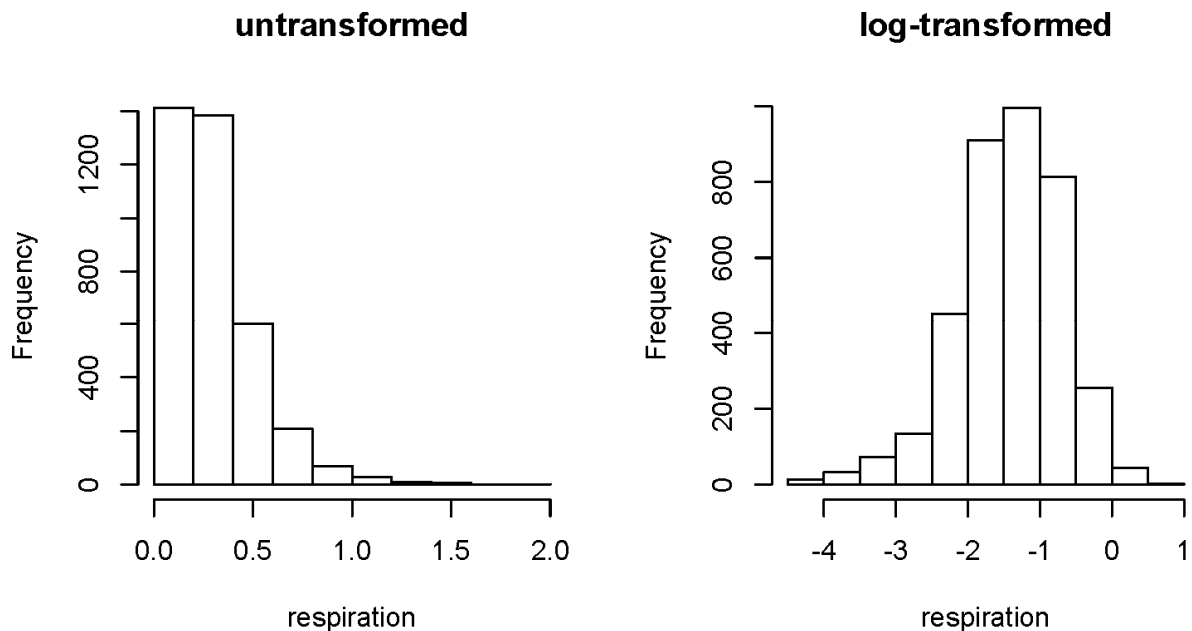


Fig. 3.1 Log-transformation of soil respiration data

The trend identification tool of ArcGIS 9.2 was used to identify spatial trends by plotting single soil respiration measurement events within a three dimensional diagram. To estimate the confidence of the observed total mean flux, N , the number of measurement locations needed for a given precision level, was calculated (Davidson et al. 2002; Yim et al. 2003; Adachi et al. 2005; Knohl et al. 2008) using equation 6:

$$N = \left[\frac{t_\alpha * s}{\text{range}/2} \right]^2, \tag{6}$$

with t the Student's t-statistic, s the standard deviation of one set of daily measurements, and range the desired interval around the daily mean. N was calculated for each measurement date separately. N was averaged to obtain a valid N for the entire study.

Potential significant differences between the soil respiration measurement location groups along the hydrologic gradient were investigated with an ANOVA for non normal-distributed data (Mann-Whitney-U-test). Therefore, the average respiration rates of respectively four measurement locations were compared with all other groups and plotted in a matrix table.

To determine possible significant differences between all datasets of soil respiration and soil moisture measurements at each measurement location in the entire research area, the non-parametric Kruskal-Wallis testing algorithm was used. The first and the second measurement series were examined separately in order to compare datasets with equal quantity, In addition to the resulting rank order table; the applied statistical software package provided the opportunity to generate a matrix of p-values indicating the probability of differences between each measurement point. The number of possible pairwise comparisons can be calculated as follows:

$$P = \frac{n^2 - n}{2} \quad (7)$$

P Number of possible pairwise combinations
n Number of measurement locations in the research area

The resulting p-value matrix allowed summarizing for each measurement location the number of all other measurement points which possessed significant different datasets within the study site. The numbers were attributed to each measurement location and visualized within a map. These numbers can be interpreted as a measure of deviation of each measurement location.

Geostatistical analysis

Pedological surveys normally produce point data, where data for the whole surface of research areas are necessary to quantify spatially averaged soil respiration. Therefore the extent of spatial variation in soil respiration must be evaluated, because the spatial variation in soil respiration is very large, whereas the area covered by one chamber is very small (Kosugi et al. 2007). For the generation of spatial data sets from point data several methods are in use. The decision about an adequate technique to extrapolate these measurements to entire study sites depends on the availability of a sufficient number of measurements and the spatiotemporal variability of the data, the scale of target map, the availability of external supporting parameters and the intended purpose of the regionalization (Zirlewagen 2003; Kosugi et al. 2007).

Upon now regionalisation methods were sparsely used for the investigation of CO₂-efflux measurements, probably because of the relatively smaller coefficient of variation of CO₂-efflux compared to other greenhouse gas emissions or other soil parameters (Ishizuka et al. 2005). Whereas Ishizuka et.al. (2005) used the inverse distance weighting method, a linear interpolation method, Stoyan et.al. (2000)(Stoyan et al. 2000), Soe & Buchmann (2005)(Soe, Buchmann 2005) and Kosugi et.al (2007)(Kosugi et al. 2007) already used ordinary block kriging as a higher sophisticated geostatistical approach.

Soe & Buchmann (2005) investigated the spatial heterogeneity of soil respiration within a small section (0.5ha) of the same research area (4.6ha) described in this study using rectangular grids with 36 (2000) respectively 144 measurement locations (2001). In the present study several designs and sampling point densities were tested and compared using geostatistics in order to find the most suitable design, the adequate sampling size and the most appropriate distance between sampling points within this old-growth temperate deciduous forest in the Hainich-National-Park. In addition the effects of external parameters like soil water content on spatial and temporal variation were incorporated too. The preferential use of geostatistics in comparison to simpler linear interpolation techniques can also be justified, as it allows determining the scale of spatial autocorrelation among measurement points and the determination of the magnitude of spatial dependence (Robertson 1987). Spatial autocorrelation or spatial dependency which means that the probability of similar data values is higher for neighbouring sample points than for points far from each other, is a essential prerequisite for the use of geostatistical regionalisation methods.

An adapted analytical approach was developed based on the procedural method described by (Franklin, Mills 2003) for microbial communities. In order to distinguish between soil respiration heterogeneity in the close-up range and spatial separation (lag distance), the overall spatial autocorrelation structure had to be analysed. All sampling points located within the two grid cells with the nested groupings were necessary to quantify autocorrelation at different spatial scale. Thus, three different sets of measurement locations for estimating the kriging parameters were used. First, only the stratified random measurement locations of the nested series with relatively large inter-measurement location distances were utilized. Then, the data of the larger groupings from the nested series and finally the data of the small scale groupings were added. The maps as well as the parameter estimates resulting from ordinary kriging with these three datasets were compared. The cell size of the maps was set to 10cm x 10cm and the maps were classified in 0.01 g CO₂ m⁻² h⁻¹ units, the same resolution as the applied measurement equipment. “Hawth’s Analysis Tool” (<http://www.spatialecology.com>,

extension to ArcGIS) was used to count the number of equal values per class. Thus, average soil respiration rates were calculated for different sampling densities and were compared (Franklin, Mills 2003; Wackernagel 2003).

In the course of calculating semivariances from field data and fitting the models to semivariograms, it was first necessary to consider the appropriate number of bins and the bin-width (lag distance). On the one hand classifying (binning) of data aims to obtain the maximum detailed resolution; on the other hand misleading structural artefacts should be excluded. Different variograms were calculated for a range of diverse lag distances and the most reasonable parameter estimates with the maximum detail were used for the kriging procedure. Kriging was carried out using the Geostatistical Analyst extension of ArcGIS 9.2 (ESRI, Redlands, USA).

The calculation of semivariances from soil respiration data and fitting the models to semivariograms was performed using “R”, a language and environment for statistical computing and graphics.

The experimental semivariogram $\gamma(\mathbf{h})$ which is a measure for the average dissimilarity between the soil respiration sampling points data separated by a vector \mathbf{h} (Goovaerts 1999; Webster, Oliver 2001) was calculated as follows:

$$\gamma(\mathbf{h}) = \frac{1}{2N(\mathbf{h})} \sum_{\alpha=1}^{N(\mathbf{h})} [z(\mathbf{u}_\alpha) - z(\mathbf{u}_\alpha + \mathbf{h})]^2 \quad (8)$$

where $N(\mathbf{h})$ is the number of pairs of points within a given class of distance and direction, $z(\mathbf{u}_\alpha)$ represents the measured value at measurement location \mathbf{u}_α and $z(\mathbf{u}_\alpha + \mathbf{h})$ is the measured value at point $\mathbf{u}_\alpha + \mathbf{h}$. The degree of relationship between soil respiration measurement locations is expressed by the semivariance. With increasing distance between them, the semivariance increases as well until it equals the variance of the whole dataset. Three different forms of semivariance curves can generally be expected. The nugget form is flat and indicates a lack of spatial autocorrelation within the dataset. The linear form represents autocorrelated data at all distances within the examination area. This empirical variogram seldom passes the origin of the graph, but indicates variability at zero distance. This also called nugget effect can occur because of measurement error, random sampling variance or spatial variability out of the scale. The linear-sill model is conceptually the same as the linear model but the function levels off at a sill, which means the range of autocorrelation ends at a

certain point. (Franklin, Mills 2003). Points within the range are spatially autocorrelated; points outside the range can be considered as spatially independent.

To optimize the kriging results I varied the lag distance until I obtained the best possible parameter estimates, which mean the maximum range. Before analysis, all datasets were checked for outliers. Outliers were defined outside the range of $1.5\delta \leq \mu \leq 1.5 \delta$ and were removed before further analysis. All kriging attempts were performed using the Geostatistical Analyst extension of ArcGIS 9.2 (ESRI, Redlands, USA).

To estimate annual fluxes based on the random series with 81 data points, regression equations using measured soil respiration, soil moisture and soil temperature data were calculated for each measurement location. Soil temperature values measured at the eddy covariance facility were used to estimate the mean flux for each measurement location each day of the year. Two methods were used for further calculation: On the one hand I calculated the final annual flux of the site from the average sum of all measurement locations; on the other hand I used a geostatistical approach. Therefore average standardised soil respiration values of each measurement location were extrapolated using ordinary kriging. A minimum convex polygon was created around the measurement points and reduced by 10m inwards to avoid border effects. The resulting polygon was used to clip the ordinary kriging result. Zonal statistics were performed to calculate the total soil respiration rate at the study site.

3.2 Results

3.2.1 Seasonal variation of soil respiration

Looking solely at the flux rates of the random series the measurements started at the 25th of August 2005 with average soil respiration rates of $0.48 \text{ g CO}_2 \cdot \text{m}^{-2} \cdot \text{h}^{-1}$, with a soil temperature of 14°C and a soil moisture of 40% (Fig. 3.2). Two weeks later, the soil temperature increased about 2°C , the soil moisture dropped slightly about 1% and the soil respiration rose to $0.50 \text{ g CO}_2 \cdot \text{m}^{-2} \cdot \text{h}^{-1}$. In the following month until the end of January 2006, the average soil respiration rate decreased constantly until it reached an absolute minimum of $0.04 \text{ g CO}_2 \cdot \text{m}^{-2} \cdot \text{h}^{-1}$. Then, in spring 2006, the soil temperature increased rapidly. This was followed with a little delay by the soil respiration rate. The two lower respiration values in the middle of May and July 2006 seem to correspond with temporal decreases in soil moisture availability. Maximum soil temperature and minimum soil moisture was measured on July 26, 2006. The average soil respiration value of $0.34 \text{ g CO}_2 \cdot \text{m}^{-2} \cdot \text{h}^{-1}$ at that day was far from its maximum of $0.60 \text{ g CO}_2 \cdot \text{m}^{-2} \cdot \text{h}^{-1}$ in June 2006.

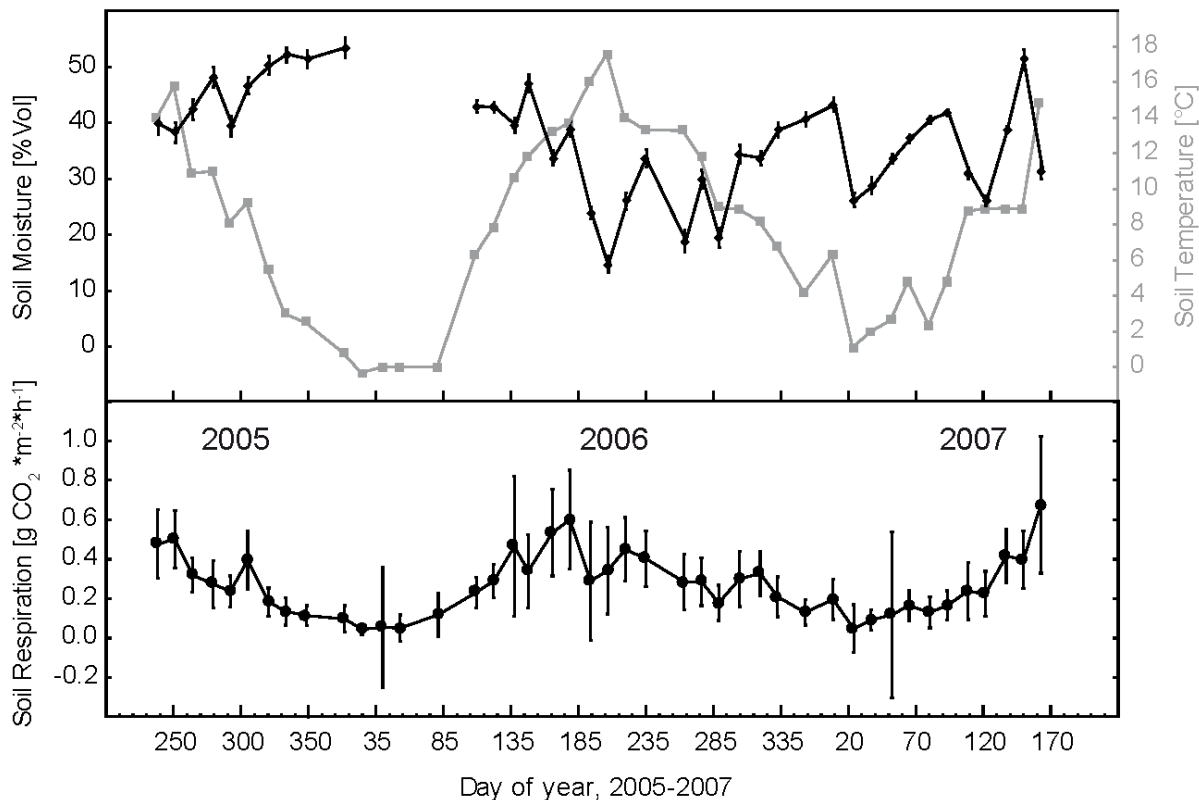


Fig. 3.2 Soil moisture, soil temperature, and soil respiration during the course of the study. The graphs base on the measurements in the 81 measurement locations of the random series. Vertical bars represent the 95% confidence interval. The annual cycle is clearly apparent. The soil moisture data gap during winter 2005/2006 is caused by ground frost. Furthermore, the soil respiration measurements show considerable heterogeneity at some of the measurement dates.

During the winter 2006/2007 non ground frost period occurred as the year before and the soil temperature and the soil respiration values seem to correspond quite well.

The variability of the soil respiration values is quite large, especially in spring 2006 during the bud break of the trees at the end of April till the end of July. The measured soil temperature values possessed a low level of variability within the entire study site. The lowest temperature difference within the site occurred in January 2007 with 0.5°C maximum difference within the site, the highest diversity with 2.6°C difference appeared twice, first in November 2005, second in June 2007. The average within-site soil temperature variability during the measurement campaign was 1.3°C. Compared to soil temperature, soil moisture showed high within-site heterogeneity as well as high seasonal variability. The two year average of volumetric water content was 37%, but it ranged from 5% till 88% at the driest, respectively the wettest places.

The seasonal variation of soil respiration is clearly temperature dependent (Fig 3.3, all data: $r^2= 0.60$, $Q_{10}=3.9$). The total average soil respiration value is $0.28 \text{ g CO}_2 \cdot \text{m}^{-2} \cdot \text{h}^{-1}$. However, the relation between soil respiration and soil temperature was much closer at measurement locations with lower soil moisture content (0-30 % Vol., $r^2= 0.69$, $Q_{10}=2.3$) compared to wetter measurement locations ($>60\text{-}90$ % Vol., $r^2=0.32$, $Q_{10}=4.1$). The highest average respiration rates ($0.30 \text{ g CO}_2 \cdot \text{m}^{-2} \cdot \text{h}^{-1}$) were observed at medium soil moisture between $>30\text{-}60$ [% Vol.].

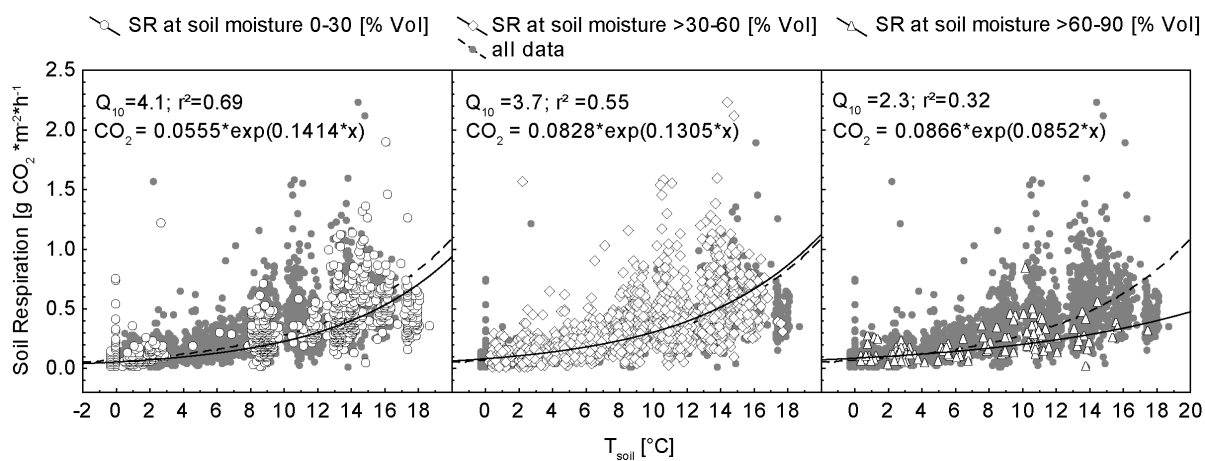


Fig. 3.3 Relationship between soil temperature and soil respiration. Q_{10} as well as the fit and the parameters of the models vary for different ranges of soil moisture. The Q_{10} for all data is 3.9 [$r^2=0.60$; $\text{CO}_2=0.0711 \times \exp(0.1365 \times x)$].

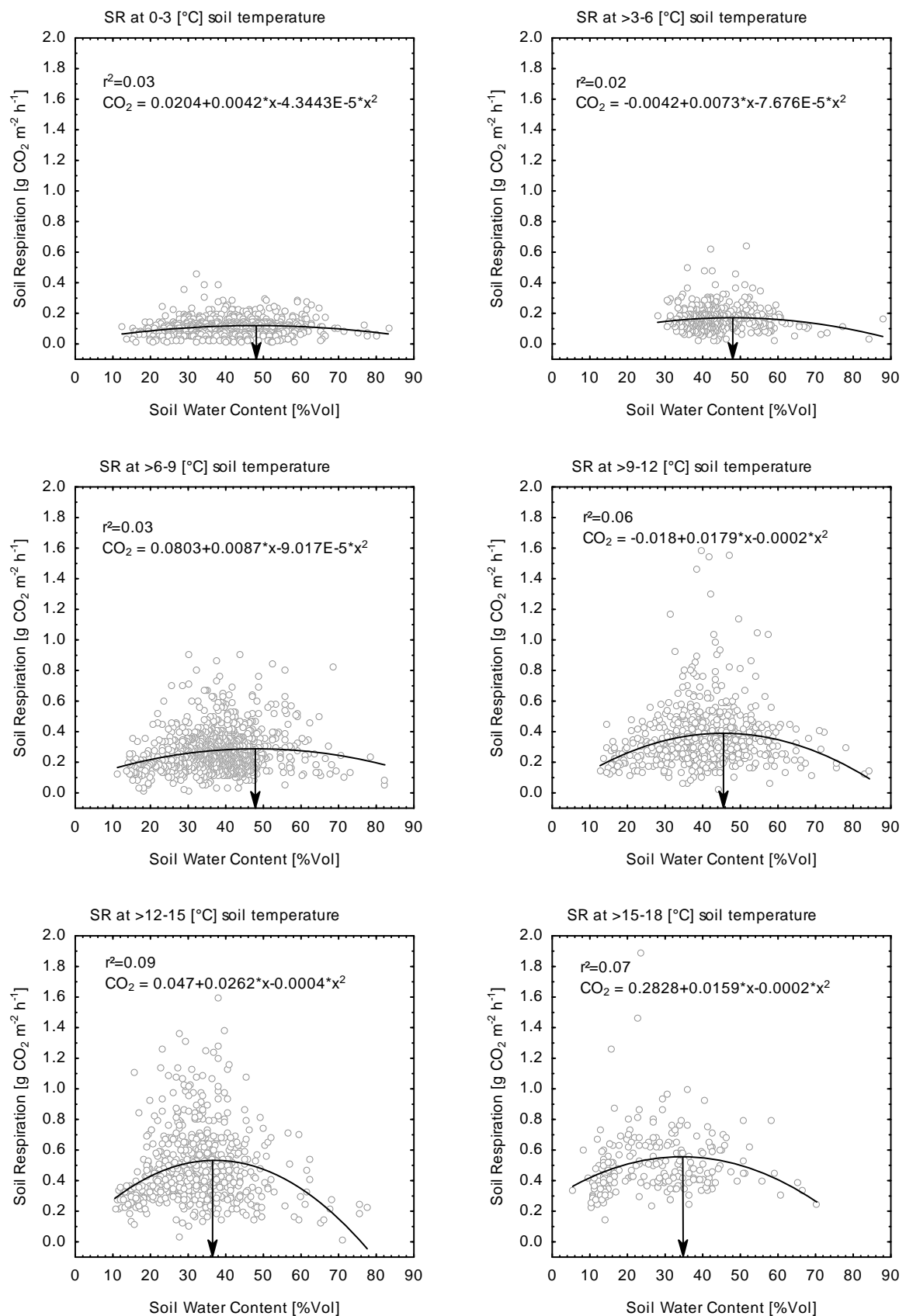


Fig. 3.4 Soil respiration versus soil water content at different soil temperature levels

These results were confirmed by the stepwise correlation of soil water content versus soil respiration rates at six different levels of soil temperature (Fig 3.4). Despite the extremely weak relationship between soil respiration rates and soil water content indicated by the coefficient of determination ranging from 0.02 to 0.09 at the different temperature levels, it is particularly noticeable that each of the analysed datasets were best fitted by quadratic functions. Furthermore, the maximum of the fitted functions which mark the highest soil respiration rates at a defined temperature level is remarkably stable between 45-50 [% Vol] soil water content at soil temperatures of 0-12 [° C]. At higher temperatures, this maximum rapidly decreased to lower levels of soil water contents of about 35 [% Vol].

Soil water content and temperature were negatively correlated across the entire measurement campaign ($r^2= 0.10$) (Fig 3.5). Plotting volumetric water content vs. soil respiration for all soil respiration data shows little correlation as seen before during the stepwise correlation at different temperature levels (Fig 3.6). The attempt to find any suitable fitting function neglects the effects of temperature. Linear, quadratic and exponential fitting functions have nearly the same extremely weak coefficient of determination ($r^2=0.024-0.028$). All fitting functions indicate a negative correlation; this finding is supported by the complete absence of higher respiration rates at very high soil moisture contents. The residuals of the regression respiration against temperature have a non-linear relation to the soil moisture content. Under very dry conditions (below soil moisture content of 20%) respiration is underestimated, whereas under medium moisture conditions the fit is generally good but can, under specific conditions driven by other variables not measured here, also be overestimated (Fig 3.7).

Soil temperature did not vary much in space (average soil temperature variability at a given measurement date was 1.3°C)(Fig. 3.8), whereas soil moisture measurements showed a considerable spatial heterogeneity as well as high seasonal variability. Total average volumetric water content was 37% with a wide range from 5% to 88%. A multiple regression model including soil moisture and soil temperature as explanatory variables slightly improves the explanation (R^2 increased from 0.60 using only temperature to 0.63). This model was used for the regionalization.

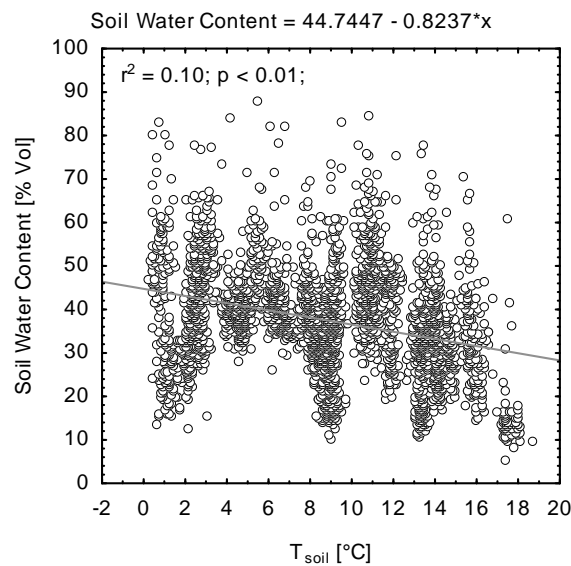


Fig. 3.5 Covariation of soil water content and soil temperature

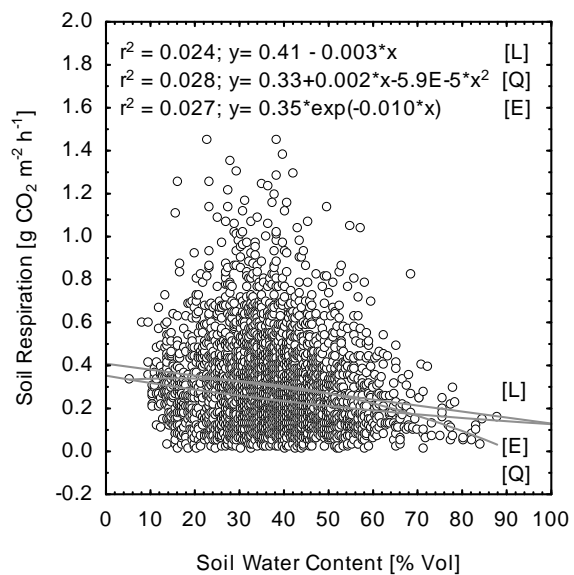


Fig. 3.6 Soil respiration versus soil water content for all data using different fitting functions

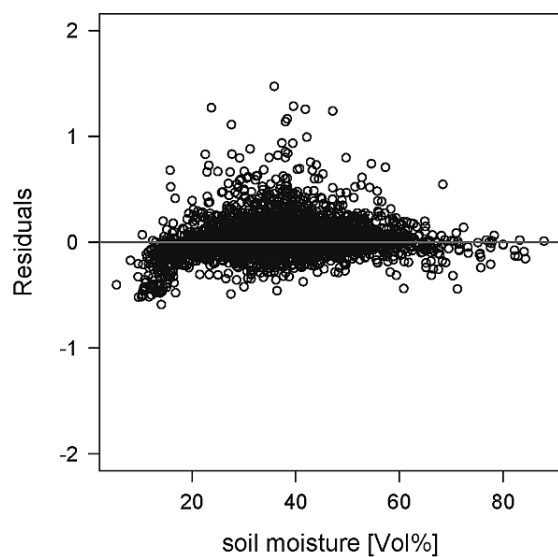


Fig. 3.7 Residuals of the regression analysis of soil respiration and soil temperature versus soil water content

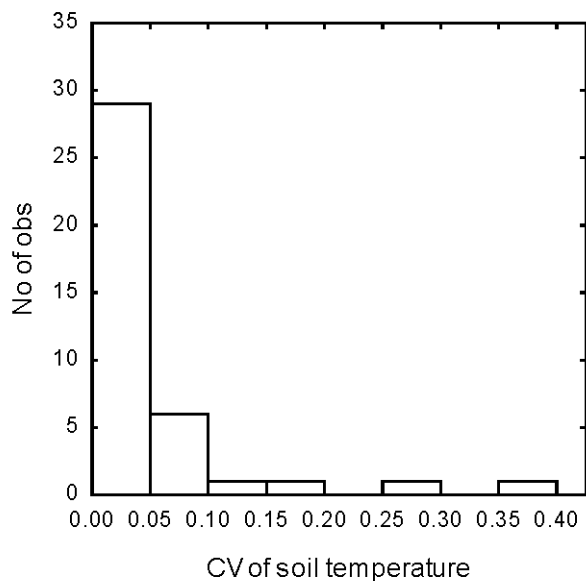


Fig. 3.8 Coefficient of variation of soil temperature of all measurement events.

3.3 Spatial distribution

3.3.1 Hydrological gradient & spatial trends

When averaged in time, soil respiration does not show a spatial trend, because the presence and absence of soil respiration hotspots rotates irregularly. This is also the case for analyzing solely possible spatial trends along the hydrologic gradient which also do not exhibit any clear trend (Fig. 3.9). Mean values over two years of continuous measurements from April 2005 till June 2007 range between $0.23 \text{ g CO}_2 \cdot \text{m}^{-2} \cdot \text{h}^{-1}$ at the third group of measurement locations till $0.28 \text{ g CO}_2 \cdot \text{m}^{-2} \cdot \text{h}^{-1}$ at the forth group 25m downhill. The difference between the median values is slightly greater, it ranges from $0.21 \text{ g CO}_2 \cdot \text{m}^{-2} \cdot \text{h}^{-1}$ at measurement location-group three till $0.28 \text{ g CO}_2 \cdot \text{m}^{-2} \cdot \text{h}^{-1}$ at measurement location group four. The coefficient of variation (CV) of the soil respiration measurements ranges between 59% (measurement location-group 1) and 63,3% (measurement location-group 3). A higher degree of variability can be found at group 5 outside the catchment area at the bottom of the valley with 79%. The results of the Mann-Whitney-U test indicate no significant differences between the five groups of soil respiration data (Table 3.1). Differences between soil moisture and soil respiration rates of all measurement location groups were not significant at $p < 0.05$. The average soil moisture is nearly the same at all measurement location groups about 32 [% Vol.], except at the upper most group (40 [% Vol.]) (Fig. 3.10). The coefficient of variation (CV) of soil moisture measurements ranges between 37% till 42%.

Opening the view from the hydrologic gradient to the entire study site supports the impression that at least half of the coefficient of variation of soil respiration during both measurement series ranged between 40% till 60%. Only a few values during the frost period in winter 2006 caused higher degrees of spatial heterogeneity, due to differences in soil temperature (Fig. 3.11 & 3.12). Therefore, ordinary kriging can be carried out without performing any trend removal procedures.

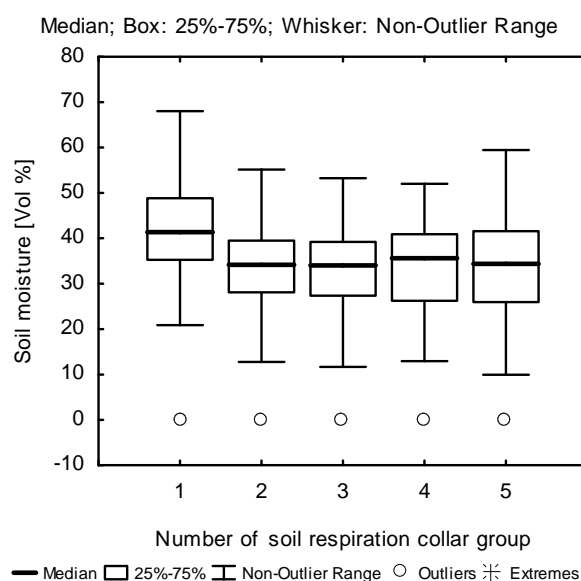
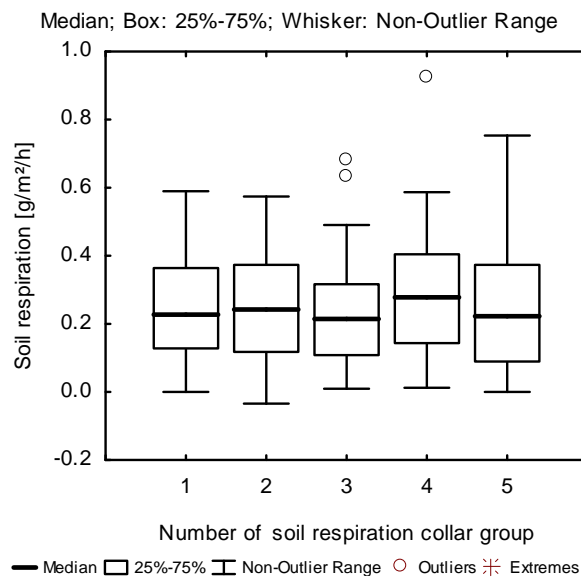


Fig. 3.9 Distribution of soil respiration along the hydrologic gradient from the upper (1) group of measurement locations downwards till group 5

Fig. 3.10 Distribution of soil moisture along the hydrologic gradient from the upper (1) group of measurement locations downwards till group 5

Table 3.1 Mann Whitney U-Test of soil respiration data at all five measurement location –groups. Non values were significant at $p < 0.05$

p-level	1	2	3	4	5
1	-	0.797	0.473	0.307	0.433
2	0.797	-	0.362	0.513	0.321
3	0.473	0.362	-	0.089	0.474
4	0.307	0.513	0.089	-	0.115
5	0.433	0.321	0.474	0.115	-

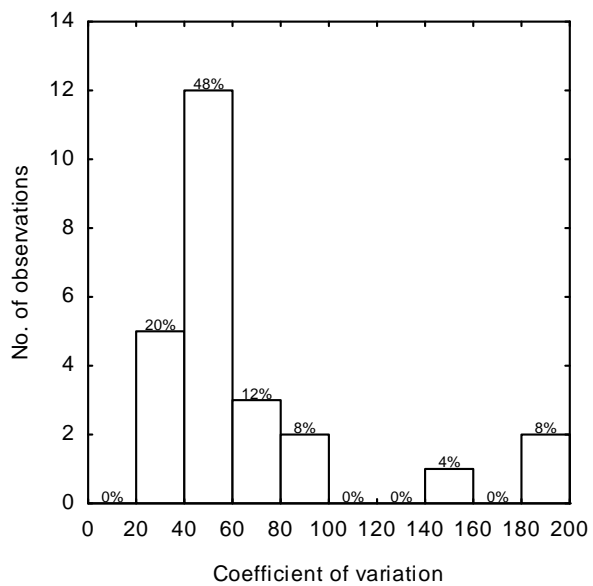


Fig. 3.11 Nested series: Coefficient of variation of soil respiration

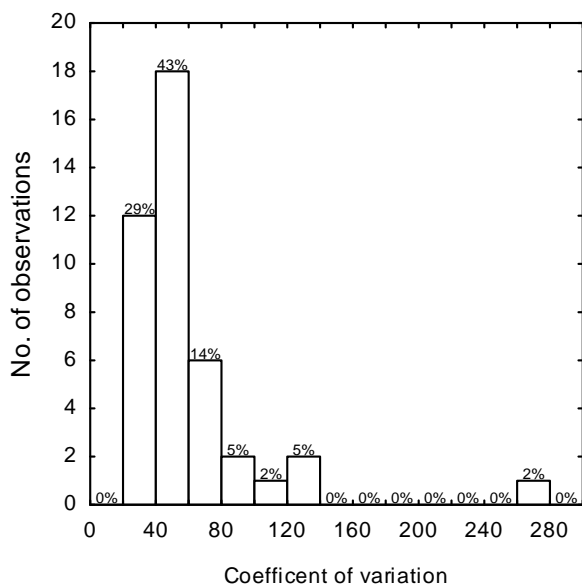


Fig. 3.12 Random series: Coefficient of variation of soil respiration

3.3.2 Outlier analysis

Small respiration collars as used in this study sometimes exhibit extremely high or low respiration rates caused by local variations in soil texture etc. Extrapolating these local outliers may lead to an overestimation /underestimation of soil respiration data of large areas within the study site. The quantity and the spatial distribution of outliers were detected using the Kruskal-Wallis one-way analysis of variance, to determine the relevance of outliers and the distance between significant different soil respiration measurement locations, in order to estimate the need of outlier exclusion before performing any kriging attempts (Fig. 3.13 – 3.15).

Within the nested series, annual mean soil respiration rates of only 28 of 99 measurement locations were significantly different from one or more other measurement locations in the research area. Altogether 50 pairs of significantly different combinations exist between these measurement locations. The values at a particular measurement location shown in (Fig. 3.13) represent the 100 end points of these connection lines. They indicate the quantity of measurement locations with significantly different soil respiration values compared to them. Only for a few of the 28 measurement locations I found more than one significantly different measurement location within the research area.

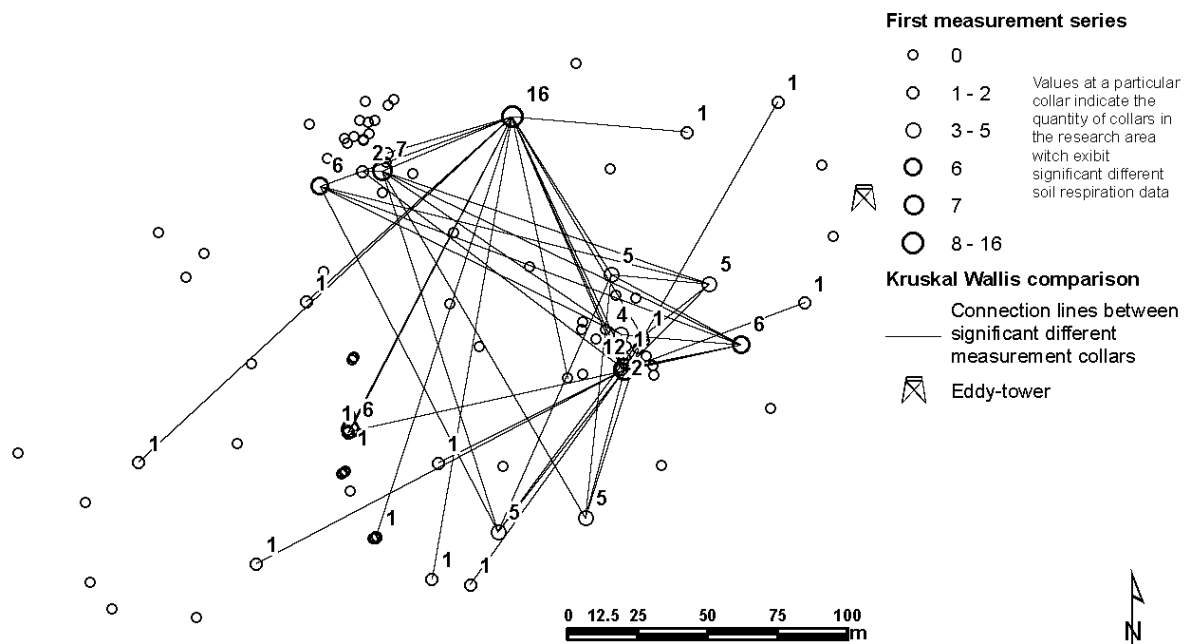


Fig. 3.13 First measurement series - Spatial heterogeneity: The size of each measurement location sign indicate how many other measurement locations in the research area exhibit significantly different values compared to them. The connection lines show which pairs of measurement locations where compared with significant differences.

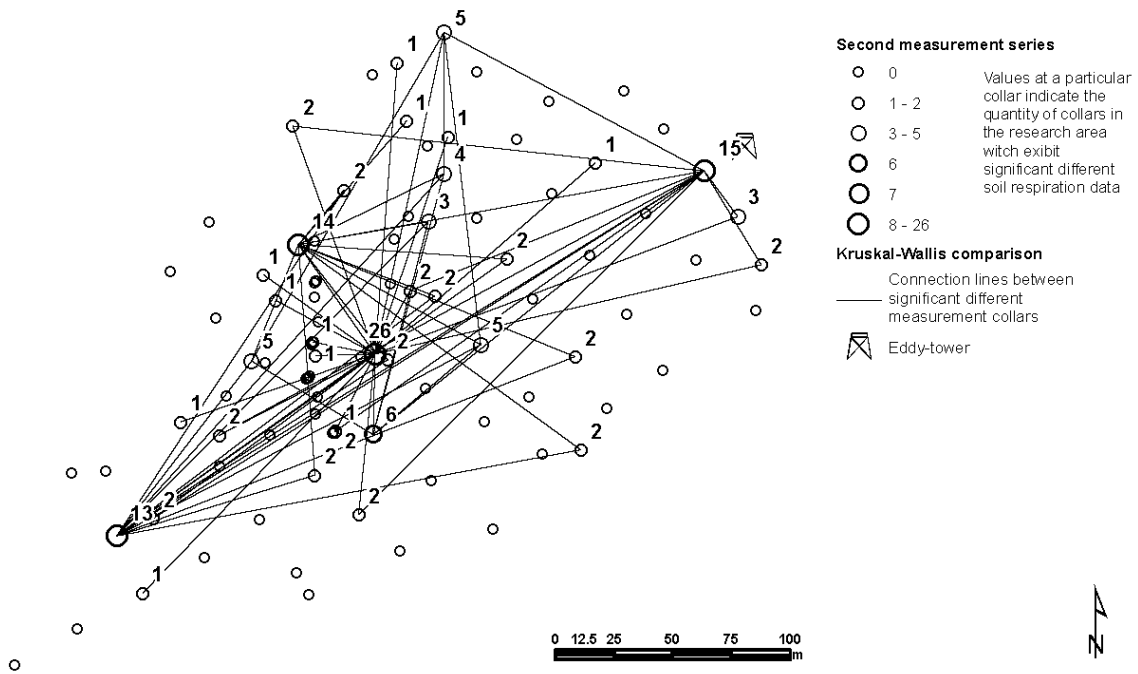


Fig. 3.14 Spatial heterogeneity of SR: The size of each measurement location sign indicates how many other measurement locations in the research area exhibit significant different values. The lines show which pairs of measurement locations where compared observing significant different values.

Only two measurement locations have double digit values, one in the centre of the eastern nest (Nest 2) and the other at the northern border of the research area. The same analysis as for the soil respiration time series was performed for soil moisture and soil temperature datasets, but without any results of significant differences.

Within the randomized measurement series 73 pairs of significantly different combinations were found between 40 collars and visualised by connection lines (Fig. 3.14). The grade of abnormality represented by the number of significant differences compared to other measurement locations is very unevenly distributed; only four measurement locations have double digit values, three at the border of the research area, one in the centre. In contrast to the first measurement series, the soil moisture values of the second series exhibit 241 pairs of significant differences between the datasets. From 101 measurement points, 97 measurement locations have one or more contrasting partner within the study site. Analogous to the soil respiration measurement results, only four measurement locations have double digit values, the high values of 30, 39, 71 and 92 significant differences to other measurement locations indicate the huge abnormality of these datasets. But these measurement locations were not identical with the four outlying results of the soil respiration measurements. As well as noticed for the first measurement series, the soil temperature values do not show any significant spatial heterogeneity.

The spatial analysis of mean annual soil respiration rates illustrates the need for exclusion of outliers in preparation for the regionalisation process. Soil temperature values do not show any significant spatial heterogeneity. This analysis demonstrates the necessity of outlier exclusion in preparation of any regionalisation of soil respiration, because it proves that significant different soil respiration collars exist even within the small nests with a high measurement density.

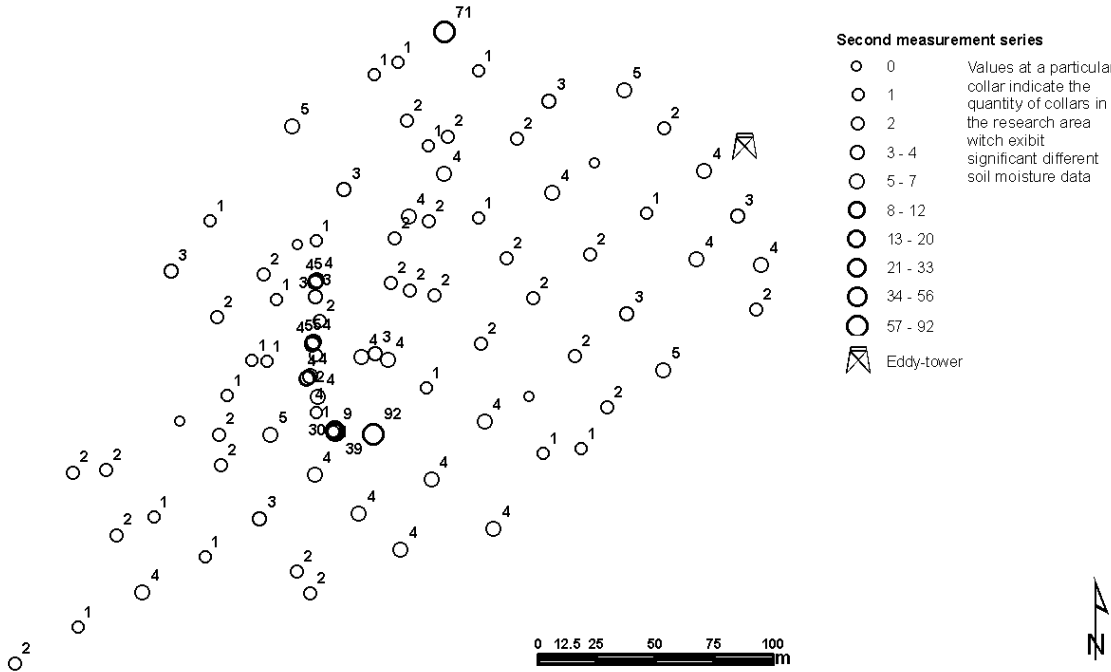


Fig. 3.15 Spatial heterogeneity of SM: The size of each measurement location sign indicates how many other measurement locations in the research area exhibit significant different values. The lines show which pairs of measurement locations where compared observing significant different values.

3.3.3 Number of measurement locations required

The outlier analysis has shown that there are few but highly significant outliers regarding annual soil respiration rates even within short distances. This illustrates the need to calculate the number of measurement points required for different levels of accuracy beforehand (Table 3.2)

Measurements from 6 ± 4 locations are necessary for a 80% confidence level with an error limit of 30% around the full population mean. Higher levels of precision require much more measurement locations. At a 95% confidence level, 16 ± 11 measurement locations are necessary for the same large error limit. Reducing this limit to 20% precision increases the required number of measurement locations up to 35 ± 26 , further precision can be achieved by using 140 ± 103 at an error limit of 10%. Data from frost periods were excluded because on the

one hand soil respiration fluxes were small and hence even small changes cause high standard deviations, on the other hand the poor fitting of the metal collar of the soil respiration chamber within the icy and sometimes deformed soil respiration measurement collar could have caused measurement errors during a high quantity of measurements. For the estimation of annual soil respiration rates these errors are of less importance because the observed fluxes are very small.

Table 3.2 Required number of soil respiration measurement points to achieve a precision of ± 10 , ± 20 , or $\pm 30\%$ around full population mean at various confidence levels (80-99%)

Interval [%]	99%	95%	90%	80%
± 10	288 \pm 213	140 \pm 103	92 \pm 68	52 \pm 39
± 20	72 \pm 53	35 \pm 26	23 \pm 17	13 \pm 10
± 30	32 \pm 24	16 \pm 11	10 \pm 8	6 \pm 4

3.3.4 Kriging preparation

Data point density was varied to optimize the kriging parameters (Fig. 3.16). This was done on subsets of the data centered around the nested cells (Fig. 2.5). That allowed testing a large range of different densities. Whereas the calculated average soil respiration rates around one of the grid cells changed little when altering sampling densities by subsampling from the available data, soil respiration rates decreased significantly with higher sampling densities. Both cells are characterized by artificial block structures at low and medium sampling point densities, indicating a distance between the sampling points wider than the range of the semivariograms. Much of the block structures can be smoothed by using a coarser scale for soil respiration, but not all.

3.3.5 Semivariograms

The adequate sampling point density used for kriging procedures depends primarily on the overall autocorrelation structure of the measured soil respiration data. Calculation of semivariograms revealed extremely heterogeneous autocorrelation ranges. First, semivariances were calculated with a lag distance of 10m using all distances. Analysis of the graphic representations of the calculated semivariances revealed flat lines which indicate a lack of spatial autocorrelation (Fig. 3.17a,b).

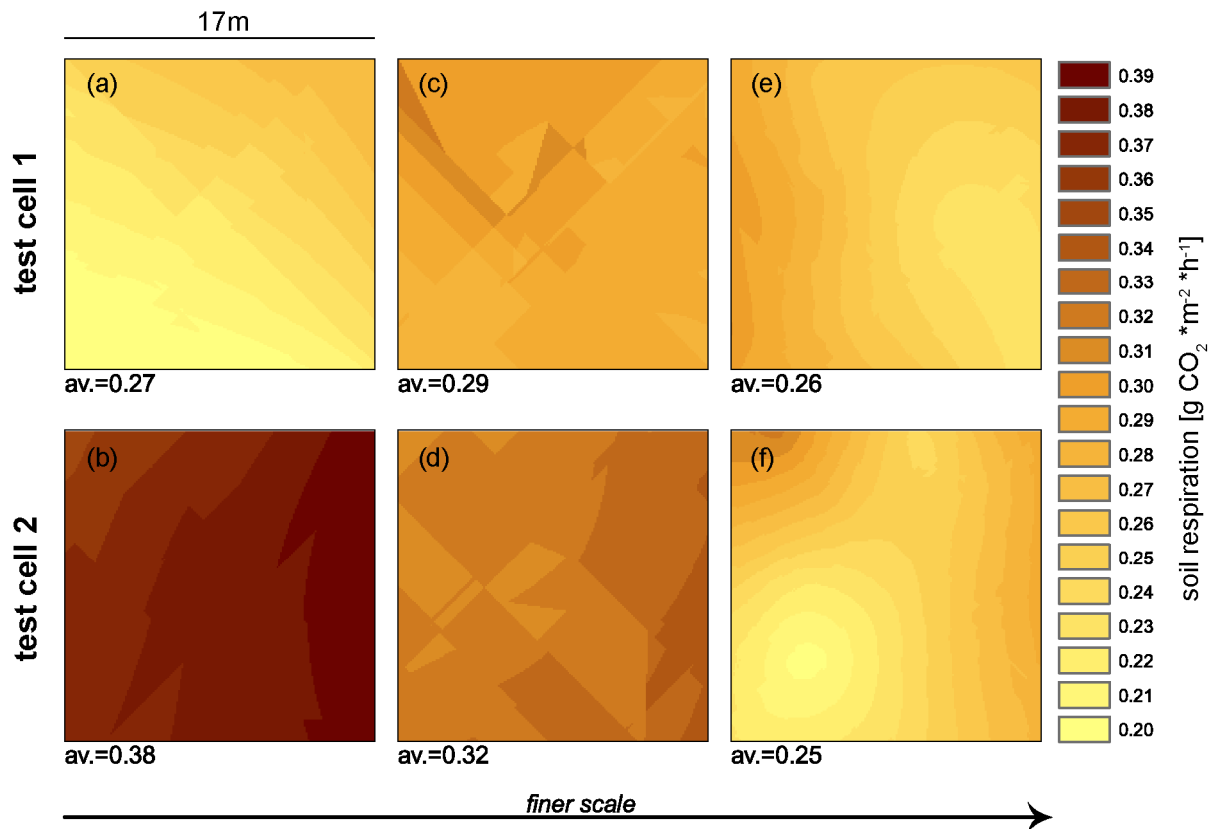


Fig. 3.16 Comparison of the soil respiration interpolation based on three different sampling densities within two test cells (see methods section for details). The resulting average soil respiration values are given below the panels. Units are $\text{g CO}_2 \text{ m}^{-2} \text{ h}^{-1}$. Fig. a & b are kriging results using only data from the stratified random distributed measurement locations, Fig. c & d represent results using the stratified random measurement locations and data from the large nests, and Fig. e & f are supplemented with data from the small nests

Zooming in the semivariograms by choosing smaller lag sizes and marginal shorter maximum distances (Fig. 3.17c,d) whilst reducing the dataset by eliminating outliers defined as bigger as ± 1.5 respectively ± 2.0 standard deviations, results in small range autocorrelation. The elimination of outliers is very important for the calculation of semivariances because single hotspot soil respiration events can adulterate not only the semivariograms but also large areas within the interpolated maps especially when the sampling density is small even when the local hot spot measurement may be functionally justified.

Ranges vary considerably from date to date (see Fig. 13.1-3 in the appendix). However, the average range of autocorrelation was determined at 9m, using lag sizes of 2m. This lag size was used in all further steps of analysis

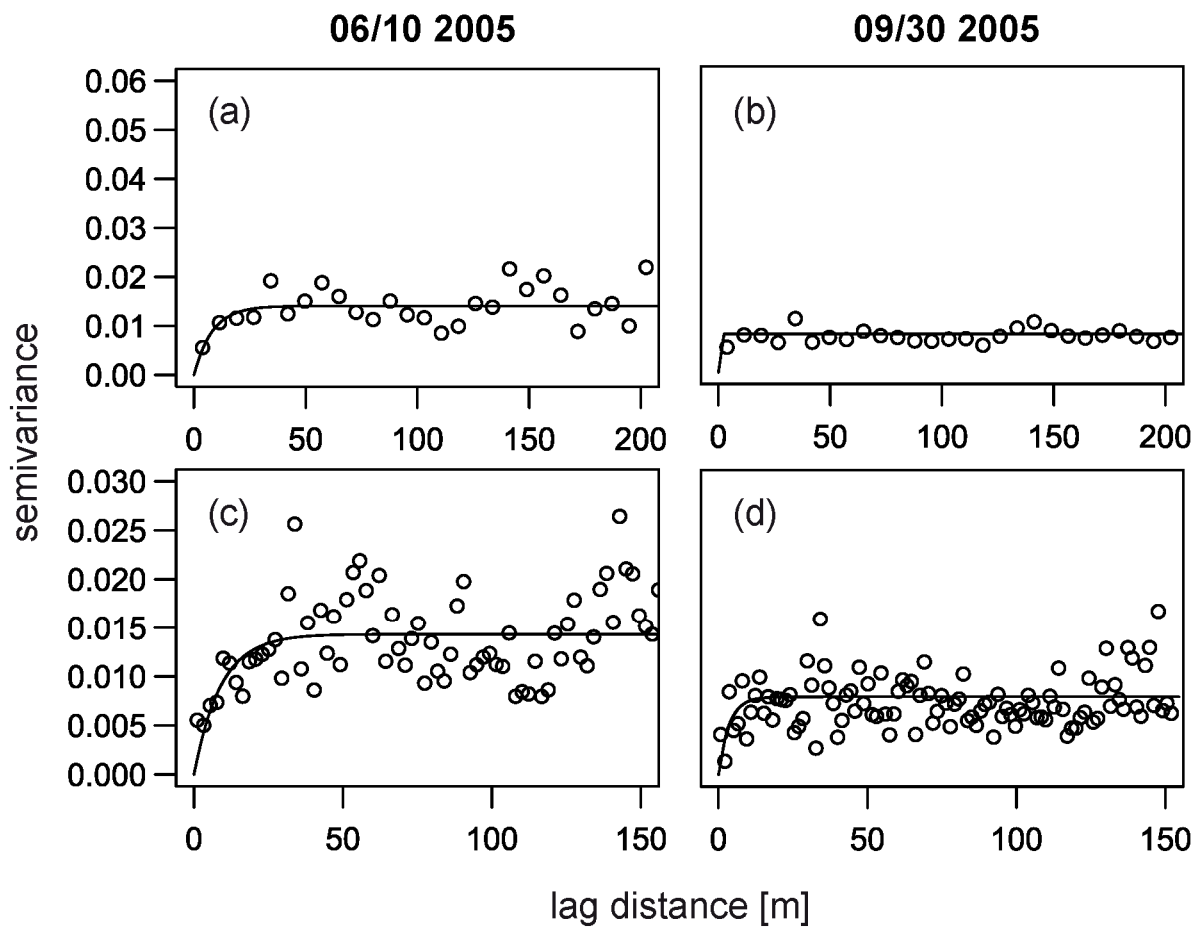


Fig. 3.17 Example semivariograms of soil respiration a, b): Bin width is 10m, all possible distances included. c, d): Bin width = 1.5m, only distances up to 150m included. Auto-correlation does only occur at very small distances between measurement locations.

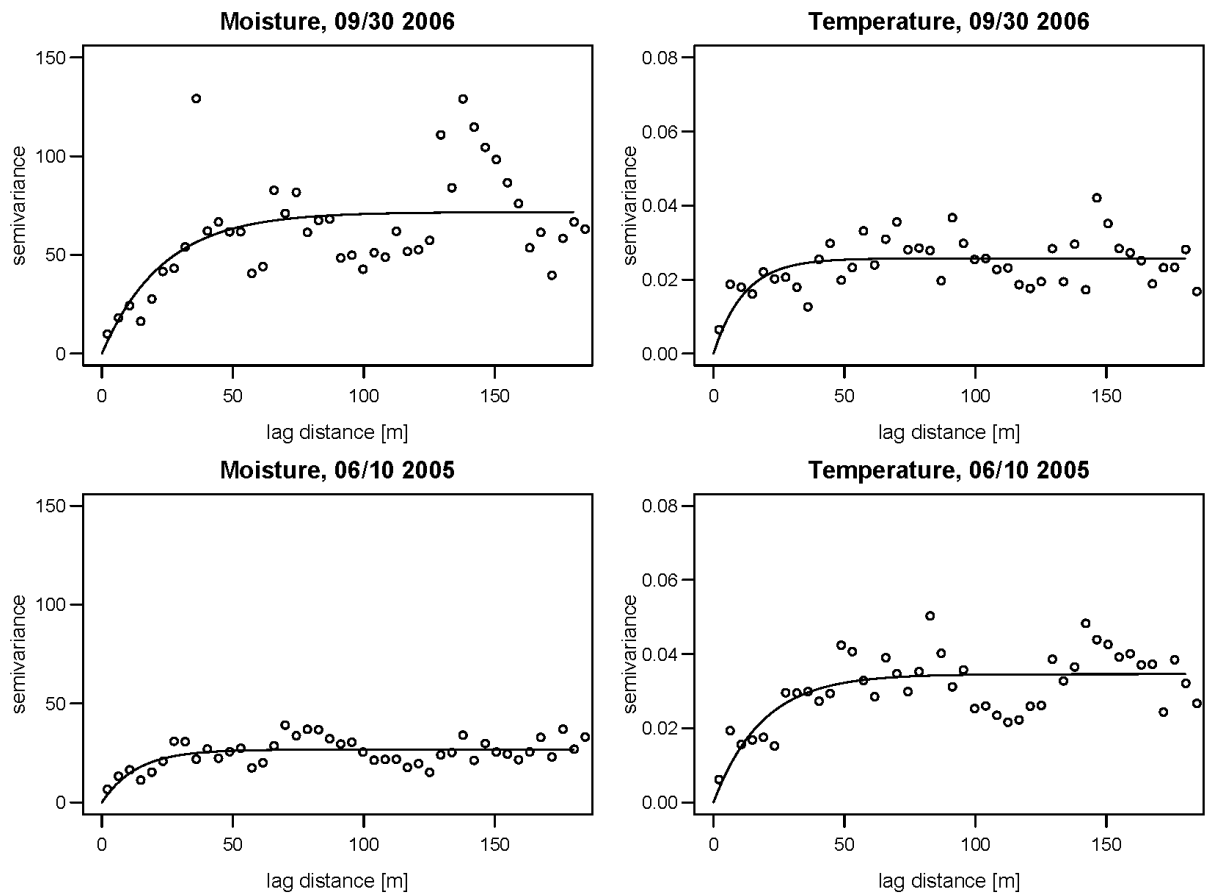


Fig. 3.18 Example semivariograms of soil moisture and soil temperature.

Fig. 3.19 Observed SR vs. predicted SR 2005

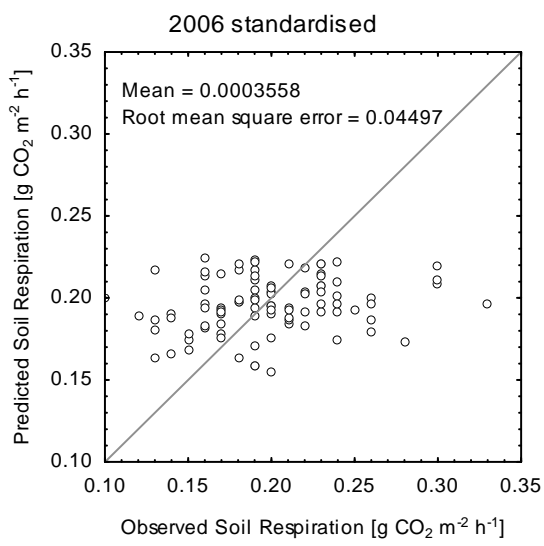
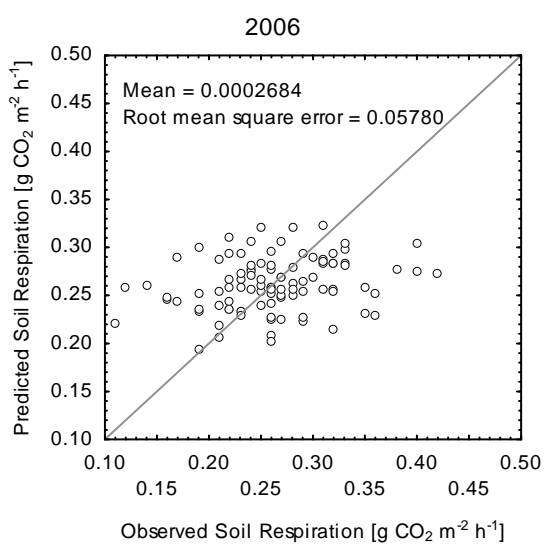
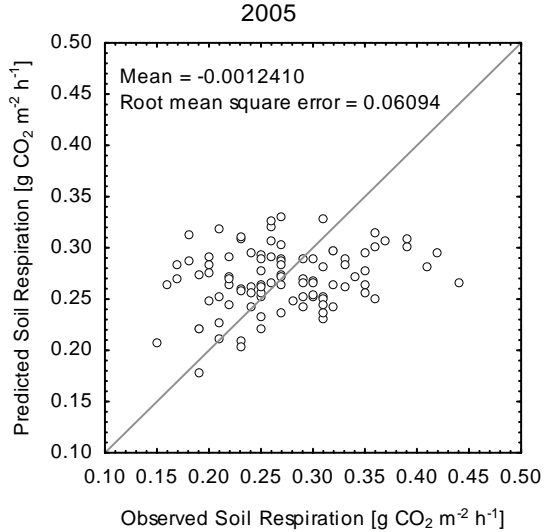


Fig. 3.20 Observed SR vs. predicted SR 2006

Fig. 3.21 Observed st.-SR vs. predicted SR 2006

3.3.6 Maps of soil respiration

Maps of soil respiration rates were extrapolated based on ordinary kriging using parameters of the beforehand calculated semivariograms. On the one hand data from the nested series were used (Fig. 3.22a). The resulting map exhibits a high level of uncertainty due to the short range of the calculated semivariogram (<20m) and the low sampling point density within the study site with distances between adjacent collars greater 25m (except within the observational cells). Even at class sizes of $0.03 \text{ g CO}_2 \cdot \text{m}^{-2} \cdot \text{h}^{-1}$ the map has many block structures (see also Fig. 3.16). The corresponding map of predicted standard errors shows concentric rings around single measurement collars with low standard error and great areas with high standard errors outside the range of the calculated semivariogram (Fig. 3.22b). Fig. 3.19 shows the scatterplot of the observed and the predicted values. The negative mean error indicates that the interpolated soil respiration data are slightly overestimated by the model.

On the other hand data from the random series was used for interpolation (Fig. 3.22c). It shows average soil respiration values between 0.16 to $0.37 \text{ g CO}_2 \cdot \text{m}^{-2} \cdot \text{h}^{-1}$ which are quite the same as for the first measurement series of 0.17 - $0.40 \text{ g CO}_2 \cdot \text{m}^{-2} \cdot \text{h}^{-1}$. Due to the higher measurement point density, the predicted standard error map is much smoother compared to results based on the nested series data (Fig. 3.22d).

3.3.7 Maps of soil respiration incorporating soil moisture and temperature

A further interpolation run is based on random series and standardized soil respiration rates (Figure 3.22e). To achieve standardized soil respiration rates average soil respiration was used with equation 5. For the 2006 series it amounts to $0.26 \text{ g CO}_2 \cdot \text{m}^{-2} \cdot \text{h}^{-1}$ and a typical soil temperature of 11.6°C . This is much higher than the total average soil temperature at the study site and caused by the exponential dependence between soil temperature and soil respiration. The corresponding soil moisture value was determined using the regression function between soil temperature and soil moisture (Fig. 3.7). Standardization causes the interval of soil respiration to shrink to 0.15 - $0.23 \text{ g CO}_2 \cdot \text{m}^{-2} \cdot \text{h}^{-1}$. The predicted standard error as well as the RMSE (0.04497) is smaller compared to the interpolation based on average soil respiration alone (Fig. 3.22f). Eliminating soil moisture and soil temperature reduces the variability of soil respiration. Comparing the maps of average soil respiration and standardized soil respiration reveals the influence of soil temperature and soil moisture. Whereas the soil temperature is mainly evenly distributed, the map predominantly shows the distribution of soil moisture deficits or excessive supply (Fig. 3.22e) which impedes soil respiration.

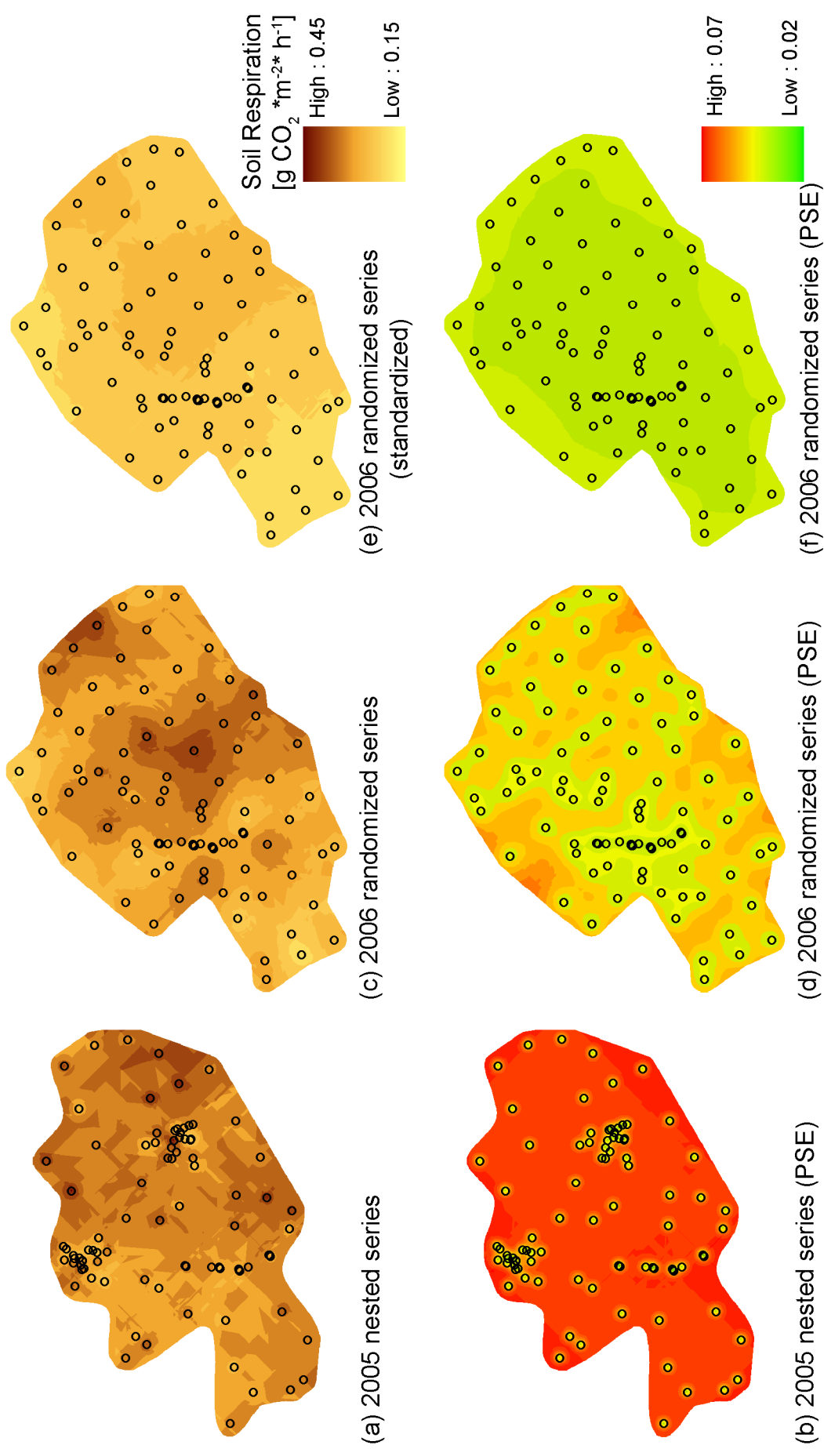


Fig. 3.22 Interpolated maps of soil respiration measurements of the nested series (a) exhibits a large predicted standard error -PSE (b), whereas the random distribution (c) shows a much smaller PSE (d). The most homogeneous result was achieved by standardizing the randomized soil respiration measurements of 2006 at 11.6°C soil temperature and correlative 35.2 % soil moisture (e) possessing little PSE (f). Units are $\text{g CO}_2 \cdot \text{m}^{-2} \cdot \text{h}^{-1}$

Table 3.3 Validation of ordinary kriging results

	Nested series	Random series	
	04/2005 - 04/2006	2006	2006 (standardised)
Mean	-0,0012410	0,0002684	0,0003558
Root-Mean-Square	0,06094	0,05780	0,04497
Average Standard-Error	0,05644	0,05180	0,04238
Mean Standardised	-0,002753	0,009261	0,01
Root Mean Square	1,107	1,114	1.0581
Standardised			

The annual flux calculated solely from 81 data points of the random series yielded a soil respiration rate of $2285.5 \text{ g CO}_2 \text{ m}^{-2} \text{ a}^{-1}$ ($\pm 480.2 \text{ g CO}_2 \text{ m}^{-2} \text{ a}^{-1}$) or $6.23 \text{ Mg C ha}^{-1} \text{ a}^{-1}$ ($\pm 1.31 \text{ Mg C ha}^{-1} \text{ a}^{-1}$) in 2006 and can be trusted at a confidence level of 90% within an error limit of 10% (or 99% confidence level at an error limit of 20%). Using the geostatistical approach accounting for the spatial distribution of the measurement locations yielded a soil respiration rate of $1875.5 \text{ g CO}_2 \text{ m}^{-2} \text{ a}^{-1}$ or $5.11 \text{ Mg C ha}^{-1} \text{ a}^{-1}$ in 2006.

4. Fine root biomass of trees as a predictor of root respiration

Whereas in the previous chapter I solely looked at total soil respiration, in the following part of this study I investigate the possibility to distinguish between the different parts of soil respiration and to use fine root biomass as a predictor of soil respiration. Therefore, total soil respiration rates were related to calculated relative fine root biomass derived from stand structure parameters, like location, breast height diameter (at 1.3m dbh) and tree type.

In early studies scientists presumed that fine roots are more or less homogenously distributed in the upper soil (Fogel 1985). Recent advances in determining fine root distribution patterns revealed that fine roots were concentrated in definite soil patches (Caldwell et al. 1996; Stoyan et al. 2000; Hölscher et al. 2002; Pellerin, Pages 1996; Ryel et al. 1996). Thereby Fleischer et al. (2006) assume that in horizontal direction roots follow the unevenly distributed soil resources (Fleischer et al. 2006). In vertical direction, fine root biomass is largest in the upper mineral layer close to the soil surface (Maier, Kress 2000), except in the organic layer (Widen, Majdi 2001). Globally, over 60% of the root biomass is found in the top 20 cm of the soil. It decreases logarithmically with depth and only 14% is found below 40cm. In contradiction, the vertical distribution of soil carbon is much smoother. Only 40% is located in the upper 20 cm and 36% is still found below 40 cm soil depth (Gleixner et al. 2009).

These findings show that knowledge on the fine root distribution in the soil should improve estimates of root and soil CO₂ efflux. In 2005, Ammer and Wagner presented a model for predicting fine root distribution patterns within a spruce forest using easy-to-measure data, despite possible limitations of uneven root distribution patterns. They assumed a proportional decrease of fine root biomass with tree diameter and an additive contribution of fine-root biomass by the surrounding trees for any given point within the forest stand (Ammer, Wagner 2005). If extended to other important tree species, validated and coupled to extensive soil CO₂ efflux measurements, the approach of Ammer and Wagner could be a valuable tool for an improved regionalisation of soil respiration.

The possibility to perform a regression kriging procedure using calculated potential fine root biomass rates for the entire study area and total soil respiration data was examined. Influences of seasonal dynamics of root growth and mortality on the quality of the regression kriging result were considered. All analyses are based on the random soil respiration series.

4.1 Materials and methods

4.1.1 Surveying and mapping of trees

The area of surveying and mapping of trees extended the calculated borders of the catchments area a little up to a size of 6ha. The precise xyz-location of each single tree and soil respiration plot were determined using a total station of Leica Geosystems (TPS1200, Munich, Germany). Therefore the geographic orientation was ascertained using several topographic reference points located next to the Hainich study site (Thuringian State Office for Survey and Geoinformation 2005). The breast height diameters of single trees with a diameter of >1cm were measured using a calliper. Additionally, tree species and the vitality of each tree (dead or alive) were recorded. Distances between each soil respiration plot and adjacent trees up to 40m were calculated using an extension for ArcGIS 9.2 (ESRI, Redlands, USA) called “Hawth’s Analysis Tool” (<http://www.spatialecology.com>) and plotted as a matrix in an Excel-file (Microsoft Excel 2003, Microsoft Corporation, Washington, USA). Distance values from the matrix were arranged at single sheets for each soil respiration measurement location.

4.1.2 Calculating point specific potential relative fine root biomass

Several approaches for modelling fine-root biomass at a given point from aboveground stand characteristics have been published in the last years (Nielsen, Mackenthun 1991; Ammer, Wagner 2002, Ammer, Wagner 2005). This study is based on an adapted numerical model which is derived by a proposal of Ammer & Wagner (2005), who calculated the potential fine root distribution within a spruce forest. The following assumptions where the model is based on were directly derived from Ammer & Wagner (2005):

1. “The maximum distance from the tree trunk where roots of a subject tree can be found depends on the dimension of the tree and exceeds the edges of the crown by a significant distance [...]
2. Fine-root biomass decreases with increasing distance from the tree trunk [...]
3. Fine-root biomass increases with the diameter at breast height (diameter at a height of 1.3m, dbh) of the tree [...].
4. The maximum fine-root biomass of a tree is not allocated directly around tree’s trunk but at some distance from the stem [...]” (Ammer, Wagner 2005)

Ammer and Wagner (2005) compared several slightly different models. For this study a tree specific adaptation of their basic approach was used, simply summarizing predicted fine root biomass values of different trees at any given point within the site. Ammer and Wagner did

not achieve any improvements in modelling fine root biomass following the assumption that the contribution of fine root biomass of a subject tree to a given point may decrease with the presence of other trees standing closer to the point of interest. In contrary, increasing the number of modelling parameters slightly decreased the quality of their modelled results.

All the above mentioned assumptions were transformed into a model. The following algorithms and parameters were formulated for spruce by Ammer and Wagner (2005).

For example, they assumed a maximum root-spread distance of 10m for a tree of 60 cm breast-height ($RD_3 = dbh/6$), RD_3 marks the maximum distance in meters, RD_2 and RD_1 are two-thirds and one-third, respectively, of this distance and RD_0 marks the trunk. The relative fine-root biomass at distance RD_0 (trunk) is $rFRB_0 = dbh/100$, $rFRB_1 = 5/3 rFRB_0$, $rFRB_2 = 5/6 rFRB_0$ and $rFRB_3 = 0$, where $rFRB_1$, $rFRB_2$ and $rFRB_3$ are the relative fine-root biomasses at distances RD_1 , RD_2 and RD_3 , respectively.

Based on these parameters for the distances RD_0 to RD_3 a third degree polynomial for the breast height diameter of each tree was calculated. This allowed the calculation of the rFRB of each tree of the stand at any soil respiration plot. The following formulas presented by Ammer & Wagner (2005) were used:

1. If $D \geq RD_3$, $rFRB=0$, where D is the distance between the tree's trunk and x,y
2. If $D < RD_3$, $rFRB$ of a tree at point x,y is calculated as follows:

$$h = RD_2 - RD_1 \quad (2)$$

$$b_0 = rFRB_0 \quad (3)$$

$$b_1 = \frac{(rFRB_1 - rFRB_0)}{1!h} \quad (4)$$

$$b_2 = \frac{((rFRB_2 - rFRB_1) - (rFRB_1 - rFRB_0))}{2!h^2} \quad (5)$$

$$b_3 = \frac{((rFRB_3 - rFRB_2) - (rFRB_2 - rFRB_1)) - ((rFRB_2 - rFRB_1) - (rFRB_1 - rFRB_0))}{3!h^3} \quad (6)$$

$$\begin{aligned} rFRB_{x,y} = b_0 + b_1(D - RD_0) + b_2(D - RD_0)(D - RD_1) \\ + b_3(D - RD_0)(D - RD_1)(D - RD_2) \end{aligned} \quad (7)$$

The relative fine root biomass of all trees contributing roots to a single soil respiration measurement location was calculated as:

$$TrFRB_{x,y} = \sum_{i=1}^n rFRB_i, \quad (8)$$

where i is the tree number of the stand. It is assumed that the total amount of fine roots at a specific soil respiration measurement location results from additive contribution of the trees,

neglecting possible competition effects between the root plates of different trees (Ammer, Wagner 2005).

The above described model was developed to predict fine root distribution patterns of spruce which usually has a shallow root system (Nielsen, Mackenthun 1991). To use this approach for other tree species requires accounting for possible differences between their genetically determined root architecture. In recent years, modelling tree root biomass has gained wide acceptance, various authors used estimated relationships between breast height diameter of tree stems and root biomass (Drexhage, Colin 2001; Le Goff, Ottorini 2001; Lee 2001; Bolte et al. 2004; Wang 2006; Tatarinov et al. 2008). Recent studies of modelling fine-root biomass at a given point from aboveground stand characteristics are rare and I am aware that attempts to model fine root distribution patterns within a broad-leaved deciduous forest stand with high tree species diversity and an uneven age class composition are difficult. Nevertheless, I do not attempt to predict absolute fine root biomass values; I am only interested in spatial patterns of fine root biomass abundance and its relation to total soil respiration. Due to the absence of existing comparative fine root biomass models relating fine root distribution to breast height diameter for different tree species, I estimated adapted tree species steering parameters for the above described model from verbal descriptions of their rooting architectures derived from a literature survey (Table 4.1):

Starting with the given parameters provided for *Picea abies* L. (Ammer, Wagner 2005; Nielsen, Mackenthun 1991), these adaptions were only made for the most frequent tree species *Fagus sylvatica* L. and *Fraxinus excelsior* L. at the study site. In contrast to spruce, beech has a heart-shaped root system (Curt, Prevosto 2003b, Curt, Prevosto 2003a; Rust, Savill 2000). Both species obtain a clustered root system, whereas spruce has a stronger clustering in smaller cluster regions, while roots of beech formed weaker clusters in larger cluster regions (Fleischer et al. 2006). Beech has a much higher root penetration intensity compared to spruce (Nielsen, Mackenthun 1991) especially near to the tree trunk. Nielsen and Mackenthun (1991) compared the estimated root penetration intensity of spruce and beech depending of the tree distance. Steering parameters of the model were adapted to get a comparable curve fitting as provided by Nielsen and Mackenthun (1991) (Figure 4.1). Beeches occupy a hemispherical volume under the base of each tree which is extremely intensively rooted (Rust, Savill 2000). Ash roots are more superficial than beech roots. As seen in mixed stands between spruce and beech (Bolte et al. 2004), root systems are separated into depth zones. Their main direction of root growth is horizontal where beech trees tend to growth downwards at an angle of 45°. Ashes have longer maximum root length compared to

beech trees. Their tough roots are oriented horizontally sending laterals vertically downwards. These roots are concentrated in clumps and between them root free zones can be found. The ash superficial root system is very intensive but compared to beech trees which uses much more efficient deeper soil layers; it is extensive (Rust, Savill 2000). While estimating the steering model parameters for ash trees, the higher maximum root length and the more evenly superficial distribution were considered.

The other tree species (*Acer pseudoplatanus* L., *Carpinus betulus* L., *Quercus petraea* L. *Acer campestre* L.) only sparsely occur at the study site. Therefore the parameters fitted for *Fagus sylvatica* L. were used to account solely for the existence of these few trees. None of the soil respiration measurement locations were significantly influenced by this species.

Table 4.1 Definition of tree type specific parameters for the calculation of relative fine root biomass. RD₃ defines the maximum extent of fine roots from the tree trunk, rFRB₀ describes the fine root biomass at the tree trunk, rFRB₁ represents the potential fine root biomass at one third of the maximum extent, rFRB₂ at two third of the maximum extent. Parameters are adapted for beech and ash (black). The other tree species (hornbeam, wych elm and sycamore maple) only sparsely occur at the study site (grey). Therefore, parameters fitted for spruce were used to account solely for the existence of these few trees. None of the soil respiration measurement locations were significantly influenced by this species.

Tree type	RD ₃	rFRB ₀	rFRB ₁	rFRB ₂
<i>spruce</i>	dbh/6	dbh/100	dbh/1.67	dbh/0.83
<i>beech</i>	dbh/6	dbh/40	dbh/0.80	dbh/0.43
<i>ash</i>	dbh/3	dbh/40	dbh/1.67	dbh/0.63
<i>hornbeam</i>	dbh/6	dbh/100	dbh/1.67	dbh/0.83
<i>wych elm</i>	dbh/6	dbh/100	dbh/1.67	dbh/0.83
<i>sycamore maple</i>	dbh/6	dbh/100	dbh/1.67	dbh/0.83

4.1.3 Calculating area-wide potential relative fine root biomass

The point-wise calculation of the potential fine root biomass by oneself is not capable to serve as a proxy for the interpolation of soil respiration data. Area-wide information is necessary to account for breaks and small scale variations, caused by differences in root distributions. Therefore, the above described model was implemented within a Java-application to calculate the potential relative fine root biomass area-wide for the entire study site. As a result, tree type specific text files as well as a summary file representing the total amount of fine roots were created. These files contained the number of columns and rows, the starting xy-

coordinate, the cell size of 10cm x 10cm and a matrix of calculated fine root biomass values of the centre coordinates of each cell of the study site. The text files were imported in an ArcGIS environment (ArcGIS 9.2, ESRI, Redlands, USA) as a grid file. The rectangular extent of the surveying and mapping area of the trees expanded by a margin which represented the maximum extent of the calculated root length for the largest trees defined the size of the thereby created maps. In contrast to the above described model, the Java-application did not calculate the distances between the soil respiration plots and the trees, but calculated the euclidean distance between each raster cell to the trees. If a cell was located within the estimated root plate of a tree the above described model was applied. If several root plates interfered with each other, single values were summarized, neglecting possible concurrence effects between tree roots.

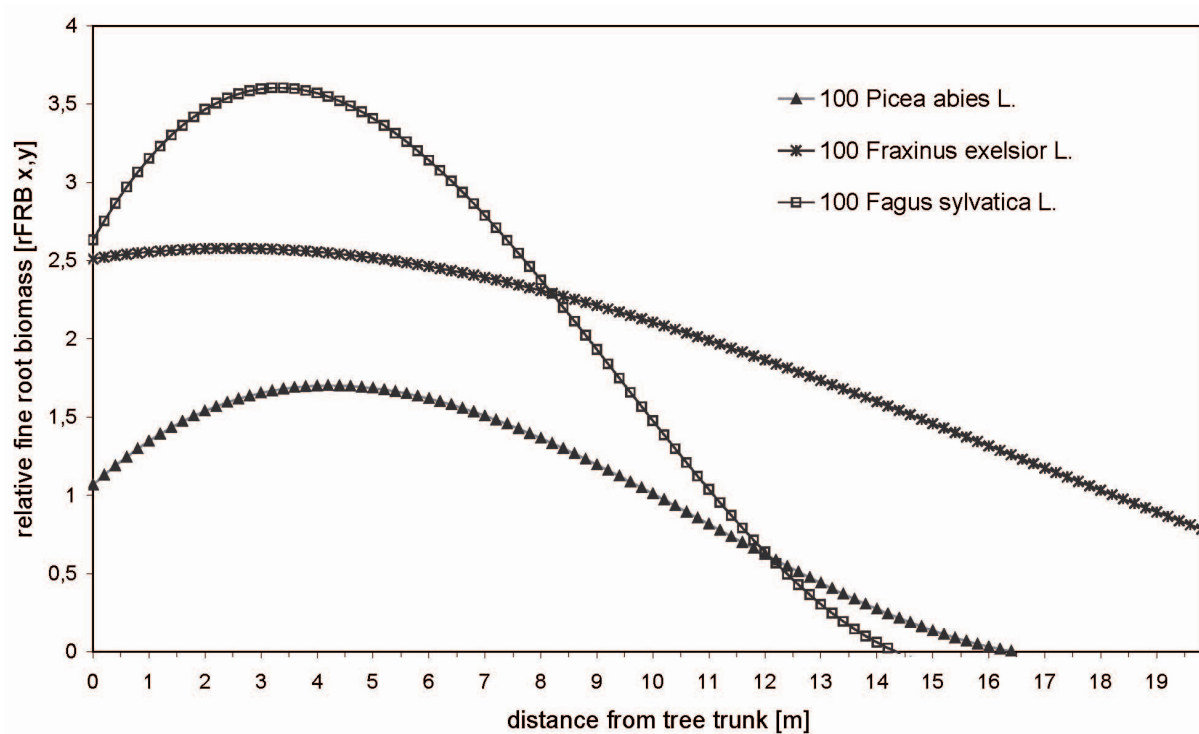


Fig. 4.1 Relative fine root biomass (rFRB) of different tree species in relation to the distance from the stem trunk and the diameter at breast height (dbh) as assumed by the model

4.1.4 Model validation

For the validation of the adapted model, fine root biomass data as well as tree parameters were used from a comparable study site 4km east of my stand (Meinen 2008). Both stands are temperate beech dominated deciduous forests with comparable species composition, age

distribution, soil type, soil texture and climatic conditions (Meinen 2008). Model validation was carried out by comparing the fine root biomass of 24 soil cores with the predicted values calculated for the core locations. The soil samples had been excavated in 2005 and 2006 from randomly selected locations along three transects of 30 m (8 per transect) within a plot of 50 m x 50 m (Meinen et al. 2009). Soil samples had been taken down to 40 cm soil depth with a soil corer of 3.5 cm in diameter (Meinen et al. 2009).

4.1.5 Statistical analysis & Regression kriging

Using calculated relative fine root biomass as a proxy for the interpolation of soil respiration data clearly presumed the documented evidence of correlation between these parameters. Therefore due to the absence of Gaussian distribution (tested with the Kolmogoroff-Smirnoff testing algorithm), non-parametric testing procedures were used for the analysis. Correlations were calculated with the Spearman's rho test using STATISTICA 7.0 (Statsoft, Oklahoma, USA).

The area-wide calculated maps provided the opportunity to perform regression kriging procedures, wherever a correlation between soil respiration data and calculated potential relative fine root biomass was proved. Odeh et al. (1995) described several procedures, which had been developed for regionalisation of soil parameters using digital elevation models. Performing regression kriging required three steps (Figure 4.2): First, the regression model determined via the correlation between potential relative fine root biomass with soil respiration efflux data was used to predict area-wide soil respiration. Therefore the calculated potential fine root biomass was multiplied using the ArcGIS RasterCalculator with the regression model (ArcGIS 9.2, ESRI, Redlands, USA). Simultaneously, an ordinary kriging was performed with the regression residuals. Finally the results were summarized (Odeh et al. 1995).

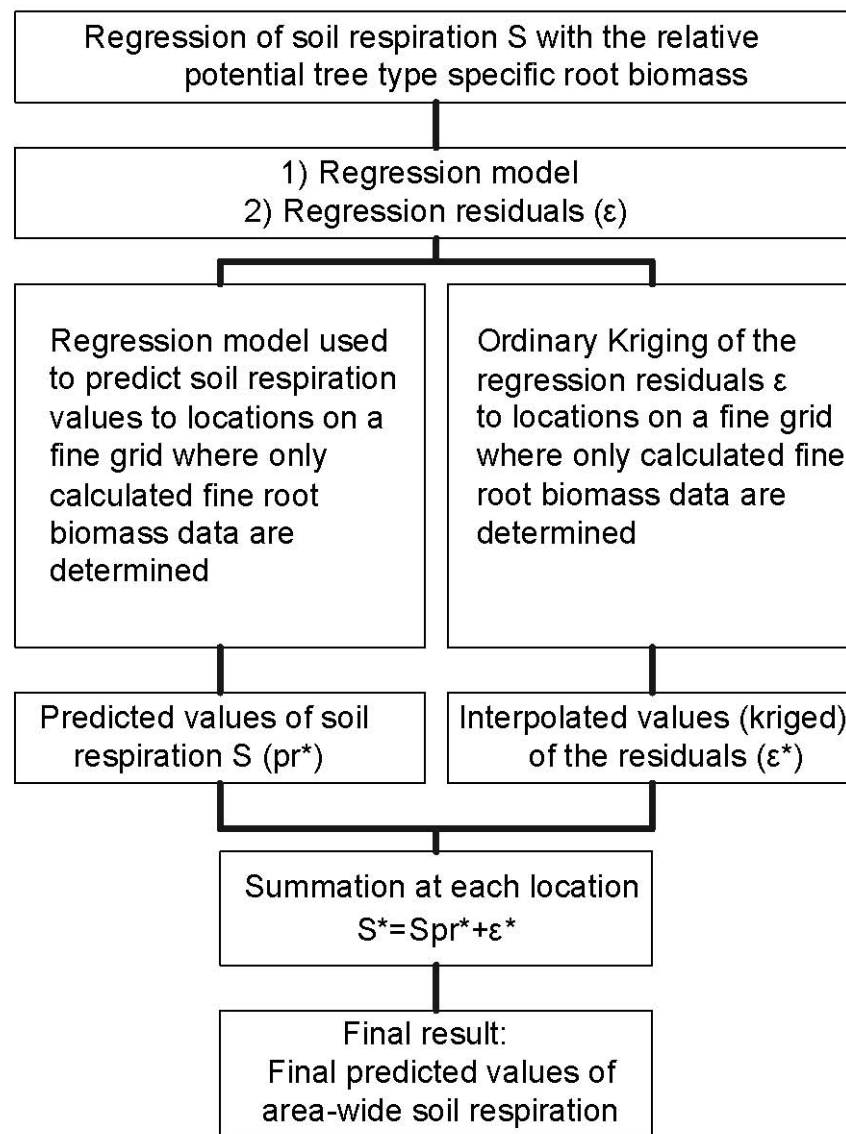


Fig. 4.2 The adapted regression-kriging-Model C of Odeh et al. 1995

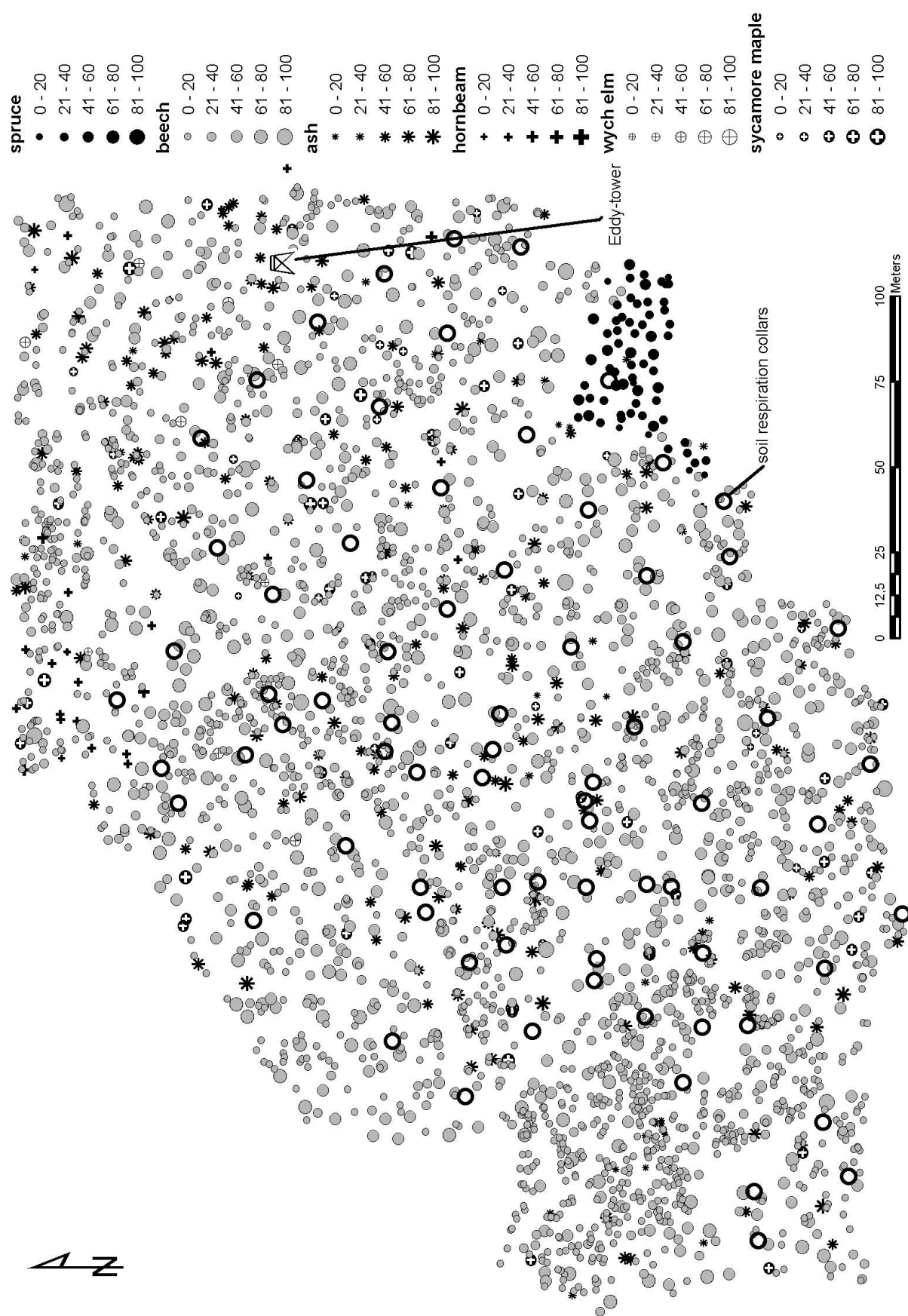


Fig. 4.3 Location, tree species and breast height diameter of all trees at the study site

4.2 Results

4.2.1 Validation results

Calculating regression equations between predicted fine root biomass and excavated fine roots revealed a significant correlation between weighted and predicted beech roots ($r^2=0.72$, $p<0.01$). Correlation between calculated fine root biomass of ash and excavated as roots were also significant ($r^2=0.60$, $p<0.01$)(Table 4.2).

Table 4.2 Results of model validation for beech and ash: Correlation between predicted fine root biomass of 24 soil cores and the weight of excavated fine roots.

	r	r^2	p
Beech	0.85	0.72	$p<0.01$
ash	0.78	0.60	$p<0.01$

4.2.2 Stand structure parameters

Within the extended research area of about 6ha, 3478 trees were surveyed and mapped (Figure 4.3). The study site is dominated (87 %) by European beech (*Fagus sylvatica* L.) followed by ash (7 %) (*Fraxinus excelsior* L.) and 2 % of maple (*Acer pseudoplatanus* L. and *Acer platanoides* L.) with minor abundance of European hornbeam (*Carpinus betulus* L.) and elm (*Ulmus glabra* Huds.). The age-class composition is diverse (Figure 4.4), but there is an unevenly distributed pattern of small areas with a high density of rejuvenating beech. Tree density is 489 stems ha^{-1} and the maximum breast height diameter is 92cm.

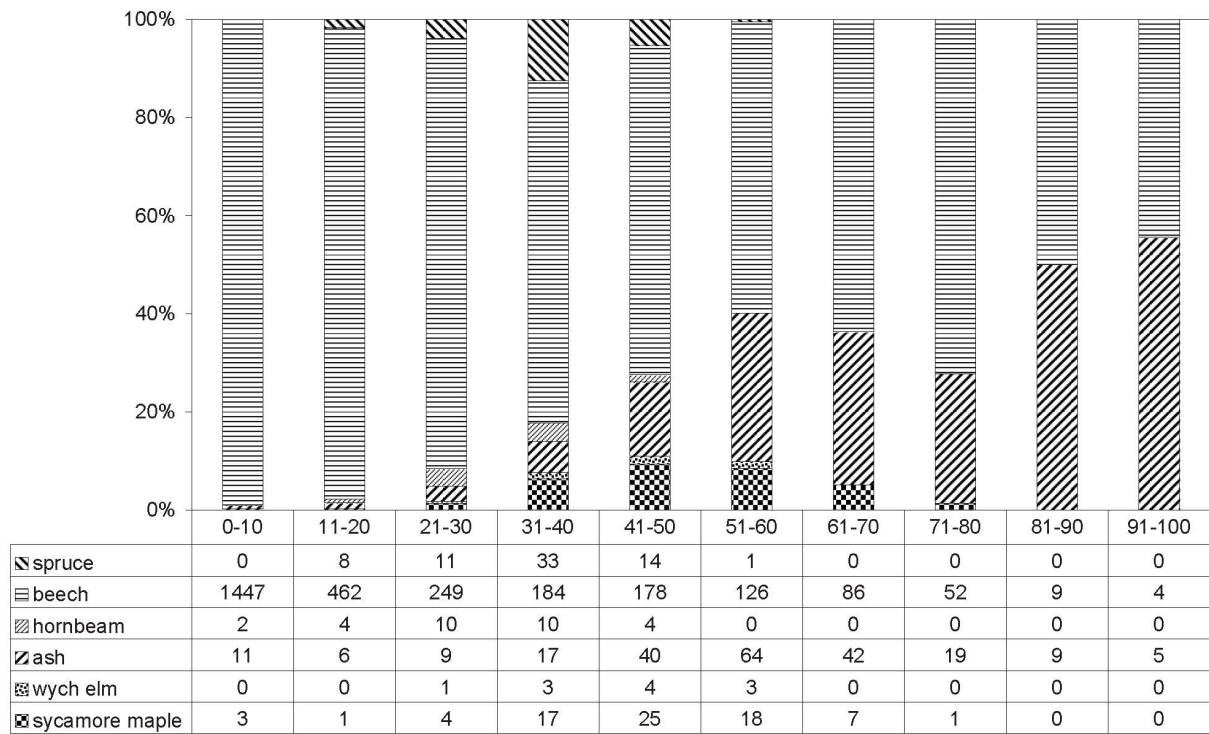


Fig. 4.4 Tree species diversity of the Hainich study site, sorted by breast height diameter

4.2.3 Calculated point specific potential fine root biomass

Compared to the dominant percentage rate of European beech (*Fagus sylvatica* L.) of 87 % of all trees, the calculated quantity of beech roots (at average 47.9%) is much lower, because of the huge amount of rejuvenating beeches. The two main tree species European beech and ash dominate the root distribution at the soil respiration measurement locations, the small root fractions of other tree species were negligible (Table 4.3). Whereas total fine root biomass map exhibited only a few areas without roots, looking solely at the distribution of beech roots features some small areas with no beech roots or only a minor presence. Although the absolute rate of ash was about 7%, their roots occurred in more than two-thirds of the study area, because of the prevalence of large trees. Maples featured 3.1 % of total fine root biomass at the soil respiration measurement locations, altogether their absolute fraction of two percent were of minor importance within the research area.

Table 4.3 Average calculated relative fine root biomass [percent of total] at soil respiration measurement locations, describing the absolute dominance of beech and ash roots at the study site. Parameters are adapted for beech and ash (black). The other tree species (hornbeam, wych elm and sycamore maple) only sparsely occur at the study site (grey). Therefore, parameters fitted for spruce were used to account solely for the existence of these few trees. None of the soil respiration measurement locations were significantly influenced by this species.

Tree type	average	min	max
<i>spruce</i>	1.1	0.0	99.7
<i>beech</i>	47.9	0.0	100
<i>ash</i>	47.4	0.0	100
<i>hornbeam</i>	0.0	0.0	0.9
<i>wych elm</i>	0.0	0.0	0.0
<i>sycamore maple</i>	3.1	0.0	100

4.2.4 Correlations between potential fine root biomass and soil respiration at different seasons

Correlations between the calculated total relative fine root biomass and total soil respiration did not exist. Performing regression analysis between beech dominated calculated fine root biomass and annual as well as monthly soil respiration rates yielded negative results as well. Only 16 ash dominated soil respiration measurement locations (>80% calculated fine roots of ash) exhibited a significant correlation between potential relative fine roots of ash and averaged monthly total soil respiration values during the summer of 2006. In June 2006, an average correlation of $r^2=0.46$ ($p<0.01$) was observed (Figure 4.5d), followed by a weak correlation in July ($r^2=0.21$, $p=0.07$) (Figure 4.5e). The best strongly significant fit was found for August 2006 ($r^2=0.50$, $p<0.01$) (Figure 4.5f), followed by an average correlation in September 2006 ($r^2=0.40$, $p<0.01$) (Figure 4.5g). Measurements in August or September 2005, May 2006, or spring 2007 did not reveal any significant correlation between soil respiration and relative fine root biomass of ash roots. Nevertheless, the summertime correlation results allow using the calculated relative fine root biomass of ash as a proxy for further regression kriging using total soil respiration measurement data of June, August and September 2006.

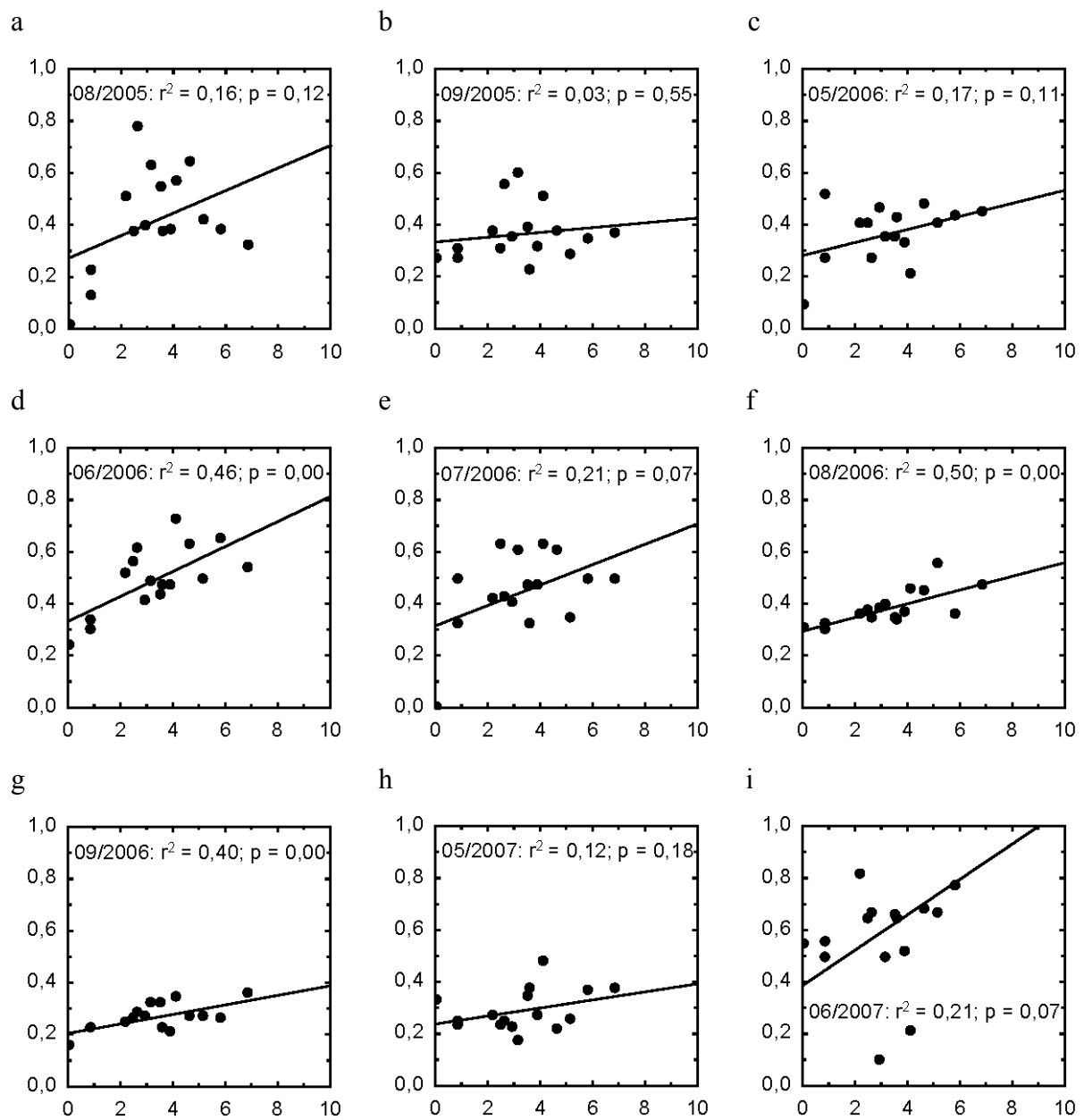


Fig. 4.5 Correlation between total soil respiration and calculated relative fine root biomass at ash dominated stands during the vegetation period of 2005 (a,b), 2006 (c-g) and 2007 (h,i).
(y-axis: soil respiration [g CO₂ m⁻² h⁻¹], x-axis: relative fine root biomass [rFRB])

4.2.5 Maps of seasonal ash root respiration

Due to the absence of a significant correlation between total soil respiration and total calculated relative fine root biomass, regression kriging was only performed using calculated relative fine root biomass of ash dominated soil respiration measurement locations (Fig. 4.6). Regression kriging was conducted using soil respiration data from June, August and September 2006. Regression analyses were performed for these three months to obtain the required regression equations as well as the associated residuals (table 4.4). The regression model was used to predict soil respiration values to locations on a fine grid where only calculated fine roots of ash biomass data were determined. An ordinary kriging procedure of the regression residuals was executed. Both results were summarized to the final maps (Figure 4.7a-c), which give an impression of total soil respiration distribution patterns at locations which are within the growing range of ash roots.

Table 4.4 Regression equations and residuals between total soil respiration and fine roots of ash from June, August and September 2006

Nr.	June 2006 $y = 0.3317 + 0.048*x$	August 2006 $y = 0.294 + 0.0264*x$	September 2006 $y = 0.2045 + 0.0183*x$
	Residual	Residual	Residual
46	0.066880	0.033001	-0.018640
29	0.034841	-0.090799	-0.052616
14	-0.079089	0.002977	0.001065
96	-0.094389	0.012763	-0.045327
16	-0.050373	-0.033045	-0.066238
12	0.081573	0.006158	0.002276
51	-0.124907	-0.006383	0.027640
18	0.150624	-0.019142	0.030339
48	-0.069588	-0.043244	0.051694
44	-0.060734	0.010327	0.012737
52	0.110840	0.017011	0.009306
73	-0.036595	-0.022118	0.000789
75	-0.086855	0.118554	-0.027818
37	0.002376	0.016639	0.057944
78	0.191788	0.053532	0.065408
27	-0.036391	-0.056230	-0.048560

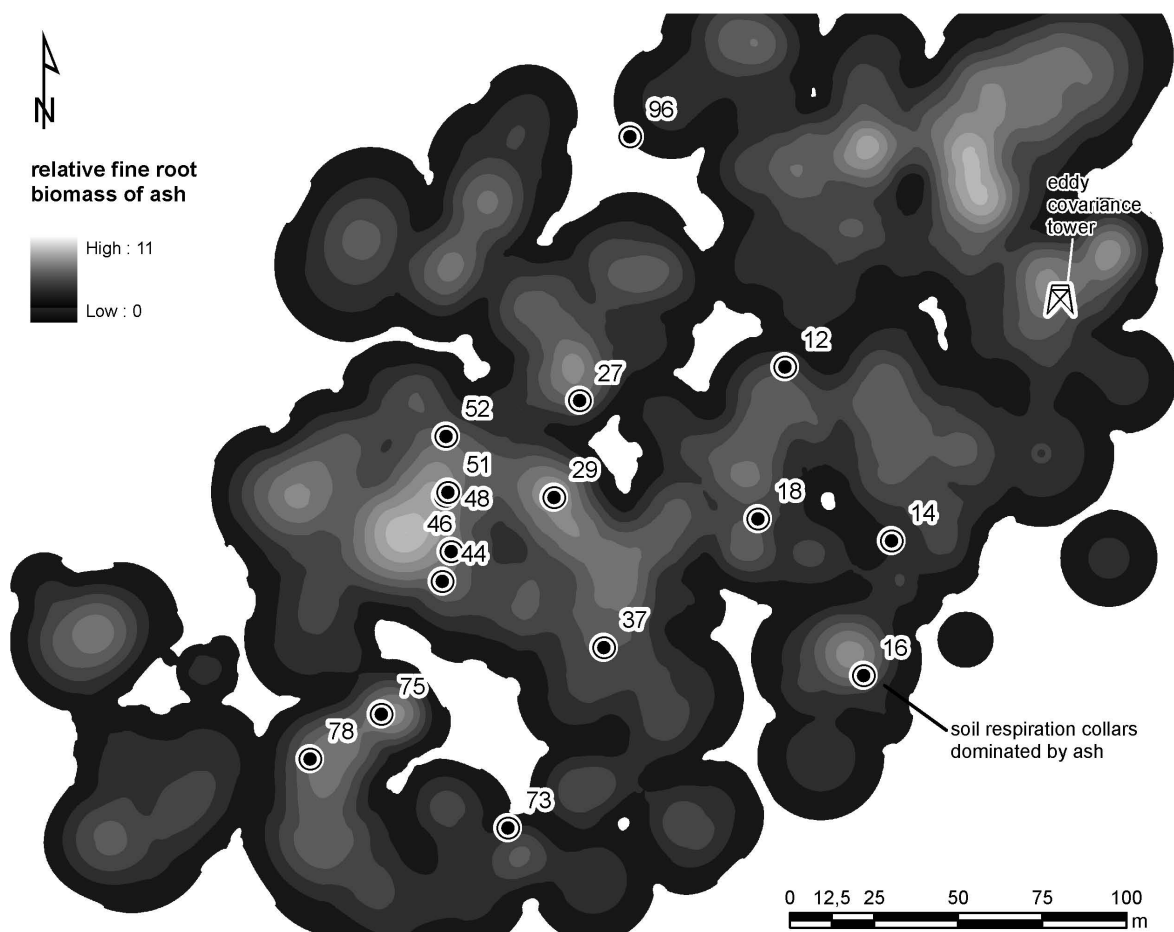
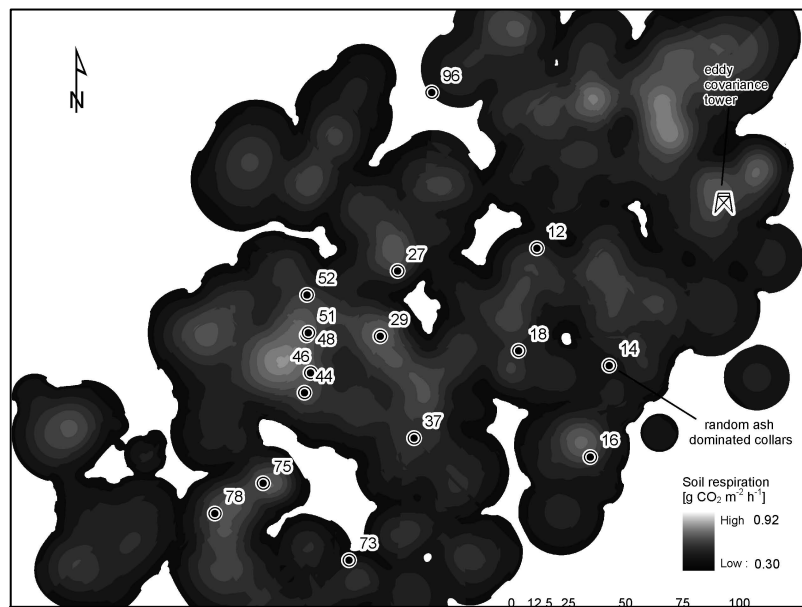


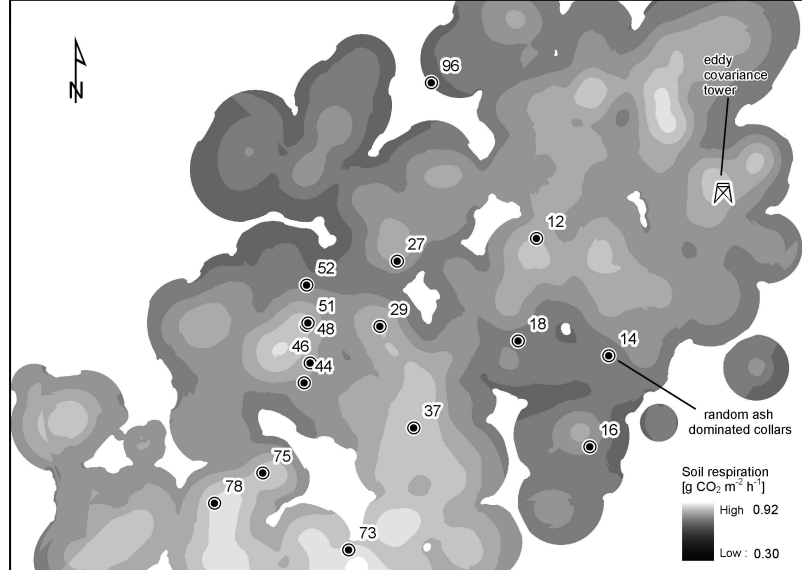
Fig. 4.6 Soil respiration measurement locations dominated by fine roots of ash (<80%)

Fig. 4.7 Root respiration derived from ash in 2006:

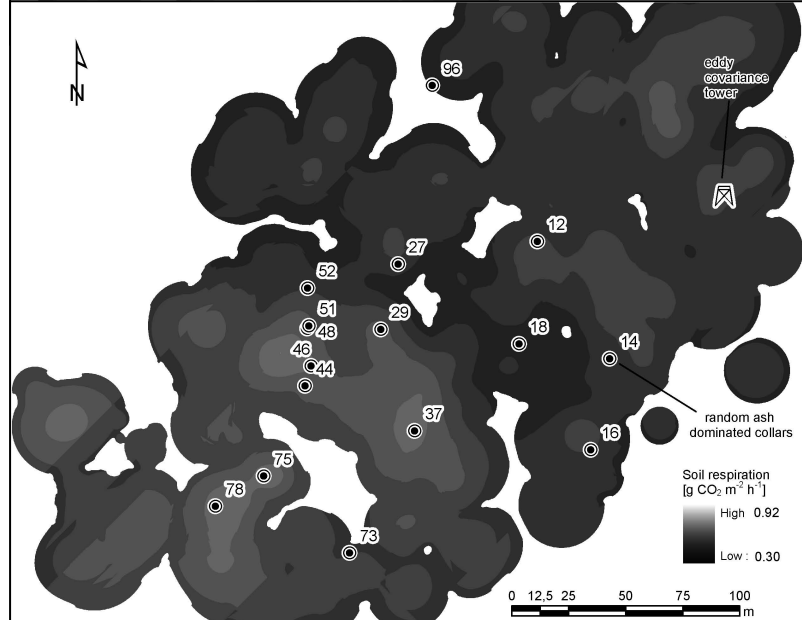
a) June 2006



b) August 2006



c) September 2006



5. Discussion

5.1 Small scale spatial heterogeneity of soil respiration

Considerable spatial heterogeneity of soil respiration rates was apparent within the 4.6 ha study site at the Hainich National Park in Thuringia due to a variety of confounding factors:

5.1.1 The influence of soil temperature

Soil temperature is an important control for the seasonal variation of soil respiration ((Davidson et al. 1998), (Janssens, Pilegaard 2003), (Reichstein, Beer 2008). Reichstein et al (2008) describe a variety of models reflecting a nonlinear positive relationship between soil respiration and soil temperature. Most often empirical models are used because the complexity of the soil environment is difficult to describe within process-based models (Janssens, Pilegaard 2003, S. 912). Two models are frequently used for soil respiration. The first presents a simple exponential relationship between soil temperature and respiration (Davidson et al. 1998). The second uses an extended Arrhenius function {Lloyd 1994 #613. In most cases the differences are small or sometimes non-existent (Gaumont-Guay et al. 2006). Here, the Q_{10} function was used (van't Hoff 1898; Jenkinson et al. 1991). It is widely accepted and often utilized (Janssens, Pilegaard 2003; Hashimoto 2005; Pavelka et al. 2007). However, it must be accepted that the Q_{10} function integrates several controls: An increase in soil temperature influences many biological and physiochemical processes e.g. root biomass distribution, litter inputs and the activity of microbial populations (Janssens, Pilegaard 2003). Interpreting the Q_{10} relationship is sometimes not straight-forward due to the possible different responses of microbial and root respiration to temperature (Davidson et al. 1998). However, the calculated Q_{10} -value of 3.9 fits well within the range of other published data of temperate deciduous forests (Raich, Schlesinger 1992; Davidson et al. 1998; Janssens, Pilegaard 2003, S. 912; van Miegroet et al. 2007).

5.1.2 The influence of soil moisture

Dividing the soil respiration data-set into three classes of different soil moisture (0-30%, 30-60%, 60-90%) reveals a much tighter relationship between soil temperature and soil respiration at dryer conditions ($r^2=0.69$, $Q_{10}=4.1$) than at wetter conditions ($r^2=0.32$, $Q_{10}=2.3$). This is in contradiction to results by Janssens et al. (2003). They also found that Q_{10} is not constant during the year, while interpreting data from a Danish beech forest. However, they observed the lowest Q_{10} values in early autumn during a period of drought stress when soil

respiration was completely unrelated to soil temperature (June– September: Q_{10} averaged 4.3) and the highest values in winter (mean $Q_{10}=16$).

Very low or very high soil water contents may limit soil respiration (e.g., Davidson et al. 1998, Sotta et al. 2006). In my data-set I did not experience drought. Instead, high soil moisture values occurred at all seasons. This might be due to pockets of high clay content (Knöhl et al. 2008) with increased soil moisture. Taking this into consideration, the low Q_{10} value in my study is more likely a characteristic feature of a few measurement locations throughout the entire year than a characteristic of seasonality.

Performing a stepwise correlation of soil water content versus soil respiration rates at six different levels of soil temperature revealed little correlation between soil respiration and soil water content. The best fit was found at 12-14°C soil temperature using a quadratic fitting function ($r^2= 0.09$). The maximum of the fitted functions which mark the highest soil respiration rates at a defined temperature level is remarkably stable between 45-50 [% Vol]. Usually it can be assumed that high water contents inhibit O₂ diffusion and dry conditions hamper biological activity (Davidson et al. 1998; Reichstein, Beer 2008), but at the Hainich study site using all data, quadratic fitting and an exponential fitting functions have nearly the same weak coefficient of determination ($r^2=0.027$ and 0.028, respectively). The reason might be, that the amount of measurements where these impeding effects play a role, are too small compared with the huge amount of all measurements. The minor importance of impeding effects at this site was also confirmed by Knöhl et.al (2008). The weak correlation between soil water content and soil respiration also indicate that other controlling parameters like fine root biomass may be of greater importance.

5.1.3 Spatial heterogeneity of soil respiration

Soil respiration as well as soil moisture did not show any spatial trends. However, soil respiration rates and soil moisture revealed a patchy pattern without any obvious structures. The spatial variability of soil temperature apparently does not drive this heterogeneity because it is very small (less than $\pm 1^\circ\text{C}$ during a single measurement day). This is in line with Yim et al. (2003) who report that soil temperature is not a dominant factor for the spatial variability of soil respiration in temperate broadleaved forests.

Primary, the Kruskal Wallis analysis of variances and the resulting p-value matrix show a defined pattern of small scale recurring measurement locations which often possess significantly different values than other measurement locations. Within the entire study site only a few measurement locations reveal such a different behaviour. At some measurement

locations these significant different values can be explained by higher soil moisture contents at shallow depressions used by animals for wallowing or by different soil moisture conditions, accumulated litter and organic debris at the bottom of small furrows (Saiz et al. 2006b) caused by erosion processes. Other significant higher soil respiration rates might be caused by single hot spots of Allium Ursinum (ramsons) in springtime. This analysis proves the existence of few but significant outliers within the study site. These values can hamper the accuracy of kriging procedures, especially when using a low sampling density.

The spatial heterogeneity of soil respiration along the hydrologic gradient did not exhibit any clear trend. The only observed difference exist between the average coefficients of variation within the study site compared to the values at the bottom of the valley, both for soil respiration and for soil moisture. In this case, the higher CV of soil moisture may explain the different CV of soil respiration. The higher variation of soil moisture itself may be caused by a large in gap the vegetation structure next to the collars and the dominance of large ashes near the collar group. Furthermore the underlying bedrock of karst limestone may have a drainage effect impeding significant higher soil moisture values and thereby significant lower soil respiration data. The expectation to detect a systematic difference in soil water content along a topographical gradient, which might be caused by water redistribution throughout the year which was pointed out by Sotta et al. (2006) could not be approved because of the special natural situation within a karst dominated landscape.

However, combining soil temperature and soil moisture effects within a single exponential equation slightly enhances the predictability of soil respiration measurements ($r^2=0.63$ compared to $r^2=0.61$). But the effect was not as pronounced as described by Knohl et.al. (2008) for the same study site (Knohl et al. 2008). Nevertheless, this equation was used to calculate standardized soil respiration measurement values for defined averaged parameters to achieve a higher level of accuracy.

The necessity of eliminating outliers was further proofed by calculating the adequate numbers of collars for the estimation of calculated annual flux rates. Due to the relatively smaller coefficient of variation of CO₂ flux in the field compared with N₂O fluxes, generally less attention has been paid to the spatial heterogeneity of CO₂ fluxes (Ishizuka et al. 2005). A wide variety of authors performed statistical analyses based on the Student's t-distribution to calculate the number of measurement locations required for an adequate level of precision (Folorunso, Rolston 1984; Davidson et al. 2002; Yim et al. 2003; Adachi et al. 2005; Knohl et al. 2008). The calculated results for different levels of precision demand a higher number of measurement locations to achieve a sufficient level of precision compared to published

studies within temperate deciduous broadleaved forest. Especially the differences to the results of Knohl et al. (2008) are remarkable, because they performed their analysis within the same research area. Knohl et al. used data from 10 different studies within the same research site, but most of these measurements were performed using much less sampling points, within smaller observational windows and only during the vegetation period. This suggests that either there sampling density was insufficient, or - and more likely - that spatial heterogeneity is increasing when all-season measurements are considered. This has important implications for the geospatial interpolation .For this analysis only value from frost periods were excluded because of suspicious measurement results due to problems with icy and snow-covered collars. The sometimes insufficient fit of the metal collar of the soil respiration chamber within the icy and, at times, possibly deformed soil respiration collar may have caused measurement errors during a high quantity of measurements. For the estimation of annual soil respiration rates these errors are of less importance because the observed fluxes are very small.

5.1.4 Optimizing the parameters for interpolation

The influence of different sample sizes was assessed using nested groupings of measurement locations that are arranged in two of the grid cells. Huge differences between the average soil respiration rates of different sampling densities can be caused by single outliers outside the considered grid cells. This led us to vary the lag distances and bin sizes when calculating the semivariograms (Franklin, Mills 2003). The observed range sizes clearly depend on the selected bin sizes. Large lag sizes (greater 10m) sometimes correspond with large range sizes indicating that some drivers of soil respiration may vary on coarser scales than others. For this study, small bin sizes were selected to determine autocorrelation at small ranges where large bin sizes did not indicate any autocorrelation, and small bin sizes were selected to consider even large variability between locations close together. However, the calculated ranges of autocorrelation also varied considerably between measurement dates. This may be caused by fluctuations in spatial patterns due to changes in microbial activity, organic matter input or root activity during the course of the year ((Saiz et al. 2006b, S. 171). The then determined average range of the semivariograms (9m) is comparable to ranges found in investigations at the same study site with a range of 6m (Soe, Buchmann 2005) and in other studies (e.g., 10m in Ishizuka et al. 2005). The increased amount of measurement locations of the random series (81) compared to the stratified random measurement locations (43) reduces the average distances and considerably enhances the validity of the kriging result proved by the associated

predicted standard error map (Fig. 3.22d). The predicted standard error decreased from 0.065 g CO₂ m⁻² h⁻¹ to 0.05 g CO₂ m⁻² h⁻¹ (at average respiration rates of 0.27 respectively 0.26 g CO₂ m⁻² h⁻¹). This results because the average distances between the measurement locations of the random series better fit to the calculated range of the semivariogram than for the stratified random series.

Single hotspot soil respiration events can adulterate not only the semivariograms but also large areas within the interpolated maps especially when the sampling density is small. The results of the nested approach measurements clearly show the misleading effect of single outliers (Fig. 3.16). Therefore, their elimination is important for the reliability of the interpolation results, even when the local hot spot measurement may be functionally justified. This was also supported by the estimation of an adequate number of collars based on the Student's t-distribution required for an adequate level of precision, which is widely used in previous studies (Folorunso, Rolston 1984; Davidson et al. 2002; Yim et al. 2003; Adachi et al. 2005; Knohl et al. 2008)

Another important factor regarding the semivariogram calculation might be the area covered by the closed chamber used for respiration measurement. Because a larger variation in emitted gas is covered with larger chambers these may require fewer sampling points compared to small chambers where the variation within one chamber is much smaller (Yim et al. 2003). The chamber used in the present study has an area of 78 cm², which is comparably small. However, with even smaller soil cores covering an area of 1.8 cm² (Robertson et al. 1997) and (Stoyan et al. 2000) found autocorrelation distances of less than 30cm. Seen in relation to this results a possible influence of the chamber size becomes obvious.

5.1.5 Interpolated maps

To avoid the influence of seasonal effects the kriging is based on mean annual soil respiration rates. Ordinary kriging was preferred to cokriging because of the bivalent nature of the supporting parameters (Pringle, Lark 2006). Soil temperature primarily accounts for seasonal changes and did not show any spatial heterogeneity. Therefore, it is a poor predictor for spatial interpolation (Yim et al. 2003). Soil moisture varies on the seasonal scale as well as on the spatial scale and the values show little autocorrelation. Therefore, the proposed approach to standardize soil respiration using defined soil moisture and temperature values seems to be more promising compared to cokriging. This should not been seen as contradictory to coregionalisation attempts. A particular model may reproduce the components of variation better at some spatial scales than it does at others (Pringle, Lark 2006). Thus, cokriging

methods may be the best choice when parameters with a better autocorrelation structure are available. But in the case of complicated autocorrelation situations like in the presented data, the standardization approach might yield better results.

5.1.6 The standardisation approach

The standardisation of soil respiration using soil temperature and soil moisture largely reduces the interpolated spatial heterogeneity of soil respiration. The remaining heterogeneity must therefore be caused by other, not measured variables.

As a result, the interpolation of soil respiration data requires large sampling densities if better, spatially autocorrelated parameters than soil moisture and soil temperature are not available. Standardizing of soil respiration can help to minimize artifacts caused by temporal and spatial small scale heterogeneity of soil moisture and soil temperature. However, to further increase the reliability of the interpolation it would be necessary to incorporate other parameters with less temporal variability and larger autocorrelation ranges. In summary, the geostatistical approach yielded slightly lower results than the statistical approach, which indicates that the calculated fluxes of even a high number of measurement locations can be further improved by involving spatial parameter.

5.2 Fine root biomass of trees as a predictor of soil respiration

5.2.1 Limitations

The second part of the study was adversely affected by the fact that the distribution of soil respiration collars had to be determined prior to the calculation of fine root biomass distribution. Therefore the detected correlation between fine root biomass and soil respiration is based on a small fraction of all measurement locations.

Further problems resulted from the derivation of tree type specific parameters from the chosen model for the root distribution. Thus, intraspecific and interspecific competition effects (Leuschner et al. 2001), (Rust, Savill 2000) were neglected.

5.2.2 Spatial patterns

In recent years, several studies determined significantly higher total soil respiration rates within close vicinity to tree stems compared to forest gaps. (Brumme 1995; Stoyan et al. 2000; Hanson et al. 2000; Wiseman, Seiler 2004; Saiz et al. 2006b). This may be caused by a higher accumulation of organic matter near the base of the trees, but also due to a higher concentration of fine root biomass next to the tree stems (Hanson et al. 2000; Saiz et al. 2006b). Significantly higher efflux rates of greenhouse gases in close vicinity to tree trunks were also reported for nitrous oxide (N_2O) and methane (CH_4). In that case, the findings were linked to different soil and soil solution properties, as well as additional input of water and nutrients via stem flow (Butterbach-Bahl et al. 2002),(Jenssen et al. 2002). Total soil respiration has been shown to correlate positively with fine root biomass in forest sites (Widen, Majdi 2001; Adachi et al. 2006; Saiz et al. 2006a) as well as in wheat plantations (Stoyan et al. 2000). In sugar maple forests, the respiration rate per mass unit of fine roots can be 2.4-3.4 times higher than that of coarse roots (Pregitzer et al. 1998) but on the other hand coarse root biomass may dominate over fine root biomass by several times, so the contribution of fine and coarse roots to root respiration is comparable (Kuzyakov, Larionova 2006).

The spatial pattern of root respiration and thereby total soil respiration is driven by seasonality. The highest differences between total soil respiration rates concentrated around tree trunks and forest gaps were found in summer, reflecting the seasonal variation of root respiration (Stoyan et al. 2000). Fine root biomass may vary considerably over a season or between years due to its high turnover rate (Vanninen, Makela 1999; Lukac et al. 2003).

Root respiration is very sensitive to temperature changes. In situ measurements determined an exponential increase of fine root respiration with root temperature. Root temperature, which

may be approximated by soil temperature, is the most important factor controlling fine root respiration (Widen, Majdi 2001). The seasonal Q_{10} of root respiration is much higher compared to heterotrophic respiration (Davidson et al. 1998; Widen, Majdi 2001; Baggs 2006). The highest relative contribution of root respiration to total soil efflux varies between the end of June (Epron et al. 2001; Widen, Majdi 2001) and early August (Moyano et al. 2008) corresponding with particular root growth (Kelting et al. 1998). In winter, the contribution of root respiration to total soil respiration is negligibly small (Kuzyakov, Larionova 2006). This is in line with my findings. Significant correlations between calculated fine root biomass and soil respiration were only found in June, August and September 2006.

5.2.3 Seasonal patterns

Root respiration may change dramatically throughout the annual cycle, whereby the contribution of root respiration to total respiration decreased till the end of the season going along with a declining importance of the overall Q_{10} value (Rayment, Jarvis 2000; Moren, Lindroth 2000). That may be a reason for the absence of significant correlations between fine root biomass and soil respiration rates in October and November during litter fall in my data. Root respiration is also linked to leaf expansion (Hanson et al. 1993; Rodeghiero, Cescatti 2006) and photosynthetic activity (Widen, Majdi 2001) whereas there is a time lag of a few days between photosynthesis and corresponding root respiration (Moyano et al. 2008). Thereby photosynthetic and temperature influences are confounding effects, which are difficult to distinguish (Moyano et al. 2008). No correlation was found between soil respiration and total fine root biomass during leaf expansion. This may be caused on the one hand by high springtime heterotrophic respiration rates due to decomposition of litter, on the other hand by confounding effects of root respiration of springtime geophytes.

Prolonged periods of drought reduce root respiration; short wilting periods are without any significant influence (Bouma et al. 1997). This may be the reason why the correlation between soil respiration and fine root biomass decreased in July 2006. During this month the lowest soil water content of the two year measurement campaign was observed (data not shown), but this period was short-lived.

5.2.4 Microbial and physical controls

Even in relatively homogeneous forest stands, heterotrophic and autotrophic respiration rates are highly variable in space and time (Rayment, Jarvis 2000; Stoyan et al. 2000; Longdoz et al. 2000), whereas the mycorrhizosphere component is spatially more variable than the

heterotrophic component (Moyano 2008). Whereas previous studies supported the assumption that roots completely and homogenously penetrate the soil (Krauss et al. 1939), more recent research supports the impression that fine roots are distributed in small clusters (Caldwell et al. 1996; Hölscher et al. 2002; Pellerin, Pages 1996; Ryel et al. 1996). The vertical distribution of fine roots can be related to the decreasing amount of nutrients with increasing depth of the soil. However, the horizontal distribution of fine roots is usually very heterogeneous, likewise following the uneven distribution of nutrients (Fleischer et al. 2006). Having in mind the differing correlations between total soil respiration and fine root biomass content of beech and ash roots it must be noticed, that root systems as well as decomposer communities are tree specific (Baum et al. 2009). Furthermore, fine root biomass of beech and ash stands may vary considerably from site to site and with stand age (Le Goff, Ottorini 2001). Therefore the incertitude of the ratio between both estimated root penetration intensities is large. Roots of ash usually grow horizontally just beneath the soil surface, while beech roots penetrate deeper soil layers (Rust, Savill 2000). As a result, the influence of autotrophic respiration from ash roots is more pronounced than from beech, because soil respiration is measured at the soil surface next to the ash roots. This proximity of ash roots to the soil surface may have contributed to higher significant correlations between soil respiration and ash fine root biomass. CO₂ originating from beech roots may leak on its way to the soil-atmosphere interface (Gaertig et al. 2002), due to differences in gas diffusion velocity, soil physical conditions, soil organisms, moisture conditions and microbial processes (Stoyan et al. 2000). The interpretation of the importance of these leaks is impeded by their interdependence (Soe, Buchmann 2005). Low gas-diffusion velocity can cause elevated soil CO₂ concentrations. This was found to lead to a significant reduction of root respiration rates of Douglas-fir roots (Qi et al. 1994), western hemlock (McDowell et al. 1999) and eastern white pine (Clinton, Vose 1999), whereas no such increase could be found in citrus or bean plantations (Bouma et al. 1997). Widen et.al. (2001) concluded that the response to ambient soil CO₂ concentration is probably species specific (Widen, Majdi 2001).

5.2.5 Synthesis

Altogether, these findings show that knowledge on the fine root distribution in the soil should improve estimates of root and thereby soil CO₂ efflux. The applied model for predicting fine root distribution patterns originally developed for spruce was successfully adapted to predict fine roots of other tree species. The validity of the results was better for beech ($r^2=0.72$) than for ash ($r^2=0.60$). However, significant correlations between soil respiration and predicted fine

root biomass could only be detected in summer month between ash roots and soil respiration ($r^2=0.40-0.50$), probably due to more shallow root distribution patterns of ash compared to beech. If extended to other important tree species, validated and coupled to extensive soil CO₂ efflux measurements, our extension of the approach of Ammer and Wagner could be a valuable tool for an improved regionalisation of summertime soil respiration. Therefore the performed regression kriging procedure (Odeh et al. 1995) using calculated potential fine root biomass rates and total soil respiration credibly depicts potential root respiration rates of ashes.

6. Conclusion

The first part of the study concentrates on the measurement location scale spatial effects, the relationships and confounding co-variations between soil temperature and soil moisture. Variations on the micro scale as well as at larger scales have to be considered whenever measurement location scale variations are influenced (Reichstein, Beer 2008). I conclude that only a combination of a randomized and a double nested sampling approach as well as the appropriate incorporation of additional parameters like soil temperature and soil moisture data may permit a sufficient estimation of the range of soil respiration, which is a prerequisite for reliable maps of soil respiration based on interpolation. Appropriate range distances should always govern the sampling design. Therefore, there is a need to estimate the range distance based on extensive pre-studies with nested measurement locations. Furthermore, my results show that the consideration of seasonal controls facilitates the interpolation of soil respiration measurements.

In the second part of the presented study it is shown that root respiration contributes to a large part of soil respiration in summer. Spatial variation of potential relative fine root biomass is high. An extensive survey of easy to measure aboveground stand characteristics provides the opportunity to relate total soil respiration data to relative fine root biomass. The successful prediction of tree species specific fine root biomass alone, however, does not guarantee a significant correlation with total soil respiration data. My approach is most valuable within stands with shallow root systems like ash dominated stands during the summer when heterotrophic soil respiration is less important. Thus the results of my study may inspire further attempts to quantify the fractions of root respiration depending on root architecture.

I also show that regression kriging is an appropriate tool for the interpolation of soil respiration datasets, wherever a correlation between soil respiration and the potential relative fine root biomass of the prevailing tree species exists. This method avoids strong impacts on the root-soil system as it is often noticed while using separation methods like trenching. Problems like increasing soil water content and rising rhizodeposition, due to higher decomposition rates of severed fine roots can not arise. In contradiction to point measurements, this method provides an area wide impression of root respiration. Due to the easy determinable above-ground stand characteristics, root respiration of larger areas can be quantified, compared to other more labour intensive methods. Both area wide prediction of root respiration and the consideration of larger areas increase the accuracy of average root respiration assessments of old-growth forest stands.

7. Summary

Soil respiration has been studied intensively in various ecosystems throughout the last decades. However, relatively little is known about micro scale heterogeneity within forest ecosystems on homogeneous soils. Here, I investigate within site spatial heterogeneity of soil respiration.

Soil respiration was measured with closed chambers biweekly from April 2005 to April 2006 using a nested design (a set of stratified random measurement locations, supplemented by 2 small and 2 large nested groupings) in an unmanaged, beech dominated old growth forest in Central Germany (Hainich, Thuringia). A set of randomly arranged measurement locations was established in August 2005 and continually sampled biweekly until July 2007.

The average soil respiration values from the random measurement locations were standardized by modeling soil respiration data at defined soil temperature and soil moisture values. By comparing sampling points as well as by comparing kriging results based on various sampling point densities, I found that the exclusion of local outliers was of great importance for the reliability of the estimated fluxes. Most of this information would have been missed without the nested groupings. The interpolation results slightly improved when additional parameters like soil temperature and soil moisture were included in the interpolation procedure. Semivariograms solely calculated from soil respiration data show a broad variety of autocorrelation distances (ranges) from a few centimeters up to a few tens of meters.

The combination of randomly distributed measurement locations with nested groupings plus the inclusion of additional relevant parameters like soil temperature and soil moisture data allows an improved estimation of the range of soil respiration, which is a prerequisite for reliably interpolated maps of soil respiration.

The second part of the study investigates the role of fine root distribution patterns as a predictor of root respiration. Relationships between tree species specific potential fine root biomass and soil respiration data were investigated. Therefore a modified heuristic model for estimating fine root biomass, originally developed for Norway spruce by Ammer & Wagner (2005), was adapted to predict potential fine root biomass at a given point within a stand for different tree species. The model is based on aboveground stand structure parameters like tree species, breast height diameter and geographic location. It is predicated on the assumption that fine root biomass decreases with tree diameter and that the contribution of fine root biomass of surrounding trees for any given point within the forest stand can be summarized. 3478 trees, their breast height diameter and geographic location were recorded. Validating the

adapted model using data from 24 soil cores revealed significant correlations between predicted and measured fine root biomass for beech ($r^2=0.72$) as well as for ash ($r^2=0.60$) roots. Correlations between the calculated total relative fine root biomass and total soil respiration as well as between soil respiration and calculated fine root biomass of beech at beech dominated soil respiration measurement locations did not exist. Significant correlations were found at 16 ash dominated soil respiration measurement locations between predicted ash fine root biomass and soil respiration in summer month ($r^2=0.40-0.50$), were heterotrophic respiration is less important. These correlations were used for a regression kriging analysis to estimate root respiration distribution patterns of ash trees within an old growth deciduous forest.

8. Zusammenfassung

Bodenatmung wurde in den letzten Jahrzehnten intensiv in verschiedenen Ökosystemen untersucht. Dabei ist bis heute relativ wenig über die kleinräumige Heterogenität in Waldökosystemen auf homogenen Böden bekannt. Hier in dieser Studie untersuche ich die kleinräumige Heterogenität der Bodenatmung.

Vom April 2005 bis April 2006 wurde Bodenatmung zweiwöchentlich mit geschlossenen Kammern in einem ungenutzten altem Kalkbuchenwald in der Mitte Deutschlands in Nationalpark Hainich in Thüringen, gemessen. Die Messhauben wurden in einem genesteten Design angeordnet, bestehend aus geschichteten zufällig verteilten Messpunkten, ergänzt durch zwei kleine und zwei große Messpunktnester. Ein weiterer Satz rein zufällig verteilter Messpunkte wurde ab August 20005 bis Juni 2007 beprobt.

Die durchschnittlichen Bodenatmungsraten der zufällig verteilten Messpunkte wurden standardisiert indem Bodenatmungsraten für definierte Bodentemperatur und Feuchte modelliert wurden. Beim Vergleich der Messpunkte ebenso wie beim Vergleich der Kriging-Ergebnisse basierend auf verschiedenen Messpunktdichten fand ich, dass der Ausschluss von lokalen Ausreißern von großer Bedeutung für die Glaubwürdigkeit der geschätzten Gasflüsse ist. Viele dieser Informationen wären ohne die Nester nicht zutage getreten. Die Ergebnisse der Interpolation wurden durch die Einbeziehung von zusätzlichen Parametern wie Bodentemperatur und Bodenfeuchte leicht verbessert. Semivariogramme, ausschließlich auf Basis der Bodenatmungsraten berechnet, weisen eine hohe Bandbreite an unterschiedlichen Autokorrelations-Distanzen (Ranges) auf. Diese reichen von wenigen Zentimetern bis hin zu einigen Dutzend Metern.

Die Kombination von zufallsverteilten Messpunkten mit genesteten Messpunkten und der Einbeziehung von zusätzlichen Parametern wie Bodentemperatur und Bodenfeuchte, erlauben eine verbesserte Abschätzung der Autokorrelations-Distanzen, was ein Voraussetzung für die Verlässlichkeit von interpolierten Bodenatmungskarten ist.

Der zweite Teil der Studie untersucht die Rolle der Feinwurzelverteilung als Vorhersageparameter für die Wurzelatmung. Die Beziehungen zwischen der baumartspezifischen potentiellen Feinwurzelbiomasse und Bodenatmung wurden untersucht. Dafür wurde ein modifiziertes heuristisches Model für die Abschätzung der Feinwurzelbiomasse, welches ursprünglich von Ammer & Wagner (2005) für Fichten entwickelt wurde, angepasst um potentielle relative Feinwurzelbiomasse na jedem beliebigen Punkt innerhalb des Untersuchungsgebietes für verschiedene Bauarten zu prognostizieren. Das Modell basiert auf oberirdischen Strukturparameter, wie Baumart,

Brusthöhendurchmesser und Position im Raum. Es gründet sich auf die Annahmen das die Feinwurzelbiomasse mit dem Durchmesser eines Baumes abnimmt und das der Anteil an Feinwurzelbiomasse an jeden Punkt innerhalb eines Waldgebietes von den nahe stehenden Bäumen aufsummiert werden kann. 3478 Bäume, ihr Brusthöhendurchmesser und ihre Position im Raum wurden aufgenommen. Die Validierung des angepassten Models anhand der Daten von 24 Bohrproben ergab signifikante Korrelationen zwischen modellierten und gemessenen Feinwurzelbiomassen sowohl für Buchen- ($r^2=0.72$) als auch für Eschenwurzeln ($r^2=0.60$). Korrelationen zwischen der berechneten potentiellen Gesamtfeinwurzelmasse und Gesamtatmung konnten ebenso wenig festgestellt werden wie zwischen Bodenatmung und berechneter potentieller Buchenfeinwurzelmasse an Buchen-dominierten Bodenatmungsmesspunkten. Signifikante Korrelationen wurden an 16 Eschen-dominierten Bodenatmungsmesspunkten zwischen der berechneten Eschenfeinwurzelbiomasse und Bodenatmung in den Sommermonaten gefunden ($r^2=0.40-0.50$), zu einer Zeit wo die heterotrophe Atmung eine geringere Bedeutung hat. Diese Korrelationen wurden für ein Regression Kriging genutzt um die räumliche Verteilung der Eschenwurzelatmung in einem alten Laubwald zu bestimmen.

9. References

- Adachi, M.; Bekku, Y. S.; Konuma, A.; Kadir, W. R.; Okuda, T.; Koizumi, H. (2005): Required sample size for estimating soil respiration rates in large areas of two tropical forests and of two types of plantation in Malaysia. *In:* Forest Ecology and Management 210, p. 455–459.
- Adachi, M.; Bekku, Y. S.; Rashidah, W.; Okuda, T.; Koizumi, H. (2006): Differences in soil respiration between different tropical ecosystems. *In:* Applied Soil Ecology 34, p. 258–265.
- Ahrns, C.; Hofmann, G. (1998): Vegetationsdynamik und Florenwandel im ehemaligen mitteldeutschen Waldschutzgebiet "Hainich" im Intervall 1963-1995. *In:* Hercynia 31, p. 33–64.
- Ammer, C.; Wagner, S. (2002): Problems and options in modelling fine-root biomass of single mature Norway spruce trees at given points from stand data. *In:* Canadian Journal of Forest Research-Revue Canadienne de Recherche Forestiere 32, p. 581–590.
- Ammer, C.; Wagner, S. (2005): An approach for modelling the mean fine-root biomass of Norway spruce stands. *In:* Trees-Structure and Function 19, p. 145–153.
- Baggs, E. M. (2006): Partitioning the components of soil respiration: a research challenge. *In:* Plant and Soil 284, p. 1–5.
- Bauer, L.; Weinitzschke, H. (1974): Naturschutzgebiete der Bezirke Erfurt, Suhl und Gera. 1. Ed. Leipzig: Urania-Verlag, Handbuch der Naturschutzgebiete der Deutschen Demokratischen Republik, 4.
- Baum, C.; Fienemann, M.; Glatzel, S.; Gleixner, G. (2009): Overstory-specific effects of litter fall on the microbial carbon turnover in a mature deciduous forest. *In:* Forest Ecology and Management 258, p. 109–114.
- Bolte, A.; Rahmann, T.; Kuhr, M.; Pogoda, P.; Murach, D.; Gadow, K. von (2004): Relationships between tree dimension and coarse root biomass in mixed stands of European beech (*Fagus sylvatica* L.) and Norway spruce (*Picea abies* [L.] Karst.). *In:* Plant and Soil 264, p. 1–11.

- Bouma, T. J.; Bryla, D. R. (2000): On the assessment of root and soil respiration for soils of different textures: interactions with soil moisture contents and soil CO₂ concentrations. *In:* Plant and Soil 227, p. 215–221.
- Bouma, T. J.; Nielsen, K. L.; Eissenstat, D. M.; Lynch, J. P. (1997): Estimating respiration of roots in soil: Interactions with soil CO₂, soil temperature and soil water content. *In:* Plant and Soil 195, p. 221–232.
- Brumme, R. (1995): Mechanisms of carbon and nutrient release and retention in beech forest gaps. 3. environmental-regulation of soil respiration and nitrous-oxide emissions along a microclimatic gradient. *In:* Plant and Soil 168, p. 593–600.
- Butterbach-Bahl, K.; Rothe, A.; Papen, H. (2002): Effect of tree distance on N₂O and CH₄-fluxes from soils in temperate forest ecosystems. *In:* Plant and Soil 240, p. 91–103.
- Caldwell, M. M.; Manwaring, J. H.; Durham, S. L. (1996): Species interactions at the level of fine roots in the field: Influence of soil nutrient heterogeneity and plant size. *In:* Oecologia 106, p. 440–447.
- Carey, E. V.; Sala, A.; Keane, R.; Callaway, R. M. (2001): Are old forests underestimated as global carbon sinks. *In:* Global Change Biology 7, p. 339–344.
- Clinton, B. D.; Vose, J. M. (1999): Fine root respiration in mature eastern white pine (*Pinus strobus*) in situ: the importance of CO₂ in controlled environments. *In:* Tree Physiology 19, p. 475–479.
- Curt, T.; Prevosto, B. (2003a): Root biomass and rooting profile of naturally regenerated beech in mid-elevation Scots pine woodlands. *In:* Plant Ecology 167, p. 269–282.
- Curt, T.; Prevosto, B. (2003b): Rooting strategy of naturally regenerated beech in Silver birch and Scots pine woodlands. *In:* Plant and Soil 255, p. 265–279.
- Davidson, E. A.; Belk, E.; Boone, R. D. (1998): Soil water content and temperature as independent or confounded factors controlling soil respiration in a temperate mixed hardwood forest. *In:* Global Change Biology 4, p. 217–227.
- Davidson, E. A.; Savage, K.; Verchot, L. V.; Navarro, R. (2002): Minimizing artifacts and biases in chamber-based measurements of soil respiration. *In:* Agricultural and Forest Meteorology 113, p. 21–37.

- Dixon, R. K.; Brown, S.; Houghton, R. A.; Am Solomon; Trexler, M. C.; Wisniewski, J. (1994): Carbon pools and flux of global forest ecosystems. *In:* Science 263, p. 185–190.
- Drexhage, M.; Colin, F. (2001): Estimating root system biomass from breast-height diameters. *In:* Forestry 74, p. 491–497.
- Epron, D.; Farque, L.; Lucot, E.; Badot, P. M. (1999): Soil CO₂ efflux in a beech forest: the contribution of root respiration. *In:* Annals of Forest Science 56, p. 289–295.
- Epron, D.; Le Dantec, V.; Dufrene, E.; Granier, A. (2001): Seasonal dynamics of soil carbon dioxide efflux and simulated rhizosphere respiration in a beech forest. *In:* Tree Physiology 21, p. 145–152.
- Fang, C.; Moncrieff, J. B.; Gholz, H. L.; Clark, K. L. (1998): Soil CO₂ efflux and its spatial variation in a Florida slash pine plantation. *In:* Plant and Soil 205, p. 135–146.
- FAO; ISRIC; ISSS (1998): World reference base for soil resources. Rome: Food and Agriculture Organization of the United Nations, World soil resources reports, 84.
- Fleischer, F.; Eckel, S.; Schmid, I.; Kazda, M. (2006): Point process modelling of root distribution in pure stands of *Fagus sylvatica* and *Picea abies*. *In:* Canadian Journal of Forest Research-Revue Canadienne de Recherche Forestiere 36, p. 227–237.
- Fogel, R. (1985): Roots as primary producers in below-ground ecosystems. *In:* Fitter, A. H. (Ed.): Ecological interactions in soil: Plants, microbes and animals. Oxford, Special publications series of the British Ecological Society, 4, p. 23–36.
- Folorunso, O. A.; Rolston, D. E. (1984): Spatial variability of field-measured denitrification gas fluxes. *In:* Soil Science Society of America Journal 48, p. 1214–1219.
- Franklin, R. B.; Mills, A. L. (2003): Multi-scale variation in spatial heterogeneity for microbial community structure in an eastern Virginia agricultural field. *In:* Fems Microbiology Ecology 44, p. 335–346.
- Gaertig, T.; Schack-Kirchner, H.; Hildebrand, E. E.; Wilpert, K. von (2002): The impact of soil aeration on oak decline in southwestern Germany. *In:* Forest Ecology and Management 159, p. 15–25.
- Gaumont-Guay, D.; Black, T. A.; Griffis, T. J.; Barr, A. G.; Jassal, R. S.; Nesic, Z. (2006): Interpreting the dependence of soil respiration on soil temperature and water content in a boreal aspen stand. *In:* Agricultural and Forest Meteorology 140, p. 220–235.

- Gleixner, G.; Tefs, C.; Jordan, A.; Hammer, M.; Wirth, C.; Nueske, A. et al. (2009): Soil Carbon Accumulation in Old-Growth Forests. In: Wirth, C.; Gleixner, G.; Heimann, M. (Eds.): Old-Growth Forests: Function, Fate and Value: SPRINGER, Ecological studies, 207, p. 231–266.
- Gomoryova, E. (2004): Small-scale variation of microbial activities in a forest soil under a beech (*Fagus sylvatica* L.) stand. In: Polish Journal of Ecology 52, p. 311–321.
- Goovaerts, P. (1999): Geostatistics in soil science: state-of-the-art and perspectives. In: Geoderma 89, p. 1–45.
- Goulden, M. L.; Munger, J. W.; Fan, S. M.; Daube, B. C.; Wofsy, S. C. (1996): Exchange of carbon dioxide by a deciduous forest: Response to interannual climate variability. In: Science 271, p. 1576–1578.
- Grossmann, M. (2007): 10 Jahre Nationalpark Hainich. Jena, Landschaftspflege und Naturschutz in Thüringen Sonderheft, 44.
- Hanson, P. J.; Edwards, N. T.; Garten, C. T.; Andrews, J. A. (2000): Separating root and soil microbial contributions to soil respiration: A review of methods and observations. In: Biogeochemistry 48, p. 115–146.
- Hanson, P. J.; Wullschleger, S. D.; Bohlman, S. A.; Todd, D. E. (1993): Seasonal and topographic patterns of forest floor CO₂ efflux from an upland oak forest. In: Tree Physiology 13, p. 1–15.
- Hashimoto, S. (2005): Q(10) values of soil respiration in Japanese forests. In: Journal of Forest Research 10, p. 409–413.
- Herbst, M.; Prolingheuer, N.; Graf, A.; Huisman, J. A.; Weihermuller, L.; Vanderborgh, J. (2009): Characterization and Understanding of Bare Soil Respiration Spatial Variability at Plot Scale. In: Vadose Zone Journal 8, p. 762–771.
- Hofmann, G. (1965): Die Vegetation im Waldschutzgebiet "Hainich" (Westthüringen). -. In: Landschaftspflege und Naturschutz in Thüringen 2, p. 1–12.
- Hofmann, G. (1974): Die natürliche Waldvegetation Westthüringens: ihre Gliederung und ihr Weiserwert für den Boden, Klima und Ertrag. Eberswalde.
- Hölscher, D.; Hertel, D.; Leuschner, C.; Hottkowitz, M. (2002): Tree species diversity and soil patchiness in a temperate broad-leaved forest with limited rooting space. In: Flora 197, p. 118–125.

Houghton, R. A.; Woodwell, G. M. (1989): Global climatic-change. *In:* Scientific American 260, p. 36–44.

Ishizuka, S.; Iswandi, A.; Nakajima, Y.; Yonemura, L.; Sudo, S.; Tsuruta, H.; Muriyars, D. (2005): Spatial patterns of greenhouse gas emission in a tropical rainforest in Indonesia. *In:* Nutrient Cycling in Agroecosystems 71, p. 55–62.

Janssens, I. A.; Pilegaard, K. (2003): Large seasonal changes in Q(10) of soil respiration in a beech forest. *In:* Global Change Biology 9, p. 911–918.

Jenkinson, D. S.; Adams, D. E.; Wild, A. (1991): Model estimates of CO₂ emissions from soil in response to global warming. *In:* Nature 351, p. 304–306.

Jenssen, M.; Butterbach-Bahl, K.; Hofmann, G.; Papen, H. (2002): Exchange of trace gases between soils and the atmosphere in Scots pine forest ecosystems of the northeastern German lowlands 2. A novel approach to scale up N₂O- and NO-fluxes from forest soils by modeling their relationships to vegetation structure. *In:* Forest Ecology and Management 167, p. 135–147.

Kalbitz, K.; Solinger, S.; Park, J. H.; Michalzik, B.; Matzner, E. (2000): Controls on the dynamics of dissolved organic matter in soils: A review. *In:* Soil Science 165, p. 277–304.

Kelting, D. L.; Burger, J. A.; Edwards, G. S. (1998): Estimating root respiration, microbial respiration in the rhizosphere, and root-free soil respiration in forest soils. *In:* Soil Biology & Biochemistry 30, p. 961–968.

Khomik, M.; Arain, M. A.; McCaughey, J. H. (2006): Temporal and spatial variability of soil respiration in a boreal mixedwood forest. *In:* Agricultural and Forest Meteorology 140, p. 244–256.

Klaus, S.; Reisinger, E. (1995): Der Hainich - Ein Weltnaturerbe. *In:* Landschaftspflege und Naturschutz in Thüringen, Sonderheft.

Klaus, S.; Stephan, T. (1998): Nationalpark Hainich. Laubwaldpracht im Herzen Deutschlands. 1. Aufl. Arnstadt: Rhino-Verl.

Knohl, A.; Soe, A. R. B.; Kutsch, W. L.; Gockede, M.; Buchmann, N. (2008): Representative estimates of soil and ecosystem respiration in an old beech forest. *In:* Plant and Soil 302, p. 189–202.

- Kosugi, Y.; Mitani, T.; Ltoh, M.; Noguchi, S.; Tani, M.; Matsuo, N. et al. (2007): Spatial and temporal variation in soil respiration in a Southeast Asian tropical rainforest. *In: Agricultural and Forest Meteorology* 147, p. 35–47.
- Krauss, G.; Müller, K.; Gärtner, G.; Härtel, F.; Schanz, H.; Blanckmeister, H. (1939): Standortsgemäße Durchführung der Abkehr von der Fichtenwirtschaft im nordwestsächsischen Niederland. *In: Tharandter Forstliches Jahrbuch* 90, p. 481–715.
- Kuzyakov, Y. V.; Larionova, A. A. (2006): Contribution of rhizomicrobial and root respiration to the CO₂ emission from soil (A review). *In: Eurasian Soil Science* 39, p. 753–764.
- Lankreijer, H.; Janssens, I. A.; Buchmann, N.; Longdoz, B.; Epron, D.; Dore, S. (2003): Measurement of Soil Respiration. *In: Valentini, R. (Ed.): Fluxes of carbon, water and energy of European forests.* Berlin: SPRINGER, Ecological studies, 163, Bd. 163, p. 37–59.
- Law, B. E.; Goldstein, A. H.; Anthoni, P. M.; Unsworth, M. H.; Panek, J. A.; Bauer, M. R. et al. (2001): Carbon dioxide and water vapor exchange by young and old ponderosa pine ecosystems during a dry summer. *In: Tree Physiology* 21, p. 299–308.
- Le Goff, N.; Ottorini, J. M. (2001): Root biomass and biomass increment in a beech (*Fagus sylvatica* L.) stand in North-East France. *In: Annals of Forest Science* 58, p. 1–13.
- Lee, D.-H. (2001): Relationship between above- and below-ground biomass for Norway spruce (*Picea abies*): Estimating root system biomass from breast height diameter. *In: Journal of Korean Forestry Society* 90, p. 338–345.
- Leuschner, C.; Hertel, D.; Coners, H.; Büttner, V. (2001): Root competition between beech and oak: a hypothesis. *In: Oecologia* 126, p. 276–284.
- Longdoz, B.; Yernaux, M.; Aubinet, M. (2000): Soil CO₂ efflux measurements in a mixed forest: impact of chamber disturbances, spatial variability and seasonal evolution. *In: Global Change Biology* 6, p. 907–917.
- Lukac, M.; Calfapietra, C.; Godbold, D. L. (2003): Production, turnover and mycorrhizal colonization of root systems of three *Populus* species grown under elevated CO₂ (POPFACE). *In: Global Change Biology* 9, p. 838–848.
- Maier, C. A.; Kress, L. W. (2000): Soil CO₂ evolution and root respiration in 11 year-old loblolly pine (*Pinus taeda*) plantations as affected by moisture and nutrient availability.

In: Canadian Journal of Forest Research-Revue Canadienne de Recherche Forestiere 30, p. 347–359.

Martin, J. G.; Bolstad, P. V. (2005): Annual soil respiration in broadleaf forests of northern Wisconsin: influence of moisture and site biological, chemical, and physical characteristics. *In:* Biogeochemistry 73, p. 149–182.

McDowell, N. G.; Marshall, J. D.; Qi, J. G.; Mattson, K. (1999): Direct inhibition of maintenance respiration in western hemlock roots exposed to ambient soil carbon dioxide concentrations. *In:* Tree Physiology 19, p. 599–605.

Meinen, C. (2008): Fine root dynamics in broad-leaved deciduous forest stands differing in tree species diversity. Dissertation.

Meinen, C.; Hertel, D.; Leuschner, C. (2009): Biomass and morphology of fine roots in temperate broad-leaved forests differing in tree species diversity: is there evidence of below-ground overyielding. *In:* Oecologia 161, p. 99–111.

Mönninghoff, W. (1998): Nationalpark Hainich. Berlin: VEBU-Verl., Edition Commerzbank, 9.

Moren, A. S.; Lindroth, A. (2000): CO₂ exchange at the floor of a boreal forest. *In:* Agricultural and Forest Meteorology 101, p. 1–14.

Moyano, F. E. (2008): Soil respiration fluxes and controlling factors in temperate forest and cropland ecosystems. Dissertation. Online available at: http://tobias-lib.ub.uni-tuebingen.de/volltexte/2008/3202/pdf/Dissertation_Moyano.pdf.

Moyano, F. E.; Kutsch, W. L.; Rebmann, C. (2008): Soil respiration fluxes in relation to photosynthetic activity in broad-leaf and needle-leaf forest stands. *In:* Agricultural and Forest Meteorology 148, p. 135–143.

Mund, M. (2004): Carbon pools of European beech forest (*Fagus silvatica*) under different silvicultural management. Göttingen, Berichte des Forschungszentrums Waldökosysteme Reihe A, 189.

Nielsen, C. C. N.; Mackenthun, G. (1991): Spatial variation of fine root biomass intensity in forest soils related to stand density - a numerical method estimating the root intensity-bell around single trees. *In:* Allgemeine Forst- und Jagdzeitung 162, p. 112–119.

- Odeh, I. O. A.; Mcbratney, A. B.; Chittleborough, D. J. (1995): Further results on prediction of soil properties from terrain attributes - Heterotopic cokriging and regression-kriging. *In: Geoderma* 67, p. 215–226.
- Pavelka, M.; Acosta, M.; Marek, M. V.; Kutsch, W. L.; Janous, D. (2007): Dependence of the Q(10) values on the depth of the soil temperature measuring point. *In: Plant and Soil* 292, p. 171–179.
- Pellerin, S.; Pages, L. (1996): Evaluation in field conditions of a three-dimensional architectural model of the maize root system: Comparison of simulated and observed horizontal root maps. *In: Plant and Soil* 178, p. 101–112.
- Pregitzer, K. S.; Euskirchen, E. S. (2004): Carbon cycling and storage in world forests: biome patterns related to forest age. *In: Global Change Biology* 10, p. 2052–2077.
- Pregitzer, K. S.; Laskowski, M. J.; Burton, A. J.; Lessard, V. C.; Zak (1998): Variation in sugar maple root respiration with root diameter and soil depth. *In: Tree Physiology* 18, p. 665–670.
- Pringle, M. J.; Lark, R. M. (2006): Spatial analysis of model error, illustrated by soil carbon dioxide emissions. *In: Vadose Zone Journal* 5, p. 168–183.
- Qi, J. E.; Marshall, J. D.; Mattson, K. G. (1994): High soil carbon-dioxide concentrations inhibit root respiration of douglas-fir. *In: New Phytologist* 128, p. 435–442.
- Raich, J. W.; Schlesinger, W. H. (1992): The global carbon-dioxide flux in soil respiration and its relationship to vegetation and climate. *In: Tellus Series B-Chemical and Physical Meteorology* 44, p. 81–99.
- Rayment, M. B.; Jarvis, P. G. (2000): Temporal and spatial variation of soil CO₂ efflux in a Canadian boreal forest. *In: Soil Biology & Biochemistry* 32, p. 35–45.
- Reichstein, M.; Beer, C. (2008): Soil respiration across scales: The importance of a model-data integration framework for data interpretation. *In: Journal of Plant Nutrition and Soil Science-Zeitschrift Fur Pflanzenernährung Und Bodenkunde* 171, p. 344–354.
- Robertson, G. P. (1987): Geostatistics in Ecology - Interpolating with Known Variance. *In: Ecology* 68, p. 744–748.
- Robertson, G. P.; Klingensmith, K. M.; Klug, M. J.; Paul, E. A.; Crum, J. R.; Ellis, B. G. (1997): Soil resources, microbial activity, and primary production across an agricultural ecosystem. *In: Ecological Applications* 7, p. 158–170.

- Rodeghiero, M.; Cescatti, A. (2006): Indirect partitioning of soil respiration in a series of evergreen forest ecosystems. *In: Plant and Soil* 284, p. 7–22.
- Rust, S.; Savill, P. S. (2000): The root systems of *Fraxinus excelsior* and *Fagus sylvatica* and their competitive relationships. *In: Forestry* 73, p. 499–508.
- Ryan, M. G.; Binkley, D.; Fownes, J. H. (1997): Age-related decline in forest productivity: Pattern and process. *In: Advances in Ecological Research* 27, p. 213–262.
- Ryan, M. G.; Law, B. E. (2005): Interpreting, measuring, and modeling soil respiration. *In: Biogeochemistry* 73, p. 3–27.
- Ryel, R. J.; Caldwell, M. M.; Manwaring, J. H. (1996): Temporal dynamics of soil spatial heterogeneity in sagebrush-wheatgrass steppe during a growing season. *In: Plant and Soil* 184, p. 299–309.
- Saiz, G.; Byrne, K. A.; Butterbach-Bahl, K.; Kiese, R.; Blujdeas, V.; Farrell, E. P. (2006a): Stand age-related effects on soil respiration in a first rotation Sitka spruce chronosequence in central Ireland. *In: Global Change Biology* 12, p. 1007–1020.
- Saiz, G.; Green, C.; Butterbach-Bahl, K.; Kiese, R.; Avitabile, V.; Farrell, E. P. (2006b): Seasonal and spatial variability of soil respiration in four Sitka spruce stands. *In: Plant and Soil* 287, p. 161–176.
- Salimon, C. I.; Davidson, E. A.; Victoria, R. L.; Melo, A. W. (2004): CO₂ flux from soil in pastures and forests in southwestern Amazonia. *In: Global Change Biology* 10, p. 833–843.
- Schimel, D. S. (1995): Terrestrial ecosystems and the carbon cycle. *In: Global Change Biology* 1, p. 77–91.
- Schlichting, E.; Blume, H.-P.; Stahr, K. (1995): Bodenkundliches Praktikum. 2. Ed. Oxford: Blackwell, Pareys Studientexte, 81.
- Schramm, H.-J. (1997): Die forstlichen Wuchsbezirke Thüringens. Kurzbeschreibung. Gotha,, Mitteilungen der Landesanstalt für Wald und Forstwirtschaft, 13.
- Schwendenmann, L.; Veldkamp, E.; Brenes, T.; O'Brien, J. J.; Mackensen, J. (2003): Spatial and temporal variation in soil CO₂ efflux in an old-growth neotropical rain forest, La Selva, Costa Rica. *In: Biogeochemistry* 64, p. 111–128.

- Scott-Denton, L. E.; Sparks, K. L.; Monson, R. K. (2003): Spatial and temporal controls of soil respiration rate in a high-elevation, subalpine forest. *In: Soil Biology & Biochemistry* 35, p. 525–534.
- Seidel, G. (2003): Geologie von Thüringen. 2. Ed. Stuttgart: Schweizerbart.
- Soe, A. R. B.; Buchmann, N. (2005): Spatial and temporal variations in soil respiration in relation to stand structure and soil parameters in an unmanaged beech forest. *In: Tree Physiology* 25, p. 1427–1436.
- Sotta, E. D.; Veldkamp, E.; Guimaraes, B. R.; Paixao, R. K.; Ruivo, M. L.; Almeida, S. S. (2006): Landscape and climatic controls on spatial and temporal variation in soil CO₂ efflux in an Eastern Amazonian Rainforest, Caxiiana, Brazil. *In: Forest Ecology and Management* 237, p. 57–64.
- Stephan, T. (2000): Nationalpark Hainich. Laubwaldpracht im Herzen Deutschlands. 1. Aufl. Wechmar: Gotha Druck GmbH.
- Stoyan, H.; De-Polli, H.; Bohm, S.; Robertson, G. P.; Paul, E. A. (2000): Spatial heterogeneity of soil respiration and related properties at the plant scale. *In: Plant and Soil* 222, p. 203–214.
- Subke, J. A.; Inglima, I.; Cotrufo, M. F. (2006): Trends and methodological impacts in soil CO₂ efflux partitioning: A metaanalytical review. *In: Global Change Biology* 12, p. 921–943.
- Tatarinov, F.; Urban, J.; Cermak, J. (2008): Application of "clump technique" for root system studies of *Quercus robur* and *Fraxinus excelsior*. *In: Forest Ecology and Management* 255, p. 495–505.
- Thüringer Ministerium für Landwirtschaft, Naturschutz und Umwelt (Ed.) (2007): Forstbericht 2007. cooperation of TMLNU, Abteilung Naturschutz, Forsten.
- van Miegroet, H.; Moore, P. T.; Tewksbury, C. E.; Nicholas, N. S. (2007): Carbon sources and sinks in high-elevation spruce-fir forests of the Southeastern US. *In: Forest Ecology and Management* 238, p. 249–260.
- van't Hoff, J. H. (1898): Lectures on Theroretical and Physical Chemistry. Part 1: Chemical Dynamics. London: Ewald Arnold.
- Vanninen, P.; Makela, A. (1999): Fine root biomass of Scots pine stands differing in age and soil fertility in southern Finland. *In: Tree Physiology* 19, p. 823–830.

- Vogel, J. G.; Valentine, D. W.; Ruess, R. W. (2005): Soil and root respiration in mature Alaskan black spruce forests that vary in soil organic matter decomposition rates. *In:* Canadian Journal of Forest Research-Revue Canadienne de Recherche Forestiere 35, p. 161–174.
- Wackernagel, H. (2003): Multivariate geostatistics. An introduction with applications : 7 tables. 3., completely revised ed. Berlin: SPRINGER.
- Wang, C. K. (2006): Biomass allometric equations for 10 co-occurring tree species in Chinese temperate forests. *In:* Forest Ecology and Management 222, p. 9–16.
- Webster, R.; Oliver, M. A. (2001): Geostatistics for environmental scientists. Chichester [u.a.]: Wiley.
- Widen, B.; Majdi, H. (2001): Soil CO₂ efflux and root respiration at three sites in a mixed pine and spruce forest: seasonal and diurnal variation. *In:* Canadian Journal of Forest Research-Revue Canadienne de Recherche Forestiere 31, p. 786–796.
- Wiseman, P. E.; Seiler, J. R. (2004): Soil CO₂ efflux across four age classes of plantation loblolly pine (*Pinus taeda* L.) on the Virginia Piedmont. *In:* Forest Ecology and Management 192, p. 297–311.
- Yim, M. H.; Joo, S. J.; Shutou, K.; Nakane, K. (2003): Spatial variability of soil respiration in a larch plantation: estimation of the number of sampling points required. *In:* Forest Ecology and Management 175, p. 585–588.
- Zirlewagen, D. (2003): Regionalisierung bodenchemischer Eigenschaften in topographisch stark gegliederten Waldlandschaften. Freiburg (Breisgau): Forstliche Versuchs- und Forschungsanst. Baden-Württemberg, Schriftenreihe Freiburger Forstliche Forschung, 19.

10. List of abbreviations

ANOVA	analysis of variance
a.s.l.	above sea level
AV	average
C	carbon
CH ₄	methane
CN ratio	carbon and nitrogen ratio
CO ₂	carbon dioxide
CV	coefficient of variation
dbh	diameter at breast height of an individual tree
DFG	Deutsche Forschungsgemeinschaft
EGM	environmental gas monitor
fdr	frequency domain reflectrometry
Gt	Giga-tons
ha	hectare
IRGA	infrared gas analysator
L.	Carl von Linné, who first described many tree species
n	number of samples
Mg	Mega-gram
N	nitrogen
N ₂ O	nitrous oxide
NPP	net primary productivity
NEP	net ecosystem productivity
O ₂	oxigen
Q ₁₀	The temperature coefficient is a measure of the rate of change of a biological or chemical system as a consequence of increasing the temperature by 10°C
RD	root distance
rFRB	relative fine root biomass
RMSE	root mean square error
SD	standard deviation
SM	soil moisture
SR	soil respiration
SRC	soil respiration chamber

T	temperature
Vol	volume
yr	year
δ	standard deviation
θ	soil moisture

11. List of tables

Table 3.1	Mann Whitney U-Test of soil respiration data at all five measurement location –groups. Non values were significant at $p < 0.05$	36
Table 3.2	Required number of soil respiration measurement points to achieve a precision of ± 10 , ± 20 , or $\pm 30\%$ around full population mean at various confidence levels (80-99%).....	41
Table 3.3	Validation of ordinary kriging results	48
Table 4.1	Definition of tree type specific parameters for the calculation of relative fine root biomass. RD ₃ defines the maximum extent of fine roots from the tree trunk, rFRB ₀ describes the fine root biomass at the tree trunk, rFRB ₁ represents the potential fine root biomass at one third of the maximum extent, rFRB ₂ at two third of the maximum extent. Parameters are adapted for beech and ash (black). The other tree species (hornbeam, wych elm and sycamore maple) only sparsely occur at the study site (grey). Therefore, parameters fitted for spruce were used to account solely for the existence of these few trees. None of the soil respiration measurement locations were significantly influenced by this species.....	53
Table 4.2	Results of model validation for beech and ash: Correlation between predicted fine root biomass of 24 soil cores and the weight of excavated fine roots.....	58
Table 4.3	Average calculated relative fine root biomass [percent of total] at soil respiration measurement locations, describing the absolute dominance of beech and ash roots at the study site. Parameters are adapted for beech and ash (black). The other tree species (hornbeam, wych elm and sycamore maple) only sparsely occur at the study site (grey). Therefore, parameters fitted for spruce were used to account solely for the existence of these few trees. None of the soil respiration measurement locations were significantly influenced by this species.....	60
Table 4.4	Regression equations and residuals between total soil respiration and fine roots of ash from June, August and September 2006.....	62

12. List of figures

Fig. 2.1	Location of study site in the Hainich National Park	12
Fig. 2.2	Geology at the Hainich-Dün growing region	14
Fig. 2.3	Distribution of vegetation communities around the study site.....	16
Fig. 2.4	Age class distribution around the study site.....	17
Fig. 2.5	Distribution of sampling locations in two series. Sampling locations of the random series (81 open circles) are distributed completely random across the site. Sampling locations of the nested series (43 dark circles and 36 triangles and 34m grid squares) are arranged in a stratified random way in 2 nested groupings: Two of the cells were chosen randomly from the grid. In both, 9 measurement locations are distributed randomly (large groupings). Both cells are further divided into quarters and in one quarter 9 measurement locations are placed at random (small groupings).	21
Fig. 3.1	Log-transformation of soil respiration data.....	25
Fig. 3.2	Soil moisture, soil temperature, and soil respiration during the course of the study. The graphs base on the measurements in the 81 measurement locations of the random series. Vertical bars represent the 95% confidence interval. The annual cycle is clearly apparent. The soil moisture data gap during winter 2005/2006 is caused by ground frost. Furthermore, the soil respiration measurements show considerable heterogeneity at some of the measurement dates.....	30
Fig. 3.3	Relationship between soil temperature and soil respiration. Q_{10} as well as the fit and the parameters of the models vary for different ranges of soil moisture. The Q_{10} for all data is 3.9 [$r^2=0.60$; $CO_2=0.0711 \times \exp(0.1365 \times x)$].	31
Fig. 3.4	Soil respiration versus soil water content at different soil temperature levels.....	32
Fig. 3.5	Covariation of soil water content and soil temperature.....	34
Fig. 3.6	Soil respiration versus soil water content for all data using different fitting functions	34
Fig. 3.7	Residuals of the regression analysis of soil respiration and soil temperature versus soil water content	34
Fig. 3.8	Coefficient of variation of soil temperature of all measurement events.	34
Fig. 3.9	Distribution of soil respiration along the hydrologic gradient from the upper (1) group of measurement locations downwards till group 5.....	36

Fig. 3.10	Distribution of soil moisture along the hydrologic gradient from the upper (1) group of measurement locations downwards till group 5	36
Fig. 3.11	Nested series: Coefficient of variation of soil respiration.....	37
Fig. 3.12	Random series: Coefficient of variation of soil respiration	37
Fig. 3.13	First measurement series - Spatial heterogeneity: The size of each measurement location sign indicate how many other measurement locations in the research area exhibit significantly different values compared to them. The connection lines show which pairs of measurement locations where compared with significant differences.	38
Fig. 3.14	Spatial heterogeneity of SR: The size of each measurement location sign indicates how many other measurement locations in the research area exhibit significant different values. The lines show which pairs of measurement locations where compared observing significant different values.	39
Fig. 3.15	Spatial heterogeneity of SM: The size of each measurement location sign indicates how many other measurement locations in the research area exhibit significant different values. The lines show which pairs of measurement locations where compared observing significant different values.	40
Fig. 3.16	Comparison of the soil respiration interpolation based on three different sampling densities within two test cells (see methods section for details). The resulting average soil respiration values are given below the panels. Units are $\text{g CO}_2 \text{ m}^{-2} \text{ h}^{-1}$. Fig. a & b are kriging results using only data from the stratified random distributed measurement locations, Fig. c & d represent results using the stratified random measurement locations and data from the large nests, and Fig. e & f are supplemented with data from the small nests	42
Fig. 3.17	Example semivariograms of soil respiration a, b): Bin width is 10m, all possible distances included. c, d): Bin width = 1.5m, only distances up to 150m included. Auto-correlation does only occur at very small distances between measurement locations.	43
Fig. 3.18	Example semivariograms of soil moisture and soil temperature.	44
Fig. 3.19	Observed SR vs. predicted SR 2005	45
Fig. 3.20	Observed SR vs. predicted SR 2006	45
Fig. 3.21	Observed st.-SR vs. predicted SR 2006	45
Fig. 3.22	Interpolated maps of soil respiration measurements of the nested series (a) exhibits a large predicted standard error –PSE (b), whereas the random	

distribution (c) shows a much smaller PSE (d). The most homogeneous result was achieved by standardizing the randomized soil respiration measurements of 2006 at 11.6°C soil temperature and correlative 35.2 % soil moisture (e) possessing little PSE (f). Units are g CO ₂ m ⁻² h ⁻¹	47
Fig. 4.1 Relative fine root biomass (rFRB) of different tree species in relation to the distance from the stem trunk and the diameter at breast height (dbh) as assumed by the model	54
Fig. 4.2 The adapted regression-kriging-Model C of Odeh et al. 1995.....	56
Fig. 4.3 Location, tree species and breast height diameter of all trees at the study site.....	57
Fig. 4.4 Tree species diversity of the Hainich study site, sorted by breast height diameter	59
Fig. 4.5 Correlation between total soil respiration and calculated relative fine root biomass at ash dominated stands during the vegetation period of 2005 (a,b), 2006 (c-g) and 2007 (h,i).....	61
Fig. 4.6 Soil respiration measurement locations dominated by fine roots of ash (<80%).....	63
Fig. 4.7 Root respiration derived from ash in 2006:.....	64
Fig. 13.1 Semivariograms of soil respiration measurements in 2006 (all data). The number at each title indicate the year (2006) and the day of measurement	135
Fig. 13.2 Semivariograms of soil respiration measurements in 2006 (data only within $\pm 2\text{sd}$). The number at each title indicate the year (2006) and the day of measurement.....	139
Fig. 13.3 Semivariograms of soil respiration measurements in 2006 (data only within $\pm 1.5\text{sd}$). The number at each title indicate the year (2006) and the day of measurement.....	143

13. Appendix

13.1 Soil respiration data

First measurement series

area	ID	x	y	05.104	05.117	05.133	05.146	05.161	05.174	05.188	05.204	05.217
s. random	1	4391604.895	5661628.494	0.23	0.28	0.27	0.47	0.31	0.62	0.48	0.56	0.58
s. random	2	4391620.649	5661605.688	0.25	0.30	0.19	0.36	0.28	0.38	0.36	0.35	0.43
s. random	3	4391624.907	5661580.230	0.32	0.27	0.22	0.36	0.21	0.37	0.17	0.31	0.41
s. random	4	4391614.449	5661556.541	0.47	0.27	0.30	0.53	0.32	0.53	0.33	0.40	0.59
s. random	5	4391602.427	5661518.704	0.33	0.25	0.16	0.36	0.30	0.47	0.28	0.37	0.44
s. random	6	4391591.741	5661541.303	0.61	0.46	0.56	0.59	0.70	0.54	0.88	1.80	0.86
s. random	7	4391580.399	5661563.194	0.38	0.38	0.30	0.67	0.44	0.84	0.47	0.72	0.83
s. random	8	4391572.452	5661617.528	0.17	0.19	0.15	0.28	0.20	0.36	0.14	0.20	0.27
s. random	9	4391544.976	5661604.496	0.28	0.25	0.23	0.12	0.36	0.46	0.41	0.47	0.57
s. random	10	4391545.126	5661566.460	0.16	0.20	0.15	0.38	0.23	0.16	0.12	0.21	0.27
s. random	11	4391548.626	5661545.321	0.46	0.35	0.38	0.81	0.53	0.94	0.42	0.49	0.70
s. random	12	4391563.446	5661498.431	0.21	0.17	0.14	0.58	0.26	0.84	0.26	0.31	0.53
s. random	13	4391535.893	5661479.661	1.00	0.33	0.37	1.57	0.75	1.00	0.89	0.96	0.80
s. random	14	4391494.662	5661455.820	0.49	0.36	0.31	0.59	0.31	0.67	0.25	0.48	0.67
s. random	15	4391504.724	5661474.618	0.35	0.36	0.16	0.72	0.40	1.36	0.58	0.69	0.99
s. random	16	4391506.676	5661498.157	0.42	0.35	0.33	0.53	0.48	0.65	0.30	0.46	0.54
s. random	17	4391498.136	5661540.994	0.21	0.22	0.15	0.41	0.26	0.35	0.26	0.30	0.38
s. random	18	4391516.068	5661569.508	0.36	0.26	0.23	0.33	0.37	0.63	0.43	0.46	0.61
s. random	19	4391532.734	5661642.273	0.48	0.41	0.36	0.51	0.42	0.56	0.43	0.53	0.75
s. random	20	4391509.732	5661622.961	0.35	0.31	0.35	0.65	0.58	0.68	0.51	0.68	0.75
s. random	21	4391467.769	5661629.274	0.31	0.27	0.35	0.56	0.38	0.48	0.40	0.42	0.30
s. random	22	4391465.143	5661609.981	0.23	0.17	0.12	0.27	0.20	0.54	0.16	0.22	0.37
s. random	23	4391474.263	5661602.622	0.19	0.31	2.03	0.51	0.22	0.47	0.28	0.32	0.54
s. random	24	4391488.978	5661581.551	0.42	0.32	0.22	0.57	0.35	0.59	0.32	0.47	0.44
s. random	25	4391487.471	5661556.030	0.37	0.28	1.80	0.52	0.26	0.74	0.35	0.49	0.79
s. random	26	4391483.389	5661499.275	0.21	0.46	0.38	0.52	0.41	0.44	0.56	0.41	0.48
s. random	27	4391481.196	5661457.727	0.19	0.22	0.19	0.32	0.25	0.38	0.22	0.30	0.44
hyd. gradient	28	4391460.255	5661472.183	0.37	0.30	0.30	0.46	0.32	0.41	0.30	0.31	0.36
hyd. gradient	29	4391460.674	5661472.478	0.17	0.47	0.41	0.68	0.25	0.53	0.42	0.38	0.42
hyd. gradient	30	4391461.035	5661472.779	0.30	0.27	0.23	0.44	0.23	0.46	0.27	0.26	0.28
hyd. gradient	31	4391461.405	5661473.111	0.37	0.47	0.44	0.78	0.53	0.58	0.49	0.61	0.52
s. random	32	4391451.977	5661488.993	0.31	0.25	0.31	0.52	0.36	0.47	0.25	0.28	0.38
hyd. gradient	33	4391448.972	5661495.268	0.33	0.21	0.20	0.26	0.28	0.44	0.33	0.41	0.56
hyd. gradient	34	4391449.468	5661495.600	0.30	0.28	0.21	0.43	0.30	0.51	0.38	0.36	0.47
hyd. gradient	35	4391449.848	5661495.817	0.41	0.19	0.27	0.38	0.30	0.48	0.31	0.32	0.44
hyd. gradient	36	4391450.401	5661496.230	0.52	0.26	0.19	0.36	0.27	0.49	0.32	0.33	0.47
hyd. gradient	37	4391450.884	5661510.067	0.17	0.21	0.19	0.21	0.26	0.43	0.21	0.25	0.33
hyd. gradient	38	4391451.228	5661510.419	0.52	0.11	0.17	0.31	0.20	0.31	0.17	0.22	0.28
hyd. gradient	39	4391451.548	5661510.724	0.42	0.23	0.22	0.42	0.27	0.38	0.26	0.30	0.37
hyd. gradient	40	4391451.904	5661511.053	0.37	0.19	0.20	0.16	0.22	0.37	0.23	0.27	0.33
s. random	41	4391452.087	5661516.596	0.86	0.27	0.21	0.36	0.35	0.47	0.35	0.40	0.44
hyd. gradient	42	4391452.556	5661535.991	0.52	0.37	0.42	0.62	0.44	0.65	0.38	0.42	0.47
hyd. gradient	43	4391452.718	5661536.216	0.23	0.28	0.33	0.38	0.32	0.53	0.37	0.35	0.44
hyd. gradient	44	4391452.932	5661536.599	0.32	0.25	0.28	0.43	0.33	0.62	0.42	0.49	0.53
hyd. gradient	45	4391453.199	5661537.090	0.26	0.22	0.25	0.42	0.30	0.54	0.27	0.40	0.37
s. random	46	4391442.573	5661567.595	0.36	0.30	0.23	0.25	0.33	0.57	0.31	0.43	0.49
s. random	47	4391435.933	5661556.862	0.80	0.14	0.19	0.26	0.23	0.48	0.15	0.26	0.41
s. random	48	4391416.637	5661534.619	0.40	0.35	-0.02	0.56	0.38	0.58	0.31	0.43	0.62
s. random	49	4391411.577	5661506.105	0.86	0.16	0.16	0.42	0.27	0.49	0.14	0.37	0.43
s. random	50	4391418.219	5661463.264	0.10	0.19	0.30	0.51	0.40	0.73	0.28	0.59	0.58

area	ID	x	y	05.230	05.245	05.261	05.273	05.294	05.302	05.315	05.327	05.341
s. random	1	4391604.895	5661628.494	0.62	0.69	0.41	0.37	0.41	0.54	0.44	0.30	0.26
s. random	2	4391620.649	5661605.688	0.40	0.48	0.23	0.25	0.33	0.48	0.23	0.14	0.11
s. random	3	4391624.907	5661580.230	0.40	0.46	0.31	0.38	0.40	0.52	0.25	0.16	0.16
s. random	4	4391614.449	5661556.541	0.59	0.85	0.48	0.43	0.69	0.48	0.38	0.19	0.33
s. random	5	4391602.427	5661518.704	0.48	0.54	0.26	0.30	0.41	0.35	0.25	0.11	0.19
s. random	6	4391591.741	5661541.303	0.88	0.98	0.95	0.89	0.37	0.62	0.41	0.40	0.22
s. random	7	4391580.399	5661563.194	0.99	0.91	0.54	0.54	0.72	0.68	0.31	0.23	0.23
s. random	8	4391572.452	5661617.528	0.28	0.30	0.19	0.16	0.27	0.37	0.17	0.15	0.11
s. random	9	4391544.976	5661604.496	0.58	0.74	0.36	0.40	0.27	0.49	0.17	0.11	0.15
s. random	10	4391545.126	5661566.460	0.26	0.23	0.12	0.14	0.31	0.36	0.32	0.12	-0.17
s. random	11	4391548.626	5661545.321	0.75	0.95	0.48	0.44	0.42	1.02	0.42	0.20	0.21
s. random	12	4391563.446	5661498.431	0.65	0.70	0.40	0.26	0.38	0.56	0.22	0.20	0.14
s. random	13	4391535.893	5661479.661	0.90	1.27	0.74	0.74	0.74	0.88	0.28	0.21	0.19
s. random	14	4391494.662	5661455.820	0.65	0.67	0.33	0.27	0.80	0.27	0.35	0.17	0.19
s. random	15	4391504.724	5661474.618	0.81	0.98	0.59	0.62	0.89	1.15	0.26	0.17	0.15
s. random	16	4391506.676	5661498.157	0.53	0.46	0.35	0.28	0.31	0.33	0.40	0.17	0.17
s. random	17	4391498.136	5661540.994	0.46	0.51	0.28	0.23	0.37	0.46	0.25	0.06	0.09
s. random	18	4391516.068	5661569.508	0.59	0.49	0.35	0.28	0.43	0.63	0.32	0.20	0.09
s. random	19	4391532.734	5661642.273	0.75	0.75	0.46	0.38	0.40	0.41	0.19	0.15	-0.22
s. random	20	4391509.732	5661622.961	0.85	1.00	0.58	0.70	0.64	0.68	0.48	0.32	0.23
s. random	21	4391467.769	5661629.274	0.42	0.51	0.26	0.23	0.28	0.35	0.19	0.14	0.10
s. random	22	4391465.143	5661609.981	0.31	0.32	0.23	0.27	0.32	0.35	0.10	0.06	0.09
s. random	23	4391474.263	5661602.622	0.49	0.37	0.28	0.25	0.27	0.31	0.22	0.11	0.09
s. random	24	4391488.978	5661581.551	0.32	0.59	0.31	0.09	0.22	0.20	0.31	0.10	0.12
s. random	25	4391487.471	5661556.030	0.67	0.68	0.38	0.27	0.28	0.57	0.22	0.15	0.11
s. random	26	4391483.389	5661499.275	0.47	0.53	0.28	0.33	0.41	0.47	0.57	0.09	0.17
s. random	27	4391481.196	5661457.727	0.36	0.30	0.20	0.17	0.20	0.28	0.14	0.11	0.09
hyd. gradient	28	4391460.255	5661472.183	0.35	0.32	0.21	0.21	0.30	0.36	0.23	0.16	0.14
hyd. gradient	29	4391460.674	5661472.478	0.40	0.44	0.25	0.25	0.32	0.33	0.27	0.16	0.11
hyd. gradient	30	4391461.035	5661472.779	0.27	0.31	0.20	0.16	0.22	0.26	0.21	0.11	0.09
hyd. gradient	31	4391461.405	5661473.111	0.53	0.57	0.33	0.31	0.27	0.32	0.15	0.06	0.12
s. random	32	4391451.977	5661488.993	0.38	0.49	0.27	0.27	0.36	0.41	0.25	0.11	0.10
hyd. gradient	33	4391448.972	5661495.268	0.69	0.52	0.38	0.59	0.44	0.42	0.16	0.12	0.10
hyd. gradient	34	4391449.468	5661495.600	0.44	0.44	0.22	0.23	0.27	0.31	0.22	0.14	0.10
hyd. gradient	35	4391449.848	5661495.817	0.38	0.49	0.21	0.25	0.32	0.31	0.25	0.14	0.10
hyd. gradient	36	4391450.401	5661496.230	0.41	0.48	0.26	0.27	0.26	0.30	0.22	0.15	0.12
hyd. gradient	37	4391450.884	5661510.067	0.28	0.37	0.20	0.19	0.26	0.32	0.20	0.15	0.14
hyd. gradient	38	4391451.228	5661510.419	0.28	0.30	0.19	0.16	0.19	0.22	0.25	0.09	0.07
hyd. gradient	39	4391451.548	5661510.724	0.42	0.44	0.25	0.27	0.27	0.31	0.22	0.10	0.11
hyd. gradient	40	4391451.904	5661511.053	0.26	0.42	0.22	0.25	0.28	0.31	0.21	0.12	0.06
s. random	41	4391452.087	5661516.596	0.46	0.52	0.30	0.31	0.35	0.42	0.26	0.19	0.14
hyd. gradient	42	4391452.556	5661535.991	0.54	0.68	0.31	0.30	0.33	0.42	0.23	0.15	0.11
hyd. gradient	43	4391452.718	5661536.216	0.47	0.23	0.14	0.11	0.19	0.27	0.15	0.11	0.07
hyd. gradient	44	4391452.932	5661536.599	0.65	0.70	0.42	0.30	0.35	0.41	0.28	0.09	0.09
hyd. gradient	45	4391453.199	5661537.090	0.37	0.37	0.22	0.22	0.35	0.44	0.27	0.14	0.10
s. random	46	4391442.573	5661567.595	0.52	0.59	0.31	0.26	0.41	0.56	0.31	0.10	0.15
s. random	47	4391435.933	5661556.862	0.43	0.33	0.19	0.16	0.21	0.27	0.17	0.10	0.10
s. random	48	4391416.637	5661534.619	0.67	0.65	0.32	0.32	0.43	0.57	0.23	0.17	0.12
s. random	49	4391411.577	5661506.105	0.48	0.33	0.30	0.23	0.26	0.33	0.22	0.11	0.11
s. random	50	4391418.219	5661463.264	0.86	0.80	0.44	0.35	0.44	0.88	0.47	0.36	0.23

area	ID	x	y	05.355	06.004	06.032	06.047	06.074	06.089	06.102
s. random	1	4391604.895	5661628.494	0.28	0.21	0.10	-0.14	0.23	0.20	0.16
s. random	2	4391620.649	5661605.688	0.16	0.23	0.04	0.05	0.16	0.19	0.10
s. random	3	4391624.907	5661580.230	0.14	-0.05	0.05	0.05	0.06	0.17	0.14
s. random	4	4391614.449	5661556.541	0.31	0.38	0.05	0.04	0.09	0.20	0.10
s. random	5	4391602.427	5661518.704	0.17	0.12	0.06	0.17	0.10	0.05	0.22
s. random	6	4391591.741	5661541.303	0.23	0.36	0.04	0.00	0.01	0.11	0.22
s. random	7	4391580.399	5661563.194	0.40	0.23	0.07	0.12	0.06	0.16	0.25
s. random	8	4391572.452	5661617.528	0.20	-	0.05	0.24	0.01	0.15	0.02
s. random	9	4391544.976	5661604.496	0.21	0.15	0.01	0.21	0.12	0.14	0.14
s. random	10	4391545.126	5661566.460	0.05	0.11	0.01	0.09	0.04	0.14	0.10
s. random	11	4391548.626	5661545.321	0.42	0.23	0.06	-0.23	-1.20	0.27	0.16
s. random	12	4391563.446	5661498.431	0.14	0.14	0.02	0.09	0.15	0.16	0.12
s. random	13	4391535.893	5661479.661	0.06	0.23	0.07	-0.05	0.06	0.27	0.25
s. random	14	4391494.662	5661455.820	0.25	0.32	0.10	0.12	0.46	0.20	0.19
s. random	15	4391504.724	5661474.618	0.38	0.14	0.26	0.13	0.11	0.22	0.35
s. random	16	4391506.676	5661498.157	0.16	0.20	0.05	-0.01	0.14	0.22	0.19
s. random	17	4391498.136	5661540.994	0.22	0.14	0.01	0.09	0.09	0.20	0.11
s. random	18	4391516.068	5661569.508	0.15	0.11	0.04	0.07	0.20	0.19	0.12
s. random	19	4391532.734	5661642.273	0.26	0.23	0.05	-0.01	0.12	0.21	0.00
s. random	20	4391509.732	5661622.961	0.27	0.27	0.16	0.04	0.15	0.43	0.64
s. random	21	4391467.769	5661629.274	0.19	0.15	0.00	-0.12	0.06	0.15	0.67
s. random	22	4391465.143	5661609.981	0.09	0.12	0.02	0.00	0.15	0.10	0.17
s. random	23	4391474.263	5661602.622	0.16	0.15	0.02	0.18	0.12	0.14	0.07
s. random	24	4391488.978	5661581.551	0.22	0.07	0.02	0.04	0.52	0.10	0.12
s. random	25	4391487.471	5661556.030	0.16	0.15	0.02	0.16	0.56	0.31	0.14
s. random	26	4391483.389	5661499.275	0.84	0.15	0.62	0.10	0.04	0.17	0.16
s. random	27	4391481.196	5661457.727	0.09	0.11	0.02	0.14	0.09	0.11	0.26
hyd. gradient	28	4391460.255	5661472.183	0.20	0.01	0.02	0.01	0.42	0.15	0.10
hyd. gradient	29	4391460.674	5661472.478	0.15	0.11	0.01	0.18	0.16	0.12	0.07
hyd. gradient	30	4391461.035	5661472.779	0.05	0.06	0.01	0.12	0.00	0.13	0.09
hyd. gradient	31	4391461.405	5661473.111	0.09	0.06	0.01	-0.07	0.07	0.13	0.07
s. random	32	4391451.977	5661488.993	0.19	0.09	0.02	0.27	0.11	0.12	0.09
hyd. gradient	33	4391448.972	5661495.268	0.09	0.16	0.01	0.16	0.32	0.24	0.11
hyd. gradient	34	4391449.468	5661495.600	0.09	0.12	0.00	0.14	0.02	0.02	0.11
hyd. gradient	35	4391449.848	5661495.817	0.07	0.09	0.01	0.06	0.05	0.06	0.12
hyd. gradient	36	4391450.401	5661496.230	0.11	0.12	0.01	-0.13	0.06	0.25	0.12
hyd. gradient	37	4391450.884	5661510.067	0.12	0.09	0.00	0.11	0.26	0.16	0.11
hyd. gradient	38	4391451.228	5661510.419	0.10	0.10	0.01	0.10	0.05	0.25	0.07
hyd. gradient	39	4391451.548	5661510.724	0.09	0.10	0.01	0.07	0.06	0.14	0.10
hyd. gradient	40	4391451.904	5661511.053	-0.12	0.10	0.01	0.00	0.04	0.28	0.12
s. random	41	4391452.087	5661516.596	0.33	0.21	0.01	0.04	0.09	-0.04	0.11
hyd. gradient	42	4391452.556	5661535.991	0.16	0.14	0.02	-0.01	0.23	0.22	0.11
hyd. gradient	43	4391452.718	5661536.216	0.09	0.09	0.01	0.01	0.14	0.18	0.15
hyd. gradient	44	4391452.932	5661536.599	0.20	0.10	0.00	0.26	0.00	0.21	0.10
hyd. gradient	45	4391453.199	5661537.090	0.14	0.07	0.01	-0.03	0.07	0.25	0.12
s. random	46	4391442.573	5661567.595	0.30	0.00	0.02	-0.02	0.11	0.24	0.10
s. random	47	4391435.933	5661556.862	0.14	0.17	0.02	-0.02	0.12	0.04	0.14
s. random	48	4391416.637	5661534.619	0.15	0.20	0.00	0.02	0.19	0.11	0.10
s. random	49	4391411.577	5661506.105	0.14	0.09	0.01	-0.01	0.04	0.30	0.12
s. random	50	4391418.219	5661463.264	0.33	0.38	0.02	0.15	0.10	0.11	0.10

area	ID	x	y	05.104	05.117	05.133	05.146	05.161	05.174	05.188	05.204	05.217
s. random	51	4391396.886	5661443.993	0.23	0.36	0.33	0.54	0.42	0.48	0.40	0.46	0.53
s. random	52	4391366.658	5661446.880	0.19	0.28	0.15	0.65	0.51	0.32	0.49	0.41	0.27
s. random	53	4391358.949	5661456.720	0.79	0.28	0.41	0.62	0.46	0.67	0.57	0.48	0.51
s. random	54	4391357.192	5661484.990	0.25	0.15	0.17	0.33	0.25	0.36	0.19	0.26	0.33
s. random	55	4391333.108	5661502.728	0.32	0.37	0.35	0.41	0.31	0.44	0.41	0.35	0.30
s. random	56	4391376.069	5661499.587	0.33	-	0.30	0.37	0.26	0.32	0.27	0.23	0.33
s. random	57	4391393.175	5661565.696	0.33	0.19	0.21	0.27	0.15	0.38	0.23	0.21	0.33
s. random	58	4391399.536	5661574.112	0.44	0.25	0.25	0.56	0.41	0.62	0.36	0.35	0.52
s. random	59	4391383.163	5661581.773	0.15	0.47	0.44	0.79	0.47	0.64	0.27	0.35	0.46
nest large 1	60	4391437.504	5661620.387	0.35	0.22	0.25	0.46	2.24	0.53	0.27	0.33	0.44
nest large 1	61	4391441.098	5661598.065	0.26	0.19	0.16	0.20	0.56	0.30	0.10	0.10	0.27
nest large 1	62	4391443.823	5661607.943	0.40	0.26	0.28	0.35	0.14	0.38	0.31	0.30	0.36
nest large 1	63	4391450.884	5661613.363	0.38	0.20	0.20	0.32	0.28	0.41	0.27	0.32	0.44
nest small 1	64	4391450.182	5661615.168	0.40	0.51	0.59	0.80	0.25	0.57	0.47	0.44	0.44
nest small 1	65	4391453.563	5661615.982	0.25	0.21	0.22	0.31	0.42	0.44	0.33	0.48	0.42
nest large 1	66	4391457.250	5661628.502	0.23	0.00	0.22	0.35	0.31	0.43	0.25	0.32	0.43
nest small 1	67	4391455.279	5661621.542	0.33	0.40	0.30	0.53	0.22	0.46	0.52	0.54	0.40
nest small 1	68	4391456.971	5661614.726	0.28	0.16	0.21	0.35	0.40	0.47	0.26	0.26	0.31
nest small 1	69	4391456.624	5661614.607	0.33	0.28	0.27	0.47	0.27	0.51	0.32	0.25	0.38
nest large 1	70	4391456.115	5661603.379	0.17	0.56	0.47	0.53	0.31	1.02	0.58	0.75	1.02
nest small 1	71	4391458.964	5661616.915	0.14	0.16	0.23	0.33	0.43	0.42	0.40	0.40	0.37
nest small 1	72	4391458.504	5661620.863	0.27	0.25	0.19	0.33	0.35	0.40	0.19	0.23	0.32
nest large 1	73	4391460.883	5661621.625	0.25	0.32	0.31	0.32	0.23	0.46	0.22	0.27	0.35
nest small 1	74	4391465.809	5661627.022	0.12	0.19	0.17	0.40	0.33	0.46	0.19	0.23	0.37
nest large 1	75	4391464.734	5661606.858	0.22	0.23	0.25	0.40	0.25	0.40	0.30	0.30	0.36
nest large 1	76	4391463.297	5661603.530	0.42	0.15	0.07	0.31	0.26	0.32	0.14	0.15	0.22
nest large 1	77	4391463.608	5661595.834	0.35	0.48	0.37	0.73	0.16	0.63	0.48	0.53	0.57
nest large 2	78	4391529.609	5661529.579	0.26	0.37	0.25	0.41	0.47	0.26	0.16	0.22	0.22
nest large 2	79	4391534.905	5661546.944	0.25	0.19	0.25	0.33	0.25	0.49	0.26	0.38	0.61
nest large 2	80	4391535.212	5661549.797	0.35	0.20	0.33	0.53	0.31	0.65	0.59	0.74	0.63
nest large 2	81	4391535.253	5661530.975	0.37	0.23	0.32	0.44	0.44	0.58	0.33	0.40	0.52
nest large 2	82	4391539.962	5661543.388	0.36	0.17	0.28	0.47	0.31	0.58	0.37	0.42	0.57
nest large 2	83	4391543.294	5661547.147	0.47	0.30	0.38	0.38	0.33	0.31	0.37	0.44	0.41
nest large 2	84	4391546.968	5661559.352	0.25	0.23	0.31	0.44	0.28	0.41	0.32	0.33	0.38
nest small 2	85	4391548.809	5661532.750	0.41	0.10	0.12	0.22	0.14	0.43	0.06	0.19	0.41
nest large 2	86	4391549.874	5661532.482	0.32	0.09	0.16	0.19	0.11	0.28	0.11	0.16	0.20
nest small 2	87	4391549.859	5661536.795	0.36	0.17	0.23	0.21	0.22	0.38	0.12	0.21	0.30
nest small 2	88	4391550.708	5661541.041	0.27	0.28	0.22	0.09	0.31	0.77	0.35	0.28	0.43
nest large 2	89	4391554.366	5661558.117	0.25	0.28	0.32	0.44	0.49	0.62	-0.06	0.37	0.52
nest small 2	90	4391554.650	5661540.165	0.22	0.32	0.33	0.61	0.27	0.57	0.36	0.37	0.30
nest small 2	91	4391556.359	5661544.376	0.21	0.19	0.20	0.36	0.26	0.41	0.21	0.19	0.31
nest small 2	92	4391557.309	5661542.682	0.49	0.28	0.28	0.44	0.31	0.44	0.27	0.25	0.33
nest small 2	93	4391557.932	5661537.527	0.31	0.15	0.20	0.40	0.23	0.57	0.17	0.26	0.48
nest large 2	94	4391560.107	5661533.968	0.33	0.30	0.35	0.47	0.31	0.75	0.32	0.31	0.47
nest small 2	95	4391560.588	5661530.736	0.31		0.23	0.53	0.14	0.61	0.33	0.33	0.44
hyd. gradient	96			0.44		0.73	0.67	0.49	0.65	0.38	0.40	0.80
hyd. gradient	97			0.28		0.38	0.46	0.37	0.51	0.35	0.43	0.73
hyd. gradient	98			0.32		0.26	0.58	0.28	0.59	0.31	0.46	0.63
hyd. gradient	99			0.36		0.31	0.63	0.35	0.42	0.23	0.30	0.85
average CO ₂				0.34	0.27	0.30	0.45	0.35	0.52	0.32	0.39	0.47
SD				0.16	0.10	0.26	0.19	0.22	0.17	0.15	0.20	0.17
CV				45.61	37.26	85.08	41.85	64.58	33.41	45.61	52.13	35.42

area	ID	x	y	05.230	05.245	05.261	05.273	05.294	05.302	05.315	05.327	05.341
s. random	51	4391396.886	5661443.993	0.51	0.57	0.30	0.28	0.30	0.43	0.31	0.14	0.14
s. random	52	4391366.658	5661446.880	0.42	0.61	0.23	0.36	0.41	0.52	0.23	0.14	0.12
s. random	53	4391358.949	5661456.720	0.46	0.58	0.05	0.22	0.27	0.22	0.20	0.06	0.10
s. random	54	4391357.192	5661484.990	0.40	0.47	0.25	0.22	0.25	0.20	0.16	0.14	0.09
s. random	55	4391333.108	5661502.728	0.44	0.56	0.25	0.21	0.27	0.37	0.26	0.12	0.12
s. random	56	4391376.069	5661499.587	0.41	0.36	0.19	0.19	0.26	0.27	0.23	0.11	0.09
s. random	57	4391393.175	5661565.696	0.32	0.28	0.20	0.16	0.23	0.28	0.20	0.12	0.09
s. random	58	4391399.536	5661574.112	0.59	0.65	0.44	0.37	0.51	0.62	0.42	0.21	0.17
s. random	59	4391383.163	5661581.773	0.41	0.40	0.23	0.23	0.33	0.40	0.32	0.14	0.12
nest large 1	60	4391437.504	5661620.387	0.53	0.79	0.37	0.35	0.38	0.40	0.35	0.26	0.19
nest large 1	61	4391441.098	5661598.065	0.22	0.19	0.14	0.09	0.14	0.11	0.21	0.11	0.07
nest large 1	62	4391443.823	5661607.943	0.40	0.52	0.21	0.23	0.20	0.21	0.19	0.10	0.07
nest large 1	63	4391450.884	5661613.363	0.48	0.51	0.32	0.27	0.31	0.30	0.25	0.15	0.14
nest small 1	64	4391450.182	5661615.168	0.63	0.62	0.40	0.32	0.35	0.36	0.40	0.15	0.14
nest small 1	65	4391453.563	5661615.982	0.58	0.63	0.28	0.31	0.26	0.28	0.26	0.17	0.16
nest large 1	66	4391457.250	5661628.502	0.51	0.53	0.26	0.26	0.27	0.23	0.22	0.11	0.10
nest small 1	67	4391455.279	5661621.542	0.47	0.56	0.31	0.32	0.30	0.28	0.27	0.07	0.16
nest small 1	68	4391456.971	5661614.726	0.31	0.31	0.21	0.23	0.32	0.30	0.28	0.12	0.11
nest small 1	69	4391456.624	5661614.607	0.40	0.56	0.22	0.23	0.26	0.27	0.28	0.12	0.19
nest large 1	70	4391456.115	5661603.379	1.12	1.21	0.51	0.58	0.53	0.49	0.58	0.22	0.16
nest small 1	71	4391458.964	5661616.915	0.40	0.38	0.26	0.27	0.31	0.31	0.33	0.17	0.16
nest small 1	72	4391458.504	5661620.863	0.38	0.38	0.21	0.20	0.25	0.27	0.20	0.09	0.09
nest large 1	73	4391460.883	5661621.625	0.37	0.46	0.25	0.22	0.19	0.19	0.21	0.12	0.09
nest small 1	74	4391465.809	5661627.022	0.33	0.32	0.11	0.20	0.25	0.32	0.37	0.12	0.11
nest large 1	75	4391464.734	5661606.858	0.43	0.49	0.21	0.23	0.22	0.14	0.00	0.11	0.10
nest large 1	76	4391463.297	5661603.530	0.17	0.15	0.11	0.10	0.17	0.12	0.12	0.06	0.06
nest large 1	77	4391463.608	5661595.834	0.63	0.56	0.27	0.28	0.32	0.26	0.30	0.14	0.17
nest large 2	78	4391529.609	5661529.579	0.26	0.30	0.12	0.15	0.14	0.15	0.16	0.11	0.04
nest large 2	79	4391534.905	5661546.944	0.58	0.62	0.32	0.27	0.21	0.27	0.19	0.23	0.01
nest large 2	80	4391535.212	5661549.797	0.61	0.95	0.32	0.28	0.22	0.30	-0.01	0.28	0.10
nest large 2	81	4391535.253	5661530.975	0.70	0.85	0.38	0.31	0.32	0.32	0.35	0.22	0.11
nest large 2	82	4391539.962	5661543.388	0.53	0.68	0.42	0.35	0.26	0.28	0.27	0.20	0.09
nest large 2	83	4391543.294	5661547.147	0.46	0.64	0.40	0.40	0.33	0.36	0.33	0.11	0.17
nest large 2	84	4391546.968	5661559.352	0.35	0.32	0.25	0.14	0.17	0.22	0.27	0.15	0.07
nest small 2	85	4391548.809	5661532.750	0.36	0.46	0.25	0.09	0.19	0.21	0.05	0.14	0.07
nest large 2	86	4391549.874	5661532.482	0.19	0.22	0.11	0.20	0.16	0.22	0.20	0.11	0.10
nest small 2	87	4391549.859	5661536.795	0.27	0.28	0.20	0.37	0.26	0.26	0.21	0.10	0.09
nest small 2	88	4391550.708	5661541.041	0.40	1.15	0.57	0.32	0.27	0.26	0.27	0.16	0.10
nest large 2	89	4391554.366	5661558.117	0.59	0.64	0.36	0.57	0.38	0.37	0.41	0.28	0.16
nest small 2	90	4391554.650	5661540.165	0.35	0.58	0.32	0.06	0.27	0.22	0.25	0.14	0.06
nest small 2	91	4391556.359	5661544.376	0.26	0.19	0.06	0.23	0.12	0.15	0.14	0.04	0.06
nest small 2	92	4391557.309	5661542.682	0.26	0.43	0.22	0.26	0.16	0.17	0.22	0.11	-0.11
nest small 2	93	4391557.932	5661537.527	0.56	0.62	0.27	0.26	0.30	0.25	0.30	0.14	0.12
nest large 2	94	4391560.107	5661533.968	0.43	0.57	0.32	0.32	0.28	0.32	0.31	0.25	0.00
nest small 2	95	4391560.588	5661530.736	0.48	0.58	0.28	0.25	0.30	0.26	0.27	0.44	0.06
hyd. gradient	96			0.48	0.46	0.27	0.26	0.23	0.20	0.22	0.20	0.12
hyd. gradient	97			0.51	0.49	0.31	0.28	0.22	0.23	0.21	0.14	-0.10
hyd. gradient	98			0.70	0.69	0.49	0.14	0.21	0.23	0.27	0.12	0.10
hyd. gradient	99			0.47	0.47	0.52	0.26	0.22	0.30	0.16	0.09	0.10
average CO ₂				0.49	0.54	0.30	0.29	0.32	0.37	0.26	0.15	0.11
SD				0.18	0.22	0.14	0.14	0.14	0.18	0.10	0.07	0.08
CV				36.58	40.88	45.39	47.91	42.80	48.99	38.65	46.08	67.75

area	ID	x	y	05.355	06.004	06.032	06.047	06.074	06.089	06.102
s. random	51	4391396.886	5661443.993	0.07	0.23	0.02	-0.07	0.31	0.10	0.22
s. random	52	4391366.658	5661446.880	0.10	0.04	0.09	-0.07	0.47	0.15	0.15
s. random	53	4391358.949	5661456.720	0.15	0.09	0.04	-0.05	0.27	0.20	0.79
s. random	54	4391357.192	5661484.990	0.06	0.15	0.04	-0.12	0.48	0.37	0.11
s. random	55	4391333.108	5661502.728	0.25	0.25	0.01	0.07	0.20	0.05	0.10
s. random	56	4391376.069	5661499.587	0.15	0.16	0.06	-0.11	0.19	0.25	0.10
s. random	57	4391393.175	5661565.696	0.02	0.30	0.02	-0.02	0.17	0.02	0.14
s. random	58	4391399.536	5661574.112	0.12	0.26	0.12	0.14	0.06	0.19	0.14
s. random	59	4391383.163	5661581.773	0.14	0.20	0.00	0.03	0.09	0.24	0.20
nest large 1	60	4391437.504	5661620.387	0.17	0.14	0.01	-0.02	0.57	0.23	0.15
nest large 1	61	4391441.098	5661598.065	0.12	0.07	0.05	-0.06	0.15	0.36	0.14
nest large 1	62	4391443.823	5661607.943	0.14	0.21	0.02	-0.11	0.02	0.24	0.09
nest large 1	63	4391450.884	5661613.363	0.16	0.22	0.07	0.02	0.07	0.28	0.11
nest small 1	64	4391450.182	5661615.168	0.25	0.11	0.02	0.10	0.20	0.28	0.11
nest small 1	65	4391453.563	5661615.982	0.19	0.17	0.02	-0.08	0.25	0.16	0.14
nest large 1	66	4391457.250	5661628.502	0.09	0.18	0.01	0.32	0.15	0.20	0.11
nest small 1	67	4391455.279	5661621.542	0.11	0.20	0.40	0.06	0.00	0.32	0.09
nest small 1	68	4391456.971	5661614.726	0.09	0.17	0.01	0.01	0.14	0.23	0.20
nest small 1	69	4391456.624	5661614.607	0.12	0.08	0.04	0.23	0.28	0.28	0.12
nest large 1	70	4391456.115	5661603.379	0.20	0.08	0.09	0.04	0.21	0.19	0.11
nest small 1	71	4391458.964	5661616.915	0.12	0.07	0.00	-0.06	0.10	0.19	0.19
nest small 1	72	4391458.504	5661620.863	0.07	0.17	0.01	0.14	0.06	0.31	0.15
nest large 1	73	4391460.883	5661621.625	0.09	0.02	0.00	-0.07	0.05	0.17	0.07
nest small 1	74	4391465.809	5661627.022	0.11	0.34	0.01	0.13	0.09	0.30	0.14
nest large 1	75	4391464.734	5661606.858	0.10	0.16	0.02	0.05	0.20	0.26	0.15
nest large 1	76	4391463.297	5661603.530	0.06	0.20	0.01	0.01	0.10	0.28	0.11
nest large 1	77	4391463.608	5661595.834	0.17	0.19	0.02	0.05	0.05	0.13	0.10
nest large 2	78	4391529.609	5661529.579	0.04	0.19	0.00	0.07	0.17	0.27	0.15
nest large 2	79	4391534.905	5661546.944	0.01	0.04	0.04	0.06	0.16	0.35	0.11
nest large 2	80	4391535.212	5661549.797	0.10	0.19	0.00	0.22	0.07	0.22	0.17
nest large 2	81	4391535.253	5661530.975	0.11	0.12	0.01	0.13	0.05	0.25	0.23
nest large 2	82	4391539.962	5661543.388	0.09	0.25	0.04	0.28	0.20	0.19	0.15
nest large 2	83	4391543.294	5661547.147	0.17	0.26	0.37	-0.03	0.01	0.19	0.15
nest large 2	84	4391546.968	5661559.352	0.07	0.24	0.01	0.01	0.01	0.23	0.23
nest small 2	85	4391548.809	5661532.750	0.07	0.32	0.00	0.04	0.11	0.08	0.14
nest large 2	86	4391549.874	5661532.482	0.10	0.20	0.05	-0.03	0.05	0.13	0.12
nest small 2	87	4391549.859	5661536.795	0.09	0.07	0.04	0.07	0.07	0.24	0.00
nest small 2	88	4391550.708	5661541.041	0.10	0.12	0.01	0.04	0.09	0.26	0.00
nest large 2	89	4391554.366	5661558.117	0.16	0.18	0.05	0.26	0.09	0.32	0.00
nest small 2	90	4391554.650	5661540.165	0.06	0.24	0.00	0.08	0.14	0.15	0.00
nest small 2	91	4391556.359	5661544.376	0.06	0.07	0.12	0.16	0.10	0.13	0.00
nest small 2	92	4391557.309	5661542.682	-0.11	0.21	0.05	0.08	0.05	0.31	0.00
nest small 2	93	4391557.932	5661537.527	0.12	0.23	0.02	0.01	0.17	0.06	0.00
nest large 2	94	4391560.107	5661533.968	0.00	0.08	0.01	0.10	0.10	0.10	0.00
nest small 2	95	4391560.588	5661530.736	0.06	0.20	0.02	-0.04	0.12	0.37	0.00
hyd. gradient	96			0.10	0.19	0.01	0.13	0.06	0.38	0.17
hyd. gradient	97			0.10	0.12	0.01	0.10	0.04	0.34	0.17
hyd. gradient	98			0.11	0.12	0.00	-0.04	0.16	0.13	0.15
hyd. gradient	99			0.05	0.02	0.01	0.07	0.04	0.36	0.14
average CO ₂				0.15	0.16	0.05	0.05	0.13	0.20	0.14
SD				0.11	0.08	0.09	0.10	0.18	0.09	0.12
CV				78.44	53.53	187.22	191.99	145.21	45.56	84.13

Second measurement series

ID	x	y	05.237	05.251	05.265	05.279	05.293	05.306	05.321	05.334	05.348	06.011	06.024
1	4391584.14	5661617.88	0.32	0.40	0.36	0.36	0.15	0.49	0.15	0.22	0.14	0.15	0.01
2	4391601.18	5661601.59	0.38	0.38	0.28	0.17	0.23	0.32	0.07	0.11	0.07	0.07	0.00
3	4391618.03	5661583.68	0.69	0.94	0.41	0.35	0.25	0.69	0.38	0.23	0.23	0.28	0.01
4	4391632.28	5661564.28	0.33	0.33	0.26	0.19	0.19	0.28	0.14	0.09	0.07	0.01	0.00
5	4391642.35	5661543.76	0.28	0.33	0.19	0.15	0.16	0.15	0.15	0.09	0.06	0.06	0.00
6	4391640.01	5661524.41	0.56	0.46	0.32	0.30	0.23	0.53	0.27	0.14	0.14	0.06	0.00
7	4391614.74	5661545.93	0.64	0.65	0.36	0.31	0.31	0.51	0.27	0.16	0.15	0.28	0.00
8	4391593.31	5661565.64	0.80	0.62	0.36	0.33	0.21	0.52	0.21	0.19	0.12	0.10	0.00
9	4391571.79	5661586.98	0.28	0.35	0.22	0.17	0.26	0.31	0.15	0.16	0.09	0.07	0.00
10	4391552.02	5661613.23	0.43	0.38	0.25	0.22	0.17	0.28	0.19	0.16	0.17	0.20	-0.01
11	4391538.22	5661596.95	0.47	0.47	0.33	0.22	0.17	0.36	0.15	0.09	0.07	0.09	0.04
12	4391553.35	5661574.24	0.51	0.43	0.31	0.36	0.14	0.33	0.16	0.11	0.09	0.02	0.04
13	4391569.49	5661547.76	0.56	0.63	0.40	0.06	0.26	0.42	0.23	0.07	0.14	0.15	0.04
14	4391585.15	5661522.70	0.22	0.42	0.20	0.22	0.27	0.32	0.11	0.15	0.10	0.30	0.04
15	4391600.88	5661498.65	0.57	0.46	0.30	0.27	0.23	0.16	0.16	0.11	0.12	0.09	0.05
16	4391576.83	5661482.75	0.38	0.41	0.22	0.19	0.12	0.40	0.12	0.11	0.07	0.09	0.05
17	4391563.07	5661504.54	0.43	0.56	0.33	0.30	0.31	0.43	0.20	0.14	0.11	0.14	0.05
18	4391545.44	5661529.22	0.78	0.62	0.48	0.44	0.23	0.28	0.10	0.11	0.11	0.07	0.05
19	4391534.02	5661546.01	0.68	0.75	0.44	0.40	0.37	0.06	0.26	0.21	0.22	0.26	0.04
20	4391521.51	5661563.32	0.35	0.44	0.25	0.17	0.28	0.77	0.19	0.09	0.10	0.06	0.02
21	4391507.32	5661582.38	0.69	0.58	0.40	0.37	0.31	0.64	0.32	0.14	0.21	0.05	0.07
22	4391509.06	5661598.16	0.30	0.36	0.19	0.17	0.13	0.35	0.12	0.07	0.07	0.02	0.04
23	4391500.26	5661594.09	0.56	0.41	0.28	0.26	0.17	0.38	0.09	0.12	0.10	0.14	0.04
24	4391491.39	5661604.94	0.68	0.51	0.38	0.31	0.26	0.56	0.21	0.20	0.16	0.12	0.06
25	4391464.89	5661575.56	0.48	0.44	0.36	0.30	0.22	0.42	0.05	0.30	0.11	0.10	0.05
26	4391486.21	5661554.78	0.56	0.47	0.28	0.26	0.21	0.40	0.25	0.25	0.14	0.04	0.05
27	4391492.33	5661564.21	0.37	0.23	0.21	0.23	0.16	0.35	0.20	0.20	0.15	0.07	0.01
28	4391500.64	5661562.11	0.89	0.86	0.58	0.54	0.23	0.65	0.26	0.16	0.14	0.07	0.04
29	4391484.73	5661535.60	0.38	0.35	0.35	0.17	0.20	0.43	0.30	0.15	0.12	0.20	0.01
30	4391492.90	5661532.59	-	0.41	0.25	0.16	0.20	0.37	0.21	0.09	0.07	0.04	0.04
31	4391503.33	5661530.52	0.38	0.44	0.25	0.22	0.20	0.31	0.37	0.14	0.09	0.14	0.04
32	4391523.02	5661509.81	0.65	0.69	0.46	0.32	0.33	0.67	0.17	0.23	0.11	0.09	0.06
33	4391543.73	5661487.49	0.31	0.61	0.37	0.31	0.04	0.86	0.17	0.14	0.10	0.10	0.05
34	4391565.52	5661465.10	0.68	0.48	0.37	0.33	0.27	0.63	0.22	0.12	0.09	0.02	0.07
35	4391549.37	5661463.21	0.40	0.62	0.27	0.26	0.26	0.63	0.17	0.15	0.10	0.12	0.06
36	4391524.52	5661476.99	0.35	0.37	0.26	0.26	0.20	0.17	0.26	0.16	0.11	0.21	0.09
37	4391499.53	5661491.06	0.63	0.77	0.43	0.25	0.27	0.26	0.22	0.23	0.15	0.22	0.14
38	4391483.30	5661503.20	0.48	0.43	0.35	0.30	0.23	0.28	0.23	0.23	0.15	0.14	0.06
39	4391477.97	5661505.58	0.57	0.73	0.43	0.32	0.38	0.85	0.51	0.64	0.46	0.27	0.09
40	4391472.17	5661504.36	0.40	0.38	0.25	0.16	0.20	0.43	0.21	0.12	0.12	0.22	0.05
41	4391452.62	5661505.19	0.20	0.38	0.23	0.14	0.17	0.20	0.11	0.06	0.06	0.05	0.06
42	4391451.20	5661509.62	0.30	0.42	0.23	0.17	0.21	0.00	0.16	0.11	0.05	0.02	0.04
43	4391451.26	5661510.46	0.26	0.36	0.21	0.10	0.19	0.31	0.11	0.12	0.11	0.04	0.02
44	4391451.55	5661510.72	0.40	0.38	0.32	0.26	0.21	0.35	0.16	0.10	0.11	0.04	0.04
45	4391452.16	5661510.92	0.35	0.38	0.31	0.20	0.20	0.41	0.14	0.07	0.07	0.02	0.02
46	4391454.16	5661519.49	0.64	0.43	0.32	0.33	0.25	0.47	0.17	0.12	0.11	0.05	0.07
47	4391452.65	5661529.84	0.31	0.37	0.25	0.22	0.21	0.42	0.12	0.09	0.09	0.05	0.05
48	4391452.56	5661535.99	0.54	0.46	0.32	0.32	0.21	0.14	0.10	0.10	0.10	0.06	0.05
49	4391452.72	5661536.22	0.28	0.32	0.17	0.14	0.17	0.27	0.11	0.06	0.06	0.04	0.02
50	4391452.93	5661536.60	0.64	0.40	0.41	0.19	0.25	0.40	0.19	0.10	0.06	0.06	0.02

ID	x	y	06.039	06.053	06.081	06.110	06.123	06.137	06.149	06.165	06.179	06.193	06.207
1	4391584.14	5661617.88	0.09	0.04	0.53	0.26	0.27	0.59	0.40	0.54	0.73	0.57	0.33
2	4391601.18	5661601.59	3.24	0.05	0.12	0.31	0.38	0.64	0.43	0.43	0.47	0.58	0.43
3	4391618.03	5661583.68	0.09	0.01	0.32	0.27	0.27	0.65	0.51	0.84	0.68	0.67	0.54
4	4391632.28	5661564.28	0.02	0.00	0.14	0.15	0.23	0.36	0.26	0.38	0.46	0.40	0.30
5	4391642.35	5661543.76	0.01	0.05	0.05	0.09	0.14	0.25	0.21	0.27	0.26	0.30	0.28
6	4391640.01	5661524.41	0.06	0.14	0.23	0.26	0.36	0.37	0.40	0.48	0.58	0.65	0.88
7	4391614.74	5661545.93	0.02	0.07	0.11	0.16	0.27	0.52	0.38	0.63	0.54	0.51	0.22
8	4391593.31	5661565.64	0.05	0.00	0.00	0.21	0.35	0.63	0.40	0.68	0.59	0.63	0.49
9	4391571.79	5661586.98	0.07	0.01	0.01	0.23	0.26	0.37	0.33	0.51	0.36	0.41	0.35
10	4391552.02	5661613.23	0.05	0.07	0.16	0.22	0.28	0.38	0.31	0.46	0.44	0.43	0.31
11	4391538.22	5661596.95	0.06	0.01	0.09	0.21	0.23	0.33	0.22	0.38	0.41	0.43	0.30
12	4391553.35	5661574.24	0.02	0.05	0.11	0.19	0.26	0.65	0.30	0.49	0.54	0.53	0.31
13	4391569.49	5661547.76	-0.17	-0.02	0.02	0.20	0.16	0.42	0.27	0.41	0.37	0.42	0.26
14	4391585.15	5661522.70	0.01	0.02	0.04	0.32	0.17	0.40	0.23	0.33	0.26	0.51	0.48
15	4391600.88	5661498.65	0.02	-0.01	0.00	0.27	0.43	0.35	0.36	0.42	0.51	0.43	0.27
16	4391576.83	5661482.75	-0.06	0.04	0.19	0.14	0.25	0.47	0.26	0.53	0.41	0.52	0.42
17	4391563.07	5661504.54	0.02	0.00	0.15	0.28	0.32	0.46	0.35	0.58	0.54	0.62	0.35
18	4391545.44	5661529.22	0.01	0.02	0.02	0.14	0.21	0.36	0.25	0.53	0.69	0.58	0.27
19	4391534.02	5661546.01	0.02	0.02	0.22	0.33	0.32	0.78	0.41	0.80	0.84	0.68	0.67
20	4391521.51	5661563.32	0.04	0.07	0.15	0.12	0.19	0.40	0.20	0.44	0.43	0.53	0.64
21	4391507.32	5661582.38	0.04	0.04	0.12	0.25	0.36	0.54	0.42	0.67	0.68	0.63	0.61
22	4391509.06	5661598.16	0.01	0.10	0.12	0.16	0.21	0.36	0.32	0.36	0.46	0.43	0.59
23	4391500.26	5661594.09	0.04	0.06	0.10	0.14	0.20	0.38	0.23	0.40	0.36	0.38	0.32
24	4391491.39	5661604.94	0.02	0.06	0.14	0.23	0.32	0.70	0.53	0.69	0.94	0.58	0.57
25	4391464.89	5661575.56	-0.04	0.10	0.14	0.15	0.26	0.27	1.14	1.23	1.07	0.80	0.61
26	4391486.21	5661554.78	0.04	0.16	0.06	0.19	0.22	0.53	0.40	0.46	0.54	0.42	0.38
27	4391492.33	5661564.21	0.02	0.09	0.14	0.19	0.30	0.62	0.36	0.43	0.51	0.40	0.25
28	4391500.64	5661562.11	0.02	0.06	0.14	0.30	0.47	1.30	0.63	1.02	1.59	1.46	1.26
29	4391484.73	5661535.60	0.04	0.05	0.15	0.31	0.36	0.44	0.49	0.73	0.57	0.56	0.43
30	4391492.90	5661532.59	0.02	0.10	0.16	0.23	0.28	0.42	0.28	0.51	0.46	0.49	0.15
31	4391503.33	5661530.52	0.05	0.07	0.11	0.17	0.27	1.58	0.54	0.64	1.25	0.81	0.43
32	4391523.02	5661509.81	0.04	0.09	0.15	0.30	0.47	0.67	0.43	0.64	1.12	0.70	0.52
33	4391543.73	5661487.49	0.04	0.06	0.10	0.17	0.28	0.79	0.40	0.38	0.51	0.68	0.73
34	4391565.52	5661465.10	0.05	0.07	0.12	0.21	0.49	0.99	0.47	0.80	0.79	0.79	0.68
35	4391549.37	5661463.21	0.05	0.10	0.07	0.25	0.31	0.41	0.36	0.51	0.64	0.65	0.54
36	4391524.52	5661476.99	0.00	0.09	0.07	0.17	0.35	0.63	0.35	0.42	0.64	0.43	0.42
37	4391499.53	5661491.06	0.04	0.12	0.09	0.30	0.31	0.43	0.31	0.48	0.49	0.65	0.56
38	4391483.30	5661503.20	0.05	0.12	0.11	0.31	0.33	1.54	0.74	0.61	0.70	0.65	0.64
39	4391477.97	5661505.58	0.04	0.06	0.10	0.35	0.47	1.46	0.94	1.09	1.38	0.62	0.26
40	4391472.17	5661504.36	0.02	0.07	0.06	0.22	0.21	0.57	0.22	0.41	0.43	0.49	0.37
41	4391452.62	5661505.19	0.02	0.07	0.10	0.19	0.26	1.04	0.38	0.40	0.47	0.62	0.38
42	4391451.20	5661509.62	0.01	0.02	0.05	0.12	0.20	0.47	0.30	0.43	0.53	0.52	0.61
43	4391451.26	5661510.46	0.04	0.02	0.04	0.15	0.21	0.47	0.20	0.33	0.33	0.48	0.37
44	4391451.55	5661510.72	0.00	0.00	0.01	0.22	0.33	0.77	0.30	0.40	0.43	0.46	0.35
45	4391452.16	5661510.92	0.01	0.00	0.02	0.15	0.20	0.83	0.23	0.36	0.42	0.51	0.46
46	4391454.16	5661519.49	0.04	0.09	0.14	0.30	0.35	0.70	0.38	0.63	0.62	0.86	0.35
47	4391452.65	5661529.84	0.00	0.02	0.07	0.22	0.23	0.47	0.30	0.42	0.37	0.42	0.40
48	4391452.56	5661535.99	0.02	0.05	0.11	0.31	0.35	0.41	0.31	0.44	0.42	0.47	0.47
49	4391452.72	5661536.22	0.01	0.05	0.02	0.22	0.23	0.54	0.28	0.32	0.28	0.40	0.48
50	4391452.93	5661536.60	0.01	0.00	0.01	0.19	0.27	0.43	0.31	0.52	0.64	0.48	0.27

ID	x	y	06.221	06.235	06.263	06.277	06.290	06.305	06.319	06.333	06.354	07.010	07.025
1	4391584.14	5661617.88	0.44	0.41	0.21	0.53	0.14	0.33	0.30	0.26	0.15	0.21	0.06
2	4391601.18	5661601.59	0.44	0.32	0.32	0.48	0.05	0.46	0.30	0.20	0.07	0.20	0.02
3	4391618.03	5661583.68	0.57	0.53	1.11	0.56	0.36	0.90	0.38	0.41	0.31	0.59	-0.23
4	4391632.28	5661564.28	0.30	0.23	0.31	0.26	0.12	0.25	0.36	0.12	0.07	0.17	0.07
5	4391642.35	5661543.76	0.21	0.19	0.22	0.25	0.15	0.23	0.28	0.16	0.07	0.17	0.09
6	4391640.01	5661524.41	0.54	0.38	0.30	0.35	0.09	0.19	0.16	0.27	0.20	0.25	0.12
7	4391614.74	5661545.93	0.53	0.37	0.32	0.27	0.20	0.31	0.32	0.27	0.14	0.23	0.04
8	4391593.31	5661565.64	0.41	0.41	0.27	0.35	0.21	0.28	0.37	0.19	0.17	0.14	0.05
9	4391571.79	5661586.98	0.25	0.19	0.19	0.19	0.15	0.19	0.38	0.19	0.12	0.15	0.09
10	4391552.02	5661613.23	0.43	0.38	0.28	0.32	0.20	0.30	0.28	0.23	0.14	0.19	0.07
11	4391538.22	5661596.95	0.41	0.41	0.35	0.37	0.19	0.36	0.28	0.23	0.15	0.17	0.06
12	4391553.35	5661574.24	0.35	0.37	0.25	0.30	0.21	0.22	0.27	0.17	0.07	0.15	0.07
13	4391569.49	5661547.76	0.33	0.36	0.32	0.33	0.20	0.27	0.48	0.23	0.16	0.25	0.01
14	4391585.15	5661522.70	0.37	0.27	0.22	0.27	0.09	0.33	0.28	0.15	0.10	0.07	0.04
15	4391600.88	5661498.65	0.38	0.44	0.33	0.27	0.26	0.27	0.31	0.28	0.14	0.21	0.06
16	4391576.83	5661482.75	0.43	0.30	0.21	0.26	0.09	0.27	0.23	0.15	0.11	0.15	0.07
17	4391563.07	5661504.54	0.44	0.36	0.30	0.37	0.21	0.35	0.32	0.22	0.14	0.25	0.09
18	4391545.44	5661529.22	0.33	0.36	0.28	0.23	0.10	0.25	0.38	0.22	0.02	0.14	0.14
19	4391534.02	5661546.01	0.62	0.57	0.33	0.31	0.22	0.31	0.49	0.33	0.15	0.20	0.02
20	4391521.51	5661563.32	0.48	0.37	0.26	0.26	0.10	0.40	0.63	0.21	0.20	0.25	0.09
21	4391507.32	5661582.38	0.53	0.56	0.35	0.35	0.22	0.43	0.48	0.27	0.12	0.31	0.06
22	4391509.06	5661598.16	0.33	0.36	0.26	0.25	-0.06	0.19	0.19	0.19	0.11	0.23	0.09
23	4391500.26	5661594.09	0.35	0.32	0.23	0.28	0.10	0.28	0.46	0.20	0.12	0.17	0.05
24	4391491.39	5661604.94	0.38	0.65	0.27	0.32	0.16	0.20	0.38	0.19	0.10	0.16	0.09
25	4391464.89	5661575.56	0.68	0.62	0.46	0.42	0.27	0.48	0.43	0.11	0.16	0.49	0.12
26	4391486.21	5661554.78	0.28	0.31	0.22	0.25	0.12	0.21	0.28	0.16	0.10	0.12	-0.47
27	4391492.33	5661564.21	0.35	0.32	0.22	0.26	0.00	0.25	0.48	0.26	0.15	0.28	0.04
28	4391500.64	5661562.11	0.64	0.59	0.33	0.46	0.14	0.32	0.46	0.25	0.10	0.21	-0.16
29	4391484.73	5661535.60	0.37	0.35	0.26	0.31	0.19	-0.09	0.33	0.20	0.12	0.15	0.07
30	4391492.90	5661532.59	0.32	0.26	0.11	0.00	-0.07	0.16	0.21	0.12	0.06	0.11	0.02
31	4391503.33	5661530.52	0.44	0.41	0.31	0.41	0.12	0.44	0.61	0.31	0.23	0.36	0.05
32	4391523.02	5661509.81	0.53	0.57	0.43	0.36	0.33	0.27	0.43	0.36	0.21	0.30	0.00
33	4391543.73	5661487.49	0.62	0.52	0.70	0.58	0.28	0.48	0.15	0.12	0.07	0.22	0.06
34	4391565.52	5661465.10	0.46	0.46	0.35	0.35	0.15	0.31	0.41	0.27	0.16	0.22	0.11
35	4391549.37	5661463.21	0.44	0.33	0.33	0.06	0.19	0.25	0.21	0.17	0.05	0.22	-0.94
36	4391524.52	5661476.99	0.37	0.36	0.23	0.33	0.20	0.20	0.41	0.28	0.12	0.17	0.05
37	4391499.53	5661491.06	0.41	0.38	0.32	0.28	0.19	0.33	0.44	0.31	0.15	0.19	0.10
38	4391483.30	5661503.20	0.48	0.44	0.35	0.42	0.19	0.35	0.36	0.21	0.14	0.21	0.07
39	4391477.97	5661505.58	0.69	0.68	0.32	0.44	0.19	0.44	0.80	1.02	0.62	0.90	0.05
40	4391472.17	5661504.36	0.37	0.30	0.25	0.26	0.12	0.43	0.32	0.19	0.11	0.15	0.05
41	4391452.62	5661505.19	0.31	0.25	0.28	0.42	0.20	0.35	0.36	0.16	0.07	0.09	0.10
42	4391451.20	5661509.62	0.42	0.40	0.33	0.31	0.17	0.61	0.31	0.07	0.14	0.23	0.01
43	4391451.26	5661510.46	0.37	0.27	0.28	0.23	0.19	0.70	0.27	0.19	0.09	0.17	-0.07
44	4391451.55	5661510.72	0.43	0.33	0.27	0.31	0.15	0.72	0.36	0.23	0.09	0.12	0.06
45	4391452.16	5661510.92	0.47	0.38	0.27	0.32	0.01	0.70	0.35	0.14	0.09	0.19	0.04
46	4391454.16	5661519.49	0.41	0.49	0.27	0.30	0.15	0.33	0.35	0.21	0.07	0.16	0.02
47	4391452.65	5661529.84	0.35	0.27	0.28	0.23	0.20	0.32	0.35	0.12	0.15	0.23	0.05
48	4391452.56	5661535.99	0.32	0.37	0.32	0.30	0.22	0.40	0.30	0.20	0.12	0.19	0.09
49	4391452.72	5661536.22	0.32	0.36	0.30	0.32	0.17	0.26	0.33	0.19	0.09	0.16	0.36
50	4391452.93	5661536.60	0.44	0.47	0.25	0.30	0.20	0.33	0.36	0.26	0.12	0.17	0.09

ID	x	y	07.038	07.052	07.066	07.080	07.094	07.108	07.122	07.136	07.150	07.164
1	4391584.14	5661617.88	0.14	0.00	0.16	0.14	0.20	0.22	0.31	0.20	0.41	0.79
2	4391601.18	5661601.59	0.10	-0.01	0.20	0.14	0.16	0.19	0.23	0.16	0.17	0.23
3	4391618.03	5661583.68	0.17	2.49	0.22	0.10	0.27	0.31	0.37	0.65	0.49	1.31
4	4391632.28	5661564.28	0.10	0.09	0.11	0.12	0.15	0.16	0.25	0.16	0.22	0.35
5	4391642.35	5661543.76	0.06	0.09	0.15	0.10	0.10	0.15	0.15	0.57	0.23	0.44
6	4391640.01	5661524.41	0.00	0.06	0.09	0.31	0.11	0.12	0.22	0.36	0.22	0.35
7	4391614.74	5661545.93	0.09	19.21	0.15	0.02	0.10	0.14	0.21	0.33	0.36	0.93
8	4391593.31	5661565.64	0.05	0.15	0.25	0.17	0.17	0.23	0.31	0.40	0.26	0.83
9	4391571.79	5661586.98	0.14	0.12	0.12	0.28	0.10	0.17	0.19	0.59	0.19	0.38
10	4391552.02	5661613.23	0.10	0.11	0.17	0.19	-0.04	0.26	0.27	0.58	0.40	0.95
11	4391538.22	5661596.95	0.12	0.11	0.14	0.16	0.11	0.16	0.26	0.49	0.23	0.47
12	4391553.35	5661574.24	0.10	0.10	0.16	0.16	0.17	0.25	0.23	0.26	0.31	0.81
13	4391569.49	5661547.76	0.11	0.10	0.16	0.09	0.09	0.21	0.22	0.22	0.41	0.58
14	4391585.15	5661522.70	0.07	0.15	0.19	0.19	0.11	0.17	0.16	0.44	0.30	0.49
15	4391600.88	5661498.65	0.11	0.15	0.19	0.38	0.16	0.21	-0.28	0.86	0.83	2.24
16	4391576.83	5661482.75	0.11	0.11	0.11	0.12	0.14	0.21	0.22	0.28	0.32	0.52
17	4391563.07	5661504.54	0.07	0.12	0.20	0.20	0.48	0.30	0.25	0.44	0.58	0.86
18	4391545.44	5661529.22	0.12	0.09	0.28	0.20	0.14	0.10	0.19	0.36	0.31	0.67
19	4391534.02	5661546.01	0.10	0.11	0.14	0.16	0.10	0.26	0.40	0.36	0.59	1.26
20	4391521.51	5661563.32	0.09	0.10	0.12	0.02	0.14	0.15	0.22	0.46	0.22	0.42
21	4391507.32	5661582.38	0.17	0.06	0.19	0.20	0.23	0.19	0.47	0.31	0.48	0.67
22	4391509.06	5661598.16	0.07	1.57	0.21	0.10	0.12	0.09	0.14	0.22	0.30	0.69
23	4391500.26	5661594.09	0.10	-3.25	0.16	0.19	0.19	0.17	0.17	0.70	0.25	0.43
24	4391491.39	5661604.94	0.11	0.00	0.19	0.11	0.20	0.28	0.35	0.42	0.47	0.88
25	4391464.89	5661575.56	0.10	0.12	0.25	0.20	0.22	0.30	0.26	0.46	0.84	1.01
26	4391486.21	5661554.78	0.06	-0.23	0.11	0.16	0.11	0.16	0.25	0.41	0.35	0.89
27	4391492.33	5661564.21	0.15	-0.04	0.22	0.04	0.23	0.32	0.27	0.19	0.47	0.64
28	4391500.64	5661562.11	0.11	-0.16	0.17	0.14	0.25	0.26	0.43	0.41	0.38	1.12
29	4391484.73	5661535.60	0.10	0.19	0.17	0.25	0.11	0.17	0.25	0.56	0.48	0.77
30	4391492.90	5661532.59	0.06	0.02	0.11	-0.02	0.14	0.21	0.17	0.37	0.36	0.43
31	4391503.33	5661530.52	0.11	0.19	0.22	0.01	0.21	0.36	0.23	0.51	0.52	0.98
32	4391523.02	5661509.81	0.15	0.20	0.20	0.17	0.20	0.31	0.43	0.32	0.28	0.67
33	4391543.73	5661487.49	0.07	0.14	0.09	0.07	0.15	0.17	0.26	0.46	0.31	0.46
34	4391565.52	5661465.10	0.12	0.16	0.23	0.15	0.26	0.26	0.17	0.38	0.40	0.58
35	4391549.37	5661463.21	0.16	0.15	0.09	0.19	0.15	0.23	0.15	0.63	0.21	0.38
36	4391524.52	5661476.99	0.11	0.15	0.17	0.11	0.21	0.27	0.30	0.32	0.54	0.80
37	4391499.53	5661491.06	0.09	0.10	0.14	0.06	0.17	0.35	0.04	0.53	0.31	0.49
38	4391483.30	5661503.20	0.09	0.14	0.11	0.20	0.19	0.28	0.48	0.22	0.33	0.54
39	4391477.97	5661505.58	0.19	0.46	0.32	0.07	0.38	1.16	0.14	0.32	0.77	1.07
40	4391472.17	5661504.36	0.11	0.10	0.14	0.20	0.23	0.32	0.15	0.20	0.20	0.74
41	4391452.62	5661505.19	0.07	0.07	0.11	0.00	0.15	0.17	0.15	0.46	0.23	0.41
42	4391451.20	5661509.62	0.11	0.11	0.14	0.26	0.20	0.40	0.16	0.19	0.35	0.58
43	4391451.26	5661510.46	0.07	0.14	0.10	0.11	0.22	0.22	0.20	0.53	0.23	0.40
44	4391451.55	5661510.72	0.10	0.11	0.14	0.16	0.11	0.26	0.15	0.22	0.30	0.10
45	4391452.16	5661510.92	0.10	0.17	0.16	0.27	0.15	0.27	0.28	0.53	0.31	0.83
46	4391454.16	5661519.49	0.11	0.09	0.12	0.14	0.17	-0.02	0.17	0.40	0.26	0.68
47	4391452.65	5661529.84	0.15	0.11	0.12	0.02	0.14	0.21	0.00	0.46	0.40	0.57
48	4391452.56	5661535.99	0.16	0.17	0.26	0.10	0.25	0.31	0.26	0.77	0.43	0.65
49	4391452.72	5661536.22	0.16	0.14	0.49	0.06	0.12	0.26	0.37	0.32	0.35	0.85
50	4391452.93	5661536.60	0.15	0.10	0.15	0.10	0.19	0.17	0.11	0.56	0.63	0.83

ID	x	y	05.237	05.251	05.265	05.279	05.293	05.306	05.321	05.334	05.348	06.011	06.024
51	4391453.20	5661537.09	0.32	0.44	0.28	0.23	0.28	0.31	0.17	0.10	0.09	0.06	0.01
52	4391452.65	5661553.71	0.37	0.41	0.21	0.27	0.23	0.41	0.14	0.12	0.12	0.09	0.09
53	4391445.40	5661552.25	0.17	0.25	0.15	0.02	0.14	0.21	0.10	0.05	0.06	0.02	0.02
54	4391430.59	5661539.41	0.44	0.44	0.30	0.23	0.21	0.35	0.14	0.06	0.09	0.12	0.04
55	4391435.71	5661528.65	0.41	0.40	0.27	0.20	0.17	0.35	0.32	0.10	0.14	0.09	0.02
56	4391410.58	5661520.99	0.54	0.51	0.37	0.25	0.23	0.22	0.26	0.10	0.10	0.17	0.06
57	4391425.38	5661502.86	1.16	0.61	0.38	0.44	0.28	0.42	0.35	0.17	0.16	0.10	0.10
58	4391431.66	5661502.18	0.62	0.59	0.36	0.38	0.23	0.42	0.15	0.02	0.11	0.05	0.06
59	4391448.97	5661495.27	0.68	0.64	0.46	1.05	0.28	0.46	0.17	0.17	0.07	0.02	-0.02
60	4391449.47	5661495.60	0.42	0.44	0.27	0.33	0.22	0.33	0.16	0.15	0.09	0.07	0.04
61	4391449.85	5661495.82	0.40	0.48	0.28	0.23	0.25	0.46	0.20	0.14	0.07	0.02	0.05
62	4391450.40	5661496.23	0.42	0.58	0.35	0.28	0.28	0.36	0.16	0.14	0.10	0.06	0.04
63	4391453.62	5661487.51	0.52	0.58	0.37	0.28	0.28	0.47	0.19	0.12	0.11	0.06	0.06
64	4391452.79	5661480.42	0.47	0.46	0.30	0.25	0.21	0.49	0.20	0.11	0.11	0.00	0.05
65	4391460.25	5661472.18	0.33	0.40	0.25	0.22	0.23	0.43	0.14	0.12	0.16	0.07	0.09
66	4391460.67	5661472.48	0.41	0.44	0.26	0.31	0.21	0.44	0.19	0.17	0.14	0.02	0.07
67	4391461.03	5661472.78	0.27	0.38	0.21	0.20	0.19	0.30	0.19	0.11	0.11	0.05	0.02
68	4391461.41	5661473.11	0.54	0.63	0.33	0.32	0.25	0.53	0.20	0.12	0.10	0.05	0.02
69	4391477.17	5661471.40	0.15	0.25	0.16	0.15	0.19	0.21	0.11	0.04	0.05	0.06	0.06
70	4391502.02	5661452.22	0.49	0.42	0.28	0.20	0.22	0.49	0.20	0.21	0.16	0.21	0.05
71	4391528.43	5661431.44	0.51	0.52	0.32	0.30	0.26	0.80	0.16	0.25	0.15	0.15	0.06
72	4391488.63	5661422.15	0.42	0.35	0.28	0.31	0.15	0.27	0.12	0.15	0.09	0.21	0.07
73	4391471.04	5661437.50	0.12	0.35	0.19	0.10	0.17	0.22	0.10	0.11	0.06	0.06	0.05
74	4391452.45	5661454.26	0.79	0.80	0.51	0.40	0.38	0.47	0.23	0.15	0.15	0.17	0.06
75	4391433.45	5661471.16	0.42	0.27	0.30	0.26	0.21	0.41	0.20	0.14	0.14	0.06	0.05
76	4391414.83	5661487.99	0.54	0.79	0.33	0.21	0.27	0.32	0.10	0.12	-0.07	0.06	0.02
77	4391411.70	5661471.33	0.37		0.30	0.23	0.23	0.36	0.11	0.07	0.09	0.16	0.05
78	4391412.29	5661457.94	0.57	0.61	0.41	0.35	0.23	0.28	0.31	0.23	0.17	0.15	0.09
79	4391428.87	5661435.47	0.58	0.35	0.36	0.35	0.23	0.37	0.17	0.14	0.11	0.00	0.07
80	4391444.86	5661412.66	0.74	0.68	0.48	0.44	0.37	0.41	0.26	0.23	0.19	0.23	0.09
81	4391450.28	5661403.64	0.59	0.44	0.31	0.30	0.22	0.36	0.27	0.14	0.14	0.15	0.05
82	4391405.56	5661419.19	0.46	0.92	0.48	0.33	0.44	0.43	0.19	0.16	0.15	0.11	0.05
83	4391379.13	5661404.07	0.79	0.77	0.48	0.16	0.40	0.23	0.11	0.12	0.06	0.09	0.00
84	4391351.43	5661388.96	0.54	0.49	0.35	0.16	0.28	0.36	0.17	0.14	0.11	0.10	0.02
85	4391324.64	5661373.70	0.73	0.63	0.56	0.42	0.67	0.49	0.17	0.05	0.12	0.01	0.12
86	4391368.01	5661428.42	0.14	0.27	0.13	0.09	0.14	0.19	0.06	0.05	0.04	0.11	0.02
87	4391383.81	5661436.08	0.44	0.62	0.33	0.27	0.23	0.59	0.17	0.15	0.14	0.07	0.04
88	4391349.24	5661454.97	0.61	0.70	0.43	0.38	0.41	0.51	0.20	0.10	0.11	0.12	0.09
89	4391363.58	5661456.04	0.70	0.65	0.46	0.41	0.37	0.61	0.31	0.06	0.15	0.07	0.07
90	4391395.39	5661476.85	0.32	0.44	0.28	0.20	0.25	0.43	0.15	0.12	0.09	0.06	0.00
91	4391391.37	5661540.60	0.48	0.53	0.36	0.43	0.26	0.31	0.22	0.15	0.15	0.05	0.11
92	4391407.60	5661561.96	0.41	0.53	0.32	0.27	0.11	0.43	0.10	0.11	0.11	0.10	0.10
93	4391443.00	5661602.56	0.42	0.37	0.22	0.22	0.19	0.31	0.10	0.11	0.09	0.04	0.06
94	4391477.28	5661624.60	0.38	0.59	0.31	0.36	0.05	0.51	0.16	0.07	0.09	0.07	0.05
95	4391487.46	5661629.54	0.65	0.79	0.41	0.42	0.33	0.40	0.16	0.11	0.12	0.07	0.06
96	4391507.39	5661642.57	0.01	0.33	0.20	0.11	0.14	0.25	0.06	0.05	0.06	0.10	0.01
97	4391521.72	5661625.72	0.72	0.72	0.43	0.57	0.31	0.42	0.20	0.17	0.17	0.27	0.06
98			0.31	0.53	0.32	0.25	0.22	0.32	0.09	0.09	0.10	0.04	0.02
99			0.44	0.48	0.31	0.33	0.17	0.30	0.17	0.10	0.10	0.02	0.04
100			0.58	0.59	0.35	0.14	0.25	0.38	0.16	0.11	0.10	0.02	0.01
101			0.42	0.52	0.33	0.26	0.22	0.25	0.14	0.07	0.07	0.01	0.01
Average CO ₂			0.48	0.50	0.32	0.27	0.24	0.39	0.18	0.14	0.11	0.10	0.04
SD			0.18	0.15	0.09	0.13	0.08	0.16	0.08	0.07	0.05	0.07	0.03
CV			38.33	30.50	28.16	46.13	35.11	39.40	41.35	54.24	47.58	73.76	66.52

ID	x	y	06.039	06.053	06.081	06.110	06.123	06.137	06.149	06.165	06.179	06.193	06.207
51	4391453.20	5661537.09	0.04	0.00	0.05	0.20	0.26	0.77	0.31	0.51	0.57	0.73	0.49
52	4391452.65	5661553.71	0.04	0.00	0.10	0.20	0.27	0.56	0.38	0.56	0.57	0.00	0.63
53	4391445.40	5661552.25	0.04	0.05	0.07	0.12	0.12	0.28	0.16	0.21	0.22	0.00	0.32
54	4391430.59	5661539.41	0.02	0.02	0.07	0.17	0.25	0.57	0.25	0.51	0.49	0.00	0.52
55	4391435.71	5661528.65	0.04	0.05	0.11	0.10	0.19	0.41	0.43	0.41	0.42	0.00	0.38
56	4391410.58	5661520.99	0.01	0.12	0.12	0.26	0.19	0.90	0.00	0.61	0.56	0.00	0.43
57	4391425.38	5661502.86	0.05	0.04	0.22	0.37	0.46	1.56	1.04	1.20	1.07	0.00	0.69
58	4391431.66	5661502.18	0.02	0.06	0.16	0.31	0.11	1.17	0.53	0.80	0.86	0.00	0.44
59	4391448.97	5661495.27	0.01	0.01	0.00	0.20	0.25	0.58	0.26	0.42	0.51	0.00	0.38
60	4391449.47	5661495.60	0.01	0.00	0.02	0.30	0.11	0.43	0.27	0.56	0.49	0.00	0.36
61	4391449.85	5661495.82	-0.05	0.00	0.01	0.19	0.28	0.80	0.32	0.47	0.57	0.00	0.37
62	4391450.40	5661496.23	0.04	-0.15	0.05	0.16	0.27	0.44	0.31	0.47	0.58	0.00	0.40
63	4391453.62	5661487.51	0.00	0.07	0.11	0.37	0.41	0.53	0.31	0.65	0.53	0.00	0.37
64	4391452.79	5661480.42	0.01	0.02	0.15	0.23	0.27	0.62	0.40	0.53	0.54	0.00	0.41
65	4391460.25	5661472.18	0.00	0.04	0.14	0.27	0.42	0.70	0.53	0.58	0.81	0.00	0.44
66	4391460.67	5661472.48	0.04	0.00	0.12	0.19	0.36	0.43	0.30	0.21	0.42	0.00	0.40
67	4391461.03	5661472.78	0.01	0.01	0.04	0.25	0.27	0.36	0.25	0.27	0.31	0.00	0.31
68	4391461.41	5661473.11	0.01	0.02	0.02	0.31	0.30	0.47	0.30	0.37	0.40	0.00	0.38
69	4391477.17	5661471.40	0.02	0.01	0.21	0.23	0.23	0.30	0.25	0.30	0.27	0.00	0.31
70	4391502.02	5661452.22	0.04	0.07	0.05	0.41	0.16	0.49	0.36	0.68	0.61	0.00	0.52
71	4391528.43	5661431.44	0.02	0.07	0.07	0.15	0.23	0.89	0.27	0.52	0.67	0.00	0.42
72	4391488.63	5661422.15	0.01	0.06	0.07	0.20	0.35	0.54	0.20	0.51	0.51	0.00	0.31
73	4391471.04	5661437.50	0.00	0.02	0.09	0.25	0.36	0.77	0.27	0.32	0.36	0.00	0.32
74	4391452.45	5661454.26	0.05	0.04	0.17	0.21	0.31	0.93	0.59	0.78	0.91	0.00	0.36
75	4391433.45	5661471.16	-0.01	0.10	0.11	0.20	0.25	0.49	0.31	0.49	0.49	0.00	0.35
76	4391414.83	5661487.99	0.01	0.04	0.06	0.19	0.38	0.83	0.47	0.64	0.65	0.00	0.38
77	4391411.70	5661471.33	0.00	0.04	0.07	0.30	0.25	0.00	0.23	0.37	0.43	0.00	0.31
78	4391412.29	5661457.94	0.02	-0.28	0.74	0.26	0.22	0.00	0.42	0.47	0.98	0.00	0.63
79	4391428.87	5661435.47	0.05	0.07	0.32	0.36	0.32	0.00	0.30	0.56	0.54	0.00	0.41
80	4391444.86	5661412.66	0.06	0.06	0.73	0.27	0.38	0.00	0.33	0.44	0.51	0.00	0.00
81	4391450.28	5661403.64	0.02	0.06	0.15	0.35	0.21	0.00	0.52	0.61	0.94	0.00	0.00
82	4391405.56	5661419.19	0.04	0.05	0.12	0.22	0.42	0.00	0.41	1.09	1.28	0.00	0.00
83	4391379.13	5661404.07	0.01	0.12	0.10	0.20	0.31	0.00	0.26	0.85	0.99	0.00	0.00
84	4391351.43	5661388.96	0.01	0.04	0.14	0.35	0.20	0.00	0.27	0.61	0.84	0.00	0.00
85	4391324.64	5661373.70	0.02	0.01	0.21	0.30	0.41	0.00	0.33	0.84	1.06	0.00	0.00
86	4391368.01	5661428.42	0.01	-0.01	0.02	0.10	0.47	0.00	0.00	0.00	0.28	0.00	0.00
87	4391383.81	5661436.08	0.04	0.07	0.11	0.27	0.30	0.00	0.22	0.00	0.58	0.00	0.00
88	4391349.24	5661454.97	0.04	0.09	0.09	0.28	0.25	0.00	0.00	0.77	0.95	0.00	0.00
89	4391363.58	5661456.04	0.02	0.09	0.16	0.36	0.46	0.00	0.00	0.86	0.88	0.00	0.00
90	4391395.39	5661476.85	0.04	0.09	0.09	0.42	0.48	0.00	0.25	0.46	0.33	0.00	0.00
91	4391391.37	5661540.60	0.01	0.09	0.10	0.25	0.30	0.00	0.61	0.99	0.67	0.00	0.00
92	4391407.60	5661561.96	0.02	0.07	0.12	0.27	0.40	0.00	0.48	0.72	0.69	0.00	0.00
93	4391443.00	5661602.56	0.00	0.31	0.09	0.16	0.28	0.00	0.32	0.36	0.37	0.00	0.00
94	4391477.28	5661624.60	0.01	0.07	0.10	0.26	0.26	0.00	0.81	0.80	0.67	0.00	0.00
95	4391487.46	5661629.54	0.02	0.41	0.10	0.23	0.10	0.00	0.00	0.00	0.83	0.00	0.00
96	4391507.39	5661642.57	0.01	0.07	0.05	0.17	0.12	0.00	0.17	0.23	0.25	0.00	0.00
97	4391521.72	5661625.72	0.02	0.06	0.14	0.20	0.31	0.00	0.28	0.00	0.63	0.00	0.00
98			0.01	0.01	0.09	0.42	0.31	0.00	0.00	0.68	0.54	0.00	0.00
99			0.01	0.02	0.10	0.33	0.27	0.00	0.00	0.59	0.68	0.00	0.00
100			0.00	0.01	0.00	0.00	0.38	0.00	0.00	0.64	0.51	0.00	0.00
101			0.00	-0.01	0.00	0.00	0.23	0.00	0.00	0.65	0.00	0.00	0.00
Average CO ₂			0.05	0.05	0.12	0.23	0.29	0.46	0.34	0.53	0.60	0.29	0.34
SD			0.32	0.07	0.12	0.08	0.09	0.37	0.20	0.23	0.26	0.31	0.23
CV			591.49	138.31	99.04	34.96	31.29	80.51	57.68	43.32	44.10	108.94	67.89

ID	x	y	06.221	06.235	06.263	06.277	06.290	06.305	06.319	06.333	06.354	07.010	07.025
51	4391453.20	5661537.09	0.49	0.44	0.36	0.36	0.23	0.32	0.42	0.25	0.16	0.25	0.05
52	4391452.65	5661553.71	0.42	0.33	0.26	0.37	0.04	0.27	0.33	0.16	0.07	0.12	0.04
53	4391445.40	5661552.25	0.15	0.17	0.16	0.15	0.10	0.19	0.20	0.15	0.07	0.15	0.05
54	4391430.59	5661539.41	0.40	0.35	0.27	0.14	0.15	0.22	0.25	0.11	0.19	0.10	0.05
55	4391435.71	5661528.65	0.33	0.31	0.19	0.20	0.12	-0.09	0.37	0.17	0.14	0.11	0.02
56	4391410.58	5661520.99	0.68	0.44	0.31	0.36	0.19	0.56	0.35	0.20	0.11	0.15	0.05
57	4391425.38	5661502.86	0.51	0.00	0.52	0.37	0.33	0.31	0.67	0.26	0.26	0.31	0.25
58	4391431.66	5661502.18	0.48	0.67	0.21	0.25	0.11	0.23	0.28	0.17	0.14	0.14	0.06
59	4391448.97	5661495.27	0.41	0.42	0.37	0.37	0.17	0.23	0.22	0.15	0.10	0.15	0.09
60	4391449.47	5661495.60	0.44	0.41	0.32	0.28	0.19	0.25	0.21	0.12	0.07	0.14	0.09
61	4391449.85	5661495.82	0.52	0.36	0.31	0.32	0.19	0.22	0.20	0.22	0.11	0.14	-0.02
62	4391450.40	5661496.23	0.56	0.41	0.32	0.33	0.17	0.30	0.28	0.22	0.10	0.15	0.05
63	4391453.62	5661487.51	0.40	0.42	0.26	0.31	0.17	0.23	0.30	0.17	0.12	0.16	0.09
64	4391452.79	5661480.42	0.40	0.44	0.32	0.33	0.22	0.30	0.33	0.21	0.17	0.17	0.12
65	4391460.25	5661472.18	0.51	0.36	0.41	0.40	0.22	0.36	0.22	0.22	0.16	0.15	0.19
66	4391460.67	5661472.48	0.27	0.33	0.27	0.26	0.20	0.20	0.36	0.19	0.14	0.27	0.09
67	4391461.03	5661472.78	0.19	0.32	0.15	0.10	0.09	0.16	0.28	0.12	0.10	0.14	0.07
68	4391461.41	5661473.11	0.30	0.16	0.21	0.14	0.15	0.16	0.22	0.15	0.12	0.14	0.02
69	4391477.17	5661471.40	0.21	0.22	0.19	0.16	0.12	0.12	0.15	0.05	0.04	0.09	0.11
70	4391502.02	5661452.22	0.43	0.19	0.35	0.33	0.30	-0.01	0.32	0.40	0.14	0.32	0.09
71	4391528.43	5661431.44	0.46	0.53	0.36	0.38	0.33	0.54	0.35	0.22	0.16	0.15	0.06
72	4391488.63	5661422.15	0.30	1.01	0.22	0.28	0.12	0.28	0.23	0.12	0.09	0.20	0.05
73	4391471.04	5661437.50	0.32	0.27	0.22	0.30	0.15	0.31	0.27	0.14	0.09	0.16	0.05
74	4391452.45	5661454.26	0.78	0.32	0.54	0.69	0.44	0.33	0.27	0.22	0.15	0.27	0.05
75	4391433.45	5661471.16	0.40	0.70	0.27	0.30	0.12	0.28	0.31	0.17	0.14	0.15	0.10
76	4391414.83	5661487.99	0.46	0.31	0.23	0.28	0.20	0.22	0.31	0.16	0.15	0.20	0.06
77	4391411.70	5661471.33	0.26	0.36	0.23	0.21	0.20	0.19	0.28	0.16	0.07	0.11	0.04
78	4391412.29	5661457.94	0.59	0.32	0.35	0.38	0.06	0.28	0.25	0.19	0.15	0.16	0.06
79	4391428.87	5661435.47	0.48	0.46	0.35	0.37	0.16	0.22	0.43	0.23	0.12	0.20	0.09
80	4391444.86	5661412.66	0.33	0.43	0.30	0.26	0.20	0.38	0.17	0.11	0.15	0.11	0.04
81	4391450.28	5661403.64	0.42	0.27	0.00	0.21	0.17	0.31	0.25	0.21	0.14	0.20	0.04
82	4391405.56	5661419.19	1.14	0.46	0.00	0.51	0.36	0.63	0.35	0.26	0.12	0.17	0.09
83	4391379.13	5661404.07	0.73	0.61	0.00	0.00	0.30	0.27	0.35	0.17	0.10	0.14	0.09
84	4391351.43	5661388.96	0.51	0.79	0.00	0.00	0.22	0.28	0.38	0.20	0.09	0.23	0.07
85	4391324.64	5661373.70	0.98	0.54	0.00	0.00	0.32	0.26	0.30	0.27	0.11	0.17	0.07
86	4391368.01	5661428.42	0.23	0.56	0.21	0.00	0.12	0.12	0.19	0.06	0.09	0.41	0.01
87	4391383.81	5661436.08	0.59	0.16	0.28	0.00	0.14	0.23	0.33	0.19	0.15	0.12	0.09
88	4391349.24	5661454.97	0.85	0.46	0.84	0.00	0.44	0.40	0.43	0.37	0.22	0.21	0.09
89	4391363.58	5661456.04	0.48	0.65	0.00	0.00	0.35	0.32	0.00	0.26	0.17	0.27	0.15
90	4391395.39	5661476.85	0.31	0.72	0.28	0.22	0.19	0.16	0.31	0.16	0.14	0.14	0.04
91	4391391.37	5661540.60	0.49	0.30	0.27	0.30	0.19	0.27	0.35	0.22	0.06	0.27	0.07
92	4391407.60	5661561.96	1.14	0.42	0.37	0.36	0.33	0.23	0.40	0.32	0.19	0.25	0.06
93	4391443.00	5661602.56	0.33	0.59	0.14	0.27	0.15	0.27	0.32	0.07	0.11	0.04	0.04
94	4391477.28	5661624.60	0.51	0.31	0.21	0.32	0.19	0.31	0.38	0.23	0.16	0.20	0.02
95	4391487.46	5661629.54	0.38	0.42	0.37	0.38	0.26	0.22	0.23	0.21	0.10	0.12	0.12
96	4391507.39	5661642.57	0.15	0.47	0.16	0.12	0.12	0.14	0.14	0.11	0.07	0.10	0.07
97	4391521.72	5661625.72	0.64	0.15	0.00	0.28	0.26	0.28	0.47	0.26	0.19	0.15	0.09
98			0.43	0.42	0.32	0.26	-0.15	0.22	0.17	0.11	0.06	0.10	0.04
99			0.42	0.44	0.25	0.22	0.21	0.17	0.44	0.20	0.09	0.19	0.00
100			0.53	0.36	0.26	0.28	0.21	0.31	0.40	0.22	0.14	0.15	0.04
101			0.47	0.47	0.28	0.23	0.19	0.21	0.02	0.12	0.09	0.10	0.02
Average CO ₂			0.45	0.40	0.28	0.29	0.18	0.30	0.33	0.21	0.13	0.20	0.05
SD			0.17	0.15	0.15	0.13	0.09	0.15	0.12	0.11	0.07	0.11	0.13
CV			38.01	37.29	52.56	44.78	52.95	49.37	36.18	51.17	52.19	54.97	273.34

ID	x	y	07.038	07.052	07.066	07.080	07.094	07.108	07.122	07.136	07.150	07.164
51	4391453.20	5661537.09	0.16	0.20	0.21	0.00	0.22	0.28	0.44	0.44	0.31	1.36
52	4391452.65	5661553.71	0.10	0.14	0.11	0.15	0.25	0.21	0.30	0.42	0.16	0.64
53	4391445.40	5661552.25	0.00	0.11	-0.09	0.07	0.11	0.04	0.20	0.16	0.43	0.28
54	4391430.59	5661539.41	0.09	0.11	0.10	0.02	0.06	0.27	0.16	0.54	0.36	0.72
55	4391435.71	5661528.65	0.06	0.11	0.11	0.16	0.17	0.05	0.28	0.36	0.80	0.58
56	4391410.58	5661520.99	0.09	0.11	0.17	0.09	0.14	0.16	0.20	0.46	0.33	0.61
57	4391425.38	5661502.86	0.20	0.22	0.48	0.19	0.19	0.21	0.19	0.53	0.69	0.98
58	4391431.66	5661502.18	0.11	0.10	0.16	0.02	0.15	0.46	0.23	0.23	0.23	0.57
59	4391448.97	5661495.27	0.07	0.09	0.11	0.09	0.26	0.42	0.14	0.33	0.49	0.47
60	4391449.47	5661495.60	0.07	0.15	0.10	0.15	0.20	0.20	0.40	0.33	0.48	0.77
61	4391449.85	5661495.82	0.14	0.14	0.19	0.12	0.19	0.11	0.31	0.41	0.26	0.58
62	4391450.40	5661496.23	0.11	0.10	0.19	0.07	0.12	0.28	0.20	0.41	0.38	0.48
63	4391453.62	5661487.51	0.15	0.14	0.16	0.22	0.10	0.32	0.21	0.52	0.32	0.04
64	4391452.79	5661480.42	0.12	0.11	0.19	0.21	0.31	0.61	0.25	0.46	0.49	0.72
65	4391460.25	5661472.18	0.22	0.17	0.30	0.11	0.04	0.30	0.25	0.40	0.56	0.62
66	4391460.67	5661472.48	0.11	0.15	0.14	0.12	0.20	0.26	0.46	0.59	0.46	0.43
67	4391461.03	5661472.78	0.07	0.05	0.10	0.17	0.26	-0.06	0.14	0.43	0.30	0.19
68	4391461.41	5661473.11	0.07	0.06	0.02	0.11	0.09	0.25	0.00	0.64	0.49	0.30
69	4391477.17	5661471.40	0.02	0.06	0.09	0.09	0.16	0.48	0.10	0.42	0.27	0.00
70	4391502.02	5661452.22	0.14	0.17	0.37	0.22	0.25	0.31	0.14	0.67	0.57	1.01
71	4391528.43	5661431.44	0.15	0.11	0.12	0.05	0.28	0.14	0.20	0.53	0.52	0.57
72	4391488.63	5661422.15	0.09	0.12	0.22	-0.05	0.20	0.23	0.19	0.35	0.38	0.61
73	4391471.04	5661437.50	0.06	0.10	0.17	0.12	0.30	0.28	0.10	0.25	0.40	0.56
74	4391452.45	5661454.26	0.11	0.20	0.20	0.04	0.04	-0.11	0.37	0.44	0.61	0.94
75	4391433.45	5661471.16	0.14	0.12	0.14	0.01	0.17	0.26	0.12	0.30	0.38	0.67
76	4391414.83	5661487.99	0.06	0.10	0.12	0.09	0.12	0.05	0.19	0.59	0.16	0.41
77	4391411.70	5661471.33	0.07	0.09	0.14	-0.01	0.06	0.25	0.16	0.16	0.37	0.36
78	4391412.29	5661457.94	0.10	0.10	0.12	0.09	0.02	0.09	0.46	0.33	0.51	0.21
79	4391428.87	5661435.47	0.09	0.17	0.17	0.20	0.11	0.33	0.20	0.47	0.22	1.02
80	4391444.86	5661412.66	0.14	0.14	0.15	0.15	0.14	0.46	0.33	0.48	0.28	2.11
81	4391450.28	5661403.64	0.10	0.12	0.14	0.01	0.10	0.43	0.27	0.52	0.31	0.77
82	4391405.56	5661419.19	0.23	0.10	0.20	0.12	0.14	-0.10	0.28	0.56	0.69	1.00
83	4391379.13	5661404.07	0.15	0.14	0.10	0.09	0.12	0.14	0.27	0.49	0.35	1.89
84	4391351.43	5661388.96	0.01	0.14	0.14	0.28	0.23	0.36	0.26	0.37	0.48	0.72
85	4391324.64	5661373.70	0.05	0.10	0.16	0.11	0.28	0.14	0.15	0.41	0.44	1.06
86	4391368.01	5661428.42	0.12	0.11	0.11	0.09	0.06	0.25	0.06	0.53	0.58	0.41
87	4391383.81	5661436.08	-0.01	0.11	0.20	0.16	0.20	0.14	0.23	0.30	0.56	0.62
88	4391349.24	5661454.97	0.00	0.20	0.31	0.11	0.16	0.21	0.25	0.37	0.21	0.81
89	4391363.58	5661456.04	0.00	0.19	0.27	0.12	0.06	0.31	0.15	0.40	0.19	0.61
90	4391395.39	5661476.85	0.00	0.07	0.12	0.09	0.16	0.46	0.09	0.31	0.33	0.42
91	4391391.37	5661540.60	0.00	0.15	0.00	0.12	0.19	0.19	0.14	0.38	0.58	0.64
92	4391407.60	5661561.96	0.00	0.16	0.19	0.11	0.22	0.27	0.46	0.40	0.52	0.68
93	4391443.00	5661602.56	0.00	0.15	0.12	0.22	0.11	0.10	0.12	0.43	0.36	0.47
94	4391477.28	5661624.60	0.00	0.11	0.19	0.12	0.11	0.01	0.19	0.62	0.36	0.68
95	4391487.46	5661629.54	0.00	0.12	0.16	0.22	0.05	0.30	-0.01	0.44	0.44	0.00
96	4391507.39	5661642.57	0.00	0.28	0.12	0.16	0.31	0.40	0.14	0.56	0.52	0.54
97	4391521.72	5661625.72	0.00	0.30	0.16	0.38	0.10	0.15	0.17	0.26	0.44	0.42
98			0.00	0.00	0.10	0.12	0.14	0.09	0.32	0.31	0.73	0.49
99			0.00	0.00	0.17	0.22	0.20	0.40	0.52	0.21	0.47	0.72
100			0.00	0.00	0.28	-0.06	0.22	0.32	0.09	0.38	0.21	0.96
101			0.00	0.00	0.07	0.10	0.09	0.23	0.23	0.53	0.40	0.49
Average CO ₂			0.09	0.31	0.16	0.13	0.17	0.24	0.22	0.42	0.40	0.68
SD			0.06	1.95	0.08	0.08	0.08	0.15	0.12	0.14	0.15	0.36
CV			60.86	636.12	48.34	64.05	46.65	64.04	53.84	34.03	38.79	53.96

13.2 Soil moisture data

First measurement series

ID	05.104	05.117	05.133	05.146	05.161	05.174	05.188	05.204	05.217	05.230	05.245	05.261	05.273	05.294
1	44.17	28.51	33.17	24.19	25.74	20.96	27.02	39.79	17.02	13.36	13.29	14.91	16.54	24.01
2	38.95	36.44	38.86	29.51	29.83	25.53	32.21	42.17	22.68	28.55	18.82	21.82	15.75	20.03
3	46.00	25.46	28.38	25.26	21.67	18.19	25.03	27.43	22.59	23.72	17.18	16.90	17.50	26.22
4	45.60	59.57	45.01	30.40	30.29	24.64	32.09	35.78	26.99	18.66	21.14	26.77	25.53	30.43
5	53.84	47.32	48.77	34.29	33.05	26.21	34.18	28.55	28.80	28.87	25.62	12.13	28.89	30.11
6	46.94	55.39	47.58	32.70	30.44	21.98	34.81	39.08	23.80	10.15	20.70	22.92	21.12	32.28
7	38.13	38.67	37.77	35.90	37.74	32.87	38.89	30.01	33.45	29.31	25.09	31.21	55.25	16.34
8	42.85	32.99	32.90	26.03	27.60	23.74	29.38	37.30	25.07	23.20	20.15	19.11	23.16	24.28
9	45.40	50.61	51.41	36.82	35.13	30.96	39.78	49.72	30.65	24.66	37.06	27.05	18.40	29.69
10	39.22	50.20	45.55	33.54	44.36	34.19	37.03	33.09	36.73	34.30	28.65	32.11	29.66	20.81
11	41.52	39.79	39.54	30.35	31.36	28.27	35.18	39.45	29.92	26.90	25.46	27.88	22.36	22.42
12	42.66	45.62	46.17	37.90	36.25	26.64	37.53	37.50	31.00	28.90	25.08	15.73	22.61	18.35
13	43.31	32.90	54.74	30.04	26.07	24.45	31.51	22.85	26.76	20.75	11.92	26.85	24.91	17.71
14	43.99	68.48	44.01	33.33	31.51	27.28	34.64	31.61	30.34	27.78	22.68	20.59	23.55	21.25
15	37.67	34.39	38.18	45.83	34.43	35.45	38.58	36.33	45.41	34.49	32.96	28.21	41.29	22.08
16	41.74	40.51	55.74	32.07	34.05	26.93	38.84	48.92	28.99	27.79	24.89	21.63	24.53	16.61
17	38.46	45.51	39.55	33.32	30.88	26.62	34.29	30.76	32.15	29.91	24.35	24.54	22.78	22.92
18	41.99	44.66	44.98	38.56	33.88	33.24	38.48	31.36	35.66	28.87	27.19	30.40	-	23.59
19	34.28	60.04	79.53	40.46	49.58	42.78	46.16	50.63	47.18	38.04	42.43	36.25	43.52	25.78
20	44.22	51.33	-	36.30	35.50	31.46	36.45	28.56	34.88	29.58	25.08	30.87	24.89	23.74
21	47.95	44.22	43.66	29.62	27.49	23.84	30.48	41.76	24.82	27.08	20.25	22.40	18.60	23.90
22	43.07	39.32	36.93	31.82	29.53	23.08	32.92	35.96	27.77	24.72	23.08	26.35	22.34	23.72
23	32.15	42.93	63.01	41.74	41.52	32.74	43.71	33.64	41.05	39.77	37.33	34.75	31.17	30.69
24	29.98	82.03	68.54	43.55	46.19	41.48	48.76	39.88	32.15	35.11	33.97	39.01	32.42	24.88
25	35.02	47.61	65.96	41.32	41.88	34.46	46.74	31.15	34.34	43.77	33.54	31.65	35.73	24.47
26	37.58	47.40	90.54	32.86	36.32	31.43	42.15	51.03	29.81	25.71	24.17	33.07	23.43	23.14
27	43.80	51.50	50.86	35.54	36.90	40.60	39.59	11.45	35.94	36.97	33.00	35.86	37.35	33.26
28	34.24	48.87	58.01	42.20	45.75	38.77	46.30	45.37	46.77	37.53	35.96	42.10	49.20	28.75
29	34.24	66.14	62.70	41.52	40.59	39.12	44.68	35.04	47.11	31.97	36.47	36.35	41.16	34.90
30	34.24	44.67	69.79	38.58	39.04	37.10	47.67	27.38	40.71	40.44	32.13	37.54	41.28	22.56
31	34.24	40.76	60.82	43.01	37.71	39.21	39.61	11.03	37.37	37.49	34.67	30.81	41.85	31.99
32	33.07	38.21	34.37	32.73	35.33	32.21	37.25	18.99	35.88	28.53	11.57	31.38	25.66	18.67
33	34.71	44.57	34.94	30.85	31.27	27.34	34.02	36.73	38.39	24.72	32.22	23.39	30.43	27.42
34	34.71	49.49	33.92	36.62	35.75	28.02	41.40	21.18	34.78	30.91	29.53	29.30	30.20	28.90
35	34.71	41.12	32.93	34.52	32.14	29.79	37.60	49.50	30.14	30.94	25.97	28.23	30.18	33.04
36	34.71	40.93	41.25	33.70	29.58	27.24	35.98	43.04	33.35	36.30	26.84	28.54	32.12	24.89
37	34.60	53.26	42.81	33.85	31.24	32.28	34.71	29.56	33.79	32.02	22.22	31.41	27.38	23.10
38	34.60	40.17	33.17	33.99	34.25	26.24	35.96	29.31	29.53	29.88	23.35	27.09	25.69	27.98
39	34.60	39.61	34.25	33.94	33.75	28.32	40.34	50.35	34.37	23.01	28.47	33.93	30.36	23.68
40	34.60	41.43	34.45	28.66	28.85	24.70	35.40	39.89	25.72	31.64	24.82	29.06	26.65	28.31
41	46.37	52.77	44.71	36.21	38.56	30.27	39.31	50.50	31.67	30.29	25.74	28.51	27.28	19.35
42	33.31	52.60	53.40	38.21	41.78	34.55	50.85	47.84	19.85	31.93	32.89	24.97	23.48	21.78
43	33.31	46.96	49.47	38.48	39.28	31.78	35.25	38.15	30.00	27.95	23.90	27.58	23.63	19.04
44	33.31	46.81	52.23	37.04	43.61	30.12	38.37	27.33	30.68	26.41	32.61	25.18	24.44	23.75
45	33.31	39.82	53.00	38.06	34.89	28.48	36.37	32.69	30.51	24.70	22.04	22.49	26.31	25.10
46	44.05	53.30	46.95	32.82	31.64	29.61	34.72	39.94	25.54	25.91	26.02	21.69	28.55	25.34
47	36.23	51.63	50.11	35.39	35.02	31.94	36.60	39.34	37.54	32.72	27.16	29.80	30.22	23.92
48	38.47	51.26	41.24	37.88	35.36	30.92	38.40	53.06	33.55	31.78	29.43	31.84	29.08	34.16
49	39.36	50.14	48.78	35.52	37.97	33.82	40.20	42.07	34.63	29.62	28.05	34.01	27.56	18.14
50	42.83	42.79	33.79	32.92	32.19	27.06	33.91	29.78	28.81	23.39	22.72	19.74	21.86	22.23

ID	05.302	05.315	05.327	05.341	05.355	06.004	06.032	06.047	06.074	06.089	06.102
1	24.65	39.10	37.59	36.71	42.83	25.42	0.00	41.80	39.09	54.07	39.80
2	20.25	27.71	39.25	39.12	38.64	32.28	0.00	41.80	39.09	46.33	43.43
3	27.10	36.63	50.23	36.35	32.91	29.49	0.00	41.80	39.09	41.80	43.27
4	31.74	42.04	30.10	26.28	40.85	35.27	0.00	41.80	39.09	55.43	43.23
5	31.39	27.12	43.33	33.51	47.03	35.95	0.00	41.80	39.09	69.13	32.15
6	33.80	33.22	47.34	41.86	45.94	39.09	0.00	41.80	39.09	46.17	47.50
7	16.17	32.57	42.65	42.07	41.32	44.01	0.00	41.80	39.09	65.37	46.10
8	24.95	34.90	47.26	29.62	34.60	32.16	0.00	41.80	39.09	58.30	44.20
9	30.93	47.15	41.63	40.76	42.52	38.91	0.00	41.80	39.09	57.30	44.87
10	21.11	36.13	37.16	57.03	39.76	38.91	0.00	41.80	39.09	61.40	48.75
11	22.89	32.24	44.85	49.23	39.51	29.89	0.00	41.80	39.09	56.50	47.60
12	18.39	25.82	34.06	56.45	37.68	36.95	0.00	41.80	39.09	56.87	41.60
13	17.69	37.01	43.68	40.76	39.72	33.09	0.00	41.80	39.09	79.47	36.30
14	21.60	35.38	45.89	40.78	46.05	41.81	0.00	41.80	39.09	45.83	40.07
15	22.52	14.33	48.38	49.97	42.49	37.54	0.00	41.80	39.09	52.78	36.13
16	16.47	30.86	43.06	28.60	53.05	39.49	0.00	41.80	39.09	44.07	42.00
17	23.44	24.75	40.76	40.50	47.27	34.27	0.00	41.80	39.09	43.07	40.40
18	24.18	20.33	39.47	51.00	26.99	38.68	0.00	41.80	39.09	57.10	47.40
19	26.61	29.14	36.24	38.66	45.16	43.02	0.00	41.80	39.09	77.30	47.30
20	24.36	45.38	31.09	46.29	47.56	41.18	0.00	41.80	39.09	77.77	46.85
21	24.53	25.27	49.58	39.39	37.91	31.25	0.00	41.80	39.09	52.97	40.73
22	24.33	33.69	33.16	52.69	38.62	29.86	0.00	41.80	39.09	45.27	38.60
23	32.04	24.72	25.69	48.25	47.31	45.75	0.00	41.80	39.09	57.63	43.30
24	25.62	30.40	27.35	39.05	45.21	50.70	0.00	41.80	39.09	62.10	45.13
25	25.16	24.92	38.07	46.41	46.05	41.17	0.00	41.80	39.09	52.23	43.97
26	23.69	28.46	35.13	39.38	39.03	42.11	0.00	41.80	39.09	54.27	42.43
27	34.87	26.74	46.07	47.35	39.74	37.71	0.00	41.80	39.09	56.80	49.97
28	29.90	20.21	41.11	40.65	41.22	41.72	0.00	41.80	39.09	68.00	51.37
29	36.69	30.23	48.92	47.63	40.08	41.85	0.00	41.80	39.09	-	53.13
30	23.05	28.21	32.66	44.69	34.87	0.00	0.00	41.80	39.09	-	50.83
31	33.48	26.13	40.50	58.59	34.43	0.00	0.00	41.80	39.09	-	48.67
32	18.74	23.16	43.30	37.73	42.59	50.86	0.00	41.80	39.09	-	37.63
33	28.43	38.59	32.99	44.66	49.19	34.07	0.00	41.80	39.09	-	42.67
34	30.06	35.83	30.64	38.71	32.42	37.00	0.00	41.80	39.09	-	31.97
35	34.64	43.86	38.57	48.89	43.77	36.10	0.00	41.80	39.09	-	45.70
36	25.62	21.38	29.28	53.01	32.05	0.00	0.00	41.80	39.09	-	45.05
37	23.64	51.66	34.25	33.78	48.13	40.88	0.00	41.80	39.09	-	47.00
38	29.04	25.07	30.80	42.57	47.04	37.21	0.00	41.80	39.09	-	45.37
39	24.28	28.38	34.95	40.27	37.73	39.18	0.00	41.80	39.09	-	44.12
40	29.41	30.56	36.07	44.92	48.12	40.07	0.00	41.80	39.09	-	40.32
41	19.50	40.75	36.94	39.54	48.32	36.64	0.00	41.80	39.09	-	47.13
42	22.19	40.14	37.86	36.63	48.58	46.07	0.00	41.80	39.09	-	44.73
43	19.15	29.82	38.82	25.10	38.21	38.74	0.00	41.80	39.09	-	45.00
44	24.37	21.09	41.29	49.07	41.43	37.25	0.00	41.80	39.09	-	43.13
45	25.85	37.48	43.16	48.35	46.52	37.81	0.00	41.80	39.09	-	48.37
46	26.13	42.24	43.06	38.17	41.50	34.89	0.00	41.80	39.09	-	27.60
47	24.55	35.85	39.39	37.10	44.90	49.72	0.00	41.80	39.09	-	38.23
48	35.88	40.36	35.86	41.39	35.02	39.53	0.00	41.80	39.09	-	47.30
49	18.16	35.79	39.08	31.54	46.16	40.60	0.00	41.80	39.09	-	44.77
50	22.69	35.34	41.00	51.34	34.05	32.20	0.00	41.80	39.09	-	54.23

ID	05.104	05.117	05.133	05.146	05.161	05.174	05.188	05.204	05.217	05.230	05.245	05.261	05.273	05.294	
51	47.55	36.18	42.97	28.67	30.06	28.07	32.25	39.09	30.83	29.23	27.84	27.01	17.76	14.74	
52	42.04	44.09	64.18	31.56	34.62	25.52	35.41	31.41	24.77	22.08	22.64	31.99	18.47	31.12	
53	36.02	41.29	36.02	32.81	34.94	26.50	37.09	31.32	28.14	25.23	23.14	24.25	12.18	20.02	
54	38.78	47.69	46.01	35.09	33.23	29.43	36.13	25.33	26.71	28.93	22.71	27.65	31.48	22.57	
55	32.04	41.88	46.89	41.82	38.79	30.03	39.49	24.60	35.96	28.60	28.77	30.11	32.11	28.31	
56	46.98		44.61	30.02	29.58	30.36	34.20	36.25	28.00	30.98	28.74	29.23	6.12	27.13	
57	42.00	62.31	56.55	40.21	39.75	37.90	42.07	30.48	39.55	31.27	38.81	50.07	39.20	28.79	
58	42.79	40.24	44.13	37.47	44.23	38.04	35.74	41.01	46.64	35.20	40.26	43.71	35.75	27.65	
59	40.93	41.61	55.16	39.25	40.96	35.59	40.70	27.24	38.40	35.73	34.50	35.85	37.59	19.65	
60	40.03	49.19	58.20	32.07	33.20	25.50	31.35	40.95	29.80	28.52	25.12	21.74	19.67	20.69	
61	33.18	32.95	32.49	30.55	35.42	24.69	29.74	37.55	28.16	27.32	15.93	26.22	29.11	28.05	
62	31.74	41.31	35.20	31.62	32.02	26.79	32.00	29.37	28.58	23.21	15.56	30.99	25.49	26.54	
63	32.02	41.41	35.83	32.31	31.74	23.73	34.19	39.81	24.38	15.42	21.85	25.88	19.02	21.40	
64	34.23	30.74	37.15	29.16	32.98	24.95	32.70	43.32	23.60	20.67	22.33	24.76	21.52	24.25	
65	33.81	40.46	43.17	29.74	31.80	26.79	32.28	21.56	24.95	22.94	26.23	26.12	22.65	25.77	
66	33.61	59.51	55.45	38.51	42.73	32.20	40.06	18.41	36.76	33.19	26.18	28.74	30.49	27.50	
67	38.67	50.06	45.67	35.19	31.09	23.78	32.67	25.96	21.15	20.25	21.07	24.45	15.67	25.79	
68	32.61	49.78	43.91	36.33	33.26	26.02	37.18	39.27	31.91	32.88	27.10	23.83	22.52	21.52	
69	32.61	40.93	42.12	32.77	34.18	26.88	37.48	41.16	28.71	25.55	16.69	20.70	21.36	32.90	
70	39.14	42.85	40.75	29.10	29.76	23.87	31.99	41.11	22.95	33.58	16.92	14.16	20.62	27.21	
71	39.79	49.50	49.40	28.87	31.05	22.54	33.51	36.64	17.51	24.38	20.42	11.78	18.04	25.52	
72	39.85	37.18	40.47	28.41	30.82	24.82	35.00	45.52	28.24	31.46	21.40	22.90	19.86	28.61	
73	41.65	40.31	39.04	29.79	33.29	24.19	28.63	30.81	24.98	21.34	21.36	22.64	22.21	28.74	
74	51.22	49.42	57.33	33.34	31.36	28.07	33.75	33.60	31.18	29.93	22.78	29.31	26.51	22.64	
75	37.38	41.51	45.52	31.53	29.11	24.57	32.88	34.39	24.43	22.66	21.28	26.71	16.33	21.47	
76	39.63	38.77	22.40	22.44	22.42	19.85	27.36	38.88	22.91	24.87	13.81	18.89	18.84	29.75	
77	57.20		36.73	30.70	29.14	31.99	33.94	34.67	31.91	25.35	27.90	23.09	27.34	20.34	
78	37.56	43.29	43.37	31.20	33.07	27.61	35.08	40.10	33.57	28.82	25.86	27.43	18.88	18.89	
79	37.88	47.21	51.63	34.65	37.19	32.02	38.80	11.01	34.09	26.96	23.67	28.20	23.70	28.13	
80	41.43	47.05	47.50	33.47	34.44	31.83	36.90	48.89	25.90	26.05	24.00	21.80	21.50	27.83	
81	35.53	48.08		37.46	36.66	37.07	41.00	21.39	38.40	27.13	26.63	30.28	28.95	34.21	
82	59.28	39.25	35.07	26.67	27.97	47.21	29.30	42.75	26.93	18.37	25.91	28.77	17.77	31.11	
83	44.21	54.92	43.43	32.67	32.23	26.42	30.69	33.64	25.86	24.21	14.12	18.39	17.50	30.54	
84	43.51	40.53	38.45	30.20	28.56	29.57	32.93	27.95	29.45	29.97	26.15	20.71	28.45	25.69	
85	41.61	43.84	49.40	34.73	32.79	36.06	38.83	23.02	34.96	31.12	30.79	30.25	27.35	25.24	
86	41.61	45.44	42.96	33.63	32.64	29.47	40.55	22.03	34.81	35.51	28.15	32.34	31.44	27.08	
87	41.55	49.47	46.06	34.21	33.57	27.02	36.87	36.24	30.12	31.64	22.87	26.84	24.30	25.13	
88	48.48		42.80	33.57	30.59	28.88	33.42	48.53	24.76	24.12	19.18	27.50	24.30	20.94	
89	28.13	48.13	41.08	36.30	32.45	27.59	39.27	35.74	34.44	32.12	23.62	29.36	20.76	18.01	
90	34.76	45.50	39.33	32.99	31.18	27.95	31.24	40.28	24.39	31.47	20.29	27.83	12.91	28.60	
91	39.68	49.21	44.07	35.02	35.19	28.36	32.11	27.17	30.71	29.06	23.72	23.19	20.44	27.04	
92	45.68	41.28	46.09	28.14	30.85	31.44	30.72	34.40	32.02	25.27	35.59	10.81	20.19	27.74	
93	39.14	43.71	47.68	33.00	34.55	30.79	36.38	37.32	35.89	31.81	27.14	25.15	21.02	26.10	
94	35.69	52.34	68.92	32.69	38.30	37.50	40.26	28.63	24.80	38.15	31.09	35.27	33.12	21.05	
95	33.45	45.34	82.16	42.08	40.28	31.81	40.02	19.04	37.81	33.36	31.04	32.12	25.16	30.27	
96	41.59		49.81	29.71	29.63	23.67	31.74	46.30	27.82	23.57	11.81	24.20	15.31	23.96	
97	41.59		85.48	29.38	27.80	25.06	31.67	33.69	29.36	29.16	16.06	22.63	23.65	21.81	
98	41.59			39.88	31.71	29.87	25.60	31.03	54.54	26.93	27.99	21.23	23.47	9.82	21.89
99	41.59			47.13	28.77	32.90	23.20	31.93	30.53	0.00	23.13	22.16	22.31	23.21	23.48
AV	39.41	45.61	46.89	33.85	34.03	29.47	36.18	35.02	30.61	28.49	25.38	27.05	25.67	25.08	
SD	5.72	8.45	12.13	4.45	5.01	5.31	4.82	9.35	6.95	5.70	6.42	6.58	8.11	4.44	
CV	14.52	18.53	25.87	13.15	14.73	18.02	13.32	26.70	22.69	20.00	25.31	24.35	31.58	17.69	

ID	05.302	05.315	05.327	05.341	05.355	06.004	06.032	06.047	06.074	06.089	06.102
51	14.40	30.07	40.55	41.88	34.77	33.36	0.00	41.80	39.09	-	57.50
52	32.51	42.98	29.16	48.98	35.21	40.24	0.00	41.80	39.09	-	47.20
53	20.24	31.35	48.09	54.40	41.76	43.04	0.00	41.80	39.09	-	49.07
54	23.06	34.20	43.04	31.29	39.53	40.02	0.00	41.80	39.09	-	41.73
55	29.41	22.97	31.79	32.42	38.07	41.92	0.00	41.80	39.09	-	42.83
56	28.10	34.69	62.47	38.14	42.42	32.71	0.00	41.80	39.09	-	42.10
57	29.94	25.70	47.64	27.71	38.40	0.00	0.00	41.80	39.09	-	44.93
58	28.68	5.96	25.82	43.08	37.36	44.53	0.00	41.80	39.09	-	50.70
59	19.83	22.82	40.59	41.52	46.10	44.94	0.00	41.80	39.09	-	32.60
60	20.98	33.87	36.26	26.08	36.10	38.17	0.00	41.80	39.09	-	38.38
61	29.12	29.87	40.33	61.69	41.63	45.49	0.00	41.80	39.09	-	39.46
62	27.45	29.37	36.77	38.45	47.48	39.63	0.00	41.80	39.09	-	41.20
63	21.77	25.21	34.06	47.78	42.64	41.51	0.00	41.80	39.09	-	34.63
64	24.92	30.06	34.01	30.91	49.02	44.63	0.00	41.80	39.09	-	36.30
65	26.59	34.60	37.34	29.39	43.03	44.08	0.00	41.80	39.09	-	47.23
66	28.51	25.40	33.36	35.27	33.70	37.99	0.00	41.80	39.09	-	46.17
67	26.62	34.84	44.59	35.22	47.90	43.86	0.00	41.80	39.09	-	43.47
68	21.90	42.26	40.03	32.91	39.14	43.37	0.00	41.80	39.09	-	50.67
69	34.48	52.93	35.40	25.10	49.67	47.55	0.00	41.80	39.09	-	46.77
70	28.19	28.32	34.76	50.15	47.20	36.14	0.00	41.80	39.09	-	43.10
71	26.33	22.84	51.31	36.36	38.28	38.26	0.00	41.80	39.09	-	38.13
72	29.73	33.11	35.49	41.06	45.27	45.54	0.00	41.80	39.09	-	46.97
73	29.88	39.78	38.82	29.27	38.30	38.12	0.00	41.80	39.09	-	36.47
74	23.14	32.58	34.30	44.24	38.66	44.94	0.00	41.80	39.09	-	31.83
75	21.85	27.61	27.01	40.38	44.09	49.15	0.00	41.80	39.09	-	40.70
76	31.00	36.26	50.76	39.91	46.79	47.34	0.00	41.80	39.09	-	52.20
77	20.59	41.89	37.33	37.09	47.09	43.13	0.00	41.80	39.09	-	43.17
78	18.98	28.19	35.31	50.28	39.61	37.32	0.00	41.80	39.09	-	44.08
79	29.20	22.55	48.07	41.70	36.21	39.28	0.00	41.80	39.09	-	-
80	28.87	17.50	29.05	37.47	43.04	46.66	0.00	41.80	39.09	-	-
81	35.93	27.22	34.17	42.30	49.03	52.98	0.00	41.80	39.09	-	-
82	32.50	42.52	34.51	54.28	50.85	47.46	0.00	41.80	39.09	-	-
83	31.87	25.32	34.08	32.12	41.35	36.62	0.00	41.80	39.09	-	-
84	26.51	20.62	53.93	28.94	50.16	39.22	0.00	41.80	39.09	-	-
85	26.01	16.30	42.67	22.46	46.56	34.76	0.00	41.80	39.09	-	-
86	28.04	32.90	40.65	32.37	37.84	43.82	0.00	41.80	39.09	-	-
87	25.89	31.91	48.01	45.28	47.81	48.78	0.00	41.80	39.09	-	-
88	21.25	46.33	29.54	29.06	55.75	43.54	0.00	41.80	39.09	-	-
89	18.01	35.99	42.15	40.63	53.16	43.16	0.00	41.80	39.09	-	-
90	29.73	22.78	47.33	32.78	31.25	49.05	0.00	41.80	39.09	-	-
91	28.00	37.29	42.70	47.70	36.23	38.60	0.00	41.80	39.09	-	-
92	28.78	38.13	39.74	32.24	35.39	44.18	0.00	41.80	39.09	-	-
93	26.96	34.72	43.95	53.90	42.00	33.05	0.00	41.80	39.09	-	-
94	21.38	28.46	43.76	40.67	48.04	39.42	0.00	41.80	39.09	-	-
95	31.57	30.97	42.23	35.70	38.78	57.16	0.00	41.80	39.09	-	-
96	24.60	38.50	46.48	37.80	43.05	45.20	0.00	41.80	39.09	-	-
97	22.22	26.52	27.70	55.79	46.62	40.80	0.00	41.80	39.09	-	-
98	22.30	28.96	32.60	43.88	51.70	37.49	0.00	41.80	39.09	-	-
99	24.07	33.74	30.83	42.61	38.05	46.87	0.00	41.80	39.09	-	-
AV	25.84	31.59	39.09	40.74	42.16	38.72	0.00	41.80	39.09	56.98	43.55
SD	4.91	8.01	6.82	8.35	5.59	9.70	0.00	0.00	0.00	10.36	5.52
CV	18.99	25.35	17.44	20.49	13.27	25.06	-	0.00	0.00	18.18	12.67

Second measurement series

ID	05.237	05.251	05.265	05.279	05.293	05.306	05.321	05.334	05.348	06.11	06.110	06.123	06.137	06.149
1	33.34	28.12	30.19	36.00	35.06	37.72	42.09	48.35	44.36	59.06	39.37	38.73	30.93	39.00
2	41.93	43.30	38.99	57.02	33.39	46.01	54.92	56.69	46.89	55.53	44.60	38.33	37.60	48.00
3	28.67	29.50	33.01	33.07	31.50	39.11	51.32	53.55	51.67	50.98	39.30	39.40	33.43	46.50
4	31.13	39.67	33.03	44.51	32.38	43.73	40.38	54.61	44.35	58.06	43.17	43.00	33.73	49.53
5	39.31	41.15	35.23	43.34	31.38	40.60	40.75	39.04	37.12	42.57	46.40	47.20	40.77	45.65
6	50.80	47.67	46.49	48.78	40.08	48.19	43.19	48.75	45.97	49.81	49.10	60.40	36.95	52.33
7	41.63	30.86	34.94	48.09	37.36	40.80	43.73	49.73	45.76	58.92	42.30	39.83	30.10	48.37
8	39.63	42.62	47.86	57.50	45.71	56.01	58.50	57.73	57.01	68.76	48.47	46.97	37.53	46.07
9	41.40	42.61	49.92	47.91	63.67	49.33	48.24	47.20	51.71	59.91	52.10	49.77	43.47	50.57
10	29.14	28.01	37.59	45.72	34.34	41.86	43.44	49.36	43.69	45.70	44.23	46.57	34.50	45.00
11	33.61	39.24	44.52	42.86	42.99	40.66	56.70	54.87	50.05	71.26	49.40	35.90	36.50	48.17
12	27.66	33.75	39.54	45.00	36.30	38.83	37.69	45.16	42.00	35.57	44.97	43.60	36.47	39.80
13	33.44	27.74	41.38	36.00	31.03	40.92	43.64	52.16	41.76	50.03	43.83	42.23	35.47	43.77
14	34.68	41.54	36.48	43.76	35.25	42.13	47.79	46.95	43.73	50.56	41.47	45.23	39.67	47.40
15	43.14	37.74	43.09	46.03	38.06	42.80	49.96	54.48	54.88	62.11	33.43	34.87	23.70	37.93
16	42.24	38.63	42.99	40.25	40.63	42.09	55.20	54.69	50.39	57.34	38.40	40.93	38.13	42.00
17	39.69	36.43	48.40	52.82	38.00	46.21	49.63	50.32	48.04	50.16	42.63	42.37	37.13	48.17
18	39.51	28.30	33.32	43.59	32.35	43.12	42.54	45.80	42.70	54.06	44.77	44.50	37.97	44.63
19	52.22	41.30	51.57	59.49	43.93	57.76	59.45	55.89	61.57	62.73	42.87	40.10	37.50	45.13
20	51.22	51.28	48.87	53.60	49.34	54.27	54.60	58.38	46.33	45.05	43.73	46.30	39.57	49.83
21	36.87	34.74	39.13	48.64	38.79	40.91	45.48	49.45	49.58	57.56	42.40	46.10	35.23	47.40
22	41.33	28.16	41.81	42.32	36.94	40.02	45.32	45.39	43.43	51.65	44.07	46.20	42.10	47.67
23	41.33	37.42	43.76	56.86	40.52	48.73	58.24	58.27	56.79	58.57	44.43	44.80	46.83	48.27
24	38.69	33.31	39.37	42.21	32.79	58.34	53.06	47.74	48.26	55.81	45.87	45.15	35.87	47.03
25	26.08	33.96	41.21	42.59	33.36	46.20	40.21	44.57	39.92	49.18	41.77	42.00	27.50	49.70
26	38.17	34.05	37.30	44.84	31.31	37.43	46.28	52.80	52.17	56.42	42.27	42.50	42.97	48.70
27	29.95	26.53	27.48	33.23	26.12	42.08	35.48	38.35	47.59	40.60	40.67	41.30	41.23	43.33
28	35.06	29.39	36.63	42.33	48.33	41.36	41.53	42.07	49.85	42.96	40.13	41.07	42.13	48.87
29	37.14	32.43	39.07	48.75	43.53	48.17	51.87	56.85	52.39	60.31	42.87	43.47	37.77	42.67
30	47.28	40.09	40.91	53.37	43.19	52.25	57.86	60.49	58.38	55.42	39.47	38.47	38.97	44.60
31	39.66	36.34	45.34	51.19	37.38	47.73	53.26	61.77	53.91	59.74	37.73	42.70	39.57	48.97
32	42.96	38.50	46.74	49.57	40.62	51.19	48.75	48.95	52.55	60.54	36.63	43.67	43.90	47.48
33	33.91	45.17	58.47	58.43	40.49	52.79	58.95	54.26	57.80	49.64	46.73	46.40	43.50	52.27
34	39.48	37.09	44.89	48.59	36.06	56.57	51.61	53.83	50.24	51.21	37.83	42.47	43.20	46.03
35	43.95	42.13	46.19	57.38	46.31	55.82	51.23	52.12	50.71	58.89	43.13	36.97	44.27	47.27
36	32.34	33.25	33.89	39.21	34.78	37.00	51.25	53.35	44.05	44.66	42.33	40.20	39.37	48.87
37	43.28	36.13	42.48	47.57	43.69	60.95	49.25	53.51	44.59	48.06	34.77	44.67	40.98	49.98
38	31.95	29.99	32.10	42.00	31.30	35.05	45.82	49.89	44.50	52.30	40.67	40.67	41.87	43.47
39	35.01	32.72	36.81	39.85	33.50	37.98	45.85	51.43	48.52	61.41	43.20	42.10	38.37	44.43
40	34.12	28.46	31.16	37.41	33.47	36.29	41.73	42.25	47.40	42.02	41.75	43.10	38.37	45.34
41	31.80	29.88	35.21	44.45	30.04	44.44	43.81	42.00	49.85	53.28	44.10	43.53	42.83	47.07
42	38.89	37.55	42.12	37.84	30.39	38.48	40.77	43.31	39.66	45.78	41.50	39.20	39.50	46.68
43	38.89	40.86	38.53	39.50	29.00	44.76	42.68	43.95	38.51	45.78	40.20	35.50	40.80	45.30
44	38.89	27.04	41.03	40.45	32.29	43.76	46.87	46.81	48.30	43.77	34.90	36.50	38.50	44.10
45	38.89	36.33	39.08	39.06	41.35	44.26	46.21	48.29	41.78	43.77	35.20	38.56	37.10	41.40
46	42.84	32.25	38.54	43.37	37.20	53.24	52.88	51.84	50.59	49.81	41.97	41.73	45.07	49.60
47	43.73	34.16	37.73	51.25	37.24	37.15	48.83	48.97	49.69	45.86	42.90	37.20	33.58	45.80
48	36.32	32.60	38.42	42.57	25.66	41.31	50.34	48.72	43.57	41.78	37.03	37.87	44.30	50.70
49	36.32	30.58	38.08	43.30	31.32	42.97	46.83	53.56	45.11	41.78	40.80	37.03	41.50	47.40
50	36.32	30.00	34.52	40.21	31.70	37.33	38.95	46.62	42.28	46.69	39.20	40.00	39.83	40.83

ID	06.165	06.179	06.193	06.207	06.221	06.235	06.263	06.277	06.290	06.305	06.319	06.333	06.354	07.10
1	24.10	20.27	17.67	5.43	20.73	25.60	10.53	23.90	15.63	25.23	31.30	34.47	31.00	38.87
2	37.23	42.83	34.23	21.50	24.67	35.87	21.47	28.57	19.53	26.83	36.50	34.50	39.63	41.77
3	27.13	32.90	19.83	13.60	23.50	31.60	15.77	26.07	15.13	30.07	37.17	37.37	34.20	41.73
4	37.63	39.40	28.23	10.70	25.87	29.97	18.03	32.67	18.77	32.53	38.33	36.30	34.63	47.67
5	33.53	37.63	23.30	10.53	28.90	35.23	17.37	29.80	18.63	28.23	38.70	37.10	36.73	44.20
6	49.10	43.27	41.80	16.37	26.80	39.40	20.80	29.93	16.60	24.00	31.03	35.53	37.63	41.47
7	33.13	32.70	23.00	10.27	23.77	32.43	19.17	26.95	16.87	27.70	35.37	38.20	38.63	45.40
8	34.60	43.90	24.83	13.67	37.37	38.48	20.83	33.30	23.30	39.80	37.07	44.20	38.77	41.83
9	45.17	51.20	37.77	13.07	33.03	40.63	18.97	31.60	22.63	36.00	39.77	45.03	39.63	42.47
10	32.07	37.93	21.43	12.72	22.80	34.80	14.40	28.47	19.47	32.67	36.63	38.40	39.80	43.00
11	35.80	35.03	33.58	14.47	22.27	39.10	19.50	30.57	20.17	37.20	34.57	39.47	37.87	45.67
12	32.67	39.30	23.20	15.07	24.07	36.27	17.53	33.40	17.27	31.80	35.57	34.77	38.97	46.07
13	33.53	41.47	32.40	10.50	31.43	40.60	24.30	36.10	22.50	32.97	37.97	34.67	38.53	44.53
14	25.97	42.83	27.47	13.40	23.90	33.77	16.93	30.30	20.33	33.97	26.37	38.77	37.03	43.83
15	25.33	26.87	21.18	10.60	24.53	25.67	14.77	25.27	14.47	22.93	26.13	29.27	31.37	35.40
16	29.77	39.57	24.77	9.60	18.87	27.27	18.57	27.40	15.47	25.50	30.77	30.20	37.73	38.47
17	41.40	36.60	27.67	15.03	23.40	28.90	16.00	32.10	17.20	31.17	34.37	36.87	38.47	44.90
18	36.67	42.40	26.77	11.73	25.57	29.07	19.77	30.87	16.97	34.77	35.07	40.67	43.93	44.13
19	32.50	33.83	22.03	12.03	19.13	28.83	15.93	25.10	16.97	28.90	29.80	37.83	37.60	37.47
20	37.20	43.67	30.13	15.20	27.27	32.75	22.50	35.33	19.93	30.50	36.70	38.87	38.97	40.97
21	25.73	34.00	22.93	13.73	19.20	31.55	15.70	27.20	13.77	28.53	34.20	38.20	39.13	39.90
22	36.13	46.47	24.47	13.40	26.27	28.00	14.77	20.80	18.60	37.87	34.07	36.10	41.73	42.00
23	30.88	38.73	23.50	13.90	21.90	35.83	16.70	30.73	17.07	36.97	36.93	37.93	41.03	40.43
24	23.50	40.33	21.67	11.73	25.70	32.63	15.47	22.53	16.10	28.73	33.07	40.37	36.77	41.10
25	36.57	32.37	20.20	8.13	26.50	35.27	16.43	31.20	15.80	38.63	32.67	36.77	44.33	41.60
26	35.93	37.13	20.17	16.53	24.03	36.47	15.97	29.30	16.77	35.23	31.63	37.60	42.00	44.30
27	21.93	32.87	15.23	12.17	21.90	30.47	12.40	26.37	-	29.83	35.30	34.90	41.10	43.23
28	30.57	38.03	22.57	15.90	24.90	33.57	15.70	33.30	14.50	33.23	30.00	33.27	44.00	46.47
29	35.13	38.03	20.70	13.53	20.50	29.00	14.87	31.90	17.70	32.53	31.20	39.43	39.37	43.73
30	32.83	36.33	22.33	14.10	23.00	33.40	15.67	33.47	15.00	35.85	32.33	35.40	40.67	43.90
31	34.87	34.87	22.57	16.03	19.43	30.53	13.00	21.10	11.20	23.03	31.07	37.83	39.87	40.80
32	36.63	40.33	20.30	15.83	30.83	32.27	18.77	37.13	23.23	30.30	36.30	36.90	40.67	39.53
33	50.57	56.97	26.90	13.00	28.17	41.73	19.40	34.40	16.47	38.50	44.23	44.53	38.20	42.40
34	38.30	45.37	34.23	23.13	34.00	41.00	31.83	37.27	15.73	36.13	35.47	39.17	39.17	46.17
35	40.93	45.10	25.40	14.00	24.37	35.90	19.73	34.57	16.67	31.93	36.43	35.37	-	43.83
36	25.57	34.03	20.88	13.90	24.37	32.73	14.07	27.07	17.43	30.03	33.73	35.83	42.60	38.00
37	39.27	40.63	28.40	14.70	25.50	36.30	17.80	31.83	28.10	35.10	35.50	39.17	40.30	47.77
38	30.57	34.53	21.00	15.07	19.30	19.83	14.73	22.73	16.23	23.33	30.93	33.87	37.13	40.73
39	33.83	39.43	20.15	13.57	19.07	24.67	15.73	26.07	16.83	29.17	32.23	38.47	42.30	43.97
40	28.37	27.27	16.27	12.53	17.70	30.13	15.03	34.17	20.17	29.83	37.30	37.43	41.57	42.53
41	34.40	43.00	26.07	13.83	23.47	30.73	21.33	37.27	20.07	28.93	31.60	38.50	35.23	45.43
42	32.12	37.57	16.20	9.63	24.77	29.93	11.57	27.90	14.97	32.53	33.20	35.87	41.30	43.67
43	28.13	33.23	17.53	12.37	26.33	28.87	13.30	22.90	14.30	25.73	30.97	35.23	34.27	39.03
44	29.03	35.77	14.67	10.97	24.30	26.13	12.83	31.80	13.83	30.07	29.67	35.23	36.70	40.40
45	29.47	32.17	25.63	13.67	22.33	24.50	11.87	26.43	18.37	28.30	30.13	37.47	39.53	37.63
46	37.17	33.47	23.30	13.73	26.57	29.63	17.13	26.27	14.67	28.60	32.07	37.10	42.17	46.37
47	30.10	33.13	20.18	15.83	26.07	29.90	18.37	31.77	17.33	31.20	34.30	39.10	36.67	40.65
48	32.60	33.83	17.80	14.80	16.77	28.63	13.20	19.67	16.17	35.07	31.60	40.77	41.70	41.07
49	34.27	35.30	19.37	11.57	22.77	18.40	14.73	25.83	15.60	30.80	26.80	35.00	39.43	42.30
50	32.07	35.50	17.43	13.13	21.07	31.17	13.90	25.45	15.40	30.43	30.57	37.43	40.73	40.40

ID	07.25	07.38	07.52	07.66	07.80	07.94	07.108	07.122	07.136	07.150	07.164
1	19.80	27.77	30.23	31.47	40.10	41.00	30.83	26.87	41.20	42.30	21.70
2	23.67	32.80	33.13	38.33	40.97	40.93	22.90	21.73	37.90	48.10	35.93
3	28.00	33.00	31.27	33.80	39.80	42.17	29.20	25.27	39.30	58.83	29.20
4	17.80	28.50	30.67	34.40	42.63	46.47	23.93	18.37	38.80	46.37	28.77
5	27.50	27.77	31.87	34.07	40.23	46.07	28.83	22.00	38.70	46.14	30.30
6	25.00	31.03	35.53	37.03	34.27	41.67	36.60	27.93	39.80	45.23	34.40
7	32.13	28.17	27.60	33.70	38.27	38.13	23.60	18.17	41.90	46.93	20.03
8	27.53	28.80	33.77	37.13	46.60	42.30	30.77	30.87	35.60	61.93	32.97
9	28.27	32.65	32.57	35.83	39.10	48.27	39.17	32.90	38.90	57.10	42.07
10	35.17	32.73	32.57	37.93	34.50	43.47	30.73	21.20	40.10	54.50	30.30
11	19.70	32.50	39.70	35.40	35.50	38.73	33.77	28.07	36.90	54.47	35.10
12	27.90	19.10	33.93	36.93	51.00	43.53	29.90	23.33	41.00	51.07	31.83
13	16.07	30.13	36.40	33.50	37.70	45.50	35.57	28.93	36.60	46.53	33.03
14	28.23	25.73	30.83	28.00	41.70	42.77	30.10	22.80	35.50	45.07	32.20
15	16.97	24.90	26.10	31.23	34.40	34.60	23.87	15.43	37.60	68.37	31.20
16	22.87	29.23	35.97	32.57	47.80	40.80	35.73	31.47	39.20	59.03	31.27
17	27.90	24.30	36.50	40.23	37.50	40.43	28.03	21.90	42.80	55.83	33.77
18	31.83	26.97	33.30	33.63	41.20	45.30	32.17	27.00	39.10	46.30	32.10
19	26.77	25.33	33.00	34.47	38.50	38.20	31.65	29.13	38.20	46.47	23.23
20	29.47	27.60	34.53	39.40	40.90	40.17	31.73	30.83	36.90	51.00	34.67
21	18.13	29.00	33.63	36.93	39.00	37.53	31.73	23.87	40.00	40.30	25.97
22	15.70	24.27	35.87	38.40	45.60	37.43	28.20	29.40	40.30	57.43	33.37
23	28.93	25.73	34.63	37.73	43.30	44.43	35.57	27.97	39.50	61.03	38.27
24	23.03	32.10	37.63	36.63	41.40	43.23	24.60	22.47	36.20	47.97	26.77
25	21.57	29.63	31.07	37.27	48.70	41.50	30.60	19.10	39.00	52.60	38.07
26	20.57	28.27	37.53	34.37	40.90	35.27	32.77	35.47	42.30	61.80	32.10
27	33.17	26.20	34.70	35.13	35.50	44.83	32.08	26.87	34.70	46.93	23.30
28	21.40	30.70	31.77	38.00	48.40	42.30	40.13	33.47	41.00	52.80	30.83
29	17.80	23.47	32.83	37.73	39.90	43.97	26.73	23.43	43.20	51.63	27.83
30	25.80	24.87	34.03	34.20	41.40	40.80	27.80	26.60	42.30	68.10	30.97
31	23.13	25.80	30.20	36.93	44.10	44.10	32.13	32.00	40.40	52.73	31.47
32	28.07	23.30	28.83	36.53	37.50	36.77	10.40	24.20	36.80	71.47	23.87
33	32.23	26.03	34.67	40.27	39.70	46.27	41.70	29.60	36.90	67.33	34.67
34	28.60	28.47	35.93	35.23	42.10	41.97	34.30	25.60	39.80	52.70	35.05
35	33.07	30.47	33.90	32.93	36.80	44.40	32.65	22.90	36.40	57.30	36.83
36	25.77	24.27	37.63	38.73	35.10	41.90	31.40	23.20	35.60	55.90	32.00
37	32.53	28.87	39.43	44.07	42.70	44.28	25.98	16.90	41.80	50.47	34.17
38	23.00	25.03	36.90	40.33	42.70	43.60	34.60	20.90	38.60	56.80	29.90
39	31.77	29.33	32.17	34.50	39.40	43.17	37.33	30.90	38.80	48.57	27.00
40	29.13	25.53	28.67	38.13	36.80	39.87	31.37	24.20	38.70	48.90	27.87
41	28.10	23.03	31.83	39.47	41.60	44.67	34.77	29.70	34.80	50.47	37.27
42	20.50	12.43	30.70	36.10	40.50	40.40	32.13	21.60	42.00	52.33	31.10
43	25.77	24.90	27.53	35.83	41.10	40.20	31.13	22.50	44.10	47.77	29.53
44	31.20	19.27	30.87	33.13	37.10	39.07	31.00	27.80	34.50	55.70	30.03
45	32.77	15.43	29.47	32.97	37.90	37.23	29.83	28.30	42.30	57.10	33.00
46	21.47	30.97	38.67	41.00	42.90	44.33	33.53	21.30	34.50	45.90	31.10
47	22.10	22.20	35.50	39.43	39.70	40.67	26.73	26.30	40.20	48.67	32.80
48	22.13	32.83	49.97	39.67	42.80	43.50	26.55	36.70	38.40	44.73	28.87
49	28.80	27.50	31.47	35.90	46.20	43.73	34.63	31.30	38.70	-	27.20
50	28.83	19.93	34.47	32.13	39.60	34.93	26.77	20.60	37.50	47.03	21.13

ID	05.237	05.251	05.265	05.279	05.293	05.306	05.321	05.334	05.348	06.11	06.110	06.123	06.137	06.149
51	36.32	29.62	31.51	39.79	32.32	42.48	42.35	41.99	43.02	46.69	39.10	37.55	40.00	39.80
52	32.41	39.32	49.67	51.05	36.64	47.06	52.48	54.46	52.84	49.08	41.77	46.10	52.87	47.03
53	31.36	36.18	43.33	44.19	41.26	47.86	47.89	45.33	51.77	53.49	45.03	42.27	42.13	49.47
54	36.63	33.91	34.92	46.42	40.58	51.82	49.59	47.22	49.81	54.39	45.87	45.50	33.00	40.60
55	39.03	49.21	41.38	49.24	42.65	49.28	46.24	60.84	49.24	65.26	42.67	45.03	42.40	47.37
56	40.70	39.87	40.96	47.96	37.72	42.90	53.86	57.67	50.45	58.80	37.00	40.24	43.63	53.40
57	40.76	44.38	40.52	56.99	39.11	53.30	55.51	63.80	61.32	60.51	48.90	46.33	47.13	57.30
58	41.14	42.49	51.81	57.47	41.72	53.77	60.94	59.08	55.42	57.99	41.97	47.53	31.20	44.50
59	41.19	31.87	40.12	54.59	38.85	35.28	53.25	54.93	54.24	46.47	35.52	37.97	28.85	39.93
60	41.19	41.18	44.52	52.25	40.91	50.85	50.37	47.90	45.36	46.47	26.20	39.53	33.45	40.23
61	41.19	44.02	42.23	50.86	38.81	43.07	50.28	51.81	44.96	48.90	46.00	37.43	36.90	44.07
62	41.19	40.09	36.63	39.65	33.21	39.88	43.96	45.37	47.27	48.90	42.50	36.27	35.70	47.83
63	29.46	34.75	34.85	40.14	36.93	39.76	41.60	43.20	52.11	41.51	43.53	38.97	39.40	47.23
64	40.96	42.72	49.47	59.54	35.02	51.48	55.55	55.63	61.14	49.29	41.33	45.85	42.23	47.80
65	41.39	55.72	56.55	49.55	56.84	58.73	56.30	62.78	60.93	75.12	39.97	47.10	43.27	47.97
66	41.39	58.87	55.28	59.81	61.01	60.76	49.37	57.93	62.85	51.53	46.10	52.60	46.17	49.03
67	41.39	65.13	64.46	75.58	63.91	57.85	56.05	56.85	65.40	51.53	47.80	45.10	38.43	46.47
68	41.39	45.90	43.51	51.75	45.38	46.01	50.68	49.30	49.87	80.00	50.50	53.10	40.20	49.40
69	66.17	70.32	75.66	84.32	68.32	58.20	68.01	65.82	77.57	80.00	78.28	51.80	77.93	75.43
70	28.95	28.60	34.23	39.38	27.60	34.88	47.97	47.52	48.03	46.23	36.13	48.40	31.43	42.77
71	31.76	28.52	32.70	37.24	27.90	35.19	44.69	41.76	42.27	48.42	45.63	46.90	38.37	46.83
72	34.50	34.97	32.73	40.22	34.14	44.05	46.44	51.25	53.87	53.46	44.30	39.50	30.50	44.50
73	28.59	33.21	28.73	37.46	24.60	37.98	41.52	42.66	43.43	38.18	40.07	50.40	34.50	43.80
74	27.63	26.77	34.80	42.31	38.79	36.37	33.42	45.02	50.78	42.62	37.73	41.30	32.63	44.85
75	29.72	31.43	30.64	42.48	31.22	37.60	41.29	48.72	48.46	47.05	37.97	34.40	45.27	43.73
76	45.63	50.99	55.35	66.08	42.63	57.78	59.24	65.75	67.99	59.97	45.90	46.70	47.13	47.80
77	43.40	38.87	50.79	52.47	43.15	54.91	54.10	57.26	56.25	54.82	44.63	50.10	40.33	47.70
78	38.88	34.19	37.53	45.71	37.78	47.45	51.35	55.29	53.88	59.06	46.87	40.00	28.90	51.00
79	34.98	31.37	38.11	46.02	33.20	44.54	47.60	52.65	49.99	48.70	44.17	48.80	33.70	40.30
80	50.03	46.14	52.76	54.73	44.43	53.79	52.94	57.51	60.91	65.01	38.33	48.40	32.20	43.78
81	44.93	42.25	38.85	48.69	40.91	48.56	50.18	54.84	48.23	54.36	44.43	43.00	45.60	44.53
82	44.37	40.56	37.30	45.42	40.57	47.40	50.61	47.36	57.65	51.70	49.30	41.80	41.80	51.90
83	35.38	31.73	32.52	40.81	34.98	38.65	56.33	56.75	49.81	48.81	37.53	34.10	49.60	44.33
84	45.14	44.53	47.39	52.38	35.93	54.24	60.23	56.40	65.78	60.18	41.30	42.90	36.60	44.87
85	46.34	30.36	36.77	46.92	34.55	44.40	51.94	64.58	47.97	52.39	42.93	46.20	46.30	49.87
86	33.77	31.40	38.01	36.75	34.18	42.77	41.66	43.29	56.64	51.36	42.77	46.80	38.10	47.67
87	44.96	52.58	51.24	53.81	45.93	45.78	56.57	53.13	53.67	60.70	47.27	42.10	41.20	45.48
88	36.76	45.58	39.84	55.07	42.06	52.85	46.74	50.84	59.46	42.72	41.03	44.90	37.30	46.98
89	59.33	33.00	37.82	46.39	44.09	48.09	52.54	50.27	50.53	53.71	36.07	45.20	35.70	48.50
90	45.62	50.91	47.06	54.25	45.83	54.03	54.72	57.62	60.27	53.39	49.60	37.50	42.90	51.60
91	33.98	27.67	37.23	39.87	33.56	42.08	41.88	44.90	41.05	45.66	46.30	33.80	54.00	46.33
92	62.47	50.88	64.72	64.85	60.26	60.43	67.58	65.44	67.03	69.98	47.23	35.80	42.50	43.93
93	30.66	24.98	35.43	40.05	27.63	41.79	38.12	41.71	46.17	39.57	46.13	47.10	43.60	43.52
94	43.67	42.57	49.06	50.74	55.57	49.98	51.76	50.25	57.58	51.65	49.70	54.50	36.60	49.77
95	51.23	58.08	70.96	64.97	61.17	72.38	87.88	77.28	76.73	77.77	45.20	43.50	34.30	55.60
96	71.19	66.53	67.47	68.90	64.77	70.51	71.53	66.29	66.11	83.21	55.00	42.80	46.60	58.83
97	56.48	42.57	55.87	54.08	45.74	47.84	60.35	60.61	66.37	59.01	43.43	40.00	38.90	48.43
98	38.02	34.06	46.12	50.91	37.94	49.93	56.58	58.73	55.38	54.48	41.73	39.20	40.80	33.56
99	38.02	37.48	45.32	52.57	41.06	49.24	60.54	54.53	56.40	54.48	41.73	37.70	40.80	35.40
100	38.02	39.43	45.19	61.75	44.86	49.44	57.61	54.22	50.26	52.10	41.73	45.70	49.80	31.40
101	38.02	36.72	40.62	46.20	38.37	43.10	63.03	49.56	51.08	52.10	41.73	37.30	34.90	32.83
AV	39.72	38.27	42.34	48.16	39.39	46.68	50.28	52.09	51.36	53.49	42.92	42.78	39.56	46.53
SD	8.51	8.97	9.01	8.87	8.85	7.68	8.13	6.91	7.83	9.22	5.62	4.83	6.59	5.23
CV	21.42	23.45	21.27	18.43	22.48	16.45	16.17	13.27	15.24	17.23	13.10	11.28	16.65	11.25

ID	06.165	06.179	06.193	06.207	06.221	06.235	06.263	06.277	06.290	06.305	06.319	06.333	06.354	07.10
51	29.33	30.10	20.80	12.37	19.03	22.23	12.10	29.47	14.53	29.60	36.47	37.13	41.67	43.10
52	34.90	48.50	32.30	17.90	28.93	34.63	18.07	36.23	18.17	37.60	33.97	42.70	42.43	41.70
53	41.73	49.67	14.60	16.83	38.73	45.47	31.63	37.00	24.70	44.50	38.70	41.37	52.77	50.97
54	36.03	41.00	28.30	14.83	25.97	35.97	16.47	34.10	19.13	34.83	33.23	37.87	42.90	43.23
55	38.30	41.33	24.10	15.50	30.33	29.20	14.63	30.45	14.97	29.03	34.27	39.53	43.23	39.03
56	36.50	35.70	22.30	16.40	25.77	29.63	20.40	24.40	16.83	33.13	34.53	39.80	40.50	44.47
57	38.00	45.27	28.80	18.37	31.77	41.30	19.53	31.63	16.20	37.47	34.97	38.87	41.17	43.93
58	32.37	44.87	21.20	16.33	19.77	32.20	18.03	23.40	17.63	35.67	41.95	37.90	41.83	42.13
59	27.53	41.13	18.10	13.53	24.03	30.83	13.80	35.93	21.27	32.57	28.50	39.77	38.57	35.70
60	31.10	38.75	25.20	12.67	21.40	32.23	17.47	27.78	17.20	31.03	32.10	36.53	40.60	39.97
61	33.67	32.53	33.80	12.53	26.30	33.50	16.03	29.03	19.67	35.57	40.43	37.70	39.70	42.43
62	30.17	35.83	31.40	12.43	21.73	37.47	13.00	25.00	19.33	33.30	32.63	32.67	41.43	40.47
63	29.17	35.73	15.50	11.07	21.93	28.90	14.23	29.83	15.63	26.87	28.40	38.10	38.80	43.03
64	35.10	40.53	32.30	15.20	22.97	40.00	16.45	32.90	19.30	37.43	33.30	38.80	39.37	43.87
65	41.77	49.07	18.30	14.23	25.93	34.67	21.40	44.67	23.97	33.33	31.87	54.40	39.53	44.60
66	36.87	48.03	24.90	30.77	40.60	48.53	31.80	36.56	38.77	46.87	33.73	49.97	46.27	54.53
67	45.83	43.70	30.30	36.40	48.23	52.67	47.60	48.47	47.67	46.92	48.00	48.30	48.20	63.80
68	41.70	37.00	29.10	41.43	46.73	49.50	43.10	44.67	46.73	56.78	49.60	51.77	49.13	55.53
69	59.83	68.27	25.10	60.83	67.53	77.60	75.70	66.10	67.83	82.87	69.50	82.30	84.03	82.20
70	31.57	40.73	23.50	13.67	23.43	33.70	15.48	31.43	14.60	35.60	29.47	34.80	40.80	43.10
71	28.33	37.67	24.70	11.13	21.77	34.30	15.50	31.43	16.57	34.20	35.00	37.17	38.60	39.50
72	27.63	35.50	12.50	13.87	20.70	29.20	16.60	28.50	15.13	31.67	32.40	36.33	38.10	39.67
73	33.57	38.43	38.50	14.20	19.67	22.60	13.37	26.67	15.97	27.47	34.83	36.40	41.03	47.53
74	28.07	33.40	21.10	9.67	27.20	33.77	18.20	34.73	20.63	39.87	35.93	43.20	38.60	42.20
75	28.03	26.73	23.60	12.80	16.30	30.80	11.30	25.73	14.27	28.43	32.17	35.17	38.10	35.93
76	33.73	39.20	27.60	10.87	25.60	28.97	17.03	29.80	14.23	33.30	26.00	34.53	37.23	37.83
77	32.63	38.23	19.40	10.73	24.27	31.60	16.80	30.20	20.57	38.67	31.60	37.30	38.20	40.43
78	29.30	33.57	25.60	16.03	22.30	32.57	15.63	24.77	19.20	36.27	30.93	37.63	37.70	43.77
79	35.87	36.57	26.90	13.67	23.57	34.00	15.87	31.20	14.73	33.37	25.83	37.23	35.70	40.87
80	23.40	33.65	21.00	17.50	22.87	31.93	13.57	25.60	17.67	34.67	23.37	33.60	39.27	41.00
81	32.67	37.93	18.50	17.40	25.07	35.25	16.48	23.28	17.30	38.13	25.77	38.30	36.70	43.40
82	24.97	38.03	18.70	14.90	27.33	32.30	14.23	27.97	18.47	39.20	36.93	38.73	42.03	44.30
83	30.13	38.03	12.90	7.60	20.33	27.97	15.94	17.43	16.63	36.90	30.47	42.20	43.27	47.63
84	34.33	40.67	24.00	7.60	22.47	36.77	12.45	14.45	16.53	39.57	36.20	41.33	39.93	43.47
85	31.60	36.18	20.70	17.40	25.97	25.03	13.78	18.98	21.47	40.57	30.37	36.93	46.07	41.10
86	-	43.20	18.90	17.50	28.57	38.07	17.13	19.30	16.17	34.80	32.13	35.70	43.87	42.03
87	-	41.97	25.20	8.20	22.58	35.23	16.00	15.45	17.87	36.97	29.53	37.83	40.97	42.63
88	28.43	33.68	23.40	15.00	23.13	36.03	16.77	15.83	14.43	32.20	28.40	37.67	42.50	36.33
89	28.80	32.93	29.50	23.20	21.73	32.47	14.98	16.30	21.33	34.47	28.03	34.27	37.83	41.53
90	37.93	45.90	31.90	2.80	32.80	40.30	13.70	40.43	27.50	45.50	34.63	41.30	39.17	42.70
91	29.50	37.50	28.70	25.90	24.90	37.07	27.27	37.47	16.60	34.43	28.70	38.47	39.20	39.67
92	32.85	32.60	23.00	11.30	22.90	35.33	19.67	22.67	19.50	40.37	27.73	33.67	33.67	36.70
93	32.50	36.60	21.80	13.80	17.70	29.30	14.93	23.80	12.70	31.20	29.37	35.80	39.43	43.33
94	33.77	45.60	26.20	12.30	30.58	36.63	11.60	24.77	18.37	34.77	32.50	39.80	42.90	42.10
95	36.70	37.90	26.90	9.70	28.20	31.23	14.30	36.10	18.53	26.05	30.23	34.40	35.87	41.33
96	55.80	60.93	25.50	19.60	59.40	61.57	58.23	65.13	60.53	73.27	57.57	65.30	73.20	71.47
97	45.60	50.34	22.70	26.90	20.47	27.00	16.60	19.30	17.63	34.43	29.17	35.20	37.53	42.33
98	26.63	39.38	25.40	3.70	28.00	35.03	61.53	34.73	17.40	34.63	29.00	36.57	36.40	44.70
99	28.90	37.58	21.30	1.00	27.67	26.83	14.07	35.87	19.00	30.27	26.80	36.73	42.27	40.83
100	30.80	38.23	13.80	19.10	32.20	32.67	16.63	28.90	19.10	33.13	31.93	39.40	40.83	44.40
101	32.20	36.21	23.10	15.90	29.83	34.10	17.05	30.73	15.83	39.40	29.03	38.73	43.53	34.10
AV	33.72	38.93	23.88	14.80	26.00	33.68	18.80	29.93	19.42	34.34	33.69	38.71	40.63	43.29
SD	6.45	6.74	5.62	7.26	7.67	7.73	9.95	8.07	8.44	8.30	6.16	6.40	6.43	6.30
CV	19.14	17.30	23.51	49.03	29.50	22.94	52.93	26.97	43.48	24.17	18.29	16.54	15.82	14.56

ID	07.25	07.38	07.52	07.66	07.80	07.94	07.108	07.122	07.136	07.150	07.164
51	30.57	31.50	35.87	37.57	41.60	40.63	34.20	23.10	32.20	58.03	27.70
52	21.27	32.40	36.00	39.47	44.50	37.10	36.20	33.30	40.50	57.58	27.43
53	34.77	30.30	29.37	41.53	44.90	42.20	37.47	19.00	42.70	46.67	37.63
54	24.93	23.93	33.30	33.07	40.40	35.10	29.60	26.30	37.90	49.00	26.73
55	36.10	26.90	30.70	36.30	40.40	42.20	33.70	26.50	34.90	55.70	24.50
56	24.27	33.07	35.70	39.47	41.30	39.90	27.60	28.80	42.10	42.10	29.47
57	23.07	27.47	35.43	42.50	42.10	42.80	33.80	22.10	42.50	41.63	39.43
58	30.27	23.43	31.10	36.33	36.70	41.20	30.00	35.50	37.60	41.77	26.07
59	27.80	22.17	29.30	30.53	40.10	38.50	24.90	28.80	34.80	64.90	19.13
60	16.07	21.47	30.47	35.03	38.00	39.40	39.20	25.60	38.50	37.70	24.97
61	25.83	29.47	32.23	36.13	41.60	40.80	28.50	23.40	41.90	62.10	21.43
62	30.97	35.63	27.77	35.00	35.00	39.20	35.70	27.60	39.40	55.90	32.07
63	29.10	33.67	34.40	36.47	39.50	40.60	40.10	18.00	38.90	49.20	27.50
64	24.47	30.47	36.23	38.30	45.50	43.80	23.40	19.60	43.20	33.00	35.13
65	23.83	25.87	33.80	37.33	38.80	44.20	31.90	19.40	40.80	51.30	34.10
66	42.83	39.20	42.83	43.93	41.50	44.40	15.20	27.20	37.80	62.20	38.97
67	38.30	32.17	43.83	50.43	42.30	42.60	32.70	16.10	38.00	48.70	37.63
68	35.60	44.10	38.77	38.83	38.20	42.80	39.70	27.90	47.10	47.50	43.70
69	50.83	65.13	53.93	57.87	38.90	45.70	27.50	25.50	36.50	59.10	51.00
70	25.37	26.53	33.77	36.03	46.40	41.50	31.50	23.10	34.30	57.20	30.03
71	25.53	29.93	28.30	37.00	37.50	38.50	29.80	22.50	39.10	47.10	32.97
72	15.80	26.00	31.40	38.27	43.20	46.60	29.40	25.70	36.10	53.80	30.10
73	24.73	32.77	33.87	39.27	39.20	41.30	37.30	30.90	41.20	52.50	26.93
74	20.77	25.40	30.73	38.77	41.90	46.20	30.90	31.00	39.20	48.20	22.93
75	20.90	29.63	27.23	36.73	39.90	41.90	23.30	27.90	37.30	42.70	23.90
76	31.30	29.67	27.33	33.00	38.50	38.70	34.50	20.30	39.20	48.00	32.37
77	19.67	27.80	31.03	32.40	40.00	44.50	30.40	19.00	41.50	46.30	27.80
78	37.23	34.33	36.07	35.57	37.50	43.10	33.60	27.10	36.00	58.70	38.07
79	22.63	25.43	30.00	36.47	41.10	42.60	33.30	27.00	43.60	66.60	28.93
80	19.63	22.73	33.73	38.97	38.10	40.50	22.00	24.00	39.40	47.70	30.83
81	34.87	30.57	35.93	40.20	42.30	39.60	26.80	28.00	40.50	40.80	33.93
82	19.37	31.17	35.67	36.70	44.70	44.60	32.50	37.50	39.70	48.90	35.90
83	24.03	33.47	37.73	36.33	34.80	37.00	25.60	19.20	35.80	55.80	23.73
84	23.67	32.37	36.37	36.80	41.60	39.70	30.00	27.10	39.10	35.00	32.43
85	17.00	31.33	37.30	42.17	40.00	41.30	33.20	26.50	37.90	56.50	28.67
86	24.33	32.93	34.97	39.80	39.20	36.40	29.70	26.00	41.40	51.90	37.73
87	29.63	34.63	29.57	36.60	44.80	42.00	29.30	37.10	41.00	48.50	30.43
88	17.37	15.13	31.07	41.40	33.80	42.80	33.50	24.50	36.80	57.30	26.70
89	18.53	16.74	29.37	31.07	45.20	45.00	39.80	31.70	34.30	64.20	27.97
90	32.43	40.28	33.80	37.03	39.90	45.80	34.90	26.30	37.00	47.30	30.50
91	32.80	37.72	33.73	31.57	32.50	45.40	24.90	24.10	35.10	53.40	31.30
92	32.20	22.52	28.90	41.00	48.40	43.90	37.80	25.70	36.80	48.90	27.83
93	13.60	23.64	30.47	36.80	43.50	35.00	28.80	26.70	44.80	41.80	21.07
94	28.20	24.63	32.50	39.03	43.90	45.20	30.00	33.30	36.60	53.30	32.57
95	26.20	36.10	30.53	36.63	36.30	42.90	34.30	21.00	34.80	44.90	35.37
96	34.97	65.13	30.73	34.77	38.60	42.10	33.60	28.90	38.70	59.00	62.47
97	28.37	19.74	31.57	35.27	38.00	41.50	24.20	29.40	39.20	63.30	40.70
98	27.40	34.73	34.63	41.23	40.20	48.20	33.10	21.10	34.30	37.60	26.90
99	25.40	35.23	30.27	41.53	41.50	43.80	30.30	22.00	37.30	36.80	31.70
100	15.43	28.54	33.13	40.40	35.80	41.40	33.40	34.20	35.80	62.50	30.67
101	19.63	30.73	39.40	37.20	42.80	44.70	26.90	32.50	37.10	54.20	29.23
AV	26.21	28.86	33.60	37.14	40.55	41.82	30.97	25.98	38.75	51.79	31.22
SD	6.41	7.42	4.29	3.91	3.57	3.04	5.07	4.91	2.76	7.76	6.19
CV	24.47	25.71	12.76	10.54	8.81	7.26	16.38	18.90	7.12	14.98	19.82

13.3 Soil temperature data

First measurement series

ID	05.104	05.117	05.133	05.146	05.161	05.174	05.188	05.204	05.217	05.230	05.245	05.261	05.273	05.294
1	8.9	7.7	6.9	11.4	9.6	13.9	12.8	13.4	12.6	12.9	16.1	10.2	10.1	9.5
2	8.6	7.4	7.0	11.5	9.7	13.8	12.9	12.8	12.5	12.6	15.7	10.1	10.4	9.4
3	8.5	7.6	7.0	11.2	9.6	13.7	12.8	13.5	12.4	13.0	15.8	10.3	10.3	9.6
4	8.2	7.4	7.2	11.0	9.5	13.5	12.8	12.5	12.7	13.0	15.9	10.2	10.4	9.6
5	8.0	7.1	6.6	11.7	9.4	13.9	13.1	13.7	12.9	13.0	16.0	10.1	10.3	9.7
6	9.5	7.6	7.3	12.6	9.5	14.5	12.8	13.3	12.8	13.3	16.0	10.5	10.4	9.5
7	8.2	7.6	7.1	11.4	9.4	13.8	12.8	12.4	12.9	12.9	15.7	10.4	10.5	9.5
8	8.6	7.4	7.1	11.8	9.6	13.7	12.7	12.2	12.5	13.0	15.8	10.4	10.5	9.7
9	8.5	7.5	7.0	12.0	9.4	13.8	12.7	12.1	12.7	13.0	16.0	10.4	10.4	9.6
10	8.5	7.5	6.8	11.6	9.5	13.8	13.0	12.2	13.1	12.9	15.7	10.5	10.3	9.4
11	8.6	7.8	7.2	11.6	9.7	14.1	12.8	12.5	13.0	13.2	15.7	10.3	10.5	9.7
12	9.1	7.4	7.5	11.6	9.7	13.7	12.9	12.4	12.6	13.3	15.6	10.3	10.6	9.5
13	8.7	7.2	7.0	10.6	9.7	13.6	12.5	12.6	12.7	13.2	15.7	10.5	10.5	9.5
14	8.5	7.5	7.2	11.6	9.3	13.7	12.8	12.1	12.9	13.0	15.9	10.6	10.3	9.4
15	7.7	7.3	7.2	10.5	9.4	13.4	12.8	12.7	12.8	13.0	16.0	10.8	10.2	9.3
16	8.6	7.4	7.6	11.7	9.9	14.2	12.9	12.4	12.6	13.2	16.0	10.5	10.2	9.7
17	8.7	7.8	7.7	12.3	9.8	13.9	12.5	12.4	12.7	13.1	16.0	10.6	10.6	9.5
18	8.9	8.7	7.4	11.3	9.5	13.4	12.5	12.2	12.5	13.0	16.0	10.6	10.5	9.6
19	8.5	7.9	7.0	11.1	9.4	13.2	12.5	12.6	12.6	12.9	15.7	11.0	10.4	9.6
20	8.6	7.4	7.2	11.1	9.4	13.8	12.8	12.3	12.7	13.0	15.7	10.5	10.3	9.7
21	9.0	7.7	7.1	12.2	9.6	13.8	12.6	12.2	12.9	12.9	15.9	10.3	10.4	9.5
22	9.7	8.0	7.8	13.4	9.5	14.3	12.8	12.2	13.1	13.2	15.8	10.0	10.5	9.5
23	8.9	7.8	7.8	12.4	9.9	13.9	12.4	12.6	13.0	13.2	16.0	10.7	10.6	9.4
24	9.2	8.4	6.7	12.2	9.4	14.2	12.6	12.2	12.7	13.1	15.8	10.3	10.5	9.6
25	8.7	7.7	7.5	11.6	9.6	13.7	12.5	12.3	12.8	13.0	16.0	10.3	10.6	9.6
26	9.3	8.1	7.4	12.6	9.6	13.5	12.7	12.4	12.2	13.1	15.8	10.5	10.4	9.7
27	8.5	7.7	7.2	11.2	9.4	13.5	12.7	12.2	12.6	13.0	15.9	10.4	10.6	9.6
28	8.5	7.5	7.3	11.3	9.5	13.4	12.6	12.4	12.5	12.9	15.6	10.9	10.5	9.5
29	8.5	7.6	7.4	11.0	9.5	13.5	12.6	12.4	12.7	12.8	15.7	10.9	10.5	9.6
30	8.5	7.6	7.4	11.4	9.5	13.6	12.6	12.3	12.6	12.9	15.7	10.7	10.4	9.5
31	8.5	7.8	7.4	11.9	9.5	13.7	12.7	12.3	12.8	13.0	15.8	10.4	10.4	9.5
32	9.3	8.2	7.7	11.9	9.8	14.1	12.7	12.5	12.6	13.1	15.9	10.3	10.3	9.4
33	9.0	8.0	7.6	11.9	9.6	13.7	12.7	12.5	12.8	13.2	16.0	10.6	10.3	9.5
34	9.0	8.0	7.8	12.1	9.6	13.7	12.8	12.5	12.8	13.1	16.2	10.6	10.4	9.6
35	9.0	8.0	7.8	11.9	9.7	13.6	12.6	12.5	12.9	13.2	16.0	10.7	10.4	9.7
36	9.0	8.0	7.8	11.9	9.7	13.6	12.6	12.5	12.7	13.1	15.9	10.8	10.5	9.6
37	9.3	7.8	7.5	12.0	9.6	14.1	12.7	12.4	12.9	13.1	15.7	10.8	10.3	9.6
38	9.3	8.0	7.6	12.2	9.6	14.1	12.6	12.4	13.2	13.2	15.8	10.5	10.3	9.6
39	9.3	7.8	7.7	11.9	9.7	13.8	12.7	12.5	13.1	13.1	15.8	10.4	10.4	9.5
40	9.3	8.0	7.7	11.6	9.7	13.8	12.7	12.5	12.9	13.1	15.8	10.5	10.4	9.6
41	8.7	8.1	7.7	11.6	9.7	13.6	12.6	12.4	12.6	13.1	15.6	10.7	10.6	9.7
42	9.7	8.1	7.9	12.2	9.9	14.0	12.7	12.6	12.8	13.2	15.8	10.8	10.6	9.6
43	9.7	8.5	8.0	12.5	9.9	14.0	12.7	12.6	12.6	13.2	15.9	10.8	10.7	9.5
44	9.7	8.4	8.0	12.6	10.0	14.0	12.7	12.6	12.7	13.4	16.0	10.7	10.7	9.5
45	9.7	8.0	7.9	12.2	10.0	14.0	12.7	12.6	12.9	13.3	16.1	10.5	10.6	9.6
46	9.1	8.6	7.8	12.3	9.6	14.0	12.6	12.6	12.5	13.4	16.0	10.9	10.5	9.4
47	8.9	8.3	8.1	12.3	9.8	13.9	12.7	12.5	12.5	13.3	16.2	10.6	10.6	9.5
48	9.2	8.1	7.4	11.9	9.5	14.0	12.4	12.2	12.3	13.2	16.1	10.5	10.6	9.5
49	9.0	8.1	7.7	11.8	9.5	13.8	12.5	12.3	12.6	13.1	15.6	10.5	10.7	9.4
50	9.1	8.0	7.5	11.8	9.4	14.0	12.4	12.2	12.8	13.1	15.7	10.3	10.8	9.5

ID	05.302	05.315	05.327	05.341	05.355	06.004	06.089	06.102
1	11.0	7.8	4.1	3.3	2.2	1.5	2.4	3.6
2	11.0	8.0	4.2	3.2	2.2	1.6	1.6	3.5
3	11.1	7.7	3.7	3.4	2.3	1.6	2.3	3.3
4	10.9	8.1	4.4	3.6	2.3	1.8	2.3	3.5
5	10.9	7.8	3.8	3.3	2.3	1.5	2.3	3.1
6	11.2	7.5	3.0	3.1	1.6	1.4	2.3	3.2
7	10.9	8.2	4.1	3.7	2.3	1.5	1.4	3.3
8	10.8	8.2	4.3	3.7	2.4	1.6	2.9	3.5
9	10.9	8.0	4.4	3.6	2.3	1.5	1.8	3.4
10	10.9	7.7	4.0	3.4	2.0	1.6	2.3	3.3
11	11.0	8.2	3.9	3.4	2.3	1.5	2.2	3.5
12	11.0	8.0	4.3	3.7	2.4	1.6	2.6	3.6
13	11.2	8.6	4.9	4.1	2.3	1.7	2.5	3.7
14	11.2	7.9	3.3	3.6	2.2	1.8	2.3	3.3
15	11.2	8.7	4.9	3.8	2.0	2.2	2.4	3.5
16	11.3	8.1	3.4	3.6	2.2	1.6	2.4	3.6
17	10.9	8.2	4.2	3.7	2.2	1.5	1.4	3.6
18	10.9	8.3	4.1	3.7	2.0	1.7	1.8	3.4
19	11.1	8.1	4.3	3.8	2.6	1.5	2.2	3.5
20	11.9	8.4	3.9	4.1	2.5	1.4	2.0	3.8
21	11.1	8.2	3.7	3.3	2.5	1.5	2.4	3.6
22	11.1	7.9	3.2	3.3	2.5	1.6	2.5	3.3
23	11.1	8.1	3.5	3.4	2.4	1.7	2.3	3.5
24	11.2	8.1	4.4	3.6	2.2	1.4	2.1	3.4
25	11.0	8.2	4.3	3.6	2.2	1.5	2.2	3.6
26	11.1	8.0	3.4	3.6	2.3	1.5	1.7	3.4
27	11.3	8.0	3.8	3.4	2.3	1.4	2.4	3.8
28	11.0	8.1	3.9	3.2	2.1	1.4	2.0	3.3
29	11.0	8.1	4.0	3.3	2.1	1.4	1.7	3.3
30	11.0	8.1	3.7	3.0	2.1	1.4	1.9	3.3
31	11.0	8.2	3.6	3.4	2.1	1.5	2.0	3.3
32	11.0	7.8	3.6	3.0	1.9	1.6	2.1	3.4
33	11.0	7.8	4.3	3.1	1.9	1.2	2.6	3.7
34	11.0	7.9	4.8	3.0	1.9	1.3	0.7	2.7
35	11.2	8.0	4.2	3.2	1.8	1.5	2.5	4.0
36	11.2	7.9	4.4	3.3	1.9	1.5	1.6	3.9
37	11.2	8.0	4.4	3.3	2.0	1.6	2.2	3.4
38	11.1	8.0	4.0	3.2	1.9	1.6	2.0	3.4
39	11.2	8.0	3.8	3.2	2.0	1.5	2.0	3.4
40	11.1	8.1	4.0	3.2	2.0	1.6	1.6	3.5
41	11.1	8.3	4.1	3.5	2.0	1.5	1.6	3.5
42	11.2	8.1	4.1	3.3	2.0	1.6	1.6	3.3
43	11.2	8.0	4.2	3.2	2.0	1.5	1.3	3.6
44	11.2	8.1	3.7	3.2	1.9	1.7	2.2	3.3
45	11.2	8.1	4.0	3.3	2.0	1.5	2.3	3.8
46	11.2	7.9	4.5	3.3	2.6	1.4	1.8	4.2
47	11.2	7.9	3.6	3.0	2.1	1.4	2.0	3.2
48	11.0	7.9	3.5	3.2	2.0	1.4	1.8	3.5
49	11.1	8.0	4.2	3.4	2.1	1.3	2.3	3.4
50	11.1	8.0	4.2	3.2	2.0	1.3	1.4	3.7

ID	05.104	05.117	05.133	05.146	05.161	05.174	05.188	05.204	05.217	05.230	05.245	05.261	05.273	05.294
51	9.1	8.2	7.6	11.6	9.6	13.6	12.6	12.4	12.6	13.0	15.7	10.5	10.6	9.6
52	9.2	8.2	7.9	12.5	9.5	14.1	12.7	12.2	12.5	13.2	16.0	10.6	10.2	9.4
53	9.3	7.9	7.8	11.8	9.7	14.0	12.6	12.8	12.7	13.7	16.1	11.0	10.5	9.5
54	8.5	8.2	7.4	11.9	9.6	13.7	12.4	12.2	12.8	13.2	15.8	10.7	10.8	9.5
55	9.2	7.9	7.9	12.7	9.7	15.3	12.6	12.4	12.5	13.7	15.6	10.3	10.4	9.6
56	9.5	8.2	7.8	11.5	9.3	13.4	12.2	12.2	12.4	12.8	15.4	11.0	10.5	9.5
57	8.8	8.3	7.7	11.6	9.6	13.7	12.6	12.4	12.5	13.2	16.1	10.5	10.7	9.4
58	9.4	7.2	7.5	11.2	9.5	13.7	12.5	12.4	12.9	12.9	16.0	10.3	11.0	9.4
59	9.2	7.8	7.5	11.2	9.5	13.7	12.6	12.4	12.8	13.2	15.9	10.4	10.4	9.4
60	8.9	8.0	8.1	12.4	9.8	14.7	12.8	12.4	13.3	13.6	16.9	10.4	10.5	9.7
61	8.9	8.2	8.2	12.7	10.0	15.1	12.6	12.4	13.2	13.6	16.0	10.7	10.3	9.5
62	9.0	7.8	8.0	12.5	9.7	14.4	12.5	12.3	13.3	13.6	16.3	10.6	10.1	9.6
63	8.7	7.5	8.1	12.4	9.7	14.3	12.6	12.3	13.5	13.5	16.1	10.7	10.4	9.7
64	8.7	7.9	8.0	12.3	9.9	14.3	12.6	12.4	12.9	13.4	16.3	10.8	10.6	9.6
65	8.7	7.8	8.2	12.7	9.9	14.7	12.6	12.4	12.8	13.5	16.3	10.7	10.5	9.6
66	9.5	7.5	8.0	12.4	9.7	14.2	12.6	12.5	13.1	13.5	16.1	10.8	10.5	9.4
67	9.1	7.9	7.9	12.3	9.5	14.0	12.5	12.0	12.8	13.5	16.2	10.6	10.6	9.4
68	9.3	8.3	8.6	13.3	9.9	15.1	12.4	12.3	12.5	14.2	16.4	10.5	10.3	9.7
69	9.7	7.4	8.1	12.7	9.9	14.9	12.5	12.3	12.6	13.8	16.5	10.4	10.4	9.4
70	8.6	8.1	7.8	12.3	9.7	14.2	12.4	12.3	12.8	13.5	16.3	10.8	10.5	9.5
71	9.0	7.4	8.1	12.8	9.8	14.6	12.5	12.2	12.7	13.6	16.2	10.6	10.5	9.5
72	9.3	8.2	8.1	12.5	9.8	14.7	12.6	12.4	12.6	13.7	16.3	10.7	10.6	9.4
73	9.4	8.0	8.2	12.4	9.8	14.7	12.5	12.3	12.8	14.0	16.2	10.5	10.4	9.6
74	8.5	8.3	7.7	12.0	9.7	14.3	12.6	12.4	12.8	13.5	16.2	10.6	10.5	9.5
75	9.3	7.3	8.1	12.6	9.8	14.5	12.6	12.4	12.8	14.0	16.1	10.6	10.4	9.7
76	9.0	7.9	8.3	12.9	10.0	14.9	12.7	12.4	12.7	13.8	16.3	10.5	10.2	9.6
77	9.0	8.4	8.4	12.6	10.0	14.8	12.6	12.5	12.6	13.7	16.4	10.4	10.5	9.5
78	9.1	7.6	7.9	12.8	9.7	14.7	12.5	12.4	12.6	13.6	16.0	11.0	10.6	9.6
79	8.8	7.8	8.5	12.4	9.8	14.3	12.6	12.3	12.8	14.2	16.1	10.8	10.7	9.6
80	8.6	7.2	7.9	11.8	9.6	15.0	12.7	12.5	12.7	13.7	16.1	10.5	10.7	9.7
81	8.9	7.2	8.3	12.3	9.8	14.2	12.5	12.4	12.9	13.5	16.0	10.6	10.6	9.7
82	9.4	8.1	7.6	11.3	9.5	14.4	12.2	12.4	12.3	13.6	16.3	10.8	10.7	9.4
83	9.1	6.7	8.4	12.6	9.6	13.7	12.6	12.5	12.8	14.2	16.2	11.5	10.2	9.4
84	9.5	7.9	8.0	12.5	9.7	14.4	12.6	12.3	12.4	13.8	16.5	11.9	10.4	9.6
85	8.5	8.1	7.8	12.3	9.7	15.1	12.7	12.3	12.8	13.7	16.5	10.6	10.6	9.4
86	8.7	7.2	7.8	11.7	9.6	14.6	12.5	12.2	12.6	13.4	16.3	10.5	10.7	9.7
87	9.0	7.7	8.2	12.5	9.6	14.3	12.6	12.3	13.0	13.6	16.4	10.8	10.5	9.8
88	9.1	7.8	8.3	11.8	9.7	14.0	12.6	12.3	12.9	13.8	16.2	10.9	10.6	9.5
89	9.2	7.6	8.0	11.9	9.8	14.2	12.7	12.3	12.8	13.6	16.1	11.0	10.5	9.5
90	9.2	7.6	8.6	13.0	9.8	15.0	12.5	12.4	12.5	14.1	16.5	10.8	10.4	9.4
91	8.8	7.6	8.9	12.7	10.0	15.5	12.5	12.4	12.8	13.6	16.6	10.7	10.4	9.6
92	9.4	7.7	8.4	12.3	9.8	14.4	12.5	12.4	12.6	14.0	16.1	10.7	10.5	9.5
93	8.8	7.6	8.6	12.8	9.7	14.4	12.6	12.4	12.7	14.0	16.5	10.9	10.4	9.5
94	9.2	7.7	8.3	12.3	9.7	14.3	12.6	12.5	12.6	13.7	16.2	11.1	10.6	9.6
95	9.4	8.3	8.2	12.0	9.8	14.2	12.7	12.5	12.8	13.8	16.5	11.2	10.7	9.7
96	9.2	8.4	8.8	12.8	10.6	15.4	12.6	12.4	12.8	14.0	16.4	11.1	10.8	9.4
97	8.9	8.3	8.9	12.7	10.6	15.4	12.5	12.4	12.5	13.9	16.4	11.2	10.7	9.7
98	9.1	8.4	9.1	13.0	10.7	15.1	12.5	12.4	12.9	14.1	16.5	11.2	10.7	9.6
99	8.9	7.8	9.4	13.7	10.7	15.9	12.5	12.4	12.6	14.2	16.5	11.2	10.7	9.6
AV	9.0	7.8	7.8	12.1	9.7	14.1	12.6	12.4	12.7	13.4	16.0	10.6	10.5	9.5
SD	0.4	0.4	0.5	0.6	0.3	0.5	0.1	0.3	0.2	0.4	0.3	0.3	0.2	0.1
CV	4.4	4.8	6.8	5.0	2.7	3.9	1.2	2.1	1.8	2.9	1.8	2.8	1.6	1.1

ID	05.302	05.315	05.327	05.341	05.355	06.004	06.089	06.102
51	11.1	8.1	4.2	3.3	2.1	1.4	1.8	3.4
52	11.2	8.1	3.6	3.4	2.8	1.8	2.4	3.0
53	11.1	7.9	4.3	3.4	2.0	1.5	2.1	3.5
54	11.0	7.8	5.5	3.3	2.0	1.5	2.2	3.2
55	11.0	7.6	4.3	3.6	2.0	1.1	2.3	3.1
56	11.3	8.0	5.2	3.7	2.1	1.2	1.8	3.6
57	11.0	7.9	4.4	3.5	2.0	1.5	1.6	3.9
58	11.0	8.5	4.9	3.6	3.2	1.5	1.9	4.0
59	11.2	7.9	4.2	3.7	1.9	1.2	2.2	3.3
60	11.1	7.9	4.3	3.3	2.3	1.4	1.7	3.4
61	11.2	7.8	3.7	3.5	2.3	1.5	1.5	3.7
62	11.0	7.8	3.0	3.4	2.0	1.3	2.5	3.3
63	11.0	7.8	4.1	3.2	2.0	1.5	1.4	3.6
64	10.9	7.9	4.2	3.4	2.2	1.5	2.7	3.7
65	10.8	7.9	4.2	3.3	2.4	1.5	1.9	3.0
66	11.1	7.8	3.9	3.3	2.1	1.7	1.8	3.4
67	11.2	7.8	4.2	3.6	2.3	1.5	2.0	3.4
68	11.0	7.8	3.8	3.6	2.0	1.2	2.4	3.8
69	11.0	7.8	4.1	3.5	1.6	1.4	2.3	3.0
70	11.1	7.7	3.6	3.3	1.9	1.6	2.2	4.5
71	11.2	7.8	4.4	3.2	2.3	1.6	2.0	3.7
72	11.3	7.8	4.7	3.3	2.2	1.6	2.5	3.7
73	11.0	7.9	4.0	3.5	2.1	1.4	2.4	3.7
74	11.0	7.7	4.0	3.4	2.3	1.3	2.3	2.5
75	11.1	7.8	3.8	3.2	2.4	1.3	2.1	3.5
76	11.1	7.5	3.3	3.1	2.4	1.2	2.1	3.2
77	10.9	7.7	3.5	3.6	2.0	1.4	2.0	3.9
78	10.9	7.9	4.1	3.6	2.1	1.6	2.4	3.7
79	11.0	7.8	4.2	3.6	2.3	1.7	1.6	3.5
80	10.8	7.8	4.2	3.6	2.3	1.3	1.6	3.1
81	10.9	7.7	3.8	3.7	2.1	1.6	1.7	3.0
82	10.9	7.9	4.2	3.9	2.1	1.4	1.9	3.5
83	11.0	8.1	3.7	3.6	1.8	1.8	2.0	3.6
84	11.0	8.0	3.5	3.1	2.0	1.5	2.0	3.6
85	11.0	8.1	3.5	3.5	2.0	1.3	1.9	3.8
86	11.1	7.9	3.9	3.6	2.2	1.3	2.5	4.3
87	11.2	8.0	3.5	3.4	2.1	1.3	1.9	3.2
88	11.3	7.8	4.1	3.7	2.2	1.5	2.4	3.5
89	11.0	7.7	4.3	3.8	2.4	1.1	1.8	3.6
90	11.2	7.8	3.7	4.1	2.1	1.4	2.3	3.7
91	11.2	7.8	3.0	3.3	2.4	1.3	1.9	2.8
92	11.1	7.9	3.5	3.3	2.5	1.3	1.8	3.2
93	11.0	7.8	4.2	3.4	1.9	1.7	2.0	3.9
94	11.0	7.8	3.7	3.8	2.2	1.3	2.1	3.5
95	10.9	7.9	4.1	3.6	2.1	1.4	1.8	3.3
96	10.8	7.8	3.8	0.3	2.3	1.9	1.7	4.0
97	10.9	7.8	3.8	3.1	1.9	1.4	2.1	3.2
98	10.8	7.8	3.8	3.2	2.2	1.6	2.1	3.2
99	10.8	7.8	3.8	3.1	2.2	1.5	2.5	3.6
AV	11.1	8.0	4.0	3.4	2.2	1.5	2.0	3.5
SD	0.2	0.2	0.4	0.4	0.2	0.2	0.4	0.3
CV	1.4	2.6	11.1	11.6	10.8	11.6	17.7	8.9

Second measurement series

ID	05.237	05.251	05.265	05.279	05.293	05.306	05.321	05.334	05.348	06.011	06.024	06.110	06.123	06.137
1	13.9	15.1	10.8	11.0	8.1	9.3	5.9	3.5	2.8	1.2	-0.3	6.0	7.6	10.5
2	13.9	15.6	10.4	10.8	7.2	8.9	5.4	3.7	2.3	0.7	-0.3	6.6	7.9	10.7
3	13.9	15.4	10.7	11.4	7.9	9.1	5.3	3.1	2.5	1.0	-0.3	6.4	7.6	10.9
4	13.8	15.6	10.6	11.1	7.7	9.1	5.4	3.1	2.5	0.8	-0.3	6.1	7.7	10.3
5	13.9	15.5	10.5	10.8	7.5	9.2	5.7	2.9	2.5	0.6	-0.3	6.2	7.7	10.2
6	13.8	15.2	11.0	11.1	7.9	9.6	6.0	4.6	2.8	0.9	-0.3	5.7	7.6	9.8
7	14.0	15.7	10.9	11.0	7.8	9.3	5.9	3.6	2.5	0.9	-0.3	6.1	7.7	10.1
8	13.9	15.6	10.4	10.8	7.3	9.0	5.1	3.0	2.1	0.4	-0.3	6.5	8.3	11.1
9	13.9	15.3	10.5	10.9	7.7	9.0	5.0	2.9	2.4	0.6	-0.3	5.9	7.2	10.3
10	13.9	15.3	10.7	10.9	7.9	9.2	5.5	3.4	2.6	0.7	-0.3	6.2	7.8	10.6
11	14.0	15.6	10.6	10.9	7.6	9.2	5.4	2.9	2.4	0.6	-0.3	6.3	7.6	10.7
12	14.0	15.5	10.8	10.9	7.7	9.1	5.2	2.4	2.2	0.4	-0.3	6.6	8.4	10.8
13	14.0	15.7	10.3	10.8	7.4	9.0	5.5	2.4	1.9	0.4	-0.3	6.3	8.0	11.0
14	14.0	15.6	10.6	10.9	7.6	9.0	5.4	2.9	2.3	0.5	-0.3	6.2	7.7	10.4
15	13.6	14.6	10.6	10.9	7.9	9.0	5.1	2.4	2.6	0.4	-0.3	6.0	7.3	10.6
16	13.8	15.6	10.9	11.0	7.9	8.9	5.8	3.1	2.4	0.8	-0.3	6.0	7.7	10.6
17	13.9	15.5	11.1	11.0	8.1	9.3	5.6	2.9	2.6	1.1	-0.3	6.2	7.6	10.6
18	14.0	15.6	10.5	10.9	7.6	9.1	4.7	2.0	1.9	0.6	-0.3	6.6	8.3	11.2
19	13.9	15.3	10.9	11.0	8.1	9.2	5.7	3.0	2.8	1.2	-0.3	6.1	7.7	10.5
20	13.9	15.6	10.7	10.9	7.9	9.3	6.0	2.9	2.8	0.9	-0.3	6.1	7.7	10.2
21	14.0	15.6	10.7	11.0	7.9	8.9	5.7	3.0	2.7	0.9	-0.3	6.2	7.8	10.7
22	13.9	15.3	10.5	10.8	7.5	9.2	5.3	2.5	2.2	0.5	-0.3	6.3	7.9	10.9
23	13.8	15.6	10.7	10.9	7.9	9.2	5.7	3.2	2.6	0.8	-0.3	6.4	7.9	10.4
24	14.2	15.9	10.7	11.0	8.0	9.1	5.2	3.0	2.6	0.9	-0.3	6.4	8.0	10.6
25	14.0	15.7	10.6	11.0	8.0	9.1	5.7	3.1	2.8	1.2	-0.3	6.2	8.0	10.5
26	13.8	15.5	10.8	10.9	8.0	8.9	5.6	3.0	2.6	0.7	-0.3	6.6	8.0	10.8
27	14.0	15.6	10.6	11.0	7.9	9.2	5.3	2.9	2.6	0.7	-0.3	6.8	7.8	10.7
28	14.0	15.6	11.1	11.0	8.2	9.4	5.9	3.6	2.9	1.3	-0.3	6.7	7.9	10.8
29	14.0	15.7	10.7	11.0	7.9	9.3	5.8	2.9	2.7	0.8	-0.3	6.5	7.7	10.5
30	13.8	15.5	10.7	10.9	7.9	9.1	5.5	2.7	2.5	0.9	-0.3	6.3	8.1	10.3
31	13.9	15.5	10.8	11.0	8.0	9.4	6.0	3.2	2.9	1.0	-0.3	6.4	7.9	10.6
32	14.2	15.7	10.6	10.9	7.9	9.2	5.6	3.0	2.6	0.9	-0.3	6.5	7.8	10.9
33	14.1	15.5	10.7	11.1	8.3	9.4	5.8	3.1	2.9	1.5	-0.3	6.4	7.8	10.8
34	14.0	15.4	10.8	10.9	8.0	9.2	5.7	3.2	2.8	0.8	-0.3	6.3	7.6	10.9
35	14.0	15.6	10.7	10.8	7.7	9.0	5.5	3.0	2.5	0.9	-0.3	6.0	7.8	10.2
36	13.9	16.0	10.8	10.9	8.1	9.2	5.7	3.3	2.8	0.9	-0.3	6.3	7.5	10.6
37	13.9	15.8	10.6	10.9	7.9	9.2	5.5	2.9	2.6	0.9	-0.3	6.1	7.7	10.8
38	13.9	15.9	10.9	11.0	8.2	9.4	5.9	3.5	2.9	1.1	-0.3	6.3	7.8	10.4
39	14.0	16.2	10.7	11.0	8.2	9.4	6.1	3.8	3.4	0.8	-0.3	6.2	7.8	10.5
40	14.0	15.7	10.7	10.9	7.9	9.3	5.7	3.4	2.9	0.8	-0.3	6.2	7.9	10.3
41	14.1	15.6	10.7	10.9	8.0	9.3	5.6	3.0	2.6	0.9	-0.3	6.3	7.8	10.2
42	14.1	15.7	10.7	10.8	7.9	9.2	5.6	2.7	2.4	0.6	-0.3	6.5	8.1	10.4
43	14.1	15.7	10.7	10.9	7.9	9.0	5.4	2.5	2.2	0.4	-0.3	6.5	7.4	10.4
44	14.1	15.6	10.8	10.9	8.0	9.0	5.5	2.7	2.2	0.5	-0.3	6.7	7.8	10.2
45	14.1	15.6	10.8	10.9	8.0	9.1	5.5	2.8	2.4	0.4	-0.3	6.6	7.7	10.5
46	13.9	15.7	10.6	10.9	8.0	9.1	5.6	3.0	2.3	0.7	-0.3	5.9	7.9	10.5
47	14.0	15.8	11.0	11.1	8.2	9.3	5.6	3.1	2.7	0.9	-0.3	6.7	7.4	10.6
48	14.1	15.8	11.0	11.1	8.2	9.2	5.4	2.9	2.4	0.6	-0.3	6.1	7.9	10.5
49	14.1	15.8	11.0	11.0	8.3	9.2	5.4	2.9	2.4	0.5	-0.3	6.3	7.9	10.5
50	14.1	15.7	11.0	11.1	8.3	9.2	5.1	2.5	2.2	0.2	-0.3	6.2	8.0	10.5

ID	06.149	06.165	06.179	06.193	06.207	06.221	06.235	06.263	06.277	06.290	06.305	06.319	06.333	06.354
1	12.0	13.4	13.2	15.5	17.4	13.7	13.0	13.2	12.1	8.3	8.6	8.3	7.0	4.4
2	11.8	13.0	13.8	16.1	17.4	13.4	12.9	13.2	11.7	8.4	8.7	8.1	6.4	4.2
3	12.0	12.8	13.4	15.8	17.5	13.7	13.0	13.4	11.9	9.0	8.8	8.2	6.9	4.1
4	12.0	13.6	13.9	15.8	17.4	13.9	13.0	13.1	11.6	8.8	9.2	8.1	6.7	4.0
5	11.7	13.4	13.4	15.9	17.5	13.7	12.9	13.2	11.2	8.5	9.0	8.1	6.8	4.0
6	11.7	13.2	14.1	15.7	17.0	13.6	13.0	13.2	11.6	8.8	9.2	8.1	7.0	4.7
7	11.4	13.3	13.9	15.8	17.4	14.0	13.1	13.4	11.9	8.6	9.0	8.1	6.8	4.4
8	12.0	12.9	13.5	16.3	17.8	13.7	13.0	13.2	11.9	8.5	8.6	8.1	6.6	3.9
9	11.6	12.9	13.2	15.7	18.1	13.8	12.9	13.0	11.8	8.9	8.9	8.1	6.8	4.3
10	11.8	13.3	13.9	15.6	17.4	14.2	13.1	13.2	11.2	9.1	9.3	8.3	7.0	4.5
11	12.3	13.2	13.7	15.9	17.3	14.2	13.0	13.4	12.0	8.9	9.3	8.1	6.7	4.2
12	11.5	13.5	14.5	16.3	17.4	13.9	13.3	13.2	11.8	8.7	8.6	7.9	6.6	3.8
13	12.1	13.0	13.7	16.4	17.6	13.8	13.1	13.4	11.6	8.2	8.8	7.9	6.5	3.9
14	12.3	13.8	13.4	16.4	17.6	13.9	13.3	13.2	12.0	8.6	9.0	8.1	6.6	3.9
15	11.9	13.1	13.9	15.6	17.3	13.9	13.0	13.1	12.0	9.0	8.6	8.3	6.9	4.1
16	12.2	13.2	13.4	16.0	17.5	13.8	13.2	13.4	11.8	8.9	8.8	8.1	6.7	4.3
17	11.8	13.2	13.7	15.9	17.4	14.2	13.1	13.2	12.2	8.9	8.7	8.2	6.9	4.4
18	11.6	13.2	14.0	16.4	17.9	13.4	13.1	13.0	11.9	8.8	8.4	8.2	6.4	3.5
19	11.9	13.6	13.9	16.0	17.4	14.2	13.1	13.2	12.0	9.3	9.0	8.4	6.9	4.5
20	11.9	13.0	14.0	16.0	17.4	14.0	13.1	13.1	11.7	8.5	9.2	8.1	6.8	4.4
21	11.7	13.2	13.8	15.9	17.4	13.9	13.0	13.3	11.9	9.1	9.2	8.2	6.8	4.0
22	11.6	13.2	13.8	16.2	17.4	13.6	13.1	13.0	11.6	8.6	9.3	7.9	6.4	4.2
23	12.1	13.6	13.7	15.9	17.4	13.8	13.3	13.2	12.0	8.8	9.1	8.1	6.9	4.3
24	11.9	13.2	13.9	16.2	18.1	14.3	13.2	13.3	12.1	8.7	9.0	8.6	6.7	4.0
25	11.6	13.1	13.7	16.0	17.8	14.2	13.3	13.3	12.1	9.1	9.2	8.3	7.3	4.4
26	11.6	13.2	13.7	15.9	17.7	14.1	13.3	13.3	12.0	8.7	9.1	8.1	6.7	4.1
27	11.7	13.1	13.7	16.1	17.5	14.0	13.3	13.2	11.8	8.7	9.2	8.2	6.7	4.0
28	11.7	13.2	13.8	16.2	17.4	14.3	13.5	13.3	11.9	9.3	9.0	8.1	6.9	4.4
29	12.1	12.9	13.9	16.3	17.3	14.1	13.2	13.3	11.9	8.7	8.8	8.1	6.6	4.1
30	11.6	13.1	14.2	16.0	17.4	13.7	13.1	13.2	11.9	8.7	8.9	8.1	6.8	4.2
31	11.6	13.2	13.7	15.7	17.3	13.9	13.3	13.2	11.8	8.9	8.9	8.0	6.8	4.1
32	11.8	13.1	13.5	16.3	18.0	14.0	13.2	13.2	11.7	8.8	9.0	8.4	7.2	4.4
33	11.6	13.1	13.4	16.2	17.3	14.3	13.3	13.4	11.9	9.4	9.1	8.1	6.7	4.7
34	11.8	12.8	13.3	15.9	17.3	13.8	13.3	13.3	11.7	8.8	8.9	8.2	6.8	4.3
35	12.3	13.7	14.0	15.8	17.3	14.0	13.3	13.2	11.8	8.8	8.8	8.2	7.0	4.2
36	12.0	12.7	13.6	16.0	17.7	14.0	13.3	13.3	12.2	8.9	8.8	8.3	6.7	4.3
37	11.5	13.4	13.8	16.3	17.4	14.0	13.2	13.2	12.0	8.7	8.8	8.2	7.1	4.1
38	11.9	13.1	13.7	16.0	17.9	14.1	13.3	13.4	12.0	9.1	9.4	8.5	7.1	4.4
39	11.6	12.9	13.7	15.7	17.3	14.1	13.3	13.3	11.8	9.1	9.1	8.2	7.1	4.7
40	12.0	13.3	13.2	16.4	17.9	14.2	13.3	13.2	11.6	8.8	9.1	8.2	6.8	4.3
41	11.4	13.2	13.5	16.2	17.9	14.1	13.2	13.3	11.8	8.9	8.8	8.1	6.9	4.2
42	11.6	13.0	13.9	16.0	18.1	14.1	13.3	13.3	11.9	8.6	8.8	8.1	6.6	4.0
43	12.0	13.6	13.6	16.0	17.7	14.1	13.4	13.3	11.8	8.6	8.8	8.1	6.6	3.9
44	11.9	13.2	13.9	16.0	17.7	14.1	13.4	13.4	11.6	8.6	8.8	8.1	6.6	4.0
45	11.5	13.3	13.9	16.0	17.2	14.1	13.3	13.3	12.0	8.7	8.8	8.2	6.8	4.0
46	11.8	13.9	13.7	16.1	17.4	14.2	13.1	13.3	12.0	8.9	8.9	8.3	6.9	4.2
47	11.6	13.0	13.2	15.9	17.3	14.3	13.3	13.3	12.0	9.1	8.6	8.4	6.9	4.4
48	11.8	13.6	13.9	16.3	18.0	14.3	13.4	13.6	11.9	8.9	9.2	8.3	6.8	4.1
49	11.7	13.3	13.6	16.3	18.0	14.3	13.4	13.5	11.9	8.8	9.2	8.3	6.6	4.1
50	11.8	12.9	13.8	16.3	17.5	14.3	13.4	13.5	11.9	8.9	9.1	8.3	6.8	4.2

ID	07.010	07.025	07.038	07.052	07.066	07.080	07.094	07.108	07.122	07.136	07.150	07.164
1	6.4	0.8	2.0	2.6	4.6	2.5	4.5	8.6	8.7	8.6	10.7	14.8
2	6.5	0.8	1.6	2.4	4.9	2.2	5.0	9.1	9.0	8.8	10.2	14.6
3	6.3	1.3	1.8	2.5	4.7	2.5	4.9	8.7	8.9	8.7	10.7	14.7
4	6.3	1.2	1.4	2.7	4.8	2.3	4.7	8.8	9.0	8.6	10.6	15.0
5	6.2	1.3	1.9	2.6	4.6	2.5	4.6	8.5	9.1	8.8	10.4	14.7
6	6.2	0.7	2.3	2.6	4.5	2.4	4.7	8.3	8.5	8.9	10.1	14.4
7	6.1	0.8	1.9	2.7	4.6	2.4	4.7	8.8	8.9	8.6	10.7	15.0
8	6.3	1.3	1.1	2.5	4.7	2.3	4.4	8.8	9.1	8.8	10.8	14.6
9	6.2	1.3	1.8	2.7	4.5	2.5	4.4	8.4	8.4	8.9	10.4	15.1
10	6.3	1.2	2.3	2.6	4.6	2.4	4.1	8.3	8.6	9.0	10.7	14.9
11	6.1	1.5	2.0	2.6	4.6	2.6	4.6	8.6	8.7	8.9	10.6	14.7
12	6.1	1.0	0.9	2.3	4.5	2.3	4.6	8.9	9.2	8.7	10.6	14.9
13	6.1	1.1	1.8	2.5	4.6	2.1	4.7	9.2	9.1	9.1	10.7	15.2
14	6.3	0.6	1.5	2.4	4.6	2.5	4.6	8.3	9.0	9.2	10.6	14.8
15	6.6	1.7	2.3	2.8	4.8	2.3	4.4	8.2	8.5	9.0	10.2	14.4
16	6.5	0.8	1.9	2.7	4.8	2.4	4.4	8.6	9.1	8.9	10.1	15.0
17	6.3	1.4	1.6	2.6	4.7	2.2	4.5	8.6	9.3	8.7	10.4	14.6
18	6.4	0.6	1.4	2.2	4.7	2.7	4.5	8.6	8.8	9.3	10.1	14.8
19	6.4	1.6	2.1	2.8	4.8	2.5	4.6	8.5	8.8	8.7	10.6	15.0
20	6.3	1.2	2.0	2.6	4.8	2.2	4.6	8.7	8.6	9.1	10.6	16.6
21	6.3	1.3	1.4	2.3	4.6	2.3	4.6	8.8	9.2	9.0	10.4	15.0
22	6.2	0.7	1.8	2.2	4.7	2.6	4.5	9.0	8.9	8.8	10.2	14.8
23	6.1	1.4	1.6	2.4	4.7	2.2	4.6	8.6	8.9	9.1	11.0	14.6
24	6.4	1.1	1.0	2.6	4.8	2.2	4.7	9.0	9.0	8.4	10.8	15.0
25	6.3	1.4	1.0	2.5	4.7	2.1	4.9	8.4	8.9	8.6	10.7	14.7
26	6.2	1.2	1.8	2.3	4.8	2.3	4.7	8.7	9.0	8.9	10.8	14.9
27	6.2	1.0	2.1	2.3	4.7	2.1	4.8	8.8	9.1	8.9	10.6	14.9
28	6.2	1.1	1.7	2.7	4.8	2.4	4.9	8.9	9.0	8.8	10.2	14.6
29	6.4	1.1	1.6	2.4	4.9	2.7	4.9	9.0	9.1	9.1	10.4	14.8
30	6.4	1.1	2.1	2.5	5.0	2.2	5.0	8.8	9.0	9.3	10.6	14.3
31	6.3	1.0	2.0	2.3	4.9	2.3	5.1	9.0	9.3	9.7	10.7	14.5
32	6.2	0.6	2.2	2.4	4.8	2.5	4.7	9.0	9.2	9.5	10.7	14.4
33	6.3	1.6	2.1	3.0	4.9	2.5	4.8	8.4	8.6	9.7	11.0	14.7
34	6.2	1.4	2.0	2.8	4.6	2.5	5.0	8.9	9.1	9.5	10.9	14.7
35	6.3	1.2	2.0	2.8	4.8	2.2	5.0	8.8	9.2	8.7	10.6	14.5
36	6.3	1.0	2.1	2.6	4.8	2.4	5.0	9.0	8.8	9.2	10.7	14.0
37	6.3	1.0	2.2	2.7	4.7	2.4	4.8	8.6	9.0	9.3	10.7	14.6
38	6.2	1.2	2.1	2.6	4.6	2.5	4.7	8.6	9.4	9.1	10.8	14.7
39	6.5	1.4	2.0	2.8	4.7	2.3	4.9	8.5	9.2	8.8	10.7	14.8
40	6.3	1.0	2.1	2.8	4.8	2.2	5.2	8.6	8.9	8.7	10.2	14.6
41	6.1	1.3	2.2	2.6	4.8	2.4	5.0	8.9	9.4	9.1	10.8	14.5
42	6.2	1.3	2.1	2.3	4.7	2.1	4.8	8.8	8.5	9.1	10.9	14.3
43	6.2	1.1	2.1	2.5	4.8	2.3	4.8	8.8	8.8	9.2	10.6	14.5
44	6.3	1.3	2.1	2.4	4.8	2.5	4.9	9.0	8.7	9.0	10.7	14.8
45	6.3	1.2	3.0	2.6	4.6	2.5	4.8	8.9	8.7	8.9	10.7	14.6
46	6.2	0.9	2.1	2.8	4.8	2.4	4.9	8.8	9.1	9.0	10.5	14.7
47	6.3	0.9	2.1	2.7	4.8	2.7	5.0	8.8	8.9	9.2	10.4	14.4
48	6.3	1.2	2.0	2.5	4.7	2.4	5.1	8.9	8.6	8.9	10.8	14.6
49	6.2	1.0	2.0	2.6	4.7	2.5	5.2	9.0	8.7	8.8	10.9	14.9
50	6.3	1.1	2.0	2.5	4.7	2.5	5.1	9.1	9.2	8.8	10.8	15.0

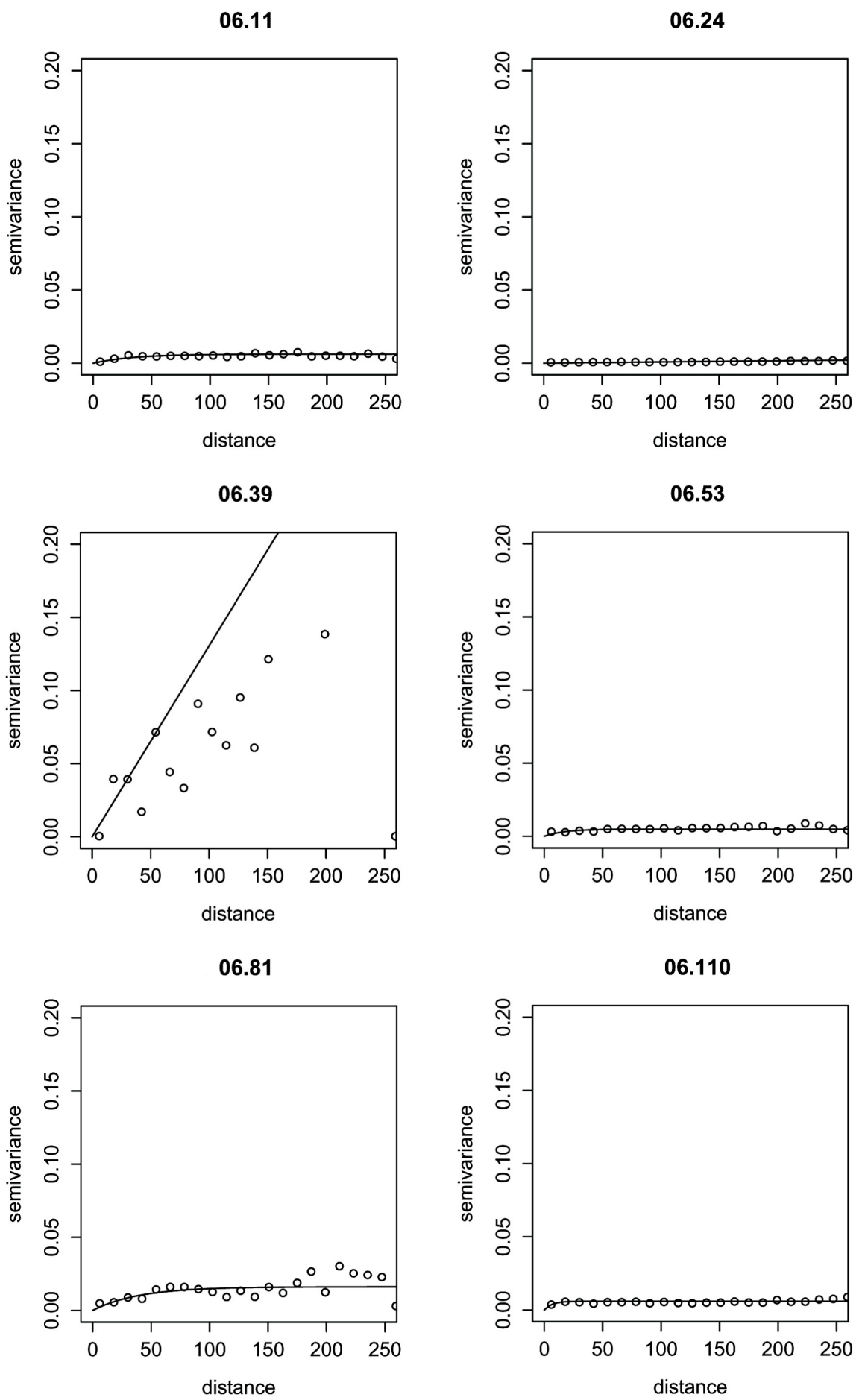
ID	05.237	05.251	05.265	05.279	05.293	05.306	05.321	05.334	05.348	06.011	06.024	06.110	06.123	06.137
51	14.1	15.7	11.1	11.1	8.3	9.2	5.4	2.9	2.3	0.5	-0.3	6.5	7.8	10.9
52	14.1	16.2	10.7	10.9	7.9	9.1	5.2	2.7	2.4	0.7	-0.3	6.5	7.8	10.6
53	14.1	15.9	10.8	10.9	7.9	9.1	5.4	2.8	2.4	0.8	-0.3	6.6	8.1	10.6
54	13.9	15.7	10.8	10.9	7.9	9.1	5.0	2.7	2.2	0.7	-0.3	6.4	7.6	10.5
55	13.9	15.7	10.8	10.8	7.9	9.2	5.4	3.0	2.6	0.6	-0.3	6.3	7.8	11.0
56	13.8	15.7	10.8	10.8	7.9	9.1	5.3	2.8	2.4	0.8	-0.3	5.8	7.9	10.8
57	14.0	15.5	11.0	11.0	8.3	9.3	5.7	3.0	2.5	0.9	-0.3	5.9	7.9	11.1
58	13.9	16.0	11.0	10.9	8.3	9.3	5.4	3.3	2.7	0.8	-0.3	6.1	8.0	10.5
59	14.0	15.6	11.1	10.9	8.0	9.1	4.7	2.4	2.2	0.4	-0.3	6.2	7.9	10.9
60	14.1	15.9	11.1	11.0	8.1	9.1	5.3	2.6	2.2	0.5	-0.3	6.2	7.6	10.3
61	14.1	15.6	11.0	11.0	8.1	9.2	5.4	2.8	2.2	0.4	-0.3	6.5	7.7	10.7
62	14.1	16.1	11.0	11.0	8.1	9.2	5.6	2.9	2.4	0.4	-0.3	6.1	7.7	10.8
63	14.2	16.6	11.2	11.0	8.1	9.1	5.2	2.6	2.2	0.6	-0.3	6.2	7.9	11.0
64	14.0	16.0	10.8	10.9	8.0	9.2	5.3	2.7	2.2	0.7	-0.3	6.1	8.0	10.6
65	13.9	15.7	11.1	10.9	8.1	9.4	5.6	3.0	2.5	0.6	-0.3	6.4	7.3	10.5
66	13.8	15.6	10.9	10.9	8.1	9.3	5.7	2.9	2.5	0.6	-0.3	6.1	7.9	10.7
67	13.9	15.6	10.8	10.8	7.9	9.2	5.5	2.7	2.3	0.5	-0.3	6.4	7.6	10.5
68	13.9	16.1	10.8	10.8	7.9	9.2	5.5	2.6	2.3	0.4	-0.3	6.4	7.9	10.8
69	13.9	15.4	10.7	10.8	7.8	9.1	5.6	3.0	2.4	1.0	-0.3	6.5	7.7	10.3
70	14.0	16.0	11.2	11.0	8.4	9.4	5.6	3.3	2.7	0.5	-0.3	6.4	7.9	10.4
71	14.1	16.1	11.3	11.0	8.4	9.4	5.5	3.4	2.7	1.0	-0.3	6.2	7.8	10.3
72	14.0	15.8	11.2	11.0	8.6	9.2	5.2	2.7	2.3	0.6	-0.3	6.3	7.7	10.5
73	14.2	16.3	11.2	11.0	8.3	9.1	5.4	2.9	2.4	0.7	-0.3	6.0	7.8	10.6
74	14.1	16.1	11.0	10.9	8.4	9.2	4.9	2.8	2.2	0.6	-0.3	6.4	7.9	10.6
75	13.9	15.6	10.9	11.0	8.3	9.2	5.0	2.9	2.5	0.9	-0.3	6.0	7.5	10.5
76	13.9	15.2	10.9	10.9	8.5	9.3	5.3	3.1	2.6	1.2	-0.3	5.8	7.8	11.0
77	13.8	15.4	10.9	10.9	8.1	9.4	5.5	3.1	2.6	0.8	-0.3	6.3	7.7	10.3
78	14.1	15.8	11.0	11.0	8.3	9.4	5.7	3.4	2.6	1.1	-0.3	6.4	7.4	10.5
79	14.2	16.0	11.1	11.0	8.4	9.2	4.9	2.7	2.5	0.9	-0.3	6.8	7.9	10.1
80	14.2	16.4	11.3	11.1	8.5	9.4	5.3	3.2	2.6	1.4	-0.3	7.0	7.8	10.9
81	14.2	15.5	11.1	11.0	8.6	9.3	5.7	3.4	2.7	1.4	-0.3	6.4	7.9	10.3
82	14.0	16.4	11.2	11.1	8.4	9.3	5.2	3.1	2.6	1.2	-0.3	6.6	7.8	10.5
83	14.7	16.6	11.4	11.4	9.1	9.5	5.4	3.0	2.3	1.2	-0.3	6.0	7.8	10.8
84	13.9	15.4	11.0	11.3	8.4	9.2	5.4	3.2	2.6	0.9	-0.3	6.2	8.1	10.7
85	14.2	15.9	11.3	11.1	8.6	9.4	5.3	3.1	2.4	1.2	-0.3	6.3	7.7	10.8
86	14.0	16.1	11.0	11.0	8.1	9.1	5.0	2.6	2.2	0.3	-0.3	6.8	7.5	10.7
87	14.0	15.7	11.2	11.0	8.3	9.5	5.4	3.4	2.7	1.0	-0.3	6.4	8.0	10.3
88	14.1	15.8	11.3	11.3	8.6	9.4	5.5	2.9	2.6	1.0	-0.3	6.4	8.0	10.4
89	14.1	16.5	11.3	11.2	8.7	9.5	5.7	3.4	2.8	1.1	-0.3	6.4	7.8	10.7
90	13.8	15.9	11.2	11.0	8.4	9.5	6.0	3.6	2.9	0.9	-0.3	6.8	7.6	10.7
91	14.0	16.1	11.2	11.0	8.2	9.3	5.4	2.9	2.4	0.7	-0.3	6.4	7.6	10.4
92	13.8	15.7	11.4	11.2	8.8	9.6	5.7	3.6	3.1	1.3	-0.3	5.9	7.7	10.6
93	14.0	16.8	11.0	11.0	8.5	9.1	4.9	2.7	2.3	0.8	-0.3	6.4	8.0	10.6
94	14.0	16.8	11.2	11.1	8.3	9.6	5.5	3.0	2.5	0.7	-0.3	6.6	7.6	10.7
95	13.8	15.7	11.2	11.1	8.5	9.5	5.5	3.3	2.7	1.2	-0.3	6.6	7.6	10.6
96	13.8	15.7	10.8	10.8	7.9	9.0	5.0	2.8	2.4	0.7	-0.3	6.4	7.8	10.4
97	14.0	15.7	11.3	11.1	8.5	9.5	5.6	3.3	2.8	1.1	-0.3	6.2	7.7	11.0
98	14.3	16.3	11.3	11.4	8.6	9.4	5.2	2.9	2.4	0.4	-0.3	6.2	7.7	10.7
99	14.3	15.8	11.3	11.3	8.6	9.3	5.2	2.7	2.4	0.6	-0.3	6.4	7.9	10.7
100	14.4	16.0	11.3	11.3	8.4	9.5	5.4	2.8	2.4	0.5	-0.3	6.5	7.7	10.7
101	14.4	16.4	11.4	11.4	8.7	9.5	5.3	2.8	2.4	0.4	-0.3	6.4	7.8	10.7
AV	14.0	15.8	10.9	11.0	8.1	9.2	5.5	3.0	2.5	0.8	-0.3	6.3	7.8	10.6
SD	0.2	0.4	0.3	0.1	0.3	0.2	0.3	0.4	0.2	0.3	0.0	0.2	0.2	0.2
CV	1.1	2.3	2.4	1.3	4.1	1.8	5.2	12.0	9.8	35.7	0.0	3.9	2.6	2.4

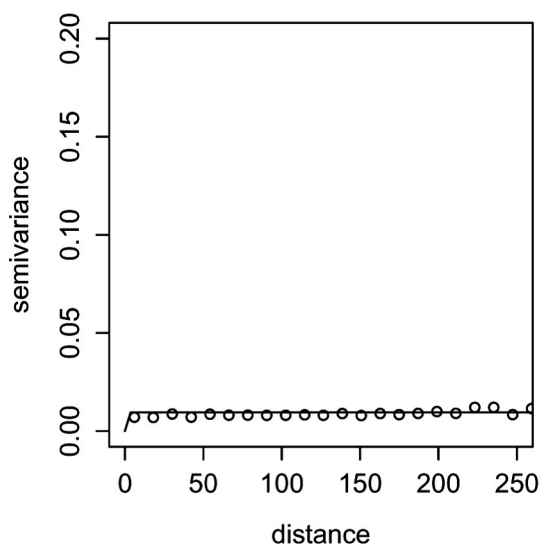
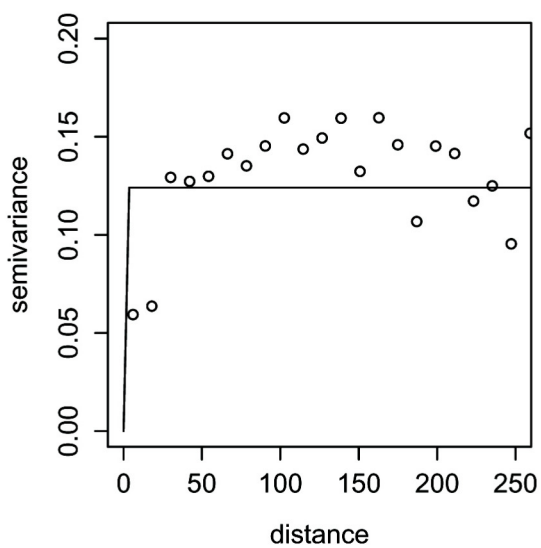
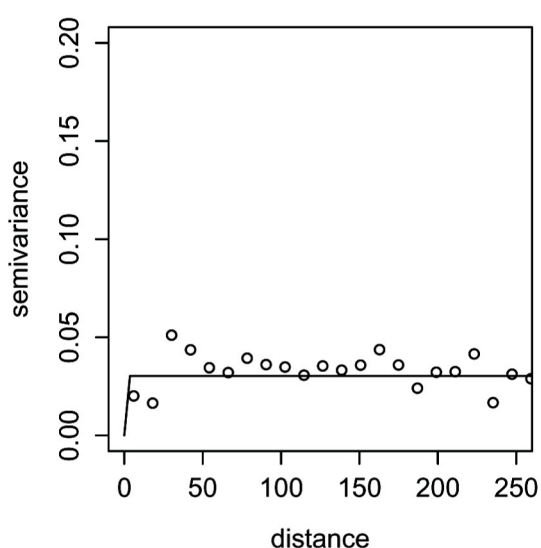
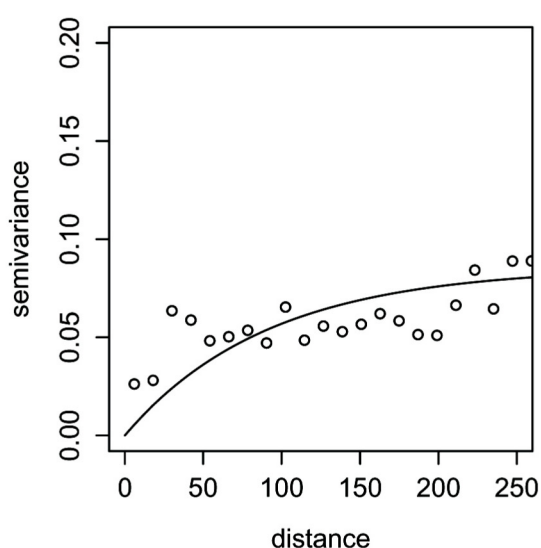
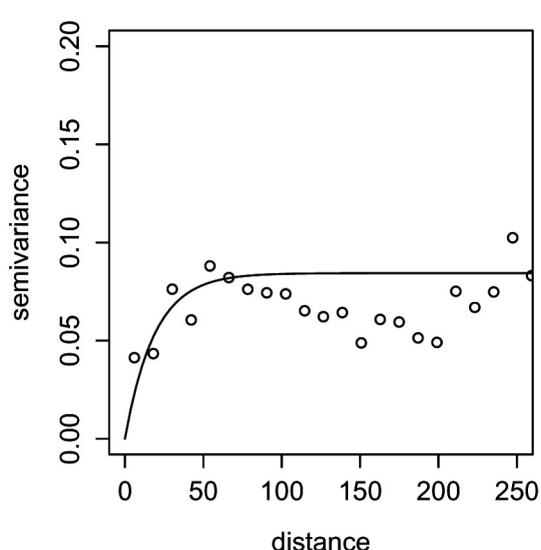
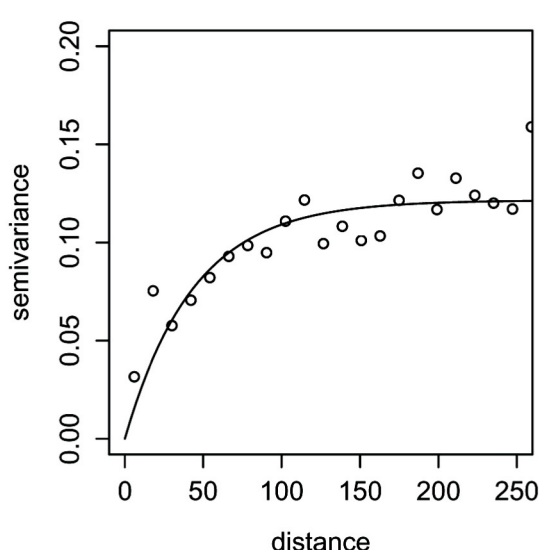
ID	06.149	06.165	06.179	06.193	06.207	06.221	06.235	06.263	06.277	06.290	06.305	06.319	06.333	06.354
51	12.1	13.6	13.6	16.3	17.3	14.3	13.3	13.5	11.9	8.9	9.1	8.4	6.7	4.1
52	11.5	13.0	14.0	15.9	18.0	14.3	13.3	13.4	11.9	8.9	9.0	8.1	6.8	4.1
53	12.2	13.3	13.5	15.7	18.0	14.1	13.3	13.3	11.8	8.7	8.8	8.1	6.8	4.1
54	11.9	13.1	13.7	16.1	18.0	13.9	13.3	13.3	11.9	8.8	8.6	8.1	6.5	4.1
55	12.4	12.9	13.3	16.3	17.4	13.9	13.2	13.3	11.8	8.8	8.4	8.2	6.5	4.1
56	11.6	13.3	13.6	16.3	17.6	14.0	13.2	13.4	12.1	8.8	9.0	8.3	6.6	3.8
57	11.4	12.8	13.4	16.4	17.4	14.0	13.3	13.3	11.8	9.2	9.4	8.2	7.2	4.4
58	12.0	13.5	13.6	15.5	17.3	14.0	13.3	13.3	11.8	9.0	9.1	8.2	7.1	4.2
59	11.6	13.4	13.2	15.9	18.0	14.2	13.4	13.5	11.8	8.9	8.7	8.2	6.6	4.1
60	12.0	13.0	13.6	16.3	17.7	14.2	13.5	13.4	11.8	8.9	8.9	8.2	6.7	4.1
61	11.9	13.1	13.5	15.7	17.4	14.2	13.4	13.4	11.8	9.0	8.8	8.3	6.6	4.1
62	11.7	13.2	13.5	15.8	17.3	14.2	13.4	13.3	11.8	8.9	8.9	8.2	6.8	4.2
63	11.5	13.1	13.7	15.6	18.0	14.3	13.4	13.2	11.7	9.1	8.4	8.2	6.8	4.0
64	11.6	13.4	14.4	15.5	18.0	14.1	13.3	13.4	11.6	8.9	8.4	8.2	6.7	4.0
65	12.1	13.2	14.0	15.8	17.5	14.1	13.4	13.4	11.5	9.0	8.8	8.1	6.9	4.1
66	11.9	13.3	13.6	15.8	17.4	14.1	13.4	13.5	12.2	8.9	8.6	8.1	6.9	4.1
67	12.4	13.2	13.8	15.5	17.7	14.1	13.4	13.4	11.6	8.9	8.9	8.2	6.8	4.2
68	12.1	13.1	14.0	15.9	17.6	14.1	13.4	13.4	11.6	8.9	8.6	8.1	6.9	4.1
69	12.1	12.9	13.7	15.9	17.5	14.0	13.4	13.3	11.6	9.0	9.5	8.0	6.8	4.2
70	11.6	13.0	13.3	16.0	17.6	14.1	13.4	13.4	11.8	9.1	8.8	8.4	7.0	4.5
71	11.5	12.6	13.7	15.9	18.0	14.0	13.4	13.6	11.6	8.9	8.8	8.2	6.7	4.2
72	12.3	13.0	13.6	15.9	17.9	14.1	13.4	13.0	11.9	9.2	8.6	8.2	6.7	4.1
73	11.7	13.2	13.7	15.9	17.9	14.2	13.5	13.5	11.4	9.2	8.4	8.2	6.9	4.0
74	11.6	13.3	13.8	16.3	18.7	14.2	13.4	13.1	12.0	8.9	8.4	8.1	6.6	4.0
75	11.9	13.3	14.1	16.0	18.0	13.9	13.4	13.1	11.8	9.0	8.5	8.2	6.7	4.2
76	11.5	13.7	13.5	16.0	17.4	13.9	13.4	13.4	11.8	8.9	8.4	8.2	6.9	4.2
77	11.6	13.0	14.2	15.9	17.4	13.9	13.4	13.5	11.1	8.9	8.6	8.2	6.9	4.1
78	11.5	13.0	13.7	16.5	17.4	14.0	13.4	13.0	11.6	9.0	9.0	8.3	6.9	4.5
79	11.5	13.5	13.5	16.2	18.0	14.1	13.4	13.3	11.9	9.2	8.9	8.2	6.8	4.0
80	11.7	13.5	13.7	16.6	17.3	14.2	13.6	13.1	11.1	9.4	9.1	8.2	7.0	4.4
81	11.6	12.8	13.7	15.8	17.5	14.1	13.6	12.9	11.7	9.4	9.1	8.3	6.9	4.5
82	12.2	13.2	13.4	16.4	17.4	14.1	13.6	13.3	11.9	9.0	8.5	8.3	7.0	4.1
83	11.4	13.2	13.8	15.6	17.7	14.1	14.2	13.4	11.6	9.5	8.9	8.4	6.8	3.9
84	11.7	13.9	13.8	16.1	17.9	14.2	13.5	13.3	12.0	9.1	8.5	8.4	6.7	4.0
85	11.4	13.4	14.0	16.2	17.3	14.5	13.6	13.3	11.7	9.2	8.9	8.1	6.9	4.2
86	11.7	13.5	13.8	16.5	17.7	13.9	13.6	13.3	12.0	8.8	8.1	8.3	6.5	3.6
87	11.7	13.3	13.8	16.0	17.2	13.9	13.6	13.5	11.8	9.2	8.8	8.3	7.0	4.2
88	12.3	13.4	13.8	15.9	17.6	14.2	13.6	13.3	11.8	9.2	8.8	8.4	6.9	4.2
89	11.7	13.0	13.9	16.2	17.8	14.0	13.6	13.2	11.8	9.2	9.4	8.4	7.2	4.7
90	11.7	13.1	13.7	15.9	17.5	14.0	13.4	13.4	11.9	9.3	9.0	8.4	7.1	4.2
91	11.8	12.7	13.7	16.2	17.3	14.1	13.5	13.2	11.9	9.1	9.1	8.1	6.8	4.0
92	11.6	13.5	13.5	15.6	17.7	14.1	13.6	13.1	11.7	9.7	9.2	8.5	7.4	4.0
93	11.6	13.3	13.6	15.8	18.0	13.9	13.5	13.0	12.6	9.2	8.4	8.1	6.6	3.8
94	11.8	13.3	14.1	15.6	17.4	14.3	13.6	13.1	12.3	9.3	8.5	8.2	6.7	4.0
95	12.3	13.1	13.4	15.9	17.4	14.1	13.6	13.4	11.4	9.7	9.0	8.3	7.0	4.6
96	11.6	13.4	13.4	16.0	17.6	13.9	13.6	13.6	12.1	8.9	9.0	8.1	6.8	3.8
97	11.6	12.8	13.4	16.0	17.6	14.1	13.6	13.1	11.6	9.4	8.9	8.1	7.3	4.6
98	11.6	13.2	13.9	15.9	17.3	14.7	13.6	13.1	11.9	9.3	9.4	8.2	6.8	4.1
99	12.0	12.9	13.8	16.5	17.3	14.7	13.6	13.7	11.8	9.3	9.2	8.2	6.7	4.1
100	11.7	13.1	13.4	15.6	17.8	14.7	13.6	13.2	11.8	9.2	9.3	8.2	6.8	4.2
101	11.7	13.1	13.7	15.8	17.5	14.7	13.6	13.3	12.0	9.2	9.2	8.2	6.8	4.1
AV	11.8	13.2	13.7	16.0	17.6	14.1	13.3	13.3	11.8	8.9	8.9	8.2	6.8	4.2
SD	0.3	0.3	0.3	0.3	0.3	0.2	0.2	0.2	0.2	0.3	0.3	0.1	0.2	0.2
CV	2.2	2.0	1.9	1.6	1.6	1.7	1.6	1.1	2.0	3.1	3.2	1.5	2.9	5.4

ID	07.010	07.025	07.038	07.052	07.066	07.080	07.094	07.108	07.122	07.136	07.150	07.164
51	6.3	0.8	2.0	2.6	4.7	2.3	4.4	9.0	8.8	9.1	10.6	14.9
52	6.3	1.4	2.1	2.5	4.8	2.5	4.6	8.9	8.5	9.2	10.6	15.0
53	6.2	1.0	2.2	2.2	4.9	2.4	4.9	9.0	9.3	8.7	10.3	14.8
54	6.3	0.8	1.9	2.6	4.7	2.6	4.7	8.8	8.5	8.8	10.6	14.8
55	6.3	1.0	1.9	2.3	4.8	2.2	4.5	8.8	9.1	9.1	11.2	14.7
56	6.3	0.5	2.2	2.8	4.8	2.3	4.7	8.7	9.1	9.0	10.5	14.8
57	6.2	1.8	2.3	2.6	4.7	2.6	5.0	8.7	9.0	8.9	10.6	14.9
58	6.3	1.3	2.2	2.8	4.9	2.1	5.2	8.6	8.8	9.2	11.0	14.6
59	6.2	1.0	2.3	2.9	4.8	2.4	4.8	8.9	9.0	8.8	10.6	14.8
60	6.3	1.2	2.1	2.7	4.8	2.1	4.6	8.6	8.9	8.9	10.1	14.8
61	6.3	1.0	2.0	2.9	4.8	2.4	4.5	8.8	9.2	8.6	10.8	14.9
62	6.2	1.3	2.2	2.9	4.7	2.0	5.1	9.3	8.9	8.9	10.6	14.7
63	6.1	1.1	2.1	2.6	4.8	2.2	5.2	9.0	8.8	9.1	10.6	14.9
64	6.2	1.0	2.1	2.4	4.8	2.3	4.7	8.6	8.6	9.1	10.8	14.7
65	6.2	1.1	2.2	2.6	4.9	2.4	4.7	9.1	8.4	9.1	11.3	14.8
66	6.2	1.0	2.0	2.5	4.8	2.5	5.0	8.4	9.1	8.7	10.1	14.8
67	6.3	1.2	2.1	2.6	4.7	2.3	5.2	9.1	8.9	9.1	10.8	14.6
68	6.2	1.1	2.0	2.8	4.8	2.3	4.6	8.5	8.8	8.9	10.6	14.8
69	6.1	1.4	2.0	2.9	4.8	2.4	5.2	9.2	9.0	8.9	10.5	14.8
70	6.3	0.9	2.2	2.4	5.0	2.5	4.7	8.9	8.8	9.0	10.5	14.7
71	6.3	1.1	2.1	2.6	4.9	2.2	4.7	9.2	8.5	9.1	10.5	14.9
72	6.2	0.7	2.0	2.5	4.9	2.5	4.6	8.5	8.9	9.2	10.3	14.7
73	6.2	1.2	2.0	2.7	4.8	2.3	4.9	8.6	9.1	9.1	10.9	15.1
74	6.2	0.9	2.0	2.7	4.9	2.3	4.7	8.8	8.9	9.1	10.5	14.6
75	6.4	0.8	2.1	2.6	5.0	2.3	5.0	8.3	8.6	8.9	10.4	14.8
76	6.2	1.1	2.1	2.7	4.9	2.4	4.5	8.7	8.7	8.9	10.9	14.3
77	6.3	0.9	2.2	2.7	4.8	2.1	4.9	9.0	8.9	9.5	10.4	14.7
78	6.3	1.2	2.0	2.6	4.9	2.0	4.9	8.6	9.3	9.0	10.3	14.5
79	6.1	1.2	2.3	2.8	4.9	2.3	4.6	8.7	8.8	8.7	10.8	14.6
80	6.2	1.6	2.1	2.7	4.8	2.0	5.2	8.4	8.7	9.2	10.4	14.8
81	6.1	1.2	1.8	2.8	5.0	2.5	5.0	9.1	8.7	8.6	10.7	15.4
82	6.4	1.1	1.9	2.6	5.1	2.6	4.9	9.1	8.9	8.8	10.5	15.1
83	6.4	0.9	2.0	2.7	4.8	2.3	4.8	8.7	8.4	8.9	10.8	16.1
84	6.3	0.7	2.0	2.8	5.2	2.2	4.8	8.8	8.7	8.5	10.2	15.3
85	6.2	1.0	2.1	2.8	4.8	2.3	4.2	8.6	9.0	9.0	11.0	14.7
86	6.4	0.4	1.7	3.0	5.2	2.5	4.9	8.9	9.0	8.8	10.8	15.0
87	6.3	1.1	1.7	2.9	4.9	2.5	4.9	8.8	9.1	8.8	10.6	14.7
88	6.3	1.7	2.1	2.9	5.0	2.3	4.8	8.6	8.6	8.4	10.7	14.5
89	6.4	1.2	1.9	2.8	5.2	2.6	5.4	8.7	8.9	9.1	10.3	14.8
90	6.3	1.2	2.0	2.7	5.0	2.2	4.9	8.9	8.7	8.9	10.3	14.6
91	6.2	0.9	2.0	2.8	5.1	2.6	4.3	8.7	9.2	9.0	10.8	15.0
92	6.3	1.9	2.2	2.6	5.0	2.4	4.7	8.7	8.8	9.2	10.7	15.2
93	6.3	0.6	1.9	2.8	4.7	2.3	4.7	8.6	8.9	8.6	10.9	15.7
94	6.2	0.9	1.6	3.1	5.2	2.5	4.7	8.6	8.9	8.9	10.9	14.2
95	6.2	1.4	2.5	3.0	5.0	2.2	4.6	8.9	9.3	9.3	10.2	15.1
96	6.3	0.7	2.0	3.2	5.1	2.4	5.0	9.1	8.9	9.0	11.1	14.5
97	6.3	1.6	2.1	3.1	5.1	2.4	4.7	8.8	8.8	9.0	10.7	14.8
98	6.3	1.0	1.5	2.3	5.3	2.5	4.7	8.6	8.7	9.0	10.3	15.7
99	6.3	1.0	2.5	2.3	5.4	2.5	5.0	8.5	8.9	8.6	10.9	15.6
100	6.2	1.3	1.9	2.7	5.3	2.4	4.8	8.6	8.9	8.7	10.4	15.7
101	6.3	0.9	2.0	2.6	5.4	2.6	4.5	8.9	8.9	9.1	10.7	15.8
AV	6.3	1.1	2.0	2.6	4.8	2.4	4.8	8.8	8.9	9.0	10.6	14.8
SD	0.1	0.3	0.3	0.2	0.2	0.2	0.2	0.2	0.2	0.3	0.3	0.4
CV	1.5	25.8	15.8	7.9	3.9	6.8	5.1	2.7	2.7	2.8	2.4	2.6

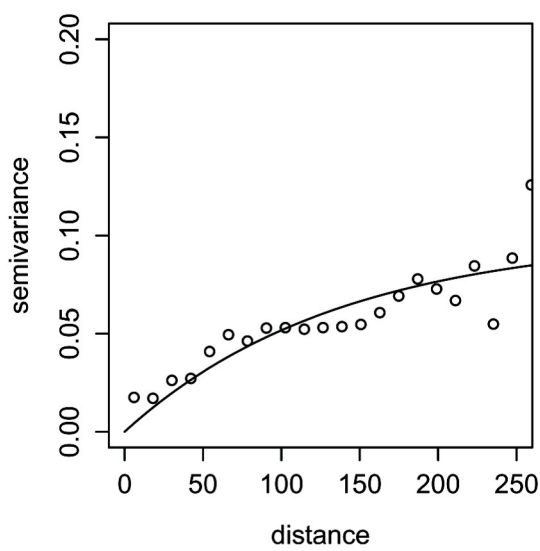
13.4 Semivariograms of soil respiration measurements

Semivariograms of soil respiration measurements of 2006 are shown, separated into “all data”, “data only within $\pm 2\text{sd}$ ” and “data only within $\pm 1.5\text{sd}$ ”.

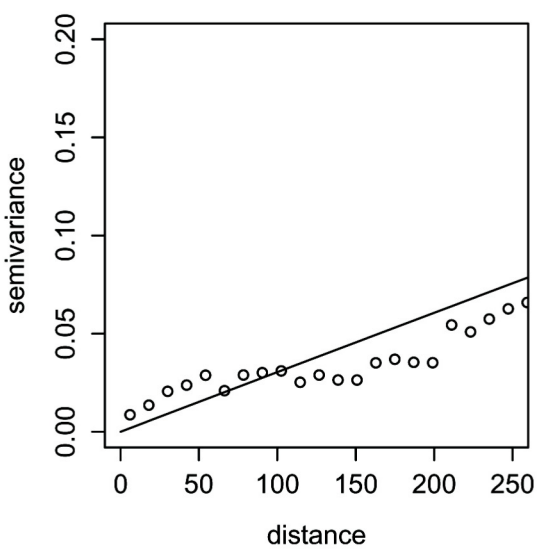


06.123**06.137****06.149****06.165****06.179****06.193**

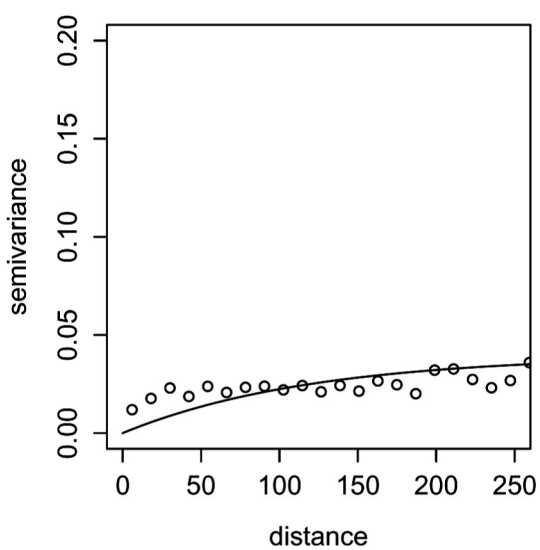
06.207



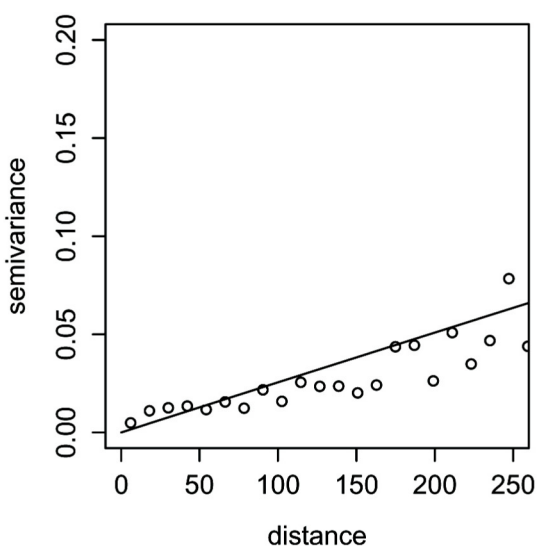
06.221



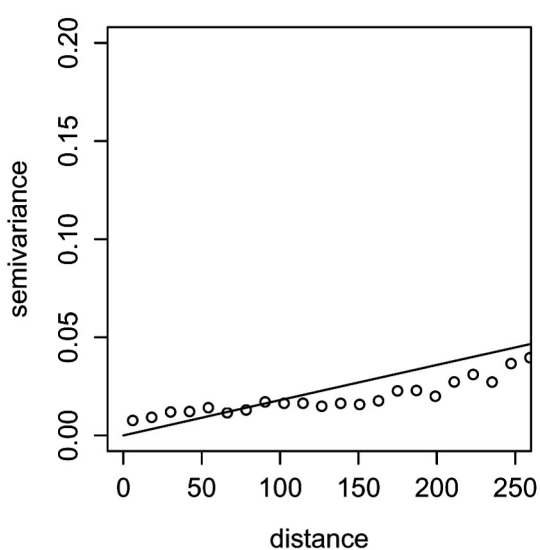
06.235



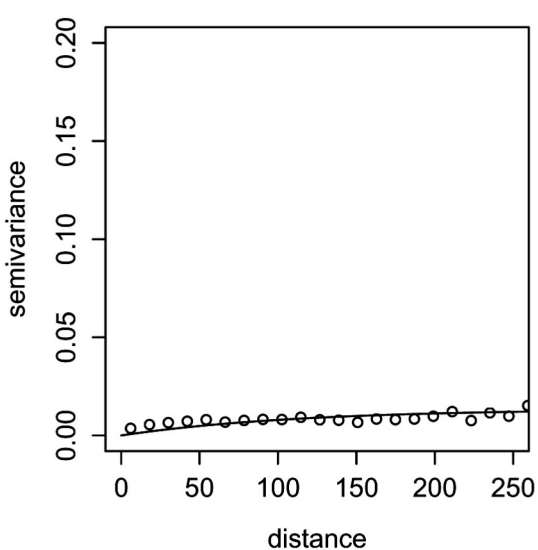
06.263



06.277



06.290



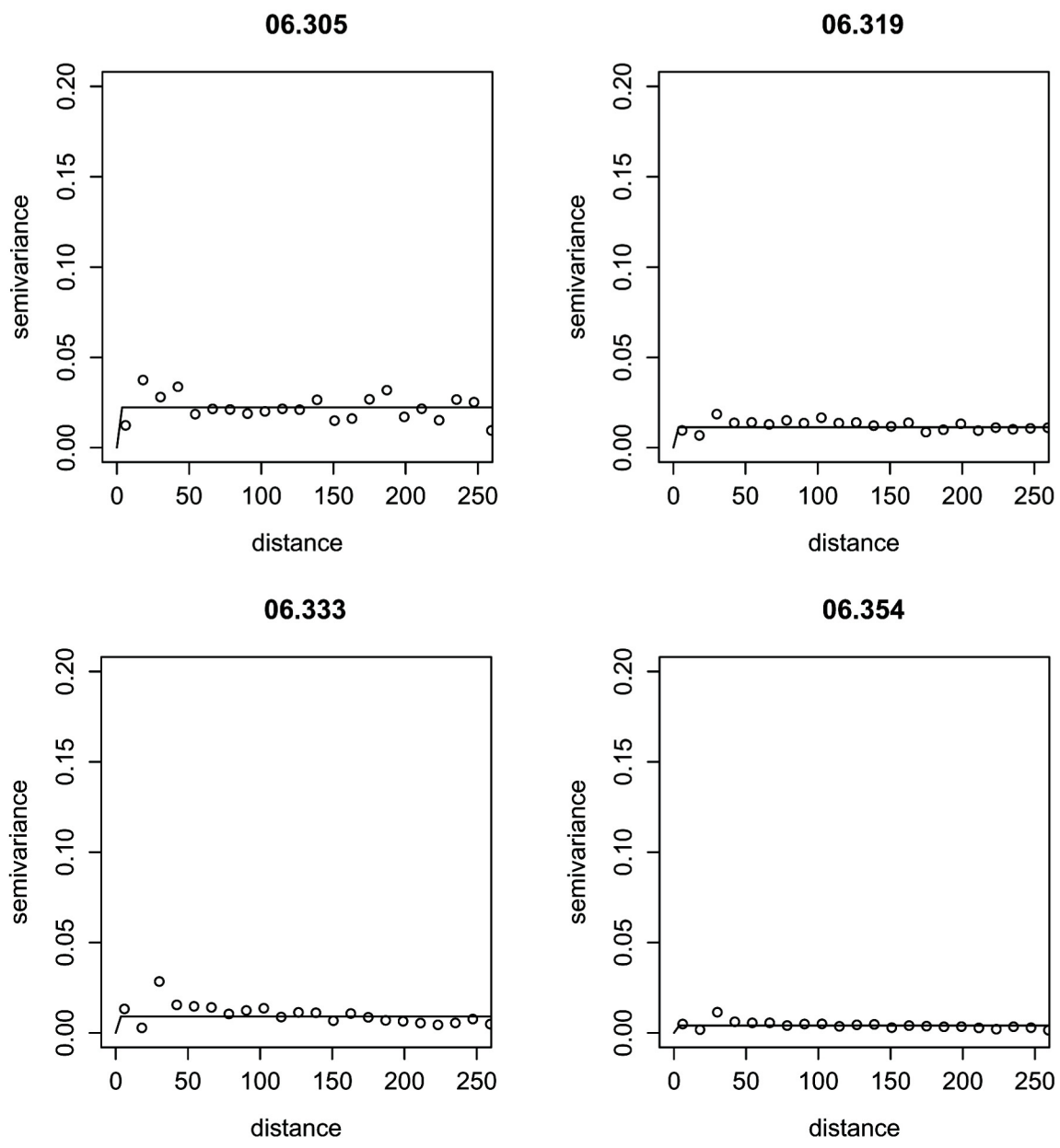
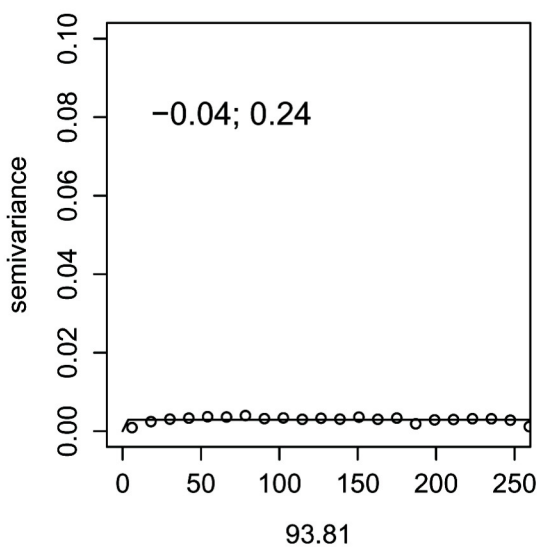
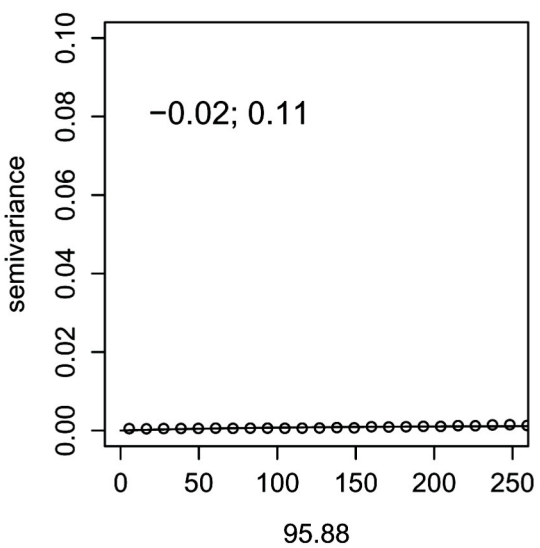


Fig. 13.1 Semivariograms of soil respiration measurements in 2006 (all data). The number at each title indicate the year (2006) and the day of measurement

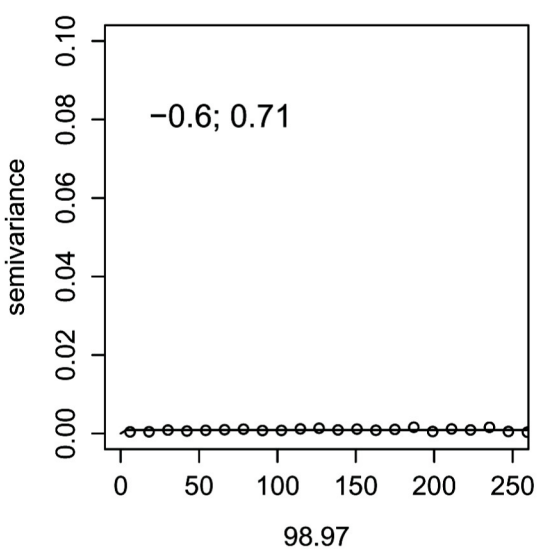
06.11



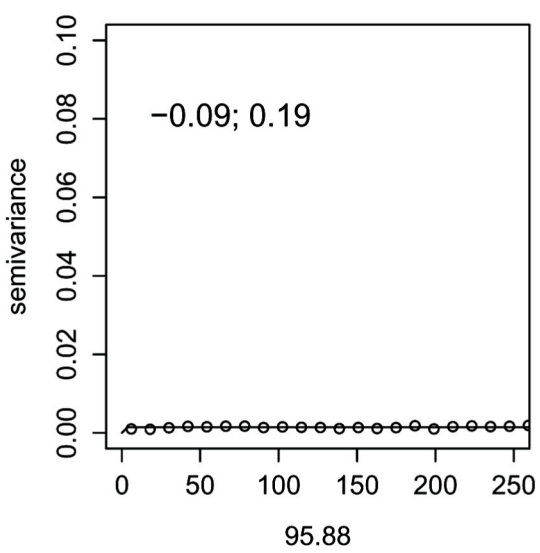
06.24



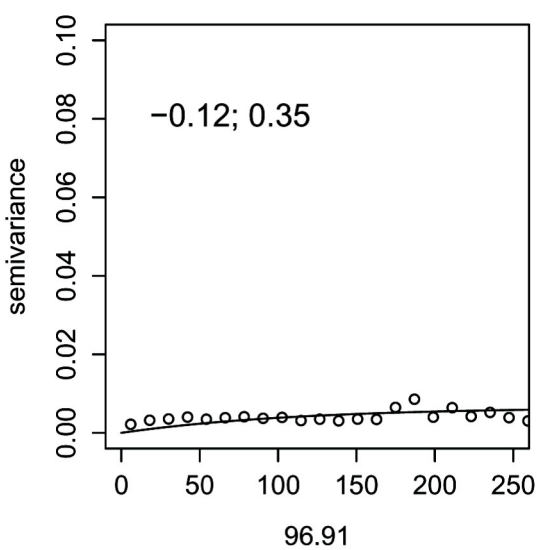
06.39



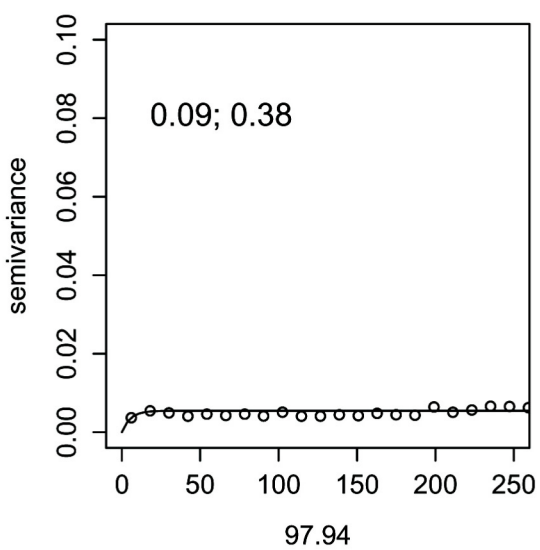
06.53



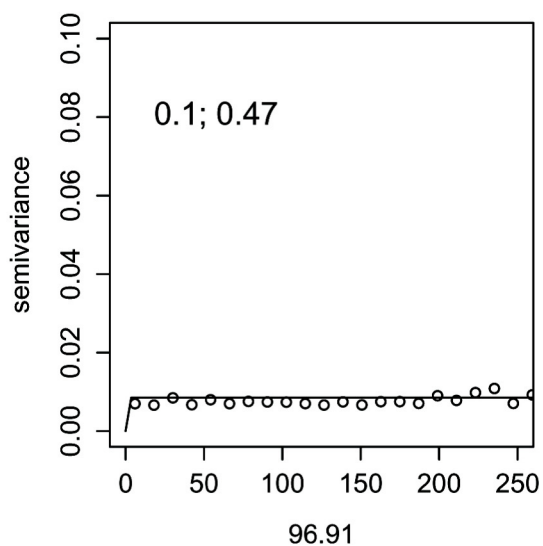
06.81



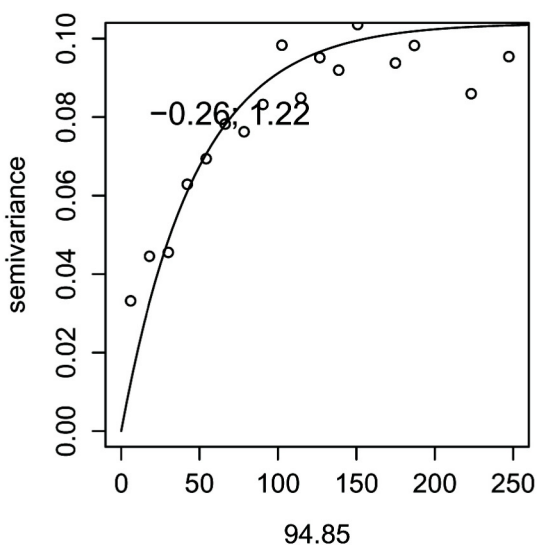
06.110



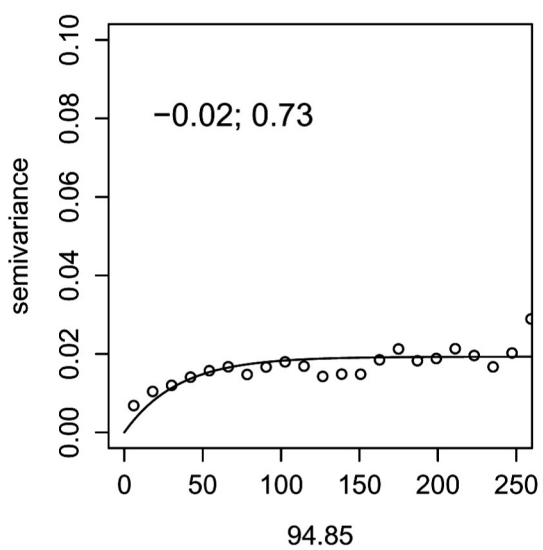
06.123



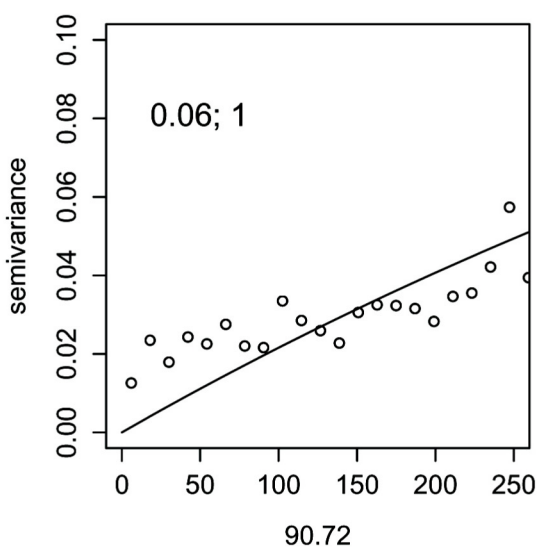
06.137



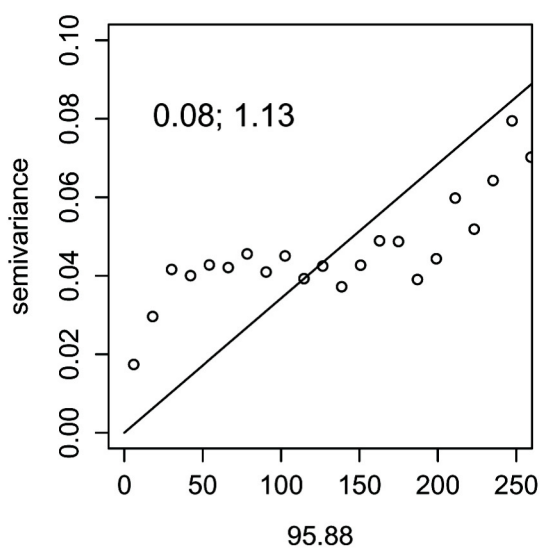
06.149



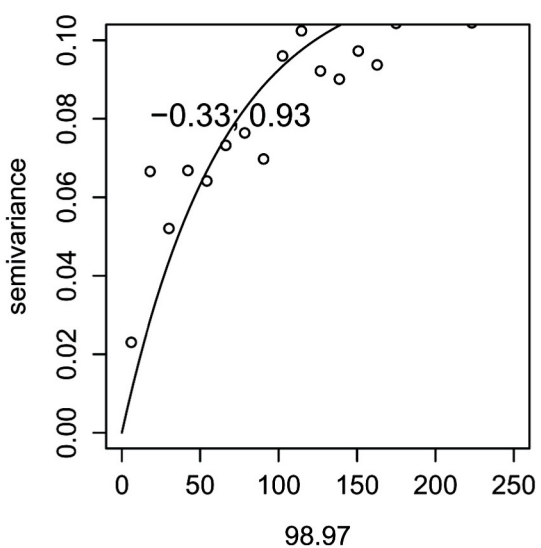
06.165



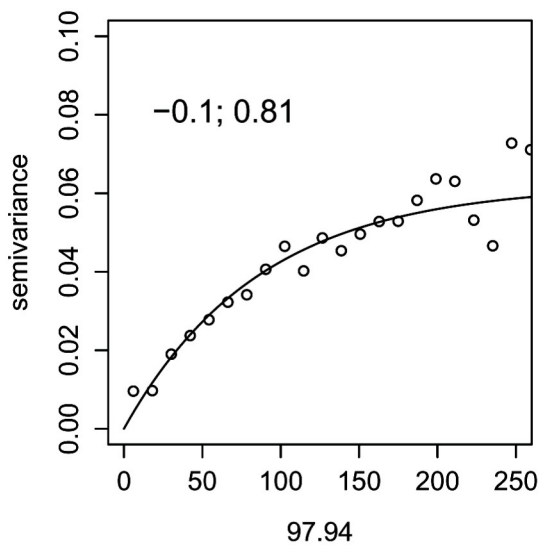
06.179



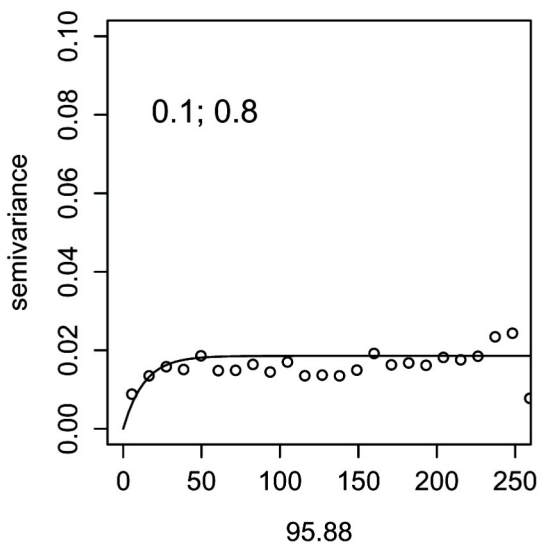
06.193



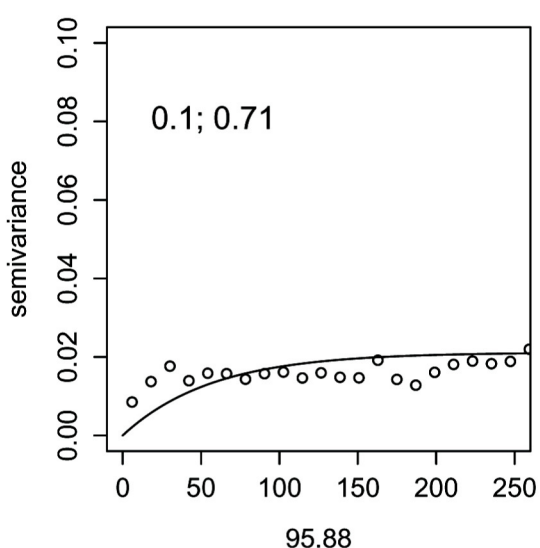
06.207



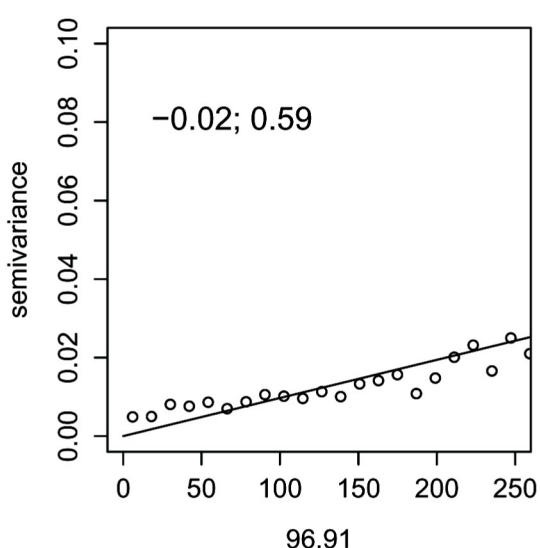
06.221



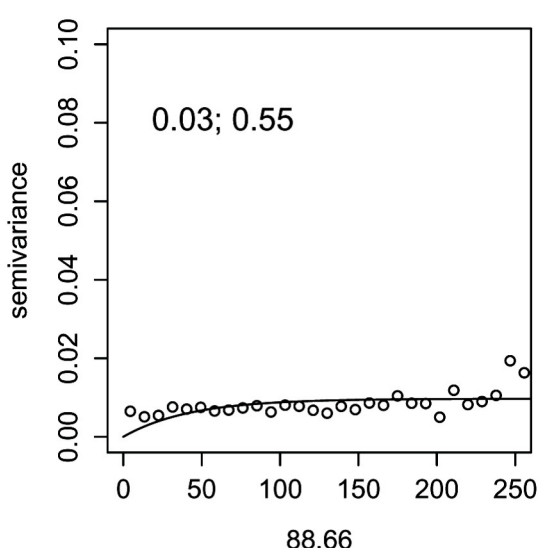
06.235



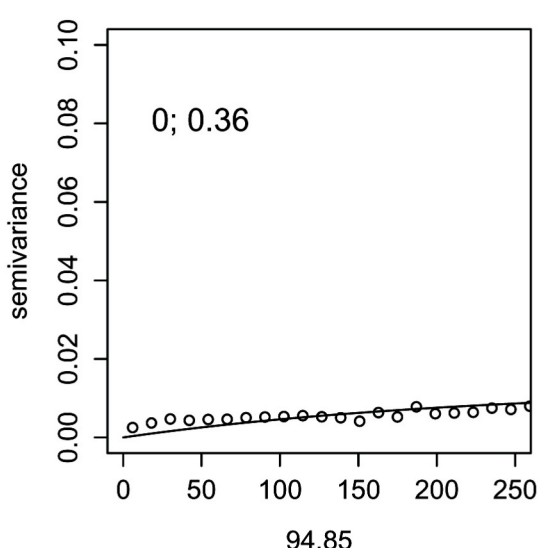
06.263



06.277



06.290



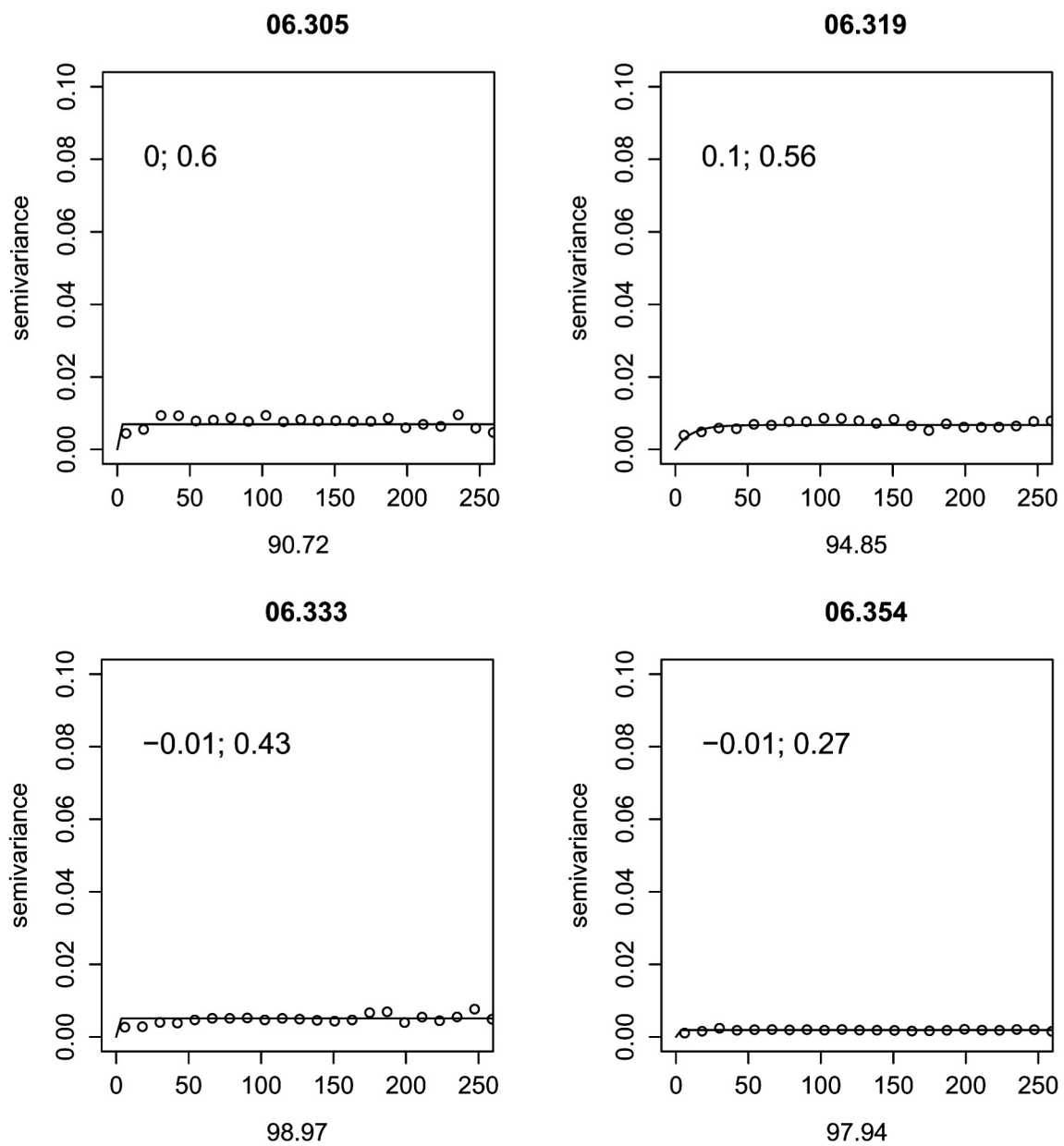
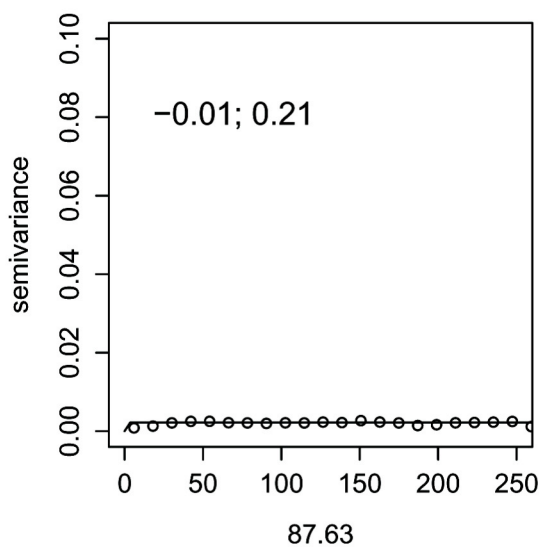
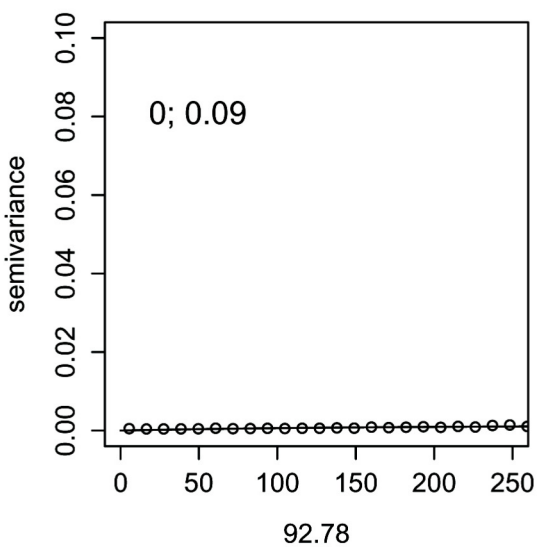


Fig. 13.2 Semivariograms of soil respiration measurements in 2006 (data only within $\pm 2\text{sd}$). The number at each title indicate the year (2006) and the day of measurement

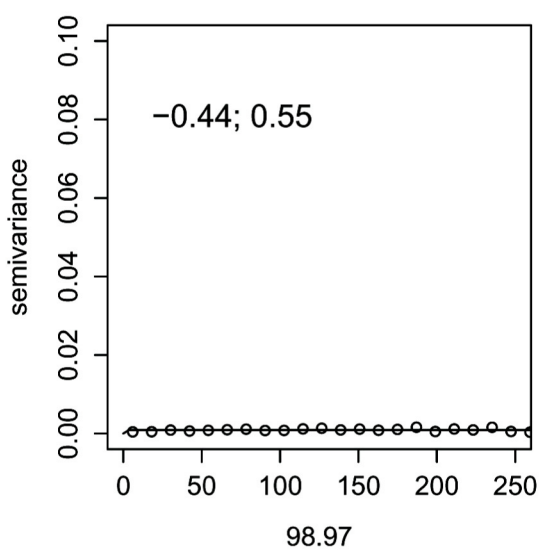
06.11



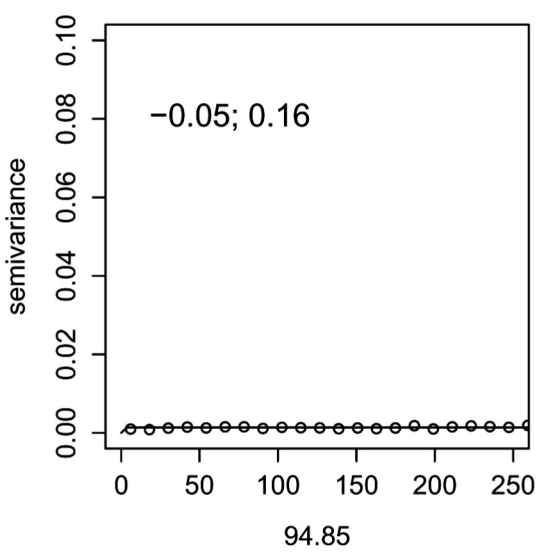
06.24



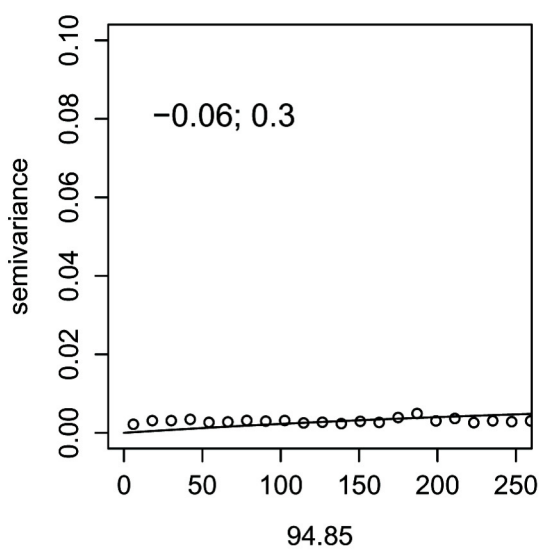
06.39



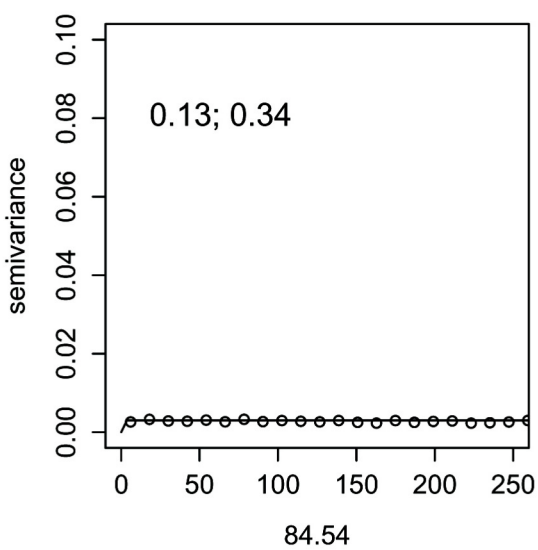
06.53



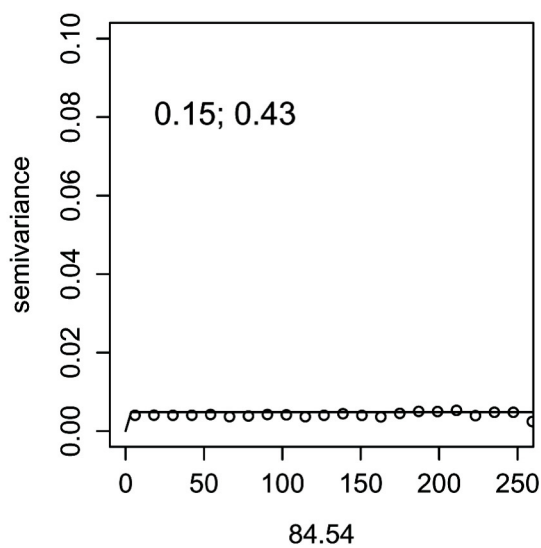
06.81



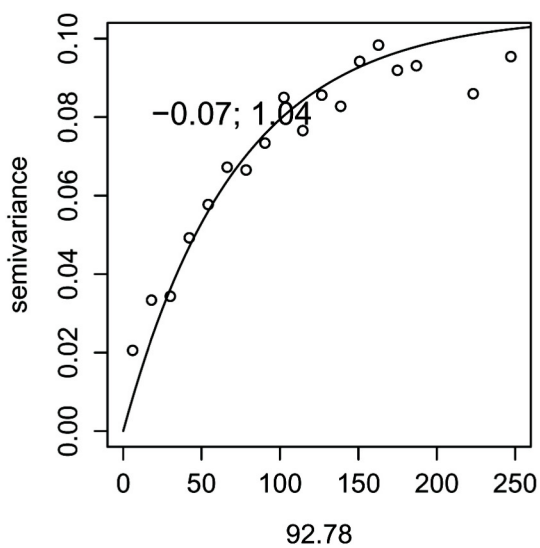
06.110



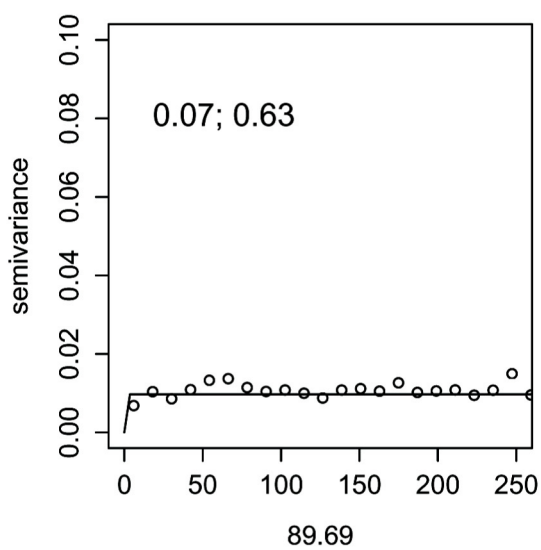
06.123



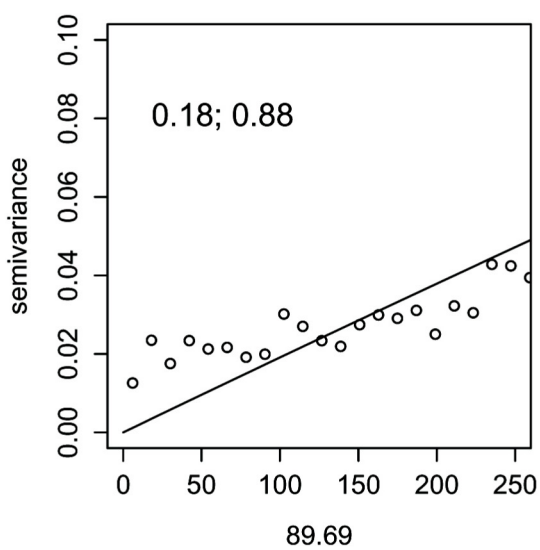
06.137



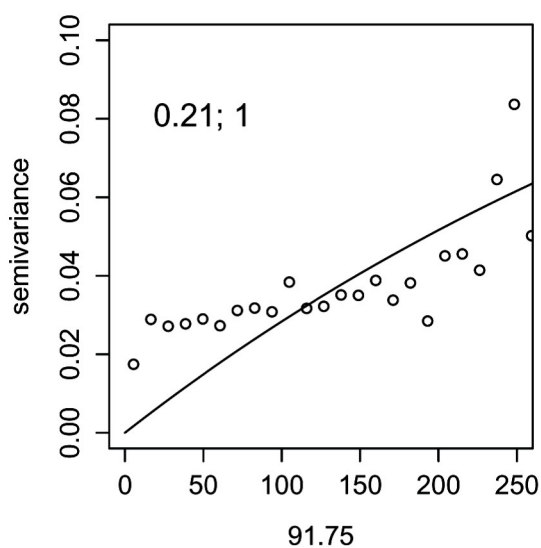
06.149



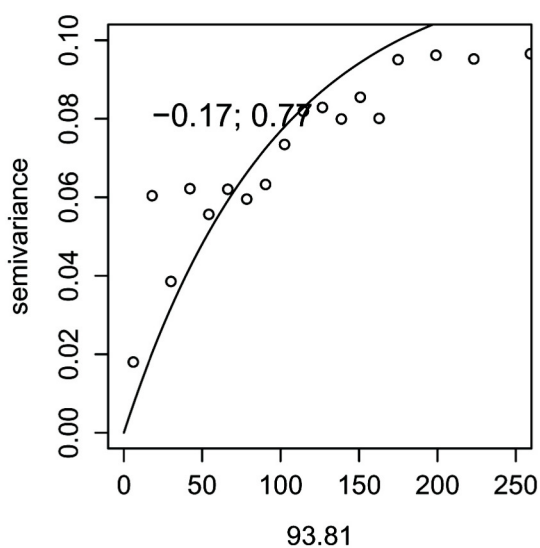
06.165



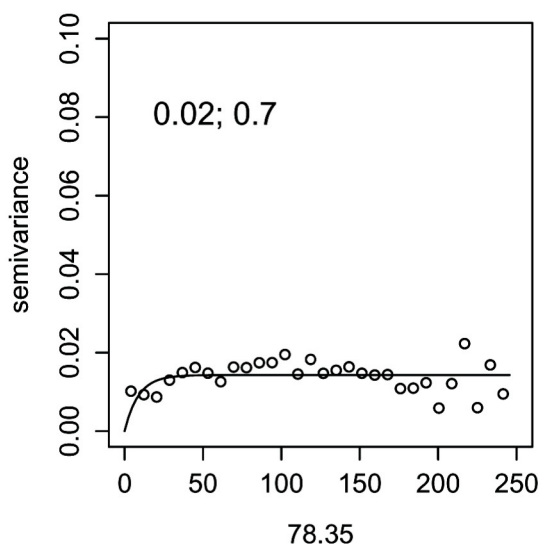
06.179



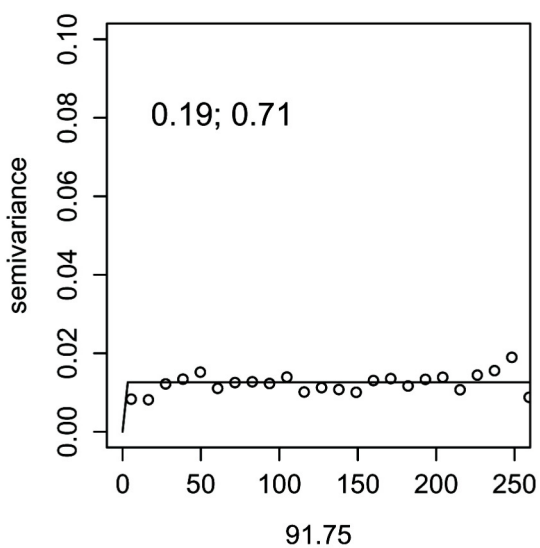
06.193



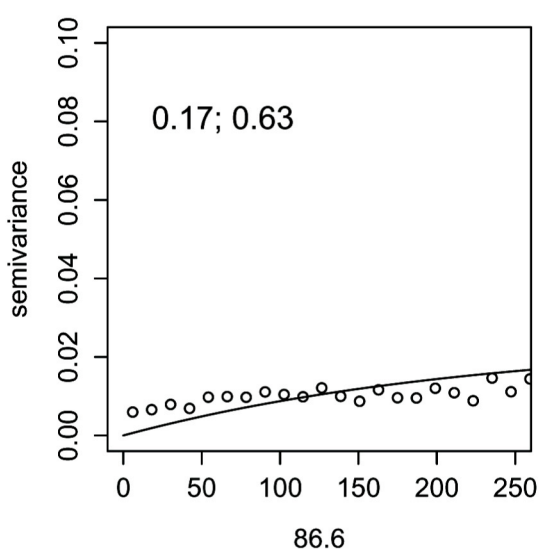
06.207



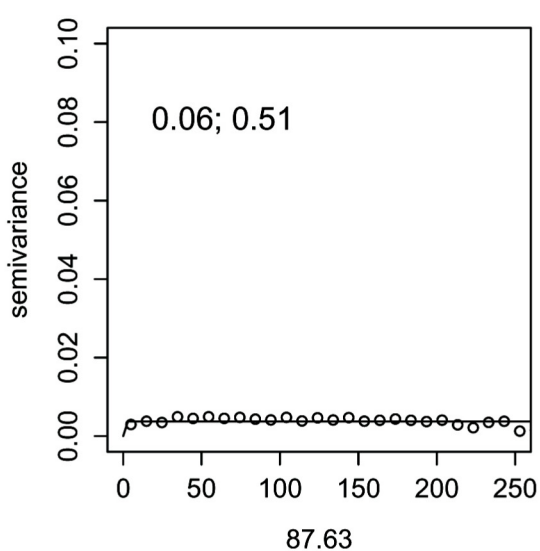
06.221



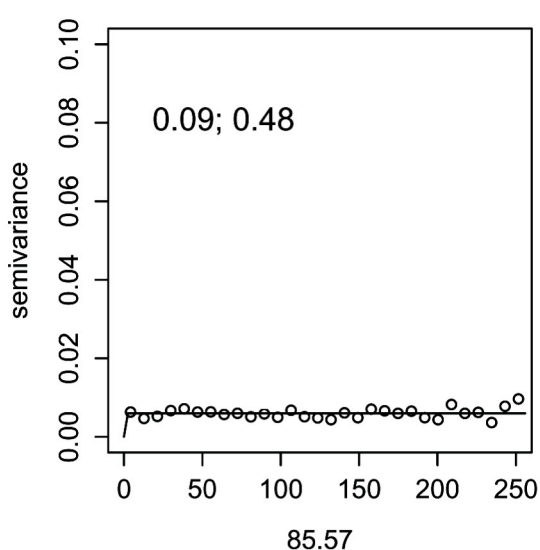
06.235



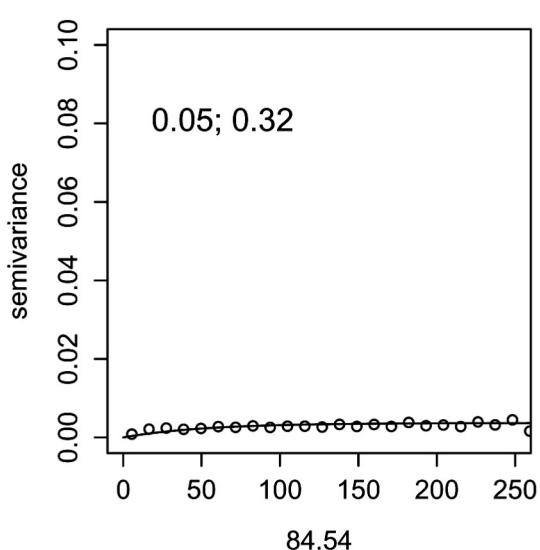
06.263



06.277



06.290



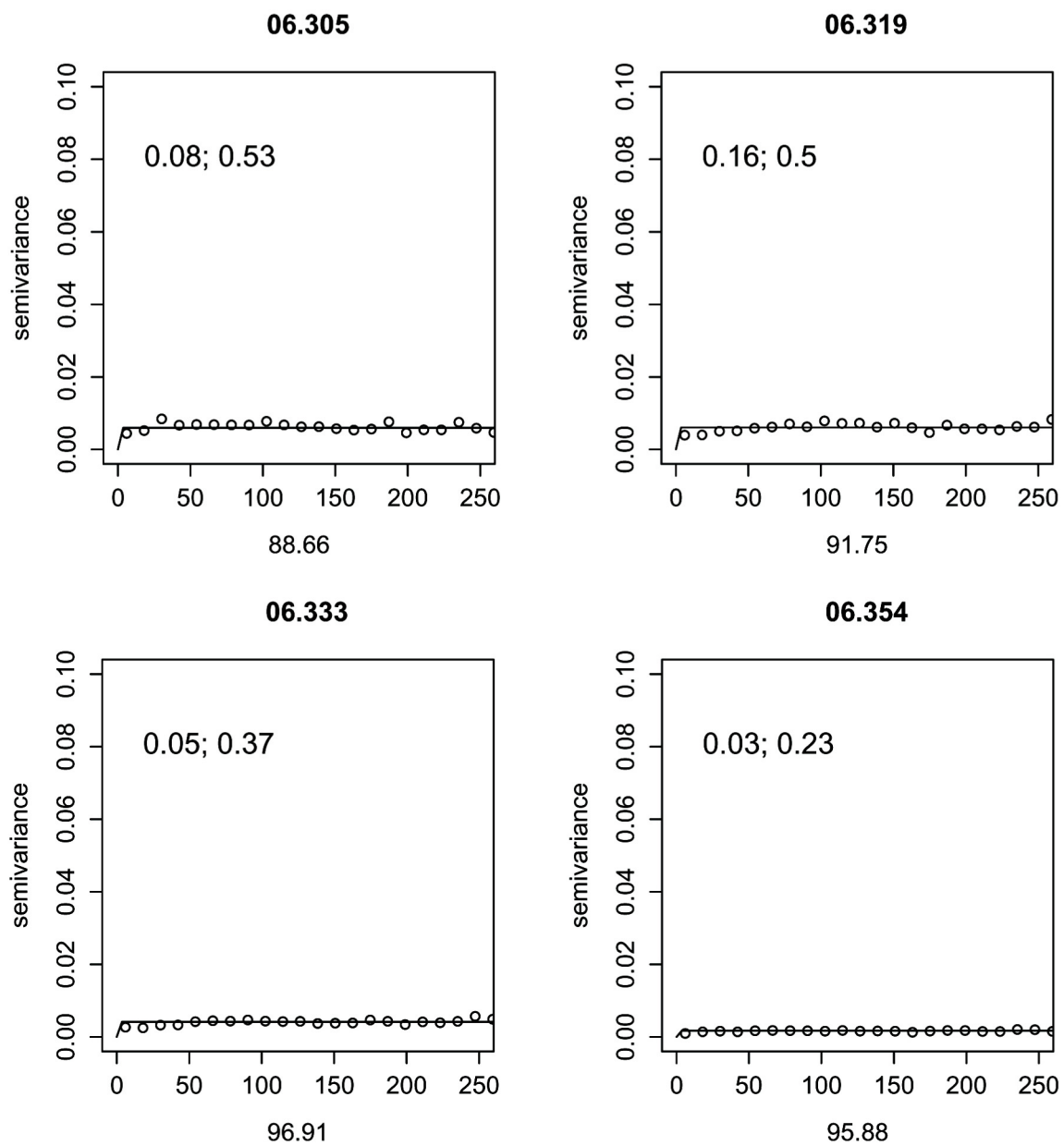


Fig. 13.3 Semivariograms of soil respiration measurements in 2006 (data only within $\pm 1.5\text{sd}$). The number at each title indicate the year (2006) and the day of measurement

13.5 Java application – Source code

```
/*
 * Main.java
 *
 * Created on 2. September 2007, 14:06
 *
 * To change this template, choose Tools | Template Manager
 * and open the template in the editor.
 */

package wurzelgitter;

import java.io.*;
import java.util.Arrays;

/**
 *
 * @author
 */
public class Main
{

    static final String BaumDatei = "C:\\\\Albrecht\\\\Baeume.txt";

    static final String ErgebnisDatei1 = "ergebnisRotbuche.txt";
    static final String ErgebnisDatei2 = "ergebnisEsche.txt";
    static final String ErgebnisDatei3 = "ergebnisHainbuche.txt";
    static final String ErgebnisDatei4 = "ergebnisBergahorn.txt";
    static final String ErgebnisDatei5 = "ergebnisBergulme.txt";
    static final String ErgebnisDatei6 = "ergebnisFeldahorn.txt";
    static final String ErgebnisDatei7 = "ergebnisFichte.txt";
    static final String ErgebnisDatei8 = "ergebnisTraubeneiche.txt";
    static final String ErgebnisDatei0 = "ergebnisGesamt.txt";

    static final int anzahlbaeume = 3142;

    static final double startx = 4391328-6;
    static final double endx = 4391664+6;
    static final double endy = 5661412-6;
    static final double starty = 5661673+6;

    static final double inkrement = 0.1;
    // static final double inkrementy = 0.1;

    /** Creates a new instance of Main */
    public Main()
    {
    }

    /**
     * @param args the command line arguments
```

```

*/
public static void main(String[] args)
{
    // TODO code application logic here
    /** Lade Baeume -----*/
    Baum[] baeume = new Baum[anzahlbaeume];
    int i=0;

    try
    {
        BufferedReader dateieingabe = new BufferedReader(
            new InputStreamReader(
                new FileInputStream(BaumDatei)));
        String zeile;
        boolean weiterarbeiten=true;

        while (weiterarbeiten)
        {
            zeile = dateieingabe.readLine();
            weiterarbeiten = (zeile != null);
            if (weiterarbeiten)
            {
                baeume[i] = new Baum();
                baeume[i].LadeBaum(zeile);
                i++;
            }
        }
    }
    catch (EOFException e) {}
    catch (IOException ioe)
    {
        System.out.println("Fehler beim Lesen aus Datei " + BaumDatei);};

    /** Initialisiere Ausgabedatei -----*/
    FileWriter[] dateiausgabe = new FileWriter[9];
    try
    {
        //Stelle Datei bereit
        dateiausgabe[0] = new FileWriter(ErgebnisDatei0);
        dateiausgabe[1] = new FileWriter(ErgebnisDatei1);
        dateiausgabe[2] = new FileWriter(ErgebnisDatei2);
        dateiausgabe[3] = new FileWriter(ErgebnisDatei3);
        dateiausgabe[4] = new FileWriter(ErgebnisDatei4);
        dateiausgabe[5] = new FileWriter(ErgebnisDatei5);
        dateiausgabe[6] = new FileWriter(ErgebnisDatei6);
        dateiausgabe[7] = new FileWriter(ErgebnisDatei7);
        dateiausgabe[8] = new FileWriter(ErgebnisDatei8);

        //Schreibe Datenkopf in Datei
        int j;
        for (j=0; j<9; j++)

```

```

{
    dateiausgabe[j].write("ncols 3481\n");
    dateiausgabe[j].write("nrows 2731\n");
    dateiausgabe[j].write("xllcorner "+startx+"\n");
    dateiausgabe[j].write("yllcorner "+endy+"\n");
    dateiausgabe[j].write("cellsize "+inkrement+"\n");
};

/** Durchlaufe Auswertungspunkte -----*/
double xtemp = startx;
double ytemp = starty;
double wurzelmasse;
double wurzelmassesumme;
int zaehler=0;

while (ytemp>=endy)
{
    xtemp = startx;
    zaehler=0;
    while (xtemp<=endx)
    {
        /** Durchlaufe alle Baeume und addiere Wurzelmasse -----*/
        wurzelmassesumme = 0;
        for (j=1; j<9; j++)
        {
            wurzelmasse = 0;
            for (i=0; i<anzahlbaeume; i++)
                wurzelmasse += baeume[i].BerechnerFRB(xtemp,ytemp,j);
        /** Speichere Wurzelmasse -----*/
        dateiausgabe[j].write(wurzelmasse+" ");
        wurzelmassesumme += wurzelmasse;
        };
        dateiausgabe[0].write(wurzelmassesumme+" ");
        xtemp += inkrement;
        zaehler++;
    };
    for (j=0; j<9; j++)
    {
        dateiausgabe[j].write("\n");
        dateiausgabe[j].flush();
    };
    ytemp -= inkrement;
    System.out.println("Zeile abgearbeitet "+ytemp+" mit "+zaehler);
};
for (j=0; j<9; j++)
    dateiausgabe[j].close ();
}
catch (IOException ioe) {System.out.println("Fehler beim Schreiben in Datei");}
}

```

```

        }
/*
 * Baum.java
 *
 * Created on 2. September 2007, 14:10
 *
 * To change this template, choose Tools | Template Manager
 * and open the template in the editor.
 */
package wurzelgitter;

/**
 *
 * @author
 */
public class Baum
{
    /** X-Koordinate des Baumes */
    public double x=0;

    /** Y-Koordinate des Baumes */
    public double y=0;

    /** Brusthöhendurchmesser des Stammes in cm */
    public double bhd=0;

    /** Baumart kodiert
     * 0 = nicht initialisiert
     * 1 = Rotbuche
     * 2 = Esche
     * 3 = Hainbuche
     * 4 = Bergahorn
     * 5 = Bergulme
     * 6 = Feldahorn
     * 7 = Fichte
     * 8 = Traubeneiche
     */
    public int baumart=0;

    /** Baumparameter RD3-Korrekturfaktor */
    public double rd3faktor=0;

    /** Baumparameter rfrb0-Korrekturfaktor */
    public double rfrb0faktor=0;

    /** Baumparameter rfrb1 */
    public double rfrb1faktor=0;

    /** Baumparameter rfrb2 */
    public double rfrb2faktor=0;
}

```

```

/** Creates a new instance of Baum */
public Baum()
{
}

/** Laedt Baum aus einer Textzeile */
public void LadeBaum(String quelle)
{
    String[] einzelwerte = quelle.split("\t");
    x = Double.parseDouble(einzelwerte[0]);
    y = Double.parseDouble(einzelwerte[1]);
    baumart = Integer.parseInt(einzelwerte[2]);
    bhd = Double.parseDouble(einzelwerte[3]);
    LadeBaumparameter();
}

/** Laedt Baumparameter in Abhaengigkeit von Baumart */
private void LadeBaumparameter()
{
    switch (baumart)
    {
        case 1:
        case 1:
            rd3faktor = 6;
            rfrb0faktor = 40;
            rfrb1faktor = 1.33;
            rfrb2faktor = 0.43;
            break;
        case 2:
            rd3faktor = 3;
            rfrb0faktor = 40;
            rfrb1faktor = 0.80;
            rfrb2faktor = 0.20;
            break;
        case 3:
            rd3faktor = 6;
            rfrb0faktor = 100;
            rfrb1faktor = 1.67;
            rfrb2faktor = 0.83;
            break;
        case 4:
            rd3faktor = 6;
            rfrb0faktor = 100;
            rfrb1faktor = 1.67;
            rfrb2faktor = 0.83;
            break;
        case 5:
            rd3faktor = 6;
            rfrb0faktor = 100;
            rfrb1faktor = 1.67;
    }
}

```

```

        rfrb2faktor = 0.83;
        break;
    case 6:
        rd3faktor = 6;
        rfrb0faktor = 100;
        rfrb1faktor = 1.67;
        rfrb2faktor = 0.83;
        break;
    case 7:
        rd3faktor = 6;
        rfrb0faktor = 100;
        rfrb1faktor = 1.67;
        rfrb2faktor = 0.83;
        break;
    case 8:
        rd3faktor = 6;
        rfrb0faktor = 100;
        rfrb1faktor = 1.67;
        rfrb2faktor = 0.83;
        break;      }
}

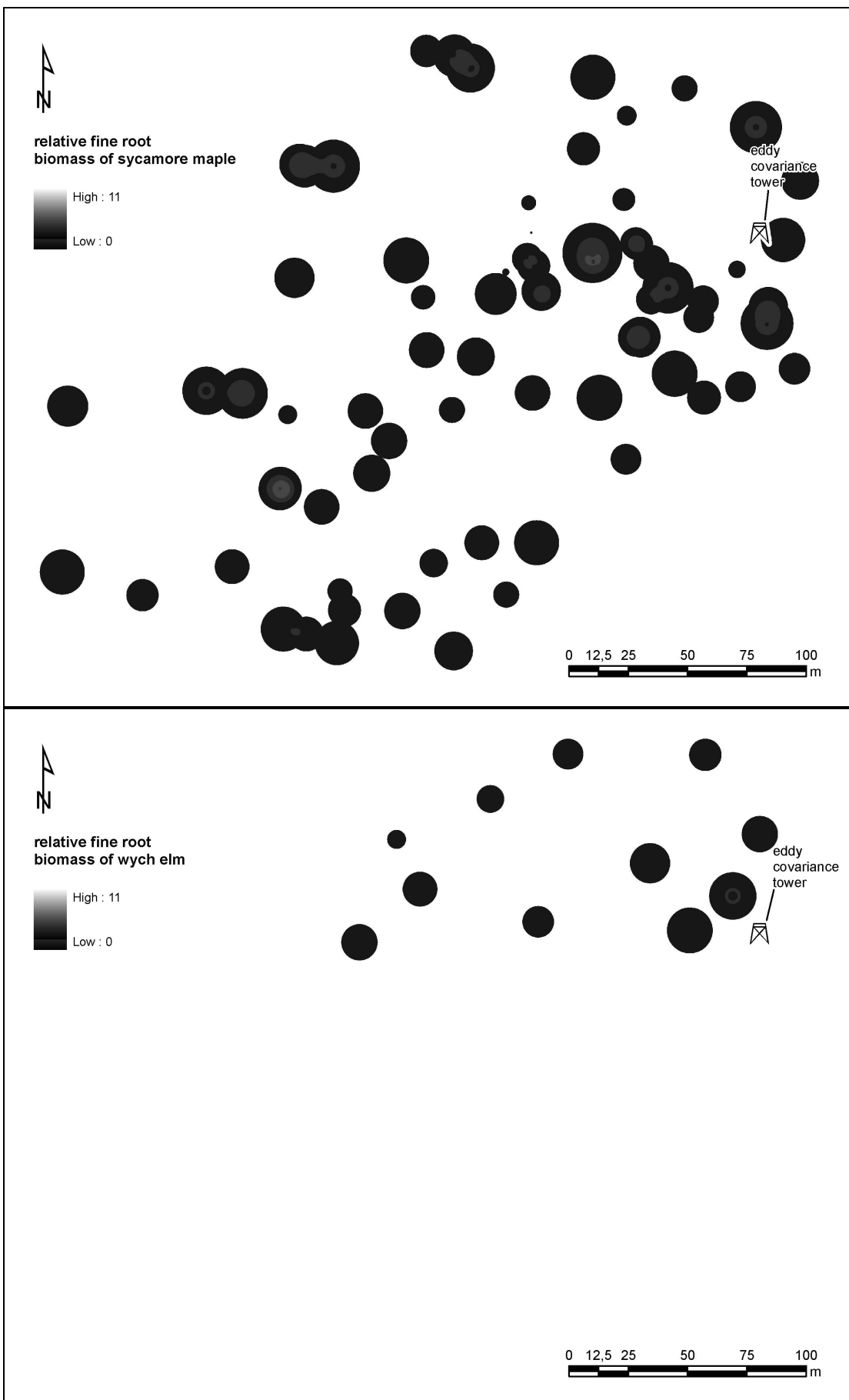
/** Berechne rFRBx,y fuer eine beliebige Koordinate */
public double BerechnerFRB(double xcoord, double ycoord, int wunschbaumart)
{
    double ergebnis=0;
    if (wunschbaumart==baumart)
    {
        double rd3=bhd/rd3faktor;
        double rfrb0=bhd/rfrb0faktor;
        double rfrb1=rfrb0*rfrb1faktor;
        double rfrb2=rfrb0*rfrb2faktor;

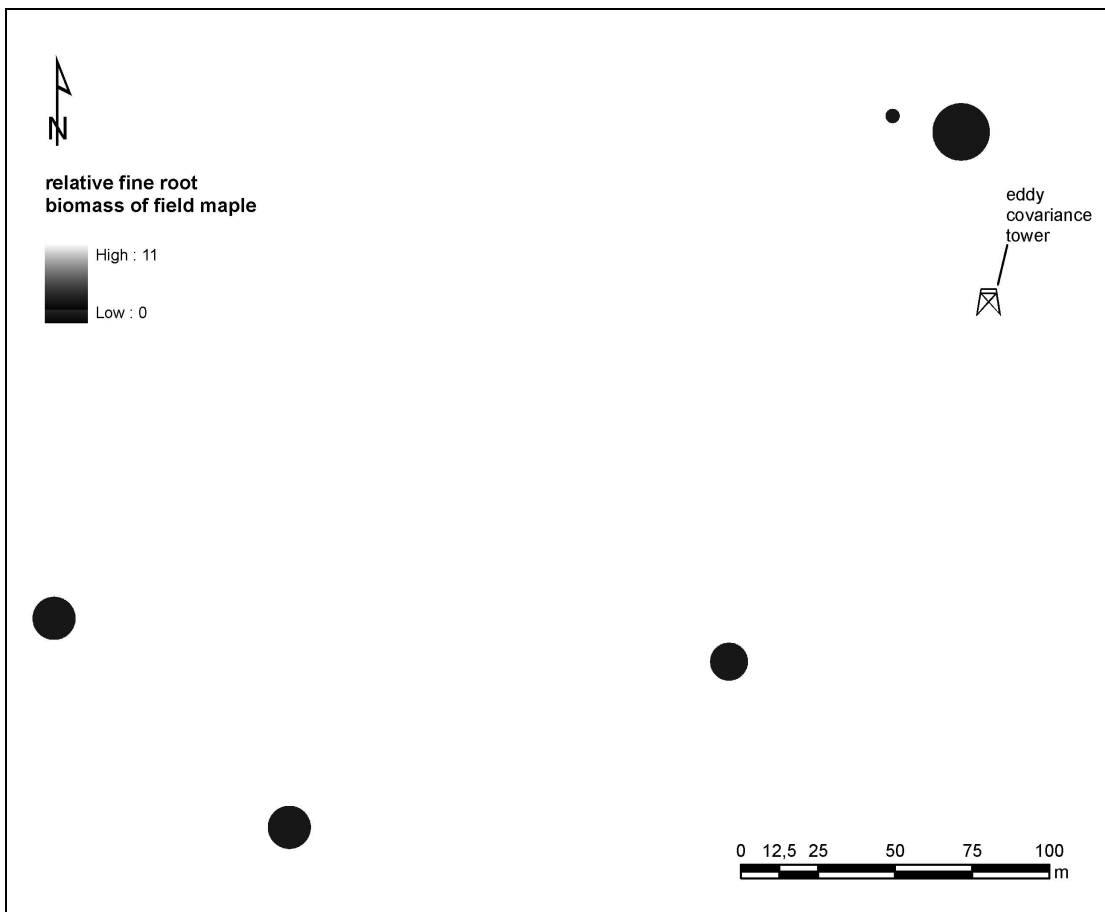
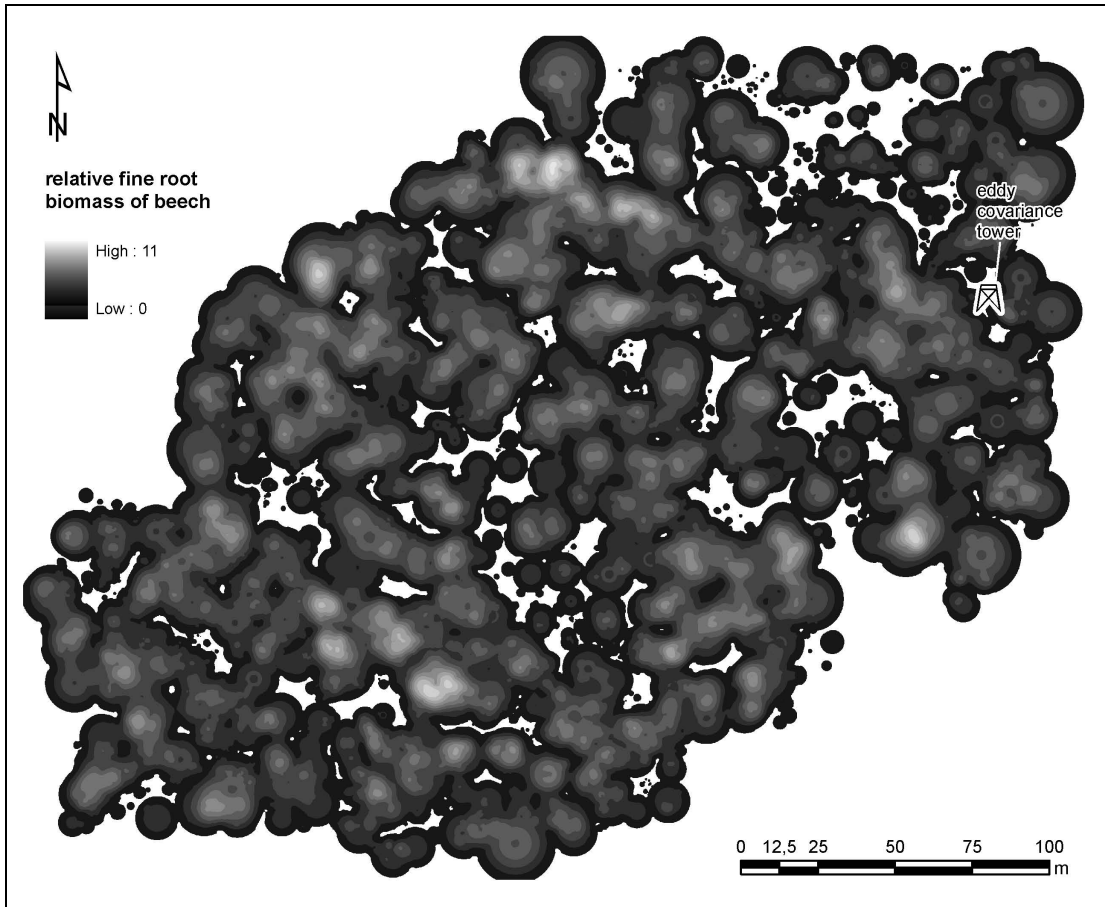
        /** Berechne Abstand zum Baum */
        double abstand = Math.hypot(xcoord-x,ycoord-y);
        if (abstand<rd3)
        {
            double h = rd3/3;
            double b0 = rfrb0;
            double b1 = (rfrb1-rfrb0)/h;
            double b2 = ((rfrb2-rfrb1)-(rfrb1-rfrb0))/(2*h*h);
            double b3 = (((0-rfrb2)-(rfrb2-rfrb1))-((rfrb2-rfrb1)-(rfrb1-rfrb0)))/(6*h*h);

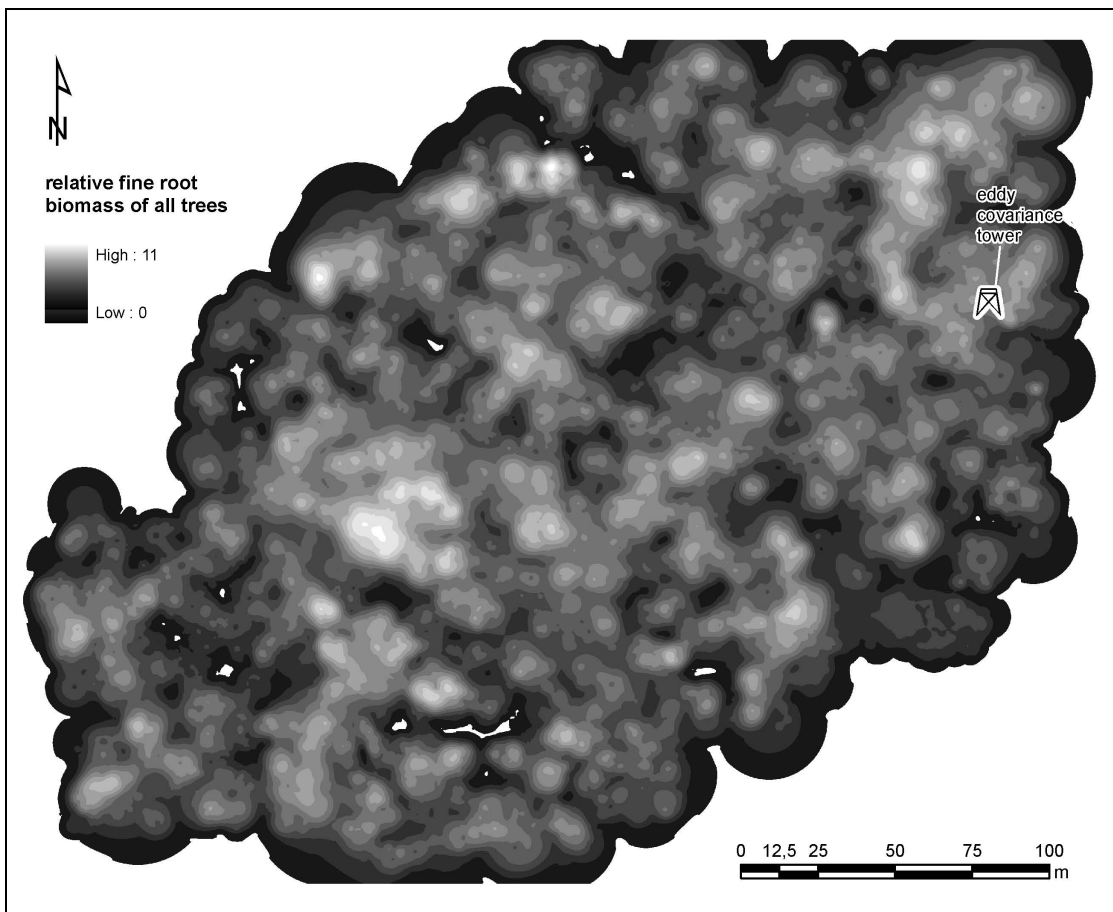
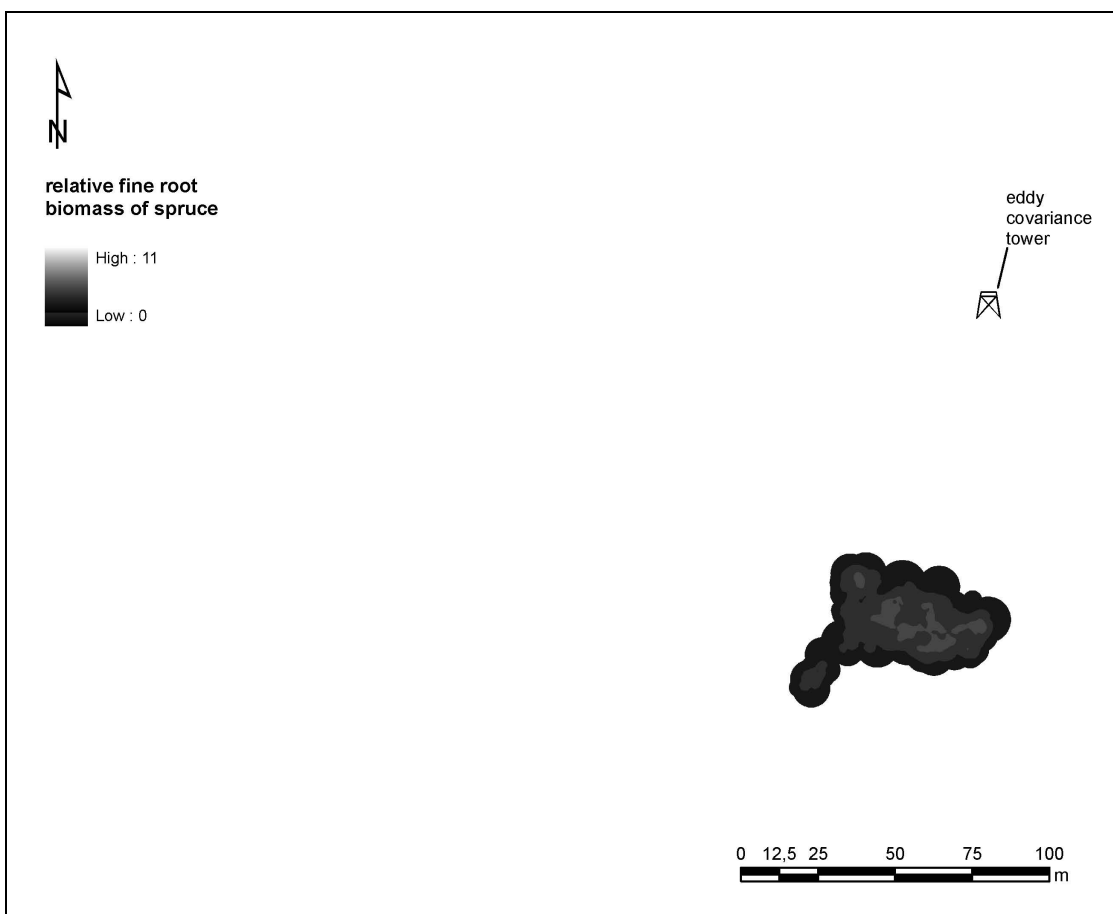
            ergebnis = b0 + abstand*(b1 + (abstand-rd3/3)*(b2 + (abstand-rd3/3*2)*b3));
        }
        else
            ergebnis = 0;
    };
    return(ergebnis);
}
}

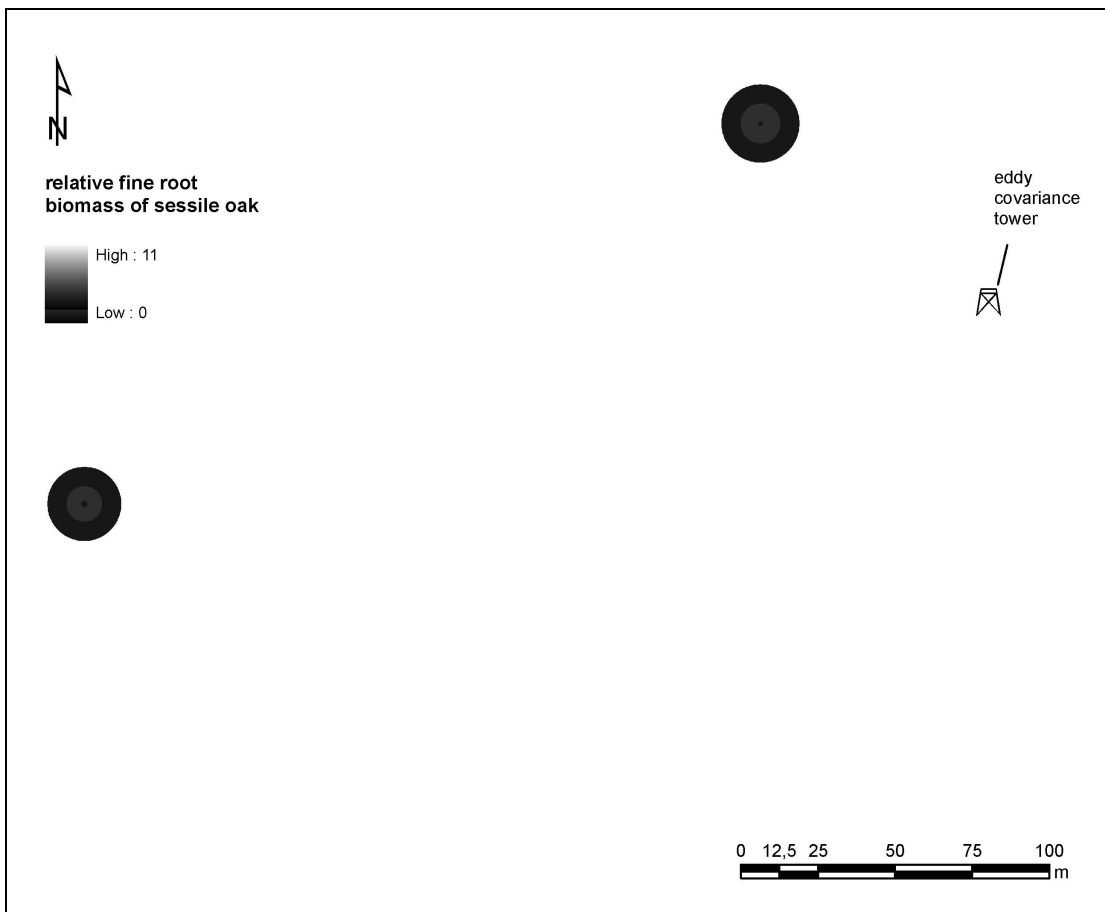
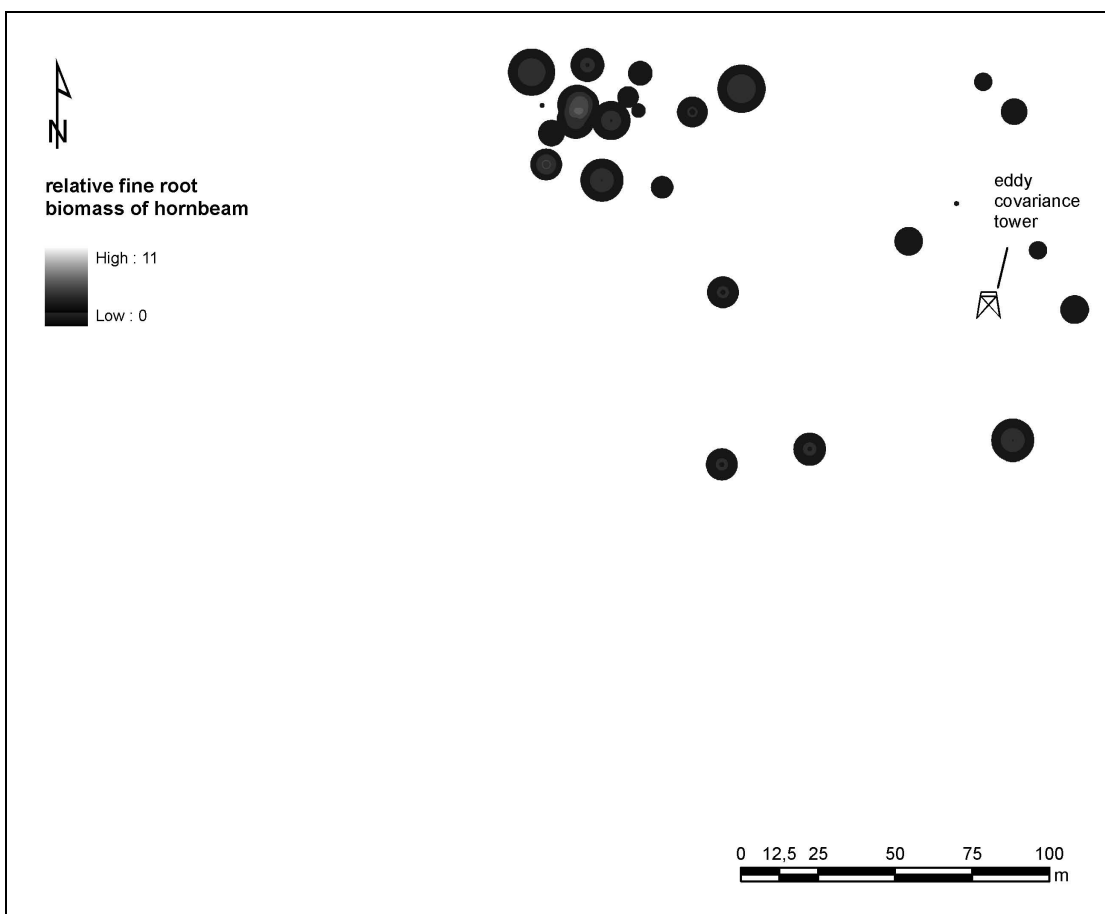
```

13.6 Potential relative fine root distribution patterns of different tree species









14. Declaration

Declaration

I do hereby declare that the present thesis is my original work and that no sources and utilities have been used other than those indicated in the thesis itself. In addition, I declare that this work and any part thereof have not been submitted elsewhere for the award of any other degree.

Erklärung

Hiermit erkläre ich, dass ich die vorliegende Dissertation selbständig verfasst und keine anderen als die von mir angegebenen Hilfsmittel und Quellen benutzt habe. Zudem erkläre ich, dass diese Dissertation weder in gleicher noch in anderer Form bereits in einem Prüfungsverfahren vorgelegt wurde.

Göttingen, Februar 2010

Albrecht Jordan

15. Acknowledgements

Many people have supported my Ph.D. study in many different ways.

I want to thank especially my supervisor **Prof. Dr. Stephan Glatzel** who was always interested in my studies and who stimulated the progress by many encouraging scientific discussions. I particularly thank him for his patience, his openness and flexibility and his support during the last years. Furthermore, I thank him for the opportunity to work at the University of Goettingen and after his call at the University of Rostock.

I am very grateful to **Dr. Gerald Jurasinski** who gave me many fruitful hints and support during the preparation of my first scientific paper.

Many thanks go to people of the landscape ecology unit of the department of Geography at the University of Goettingen:

Prof. Dr. Gerhard Gerold for the opportunity to work in his team.

Prof. Dr. Karl-Heinz Pörtge for his financial aid during the acquisition of a frequency domain reflectrometry equipment.

Dr. Jürgen Grotheer, the head of the laboratory and his team members **Petra Voigt** and **Anja Södje** for their advices and assistance with the laboratory work.

Anika Bargsten, who first worked as student assistant helping me to gather measurement data even at severe frost periods. She was an unplayable aid during the first part of mapping and surveying of all trees within the study area. Later she worked as diploma student in the team.

Isabell Kiepe, who determined soil respiration data for the first month of the second measurement series, in preparation of her diploma thesis. She also helped to map and survey a large area of trees.

Philipp Riesmeyer, Björn Todt and Tim Coldewey, who worked as student assistants in the project. They helped to gather soil respiration data as well as data about the distribution of tree species.

Petr Holy, who supports me with additional information about the research area.

René Trujillo, who was an inestimable aid during all computer problems.

Many thanks go to **Catharina Meinen**, who provided me useful data for the validation of the adapted potential relative fine-root prediction model.

I thank **Olaf Kolle** for helping me with data from the eddy-covariance-facility.

Many thanks go to **PD. Dr. Gerd Gleixner** and **Cindy Tefs** from the Max-Planck-Institut for Biogeochemie, Jena for critical but always motivating discussions.

Further, I have to thank **Prof. Dr. Uwe Eduard Schmidt** and **Matthias Hammer** for many valuable inputs concerning forest history of the study site.

I thank **Manfred Grossmann** and **Karola Marbach** for their support of my research in the Park and for providing much information about the Hainich National Park.

Special thanks go to my friend **Stefan Heinrichs**, who inestimably helped me programming the Java application.

I thank my parents **Liselotte** and **Ingo Jordan** and my sister **Anja** for their encouraging support and trust in me throughout my life.

In particular I thank my partner **Corinna Wörner** for her support and patience during the last years.

16. THESIS

“GIS-based interpolation methods for soil CO₂ respiration data in a temperate deciduous forest”

Submitted by Dipl.-Umweltwiss. Albrecht Jordan

Background and aims

1. Soil CO₂ is one of the largest carbon flux components. Even small shifts between carbon release and photosynthetic uptake can have a significant influence on the atmospheric carbon budget. An improved scientific understanding of the key factors driving soil respiration as well as a better knowledge about mean soil efflux rates of the major biome types, are of great interest. However, mean soil efflux rates show high variability even within small measurement sites. Thus, there are large uncertainties in the annual averages of, inter alia, site specific soil efflux rates of forest.
2. Small-scale heterogeneities in soil efflux rates are, among others, caused by forest age, the high variability of soil structure, soil moisture, bacterial & fungal communities, root density, soil organic matter content, wind speed at the soil surface, pressure patterns and forest stand structure.
3. Studies describing within site "spatial heterogeneity" that means micro scale spatial heterogeneity within old growth temperate deciduous forests with otherwise relatively homogeneous site conditions, are rare. Many studies in the past few years partitioned soil respiration into autotrophic and heterotrophic components and advances have been made in understanding the dynamics of a wide range of soil C pools and their effects on soil respiration. However, it still remains unclear on which scales factors influencing soil respiration vary, while influencing total soil respiration rate.
4. Various factors must be taken into account when reliable estimates of site scale flux rates are to be extrapolated from point measurements, but these factors do not take effect on the same scales within a given site. Therefore a nested as well as a random soil respiration measurement series were implemented, an approach spanning various spatial scales. Additional parameters like soil temperature and soil moisture were determined to test whether they are ample to improve ordinary kriging results of soil respiration. Soil respiration data were standardised using soil temperature and soil moisture, to account for spatial and seasonal influences. Average annual soil

respiration rates calculated statistically from soil respiration data were compared with average standardised respiration rates derived from interpolated maps of standardised soil respiration.

5. Root respiration significantly contributes to net carbon dioxide (CO_2) flux from soils, but its reliable quantification is difficult. Therefore in recent years various techniques were developed to separate different fractions of soil respiration with both direct (i.e. girdling, trenching) and indirect methodologies (i.e. stable and radioactive C isotopes). The reliability of the results is bound by assumptions and simplifications on which the applied methodologies are based on. Separation methods like trenching, which are commonly used in forest ecosystems, involve strong impacts on the root-soil system by increasing soil water content and rising rhizodeposition. Therefore I investigated the possibility to use calculated relative fine root biomass as a predictor of root respiration. Preparing this analysis, stand structure parameters like location, breast height diameter (at 1.3m dbh) and type of each tree were recorded and potential fine-root biomass rates were calculated at each soil respiration measurement location using an adapted modeling approach of Ammer and Wagner (2005). In a second analysis, it is examined whether the expected correlation results can be used to improve the regionalisation of total soil respiration measurements. Therefore a regression kriging procedure using calculated potential fine root biomass rates of the entire study area and total soil respiration data were performed. It was studied how tree type and seasonal dynamics of root growth and mortality influence the quality of the regression kriging results.

Results and conclusions

1. Soil respiration as well as soil moisture did not show any spatial trends. However, soil respiration rates and soil moisture revealed a patchy pattern without any obvious structures. The spatial variability of soil temperature apparently did not drive this heterogeneity because it is very small (less than $\pm 1^\circ\text{C}$ during a single measurement day).
2. Combining soil temperature and soil moisture effects within a single exponential equation slightly enhanced the predictability of soil respiration measurements ($r^2=0.63$ compared to $r^2=0.61$). But the effect was not as pronounced as described in the literature.

3. Spatial heterogeneity of soil respiration increased when all-season measurements were considered, compared to studies which focuses solely on the vegetation period. The calculated ranges of autocorrelation varied considerably during the season. The determined average range of the semivariograms (9m) was comparable to ranges found in other studies. Semivariograms solely calculated from soil respiration data showed a broad variety of autocorrelation distances (ranges) from a few centimeters up to a few tens of meters.
4. The standardisation of soil respiration using soil temperature and soil moisture largely reduced the interpolated spatial heterogeneity of soil respiration. The remaining heterogeneity must therefore be caused by other, not measured variables.
5. The interpolation of soil respiration data requires large sampling densities if better, spatially autocorrelated parameters than soil moisture and soil temperature are not available. Standardizing of soil respiration can help to minimize artifacts caused by temporal and spatial small scale heterogeneity of soil moisture and soil temperature.
6. The geostatistical approach yielded slightly lower results than the statistical approach, which indicates that the calculated fluxes of even a high number of measurement locations can be further improved by involving spatial parameter.
7. The spatial pattern of root respiration and thereby total soil respiration was driven by seasonality. Significant correlations between calculated fine root biomass and soil respiration were only found in summer (June, August and September 2006). These findings correspond with previous studies, because in winter, the contribution of root respiration to total soil respiration is negligibly small.
8. The influence of autotrophic respiration from ash roots was more pronounced than from beech, because soil respiration was measured at the soil surface next to the ash roots. This proximity of ash roots to the soil surface may have contributed to higher significant correlations between soil respiration and ash fine root biomass.
9. The applied model for predicting fine root distribution patterns originally developed for spruce was successfully adapted to predict fine roots of other tree species. The validity of the results was better for beech ($r^2=0.72$) than for ash ($r^2=0.60$). Significant correlations between soil respiration and predicted fine root biomass could only be detected in summer month between ash roots and soil respiration ($r^2=0.40-0.50$), probably due to more shallow root distribution patterns of ash compared to beech roots.

Outlook:

1. To further increase the reliability of the interpolation of total soil respiration data it is necessary to incorporate (besides soil moisture and soil temperature) additional parameters with less temporal variability and larger autocorrelation ranges.
2. Only a combination of a randomized and a double nested sampling approach as well as the appropriate incorporation of additional parameters may permit a sufficient estimation of the range of soil respiration, which is a prerequisite for reliable maps of soil respiration based on interpolation. Future estimations of average soil respiration rates of forest sites should consider spatial as well as temporal steering parameters of soil respiration. Thereby, appropriate range distances should always govern the sampling design. Therefore, there is a need to estimate the range distance based on extensive pre-studies with nested measurement locations. My results show that the consideration of seasonal controls facilitates the interpolation of soil respiration measurements.
3. Future attempts quantifying root respiration at forested sites may profit from an additional method as proposed in this study, which avoids strong impacts on the root-soil system. This approach is most valuable within stands with shallow root systems like ash dominated stands during the summer. Thus the results of this study may inspire further attempts to quantify the fractions of root respiration depending on root architecture. In contradiction to well-known soil respiration separation methods in previous studies, this method provides an area wide impression of root respiration. Due to the easy determinable above-ground stand characteristics, root respiration of larger areas can be quantified, compared to other more labour intensive methods. Both, area wide prediction of root respiration and the consideration of larger areas increase the accuracy of average root respiration assessments of old-growth forest stands.